Nachtelijke natuurlijke ventilatie in kantoorgebouwen
Evaluatie van de prestaties met simulatie, onzekerheids- en gevoeligheidsanalyse

Natural Night Ventilation in Office Buildings
Performance Evaluation Based on Simulation, Uncertainty and Sensitivity Analysis

Hilde Breesch

UNIVERSITEIT
GENT

Examencommissie:
Prof. Ronny Verhoeven (UGent, voorzitter)
Prof. Dirk De Meester (UGent, secretaris)
Prof. Arnold Janssens (UGent, promotor)
Prof. Michel De Paepe (UGent)
Prof. Filip Descamps (VUB)
Prof. Erik Dick (UGent)
Prof. Mattheos Santamouris (University of Athens)
Prof. Peter Wouters (UCL)

Het moet zowat op het einde van het laatste jaar middelbaar geweest zijn. De hele klas had geen zin in de les godsdienst van dat lesuur. En zoals we goed wisten, had de leraar een zwak voor klasdiscussies. Het thema deze keer was "wat we later gingen worden". Ieders toekomst werd om beurten voorspeld. Toen het aan mij was, zei een klasgenootje heel beslist: "iets met wetenschap en schrijven, redacteur bij Natuur en Techniek ofzo". De rest van de klas ging volmondig akkoord.

Ongeveer twaalf jaar later leg ik de laatste hand aan mijn doctoraatstekst. Ik wil dan ook graag een woordje richten tot enkele mensen.

Aan mijn promotor zeg ik graag: "Arnold, ik ben er fier op je eerste doctoraatsstudent te zijn! Ik ben er zeker van dat er nog velen zullen volgen."

Aan de leden van mijn examencommissie, en speciaal aan Peter en Erik die ook lid waren van mijn begeleidingscommissie: "Dank voor jullie – in mijn ogen soms tè - kritische opmerkingen en raadgevingen. Ik heb er veel van geleerd"

Aan al mijn "oude" collega's op de vakgroep en speciaal aan mijn collega's van ons klein maar gezellig labootje bouwfysica en installaties: "Dank voor alle joviale opspattingen van collegialiteit. De groepsfoto krijgt een ereplaatsje op mijn nieuw bureau." Aan mijn "nieuwe" collega's op de KaHo: "Ik kijk er al naar uit om voltijds lid te zijn van de bouwkundefamilie."

Aan mijn vriendjes en vriendinnetjes: "Dankjewel voor de zalige zangstonden, de spannende spelletjesavonden, het leuke lopen, de winterse wandeltochten, de enige etentjes, het keigezellig kletsen en de bonte bezoekjes tussen het werken door!"

Aan mijn ouders, broer, zus, neefje, nichtje, schoonzussen, bijna-schoonbroer, schoonpa en -vriendin, schoontante en –nonkel, schoonnicht en zwager, schoonachternichtje en – neefjes: "Ik hoop dat ik jullie een beetje kan meegeven wat ik de afgelopen 6 jaar heb gedaan in - het soms wel verre – Gent"

En tenslotte, aan mijn "trouw"ste supporter: "Jan, nu is het aan u!"

Contents

SUMMARY

The International Energy Agency forecasts an increase of primary energy demand of 60% by 2030. In addition, the building sector is responsible for 40% of the final energy demand in Europe. On the other hand, the fossil-fuel energy resources are running out causing a predicted increase in energy prices. In addition, the Kyoto protocol binds the governments to reduce the collective emissions of the greenhouse gases. Consequently, energy savings in the building sector can deliver a contribution to smooth the predicted increase in energy demand and to reduce the emissions of greenhouse gases. For this purpose, the European Parliament ratified the Directive on the Energy Performance of Buildings 2002/91/EC, which has been implemented by the member states from January 2006. In Flanders, this energy performance is defined by comparing the building's total annual primary energy consumption to the consumption in a reference building. This total energy consumption on its turn is calculated from the consumption of heating, cooling, lighting, energy for humidifiers, fans and other equipment.

The energy performance of an office building may amongst other things be improved by implementing natural night ventilation instead of air-conditioning. Natural night ventilation reduces the electricity consumption of cooling and fans in the air-conditioning and ventilation system while providing a good thermal comfort. Natural night ventilation is a convective passive cooling method, driven by natural driving forces. It uses outside air at night to cool down the exposed building structure in which the heat of the previous day is accumulated. The performances and potential energy savings of natural night ventilation can be predicted by building simulation. Nevertheless, the reliability of these simulation results with regard to the assumptions, made by the user in the input, is still unclear. This uncertainty can be very important in the decision process.

Therefore, this research aims to develop a methodology to predict the performances of natural night ventilation with building simulation taking into account the uncertainties in the input. Moreover, practical guidelines for design engineers to evaluate the design of natural night ventilation are derived from these general results.

To evaluate the performances of natural night ventilation, two suitable criteria of thermal comfort are selected: the weighted temperature excess method, based on Fanger's comfort theory, and the adaptive temperature limits indicator, based the adaptive theory of thermal comfort. Furthermore, the saved cooling demand, compared to the case without natural night ventilation, is predicted based on the adaptive temperature limits indicator. To predict these performances, the existing coupling between the multi-zone thermal simulation software TRNSYS and the infiltration and ventilation simulation software COMIS is chosen. Uncertainty and sensitivity analysis are used to take into account the uncertainties in the input of this building simulation tool. Uncertainty analysis defines the variation on the reached thermal comfort due to the variations in the input. Sensitivity analysis studies how this variation in thermal comfort is attributed to the variations in the input parameters. A Monte Carlo Analysis (MCA) with a Latin Hypercube sampling (LHS) design investigates the uncertainty on the output. To characterize the sensitivity of the output to the uncertainties in the input, the Standardized Regression coefficient (SRC), based on the global sensitivity MCA, is selected. The uncertainties on the input parameters of the simulation of natural night ventilation are estimated from data in literature and standards.

The result of the uncertainty analysis is the distribution of thermal comfort and the probability of good thermal comfort in a representative office. This distribution gives more reliable information on the predicted thermal comfort than the result of one single simulation. Sensitivity analysis results in the following list of input parameters which have the most important impact on the thermal comfort: the internal heat gains, the air tightness, the solar heat gain coefficient of the sunblinds, the solar radiation controlling the sunblinds, the internal convective heat transfer coefficient, the temperatures controlling the natural night ventilation at night, the wind pressure coefficient Cp and the discharge coefficient C_d of the night ventilation opening.

This list of influencing input parameters is a start to optimize the building and system design to increase the reliability of thermal comfort when natural night ventilation is applied. To ensure a high probability of good thermal comfort two conditions have to be fulfilled. Natural night ventilation has to be applied in a low energy office building with restricted fenestration and internal heat gains and sufficiently exposed thermal mass where an exposed ceiling is preferred to an exposed floor. In addition, natural night ventilation may be combined with additional cooling techniques like top cooling, increased ventilation flow by day or window opening by the users by day. Moreover, extremely warm weather data have to be taken into account to evaluate the design properly. The combination of a standard and extremely warm weather data set is preferred to evaluate the performances of a natural night ventilation design.

Practical guidelines to pre-design natural night ventilation are derived from the results of the simulations. The cooling load defines the amount of exposed thermal mass. Besides, the expected flow rates, indoor-outdoor temperature difference when night ventilation is in operation and opening duration are derived from these simulations as well. These assumptions can be used to (pre-)design the effective area of the night ventilation openings. These pre-design rules are applied to design the natural night ventilation system in the office building "Sint-Pietersnieuwstraat" (Belgium).

Furthermore, although both criteria of thermal comfort are assumed to correspond, large differences in the predicted thermal comfort by GTO and ATG are noticed. This difference can be significantly diminished by tolerating excess hours in the determination of the comfort levels in the adaptive temperature limits indicator.

The main disadvantage of the uncertainty and sensitivity analysis is the huge computational cost. These analyses require a large amount of simulations and thus prevents building engineers to use uncertainty and sensitivity in the evaluation of the performances of natural night ventilation. Therefore, two easy-to-use methods are developed. The probability of good thermal comfort and the standard deviation of this distribution are predicted from the result of one simulation. In addition, three simulations, in which only the most input parameters from the sensitivity analysis are varied, can predict the uncertainty interval of the thermal comfort.

This latter simplified method has been applied on the evaluation of the comfort in the PROBE and "Sint-Pietersnieuwstraat" office building (Belgium). It has been concluded that these three simulations could very well predict the distribution of the thermal comfort in the first case study because the list of important input parameters in this office building

corresponds rather well with the list mentioned above. Furthermore, although an acceptable average thermal comfort level can be noticed on all floors in the latter case study, thermal comfort has a large uncertainty interval.

Samenvatting

Het Internationaal Energieagentschap voorspelt enerzijds tegen 2030 een toename van het primair energieverbruik van 60%. Daarbij komt dat de gebouwsector in Europa verantwoordelijk is voor 40% van het energieverbruik. Anderzijds geraken de fossiele brandstoffen uitgeput, met een vermoedelijke stijging van de energieprijs tot gevolg. Bovendien verbindt het Kyotoprotocol de overheden ertoe de uitstoot van de broeikasgassen te verminderen. Bijgevolg kunnen energiebesparingen in de gebouwsector bijdragen tot zowel een afzwakking in de toename van het energieverbruik als een reductie van de uitstoot van broeikasgassen. Om deze doelstelling te verwezenlijken keurde het Europees Parlement de Richtlijn betreffende de Energieprestatie van Gebouwen 2002/91/EG goed. Deze richtlijn is sinds 1 januari 2006 van kracht in de lidstaten van de Europese Unie. In Vlaanderen wordt de energieprestatie van een gebouw gedefinieerd als de verhouding van het totale jaarlijkse primaire energieverbruik van het betrokken gebouw tot het energieverbruik in een referentiegebouw. Het totale jaarlijks energieverbruik omvat het verbruik van de verwarming, koeling, verlichting, bevochtiging, ventilatoren en andere apparatuur.

De energieprestatie van een kantoorgebouw kan o.a. verbeterd worden door te koelen met nachtelijke natuurlijke ventilatie i.p.v. met een centraal luchtbehandelingssysteem. Nachtelijke natuurlijke ventilatie reduceert het elektriciteitsverbruik dat nodig is voor de koeling en voor de ventilatoren in het luchtbehandelingssysteem. Deze convectieve passieve koeltechniek wordt gedreven door natuurlijke drijvende krachten zoals wind en thermische trek. Deze zorgen er voor dat 's nachts koele buitenlucht doorheen het gebouw stroomt en daarbij de thermische massa afkoelt waarin de warmte van de voorgaande dag is opgeslagen. De prestaties en de potentiële energiebesparingen van nachtelijke natuurlijke ventilatie kunnen met gebouwsimulatie voorspeld worden. Nietemin bestaat er nog onduidelijkheid over de betrouwbaarheid van deze simulatieresultaten o.w.v. de aannames die de gebruiker maakt in de invoer. De onzekerheid die dit met zich meebrengt, kan belangrijke gevolgen hebben voor het beslissingproces.

Daarom heeft dit onderzoek tot doel een methodologie te ontwikkelen die de prestaties van nachtelijke natuurlijke ventilatie met gebouwsimulatie evalueert, rekening houdend met de onzekerheden in de invoer. Daarnaast wil dit onderzoek praktische richtlijnen afleiden die ontwerpingenieurs in staat stellen het ontwerp van nachtelijke natuurlijke ventilatie te evalueren.

Twee criteria van thermisch comfort worden geselecteerd om de prestaties van nachtelijke natuurlijke ventilatie te evalueren. Dit zijn de gewogen temperatuuroverschrijdingsuren (GTO), gebaseerd op de comforttheorie van Fanger, en de adaptieve temperatuur grenswaarde indicator (ATG), gebaseerd op de adaptieve comforttheorie. Op basis van deze laatste methode wordt ook de uitgespaarde koelbehoefte berekend in vergelijking met het geval zonder nachtventilatie. Deze prestaties worden berekend met de bestaande koppeling tussen de multizonale thermische dynamisch simulatiesoftware TRNSYS en het infiltratie en ventilatie softwarepakket COMIS. Bovendien worden onzekerheids- en gevoeligheidsanalyse aangewend om rekening te houden met de onzekerheden in de invoer van deze gebouwsimulatiesoftware. Onzekerheidsanalyse bepaalt de variatie op het voorspelde thermisch comfort t.g.v. de variaties in de invoer. Gevoeligheidsanalyse

bestudeert vervolgens hoe de variatie op de uitvoer te wijten is aan de variaties in de invoerparameters. Hiervoor wordt een Monte Carlo analyse geïmplementeerd waarbij de bemonstering gebeurt met de methode van het Latijnse Vierkant. De gestandardiseerde regressiecoëfficiënten karakteriseren vervolgens de gevoeligheid van het thermisch comfort. De gebruikte onzekerheid op de invoerparameters is gebaseerd op gegevens uit de literatuur en diverse normen.

Het resultaat van deze onzekerheidsanalyse omvat de distributie van het thermisch comfort en de kans op goed comfort in een representatief kantoormodel. Deze verdeling geeft meer informatie over het voorspelde comfort dan het resultaat van één enkele simulatie. Het resultaat van de gevoeligheidsanalyse is een lijst van invoerparameters die de grootste impact hebben op het thermisch comfort bij nachtelijke natuurlijke ventilatie. Dit zijn de interne warmtewinsten, de luchtdichtheid, de zonnetoetredingscoëfficiënt van de zonwering, de invallende zonnestraling die de zonwering regelt, de interne convectieve overgangscoëfficiënt, de nachtelijke temperaturen uit het regelsysteem van de nachtelijke natuurlijke ventilatie, de winddrukcoefficiënt Cp en de ladingscoëfficiënt C_d van de ventilatie-opening.

Deze lijst van invloedrijkste invoerparameters leidt tot maatregelen om het gebouw en de systemen te optimaliseren en zo de betrouwbaarheid van het thermisch comfort te vergroten bij toepassing van nachtelijke natuurlijke ventilatie. Twee voorwaarden moeten vervuld zijn om een grote kans op goed comfort te waarborgen. Ten eerste moet nachtelijke natuurlijke ventilatie toegepast worden in een laag-energiegebouw met beperkte glasoppervlakte en interne warmtewinsten en voldoende bereikbare thermische massa. Hierbij geniet een thermisch massief plafond de voorkeur boven een thermische massieve vloer. Daarnaast moet nachtelijke natuurlijke ventilatie aangevuld worden met andere koeltechnieken zoals topkoeling, een verhoogd hygiënisch ventilatiedebiet of het openen van ramen door de gebruikers overdag. Bovendien is het ten zeerste aan te raden om de prestaties van nachtelijke natuurlijke ventilatie te evalueren bij zowel normale als extreem warme weercondities.

Uit de resultaten van de simulaties worden praktische richtlijnen afgeleid om nachtelijke natuurlijke ventilatie te ontwerpen. De koellast bepaalt de nodige hoeveelheid thermische massa. Daarnaast volgen uit deze simulaties de te verwachten debieten, het temperatuurverschil binnen-buiten wanneer nachtventilatie in werking is en de tijd dat de ramen geopend zijn. Deze aannames laten de gebruiker toe om de effectieve oppervlakte van de openingen voor nachtelijke natuurlijke ventilatie te bepalen. Deze regels worden toegepast om het nachtelijk natuurlijk ventilatiesysteem in het kantoorgebouw "Sint-Pietersnieuwstraat" van de Universiteit Gent (België) te ontwerpen.

Alhoewel de evaluaties van beide comfortcriteria zouden moeten overeenstemmen, zijn er grote verschillen te noteren tussen het door ATG en GTO voorspelde thermisch comfort. Dit verschil verkleint significant wanneer er overschrijdingen worden toegestaan bij de bepaling van de klasses in de ATG-methode.

Het grootste nadeel van onzekerheids- en gevoeligheidsanalyse is de lange rekentijd. Deze analyses vereisen immers erg veel simulaties. Dit vormt een hinderpaal om onzekerheids- en sensitiviteitsanalyse in de praktijk te gebruiken bij de evaluatie van de prestaties van

nachtelijke natuurlijke ventilatie. Daarom worden in dit onderzoek twee methodes ontwikkeld die de onzerheid op een eenvoudige manier kunnen inschatten. De ene methode voorspelt de kans op goed comfort en de standaarddeviatie van deze distributie op basis van één simulatie. In de andere wordt het onzekerheidsinterval van het thermisch comfort geschat aan de hand van drie simulaties waarbij enkel de belangrijkste parameters volgend uit de gevoeligheidsanalyse gevarieerd worden.

Deze methodologie wordt toegepast bij de evaluatie van de prestaties van nachtelijke natuurlijke ventilatie in het kantoorgebouw van PROBE en "Sint-Pietersnieuwstraat" (België). Deze eerste gevalstudie toont aan dat deze drie simulaties de distributie van het thermisch comfort goed kunnen voorspellen. De lijst van belangrijkste invoerparameters in dit kantoorgebouw komt immers goed overeen met de lijst die algemeen wordt afgeleid. Alhoewel in de laatste gevalstudie simulaties gemiddeld een aanvaardbaar thermisch comfort voorspellen, stelt de vereenvoudigde methode een groot onzekerheidsinterval vast.

Nomenclature

Abbreviations

ATG	Adaptive temperature limits indicator
CFD	Computational fluid dynamics
CHTC	Convective heat transfer coefficient
COP	Coefficient of performance
FAST	Fourier amplitude sensitivity test
GTO	Weighted temperature excess
IDA	Indoor air quality
IFFD	Iterated fractional factorial design
IHG	Convective internal heat gains
LHS	Latin hypercube sampling
MCA	Monte Carlo analysis
OAT	One-at-a-time
p.p.	Per person
PMV	Predicted mean vote
PPD	Predicted percentage of dissatisfied people
RH	Relative humidity
SRC	Standardized regression coefficient
SRRC	Standardized rank regression coefficient
TO	Temperature excess
TRY	Test reference year
WF	Weight factor

Symbols

a	Absorption coefficient (-), thermal diffusivity (m^2/s), wind profile exponent (-),
b	Thermal effusivity ($J/m^2.K.s^{0.5}$), regression coefficient
c	Specific heat capacity (J/kg.K)
c_{sys}	Specific fan power (Wh/m^3)
d	Depth (m), thickness (m)
f	Conversion coefficient (-)
f_{fan}	Time fraction of the fan (-)
g	Gravitational acceleration (m/s^2), solar heat gain coefficient (-)
h	Height (m)
m	Mean air mass flow rate (kg/s)
n	Flow exponent (-), airflow rate (h^{-1})
n_{50}	Leakage flow rate at 50 Pa (h^{-1})
p	Air pressure (Pa), probability (-)
q	Heat flux (W/m^2)
t	Time (s)
u	Moisture content (kg/kg)
v	Velocity (m/s)
$\dot{v}_{50}$	Leakage flow rate at 50 Pa per area of external walls ($m^3/h.m^2$)
var	Variance
x	Input parameter

y	Output parameter
w	Width (m)
z	Vertical dimension (m)
z_0	Neutral plane (m), roughness height (m)
A	Area (m^2)
C	Effective heat capacity (J/K), Flow coefficient ($kg/s.Pa^n$), sensible heat loss (W), Convective heat exchange (W)
C_d	Discharge coefficient (-)
C_p	Wind pressure coefficient (-)
D_h	Hydraulic diameter (m)
E	Short-wave radiation (W), latent heat loss (W/m^2)
ET*	Effective temperature (°C)
F	Conversion factor (-)
G	Mass flow rate (kg/s)
H	Internal heat production (W/m^2)
I_s	Irradiance (W/m^2)
I_{cl}	Clothing insulation (Clo)
L	Length (m)
LTA	Light transmission coefficient (-)
M	Metabolism (W/m^2), mass (kg/m^2)
N	Total number of samples
P	Perimeter (m)
Q	Heat (J)
R	Radiative heat exchange (W), thermal resistance (K/W)
R_y^2	Model coefficient of determination (-)
S	Absorbed radiative gains (W/m^2)
T	Temperature (K)
$\bar{T}$	Average temperature (K)
U	Thermal transmittance (W/m^2K)
V	Volume (m^3)
$\dot{V}$	Volume flow rate (m^3/h)
W	Effective mechanical power (W/m^2), electrical consumption (kWh)
WG	Wall gain (W)
X	Input vector
Y	Output vector
α	Heat transfer coefficient (W/m^2K)
φ	Relative humidity (%)
λ	Thermal conductivity (W/mK)
μ	Average
θ	Temperature (°C)
ρ	Density (kg/m^3)
σ	Standard deviation
ξ	Flow resistance coefficient (-)
Δ	Difference
Φ	Heat flow (W)
Ψ	Moisture content (m^3/m^3)

Subscripts

a	air
b	bottom
bound	boundary
c	convective
cplg	coupling
comf	comfort
dif	diffusion
diff	diffuser
e	exterior
eff	effective
equ	equivalent
f	fluid
g	gain
i	interior
inf	infiltration
m	meteorological station, moisture
max	maximum
mean	mean
min	minimum
mrt	mean radiant
o	operative
out	outdoor
r	relative, radiant
ref	reference
res	respiration
s	surface, short-wave, skin, stack
sw	sweat
t	top
T	temperature
tot	total
v	ventilation, vapour
w	wind
0	on site

1   INTRODUCTION

The report of the International Energy Agency "World Energy Outlook 2004 and 2005" (IEA, 2004, 2005) forecasts an increase of primary energy demand of 60% by 2030, with an annual growth rate of 1.7%. Two-thirds of this increase will come from developing countries, mainly caused by the booming economies in India and China. In an alternate scenario, the global primary energy demand would be about 10% lower in 2030 than in this reference scenario (IEA, 2004, 2005). This alternate policy scenario takes into account that countries around the world will implement a set of policies and measures that are currently in consideration or might reasonably be expected to adopted. These policies include fast deployment of more energy efficient and cleaner technologies. Besides, the cooling energy demand has increased worldwide and in particular in Europe. The demand for room and packaged air conditioners has grown between 2000 and 2003 with respectively 30 % and 50% (JRAIA, 2005). Furthermore, the building sector, including the residential and the tertiary sector, is noticed to be the main consumer of energy in Europe. In 2000, buildings were responsible for 40% of the final energy demand while transport and industry consumed respectively 32% and 28% (EC, 2003). This energy consumption includes mainly heating, but takes also the consumption of cooling, lighting, production of sanitary warm water and equipment into account. In a typical air-conditioned office building in the United Kingdom e.g., heating is responsible for 48% of the total end energy consumption. The other half is caused by electricity consumption of cooling and fans in the air conditioning and ventilation system (29%) and lighting and office equipment (23%) (Thomas, 1996).

On the other hand, the fossil-fuel energy resources are running out. While the "World Energy Outlook 2004" report supposes that these resources are more than adequate to meet the demand until 2030 and well beyond, the cost to extract these resources and deliver them to the consumers is less certain (IEA, 2004). An increase in energy prices is estimated (IEA, 2005). Moreover, the Kyoto protocol binds the developed countries to reduce the collective emissions of six key greenhouse gases - among which CO_2 - at least by 5 % by 2008-2012. This protocol encourages the governments amongst others to improve energy efficiency and to promote renewable energy (EU, 2005).

Energy savings in the building sector can deliver a contribution to smooth the predicted increase in energy demand and to reduce the emissions of greenhouse gases. The reduction of the energy intensity, i.e. the amount of energy per unit activity or product, is in particular focussed (D'haeseleer, 2005). The "Green paper on energy efficiency" of the European Commission (2005) sets out an energy policy to the EU to save 20% of its current energy use in a cost-effective manner. This policy includes, amongst others, the implementation of the Directive on the Energy Performance of Buildings 2002/91/EC (EPBD) (EU, 2002) from January 2006. The objective of this directive is to promote the improvement of the energy performance of buildings, taking into account outdoor climatic and local conditions, indoor climate requirements and cost-effectiveness. As the EPBD is a directive, it only imposes a general framework. The detailed implementation to calculate the energy performance of buildings and the targets for the minimum energy performance have to be specified by the member states. In Flanders, minimum requirements are enforced with regard to energy performance, thermal insulation and indoor climate. The energy performance is defined by comparing the building's total annual primary energy

consumption to the consumption in a reference building. This total energy consumption is calculated from the consumption of heating, cooling, lighting, energy for humidifiers, fans and other equipment.

The energy performance of an office building may amongst other things be improved by implementing natural night ventilation instead of air-conditioning. Natural night ventilation reduces the electricity consumption of cooling and fans in the air-conditioning and ventilation system while providing a good thermal comfort. This cooling technique is driven by wind and thermally (stack) generated pressures and cools down the exposed building structure at night. Consequently, heat may accumulate the next day and temperature peaks will be reduced and postponed consequently. The benefits of natural night ventilation are not yet applied in the energy performance of building regulations. It has to be assessed as an innovative system in this framework (Wouters et al., 2004). The performances and potential energy savings of natural night ventilation can be predicted by building simulation. Nevertheless, the reliability of these simulation results with regard to the assumptions, made by the user in the input, is still unclear. This uncertainty can be very important in the decision process. Therefore, it seems essential that the various decision makers are informed about the potential uncertainties (Wouters, 2000). In addition, to make effective use of simulation, designers require information on performance robustness rather than performance quantification with no account taken of uncertainty (Macdonald and Strachan, 2001). Wouters (2000) also recommends uncertainty analysis in decision making because a probability distribution curve gives substantially more information than the outcome of a single simulation.

The objective of this research is to develop a methodology to predict the performances of natural night ventilation with building simulation taking into account the uncertainties in the input. Moreover, practical guidelines for design engineers to evaluate the design of natural night ventilation will be derived from these general results.

To evaluate the performances of natural night ventilation, suitable criteria of thermal comfort are selected. An appropriate building simulation tool is chosen to predict these evaluation criteria. Uncertainty and sensitivity analysis are used to take the uncertainties in the input of this tool into account. Uncertainty analysis defines the variation on the reached thermal comfort due to the variations in the input. Sensitivity analysis studies how this variation in thermal comfort is attributed to the variations in the input parameters. These latter variations are estimated from data in literature and standards.

The reflection on this research starts in **chapter 2** with a description of the state-of-the-art of natural night ventilation. **Chapter 3** presents the monitored performances of this passive cooling technique in two case studies. **Chapter 4** elaborates on the building simulation tool to predict the performances, the uncertainty on each input parameter and the uncertainty and sensitivity analysis to take these uncertainties into account. **Chapter 5** consequently discusses the results of the uncertainty and sensitivity analysis of the performances of natural night ventilation: the surplus and the practical use of these analyses is studied. In addition, practical guidelines to evaluate the design of natural night ventilation are derived. In **chapter 6**, the developed methodology is tested in a case study. Practical guidelines to design the natural night ventilation system and to evaluate this design are illustrated in **chapter 7**. Finally, **chapter 8** formulates the conclusions of this research.

2 Natural Night Ventilation

This chapter discusses the passive cooling technique of natural night ventilation. The first section presents its general principles. A definition and the physical background of natural night ventilation are given. The performances of natural night ventilation are defined by the level of thermal comfort. Fanger's theory and the adaptive thermal comfort theory are discussed and evaluation criteria are selected. The second section discusses the state of the art of natural night ventilation. An overview of international projects and research concerning natural night ventilation is given. The aims and the results are discussed, paying special attention to dimensioning and early design tools.

2.1 General principles

2.1.1 Definition

Natural night ventilation uses the outside air at night as a heat sink to cool down a building as follows. Cold outside air enters the building at night and cools down the exposed building structure, in which the heat of the previous day is accumulated. The heated air subsequently leaves the building. This airflow is driven by natural ventilation forces as temperature difference and wind. Consequently, the indoor temperature peaks during daytime are reduced and postponed. Fig. 2.1 shows this effect by means of a calculation example. The calculated indoor operative temperatures on the second floor of the "SD Worx" building in Belgium with and without natural night ventilation are compared. A significant temperature reduction can be noticed when natural night ventilation is applied.
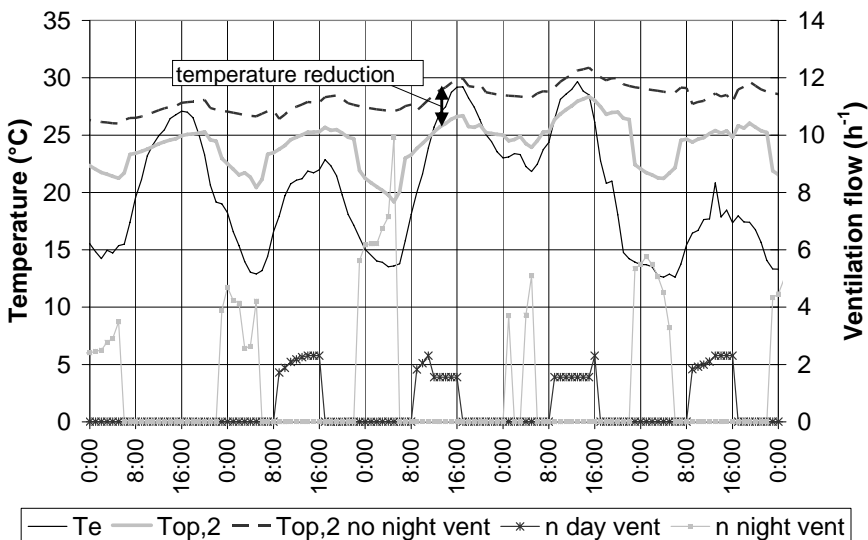
Fig. 2.1 Comparison of simulated indoor operative temperature with and without natural night ventilation on the second floor of "SD Worx" building (Kortrijk, Belgium)

Different strategies of natural night ventilation design can be distinguished: single-sided, cross and (passive) stack ventilation (Fig. 2.2). Single-sided ventilation relies on ventilation openings on only one side of the building. The main driving force is wind turbulence and stack effect. Cross ventilation occurs when ventilation openings are provided on both sides

of a room and is wind driven. In passive stack ventilation, the extraction is enforced by the stack effect. The effectiveness can be enhanced by providing the outlet chimney(s) in a wind-induced negative pressure zone.
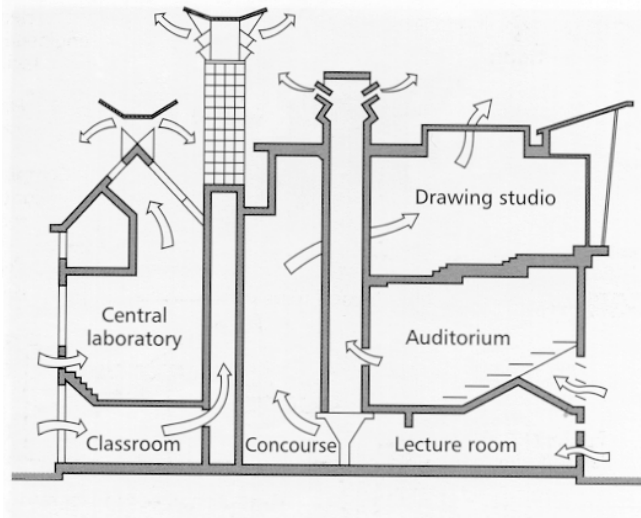
Fig. 2.2 Stack ventilation in the De Monfort University (United Kingdom) (CIBSE, 1997)

2.1.2 Physical background

The performance of buildings with natural night ventilation may be predicted using building simulation tools. These tools calculate the airflow rates, temperatures and cooling load based on mass and heat conservation laws.

2.1.2.1 Mass balance

Natural night ventilation flow rates are driven by wind and thermally (stack) generated pressures. Wind blowing on a rectangular shape induces a positive pressure on the windward side and negative pressures on the opposing side and in the weak region of the side faces i.e. the leeward sides. This pressure difference causes air entering the openings and passing through the building from high to low pressure areas. In addition, thermal buoyancy (stack effect) creates a pressure difference as the result of differences in air density (or air temperature) between the inside and the outside of the building. When the inside air temperature exceeds the outside, the air enters through openings in the lower part of the building and leaves through openings on a higher level. The flow direction is reversed when the outside air temperature exceeds the inside (Liddament, 1996). Both driving forces are illustrated in Fig. 2.3.
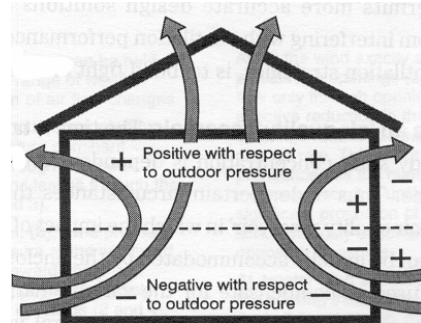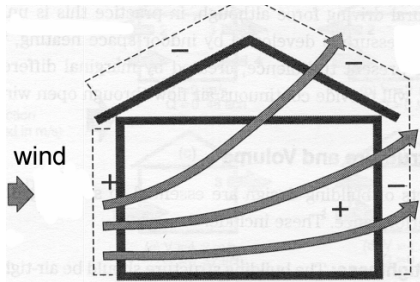
Fig. 2.3 Natural driving forces: wind (left) and thermal stack (right) (Liddament, 1996)

The total pressure difference across an opening at height z is written as the sum of the wind and stack pressure minus the unknown pressure difference at reference height (Eq. 2.1) (ASHRAE, 2005):

$$p_e(z) - p_i(z) = \frac{1}{2}\rho_e C\rho v^2 - (\rho_e - \rho_i)g(z - z_{ref}) - (p_{e,ref} - p_{i,ref}) \qquad \text{Eq. 2.1}$$

where $p_e(z)$ and $p_i(z)$ are the external and internal air pressure at height z respectively, ρ_e and ρ_i the external and internal air density respectively, Cp the wind pressure coefficient, v the wind velocity, z_{ref} the reference height, g the gravity acceleration and $p_{e,ref}$ and $p_{i,ref}$ respectively the external and internal air pressure at reference height.

At low wind velocity, the pressure difference in Eq. 2.1 is dominated by the stack effect $-(\rho_e - \rho_i)g(z - z_{ref})$. At high wind velocity, the wind component $\frac{1}{2}\rho_e C\rho v^2$ dominates the total pressure difference. At normal wind speeds, the effects of wind and thermal buoyancy can complement or oppose each other (Breesch and Janssens, 2001). A good natural ventilation system is designed in such a way to ensure both effects complement each other most of the time.

The flow rate through a flow path is related to this total pressure difference by a non linear equation, e.g. the power law equation in Eq. 2.2:

$$G = C(\Delta p)^n \qquad \text{Eq. 2.2}$$

where C is the flow coefficient (kg/s.Pa^n) and n the dimensionless flow exponent and Δp the pressure difference.

The steady-state mass conservation laws constitute a set of non-linear equations. Solving these equations determines the pressure and the airflow through the flow path.

The energy balance of a room and an internal surface are respectively given by Eq. 2.3 and Eq. 2.4:

$$C\frac{dT_{ai}}{dt} = \Phi_I + \sum_{j=1}^{n}\alpha_{cj}A_j\left(T_{sj} - T_{ai}\right) + \rho c \dot{V}\left(T_{ae} - T_{ai}\right)$$ Eq. 2.3

$$-\lambda \text{grad}T\big|_s = \alpha_{cj}\left(T_{sj} - T_{ai}\right) - a_{sj}E_j + \Phi_{rj}$$ Eq. 2.4

where C is the effective heat capacity of the room, T_{ai} and T_{ae} respectively the internal and external air temperature, Φ_I the convective internal heat gains, α_{cj} the internal heat transfer coefficient, A_i the area of the internal surface, T_{sj} temperature of the internal surface j, ρ and c the density and the specific heat capacity of the air respectively, $\dot{V}$ the volume flow rate, λ the thermal conductivity of the surface material, a_{sj} and E_j respectively absorption coefficient and the flux of the short-wave radiation on surface j and Φ_{rj} is the net long-wave radiation exchange between surface j and the other internal surfaces.

Solving these energy balances results, on the one hand, in the internal air temperature and the surface temperature of every internal surface. On the other hand, the heating and cooling load need to be calculated from these equations by defining an indoor set point temperature. The cooling load is the amount of heat that must be removed from a building to maintain comfortable indoor temperature and humidity conditions.

In standards and guidelines, e.g. the German standard VDI 2078 (1996), the maximum cooling load during a typical hot period is predicted to size the active cooling equipment. However, as passive cooling has no active control on the indoor temperature, the performances are evaluated based on the predicted indoor temperature without cooling (see below).

2.1.2.3 HEAT TRANSFER AND STORAGE

The cooling mechanism of natural night ventilation is based on the convective heat transfer from the exposed building structure to the cold air flow at night, i.e. when the indoor-outdoor air temperature difference is maximal. By day, these walls are (re)heated by solar and infrared radiation and room air convection. To make natural night ventilation work, heat storage in the internal structure is necessary. The phase difference between heat transfer to and from the building structure has to be bridged.

When the wall is subject to periodic variations of the boundary conditions, the ease of the heat accumulation of a wall is characterized by the admittance. This is the ratio of the complex heat transfer to the complex temperature at the internal surface. The admittance informs how well the variation in temperature at the surface is translated in a heat transfer and storage at this surface. A large value of the admittance corresponds to a large value of the thermal effusivity b (Eq. 2.5). This coefficient depends on the thermophysical properties of the wall materials. A material (e.g. concrete) with high values of the density ρ, thermal capacity c and thermal conductivity λ has a high heat storage capacity (Balaras, 1996). The thermal effusivity also indicates the ease of the heat accumulation of a wall

when an a-periodic temperature variation occurs (Hens, 1997). This layer has to be at or near the surface of a multi-layer wall to result in a high capacitive wall.

$$b = \sqrt{\rho c \lambda}$$

In addition, the depth the diurnal heat wave penetrates the material, is defined as follows (Eq. 2.6):

$$\delta = \sqrt{\frac{\lambda T}{\pi \rho c}} = \sqrt{\frac{aT}{\pi}}$$

where T is the period of the temperature variation. The effective periodic penetration depth corresponds to the depth where the amplitude of the temperature variation in a half-infinite material equals the original amplitude of the temperature variation at the surface divided by 2.72. This depth depends on the period of the temperature variation and the thermal diffusivity a. A material with a high value of the thermal diffusivity is more effective for cyclic heat storage at greater depth than a material with a low value. A 5-10 cm wall thickness is usable for diurnal heat storage and release (Balaras, 1996). This is confirmed by measurements in concrete with high density (Kolokotroni, 1995).

2.1.3 COMFORT ASSESSMENT

To evaluate the performances of natural night ventilation, i.e. the achieved indoor climate, the maximum indoor air temperature without cooling may be calculated (see above). But how people react on the thermal indoor environment depends on more conditions than air temperature alone. All these parameters are included in the concept 'thermal comfort'. Therefore, the performances of natural night ventilation are evaluated by thermal comfort.

2.1.3.1 THERMAL COMFORT

Thermal comfort is defined as "the condition of mind which expresses satisfaction with the thermal environment" (ISO, 1996). Thermal comfort depends on the human thermoregulation. Man has a very effective temperature regulatory system ensuring the body's core temperature constant at approximately 37°C. When the body becomes too warm, two processes are initiated to cool it down. The blood vessels expand increasing the blood flow in the skin and subsequently one begins to sweat. Reversely, when the body is getting too cold, the blood vessels shrink reducing the blood flow. The internal heat production is also increased by stimulation the muscles, which causes shivering (ASHRAE, 2005).

2.1.3.2 FANGER'S COMFORT THEORY (FANGER, 1972)

Fanger gives 3 basic requirements for thermal comfort. The first one is the heat balance of the human body (Eq. 2.7):

$$H - C_{res} - E_{res} - E_{dif} - E_{sw} = R + C$$

where H is the internal heat production of the body, C_{res} the sensible and E_{res} the latent heat loss by respiration, E_{dif} the latent heat loss by vapour diffusion through the skin, E_{sw} the

latent heat loss from evaporation of sweat and R and C the radiative and convective heat exchange from the clothed body. Based on experiments, Fanger reformulated Eq. 2.7 as follows:

$$f(H, I_{cl}, \theta_a, \theta_{mrt}, p_a, v_{ar}, \theta_s, E_{sw}) = 0 \qquad \text{Eq. 2.8}$$

where I_{cl} is the clothing insulation, θ_a the air temperature, θ_{mrt} the mean radiant temperature, i.e. the uniform temperature of an imaginary black enclosure which would result in the same heat loss by radiation from the person as the actual enclosure, p_a the partial vapour pressure in the air, v_{ar} the relative air velocity and θ_s the average skin temperature. In addition, Fanger formulated empirical relationships for the physiological parameters, i.e. the skin temperature and the sweat evaporation, depending on the internal heat production. These relationships are the second and third requirement for thermal comfort. Finally, these three requirements for thermal comfort are summarized in one equation with six variables (Eq. 2.9).

$$f(H, I_{cl}, \theta_a, \theta_{mrt}, p_a, v_{ar}) = 0 \qquad \text{Eq. 2.9}$$

Eq. 2.9 makes it possible to find a situation of neutral comfort for an average person in every condition of activity level and clothing resistance and every combination of air and radiant temperature, humidity and relative air velocity.

The sensation of the comfort is quantified in a scale (Fig. 2.4), ranging from −3 (cold) to +3 (hot), where 0 represents the neutral thermal sensation. To take into account the differences in individual perception of thermal comfort, Fanger measured the comfort sensation of different test persons. The prediction of the average sensation of a given environment or PMV (predicted mean vote) (Eq. 2.10) and the deviation of this average value or PPD (predicted percentage of dissatisfied) (Fig. 2.4) are derived from these tests.

$$PMV = f(M, W, \theta_a, \theta_{mrt}, p_a, \theta_{cl}, f_{cl}, h_c) \qquad \text{Eq. 2.10}$$

where M is the metabolism, W the effective mechanical power, θ_{cl} the surface temperature of the clothing, f_{cl} the clothing area factor i.e. the ratio of the surface area of the clothed body to the surface area of the naked body and h_c the convective heat transfer for convection.

PPD reports the percentage of people that probably feels uncomfortable (see Fig. 2.4), i.e. the percentage evaluating the environment with a given PMV cool (-2 on the comfort scale), cold (-3), warm (+2) or hot (+3). As a result, 5% of the people feels uncomfortable even when the average thermal sensation is neutral (PMV = 0).
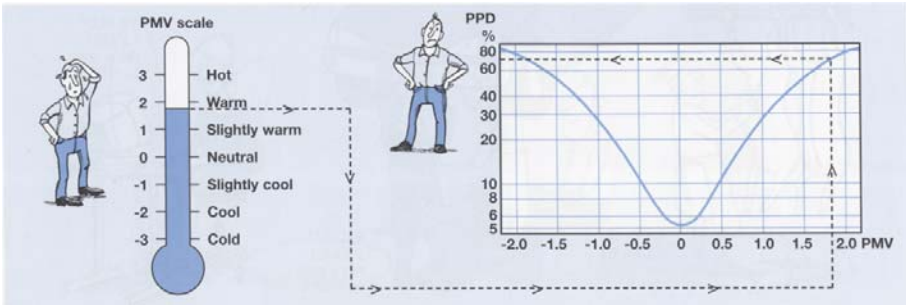
Fig. 2.4 PPD as a function of PMV (Innova, 2002)

2.1.3.3 ADAPTIVE COMFORT THEORY

The comfort theory of Fanger was developed, based on experiments with individuals in a test room under constant conditions like in fully closed buildings with air conditioning. Since 1970, international research showed discrepancy between the PMV scale and the thermal sensation of users of free-running buildings, i.e. buildings which are not heated or cooled. Humphreys (1976) proves that the neutral or comfort temperature in free-running buildings is higher and depends stronger on the monthly average outdoor temperature than in buildings with a centrally controlled HVAC (see Fig. 2.5).
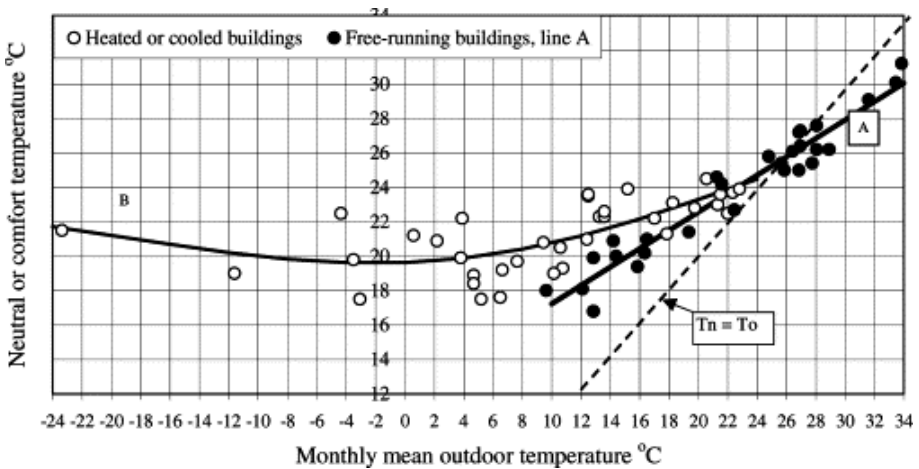
Fig. 2.5 The change in comfort temperature with monthly mean outdoor temperature
(Humphreys, 1976)

De Dear et al. (1997) summarized the experimental results of 160 buildings worldwide. In buildings with operable windows and opportunities for individual influence of the indoor environment, the comfort indoor temperature, i.e. the preferred indoor temperature by users, is noticed to depend more on the mean outdoor temperature recorded for a longer period than can be explained by the PMV model (Fig. 2.6) (de Dear and Brager, 2002). They concluded that the reason for this discrepancy is the result of adaptations of the users to the indoor environment (de Dear et al., 1997). Nicol and Humphreys (2002) defined the adaptive principle as "if a change occurs such as to produce discomfort, people react in ways which tend to restore their comfort". This is caused by behavioural and psychological

thermal adaptation (Brager and de Dear, 2000). Behavioural adaptation refers to any (un)conscious action a person might make to alter the body's thermal balance, including changing clothes, opening windows, etc. The model of Fanger partly takes these phenomena in account. Psychological adaptation means that the perception of thermal conditions depends on experiences and expectations. Therefore, de Dear and Brager (2002) use an average outdoor temperature over a long period (week or month).
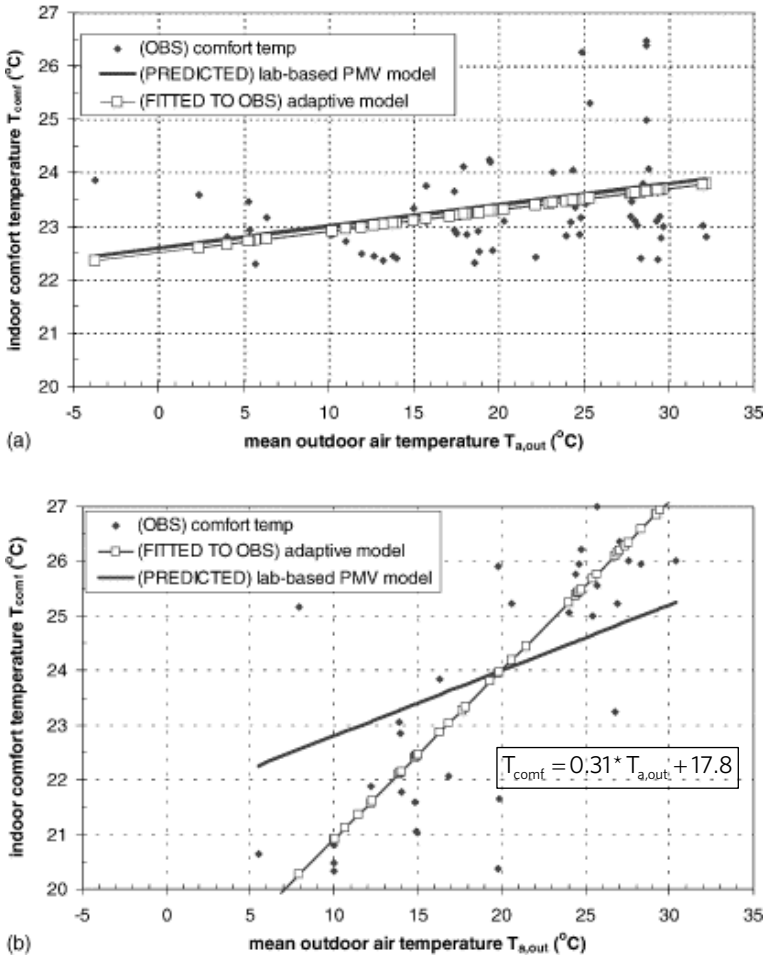
Fig. 2.6 Observed and predicted indoor temperatures in centrally air conditioned (above) and free-running buildings (below) (de Dear and Brager, 2002)

Brager and de Dear (2000) developed two separate models to evaluate the thermal comfort in either air conditioned buildings, i.e. sealed, centrally air conditioned buildings with open plan floor layouts that provide minimal adaptive opportunity where the occupants are presumed to have no option to open/close the windows, or naturally ventilated buildings, i.e. buildings with operable windows and ceiling fans within small single- or dual occupant offices that afford high degrees of adaptive opportunity. Two comfort zones, corresponding to 90 and 80% thermal acceptability, are defined depending

on the outdoor effective temperature ET* (Brager and de Dear, 2000) and on the dry bulb outdoor temperature $T_{a,out}$ (de Dear and Brager, 2002). The outdoor effective temperature ET* is theoretically more adequate because it takes in account both air and radiant temperature and humidity (ASHRAE, 2005) but requires both specialized experience and software most practicing HVAC engineers are unlikely to possess. Furthermore, the range of thermal acceptability of the comfort zones is defined as follows (de Dear and Brager, 2002). Only a small subset of the buildings in the database included direct assessment of thermal acceptability, which was in addition not statistically significant. Therefore, the acceptability was calculated from thermal sensation votes, starting from the relationship between PMV and PPD. This relationship indicates that a large group of subjects expressing a mean thermal sensation vote of ± 0.5 (± 0.85) could expect to have 10% (or 20%) of dissatisfied people. Moreover, a regression model of the thermal sensation as a function of the indoor operative temperature was created for each building. Applying the ± 0.5 and ± 0.85 criteria on these regression models produced a 90 and 80% acceptable comfort zone for each building. Averaging those comfort zone widths across all the naturally ventilated buildings produced a mean comfort zone band of 4.9°C for 90% acceptability and 6.9°C for 80% acceptability, both centred around the optimum comfort temperature (see Fig. 2.8). The comfort zones in centrally air-conditioned buildings are smaller: 2.4°C and 4.1°C for 90% and 80% acceptability respectively (see Fig. 2.7).
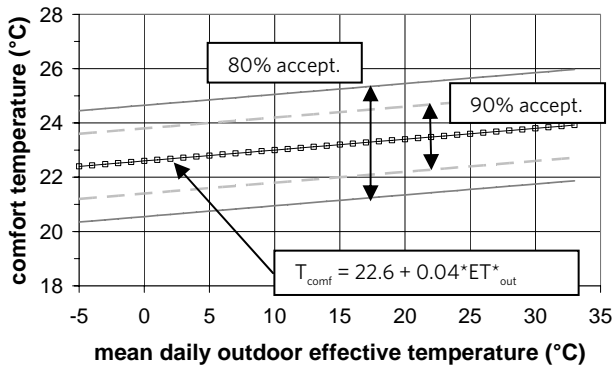
Fig. 2.7 Comfort zones of 90 and 80% thermal acceptability in buildings with centralized HVAC (de Dear et al., 1997)
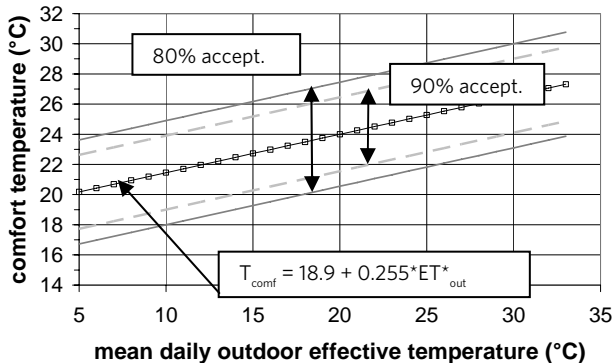
Fig. 2.8 Comfort zones of 90 and 80% thermal acceptability in buildings with natural ventilation (de Dear et al., 1997)

2.1.3.4 STANDARDS AND GUIDELINES

Different criteria exist to evaluate the level of thermal comfort, as discussed in the previous paragraphs. The aim of this paragraph is to investigate which method is a suitable performance indicator for evaluation of natural night ventilation.

Firstly, the ASHRAE and European standards defining the thermal comfort conditions are discussed. These standards are based on Fanger's comfort theory. The adjustments made for adaptive comfort are studied as well. Secondly, guidelines for long-term evaluation are presented: (weighted) temperature excess (based on Fanger's comfort theory) and the adaptive temperature limits guideline (based on the adaptive comfort theory).

2.1.3.4.1 Standards defining thermal comfort conditions

2.1.3.4.1.1 ASHRAE Standard 55-1992 (ASHRAE, 1992) and ASHRAE 55-2004 (ASHRAE, 2004)

The ASHRAE Standard 55-1992 (ASHRAE, 1992) is based on Fanger's comfort theory and defines the conditions of operative temperature and humidity where 80% of sedentary or slightly active persons find the environment thermally acceptable (Fig. 2.9). The clothing resistance in summer is typically 0.5 Clo. The comfort zone is based on measurements under constant conditions and corresponds to thermal sensation ranging from -0.5 to 0.5 on the comfort scale of Fanger. On normal relative humidity values (50 – 60%), the operative temperature for good thermal comfort ranges from 23 to 26°C in summer. For lower relative humidity values, the upper limit increases, e.g. 27°C corresponds to 30% relative humidity.
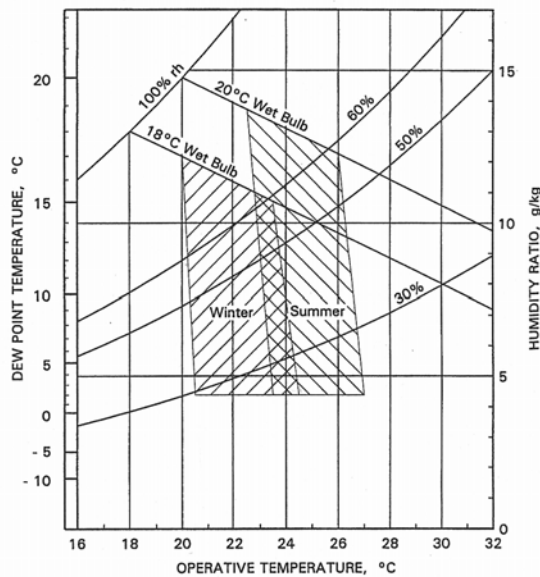
Fig. 2.9 ASHRAE summer and winter comfort zones (ASHRAE, 1992)

In the ASHRAE Standard 55-2004 (ASHRAE, 2004), the adaptive model for the naturally ventilated buildings of de Dear and Brager (2002) is added to the ASHRAE Standard 55-1992. Fig. 2.10 shows the adjustments, valid for mean outdoor temperatures between 10 and 33°C. The original requirements of the comfort zone of the ASHRAE Standard 55-1992 (based on Fanger's comfort theory) are maintained for other buildings.
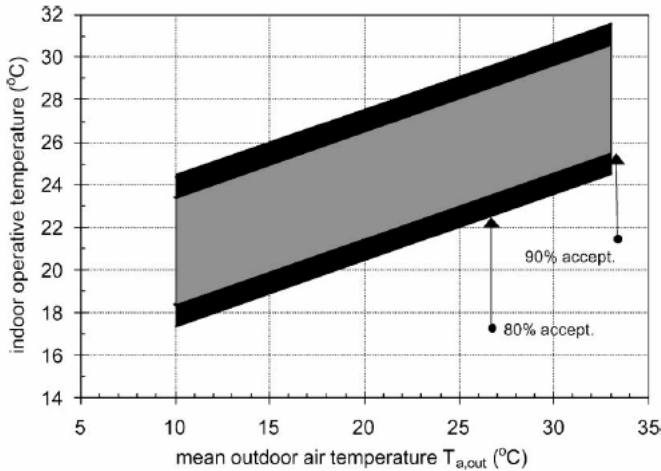
Fig. 2.10 Comfort zones of 90 and 80% thermal acceptability in naturally ventilated buildings in ASHRAE 55-2004 (de Dear and Brager, 2002)

2.1.3.4.1.2 EN ISO 7730-1996 (ISO, 1996), (Olesen and Parsons, 2002)

The European standard EN ISO 7730-1996 is based on the ASHRAE 55-1992 standard (ASHRAE, 1992) for thermal comfort and the European standard CR 1752 (CEN, 1998a) for the indoor environment for ventilation systems. Three categories of thermal comfort can be distinguished. The corresponding ranges of comfortable operative indoor temperature in summer in office buildings are presented in Table 2.1. Level B is sensated by the users as 'average to good' and corresponds to the limits of the comfort zone in the ASHRAE 55-1992 standard.

Table 2.2.1 Example criteria for operative temperature and mean air velocity for offices in the cooling season (relative humidity is assumed 60% for summer) (Olesen and Parsons, 2002)

Clothing (Clo)	Activity (met)	Category	PPD (%)	PMV	Operative temperature (°C)	Mean air velocity (m/s)
0.5	1.2	A	<6	± 0.2	24.5 ± 0.5	0.18
		B	<10	± 0.5	24.5 ± 1.5	0.22
		C	<15	± 0.7	24.5 ± 2.5	0.25

Adjustments to EN ISO 7730-1996 for naturally ventilated buildings as a consequence of adaptation are proposed (Olesen and Parsons, 2002). It will be recommended to use a wider PMV-range (class C in Table 2.1) for design and evaluation of the thermal environment in such buildings. This means the operative temperature in offices during summertime may range from 22 to 27 °C, independently from the average outdoor temperature.

2.1.3.4.2 Guidelines for long-term evaluation

2.1.3.4.2.1 Temperature excess (GBA, 1999)

The Dutch Government Buildings Agency (GBA) requires that during 90% of the working hours, minimum 90% of the occupants are satisfied with the thermal environment in office buildings. This means that the PMV has to be in between -0.5 and 0.5, i.e. a PPD of 10%, during 90% of the working time. Each of these comfort limits may only be excessed during 5% of the working hours. This requirement corresponds to a critical indoor operative temperature of 25.5°C assuming seated office work (metabolism of 65 W/m^2) and light working clothes (0.7 Clo) (ISSO, 1990). The temperature excess method requires the number of hours exceeding 25.5°C to be limited to 100 during occupancy, i.e. 5% of the working hours. Additionally, a maximum of 20 excess hours above 28°C is required. The reference weather data is the Dutch weather data of 1964.

Applying this method, differences in thermal comfort were noticed between light and heavy buildings (van der Linden et al., 2002). The thermal sensation in the light buildings was worse than in heavy buildings with the same temperature excess hours because the indoor temperature during these excess hours was on average higher in light than in heavy buildings. Therefore, the GBA developed a method taking the extent of excess into account, i.e. the weighted temperature excess hours.

2.1.3.4.2.2 Weighted temperature excess (van der Linden et al., 2002)

The weighted temperature excess method is also based on the PMV model (Fanger, 1972) and is determined as follows. The hourly weight factor (WF) takes the degree of discomfort in consideration and is directly proportional to the increase of the predicted percentage of dissatisfied people (PPD): one hour with 20 % dissatisfied people is equal to two hours with 10 % dissatisfied. A PMV of 0.5 corresponds to a WF of 1 (see Eq. 2.11). The weighted temperature excess hours are the sum of these hourly weight factors during working hours.

$$\text{if PMV} < 0.5$$
$$\text{then } WF = 0 \qquad\qquad \text{Eq. 2.11}$$
$$\text{else } WF = 10 - 9.5 \exp\left[-\left(0.03353 \, PMV^4 + 0.2179 \, PMV^2\right)\right]$$

A number of weighted working hours less than 150h, means a good thermal summer comfort. This corresponds to 5% excess hours, i.e. 100h, with on average 15% of dissatisfied people (or WF = 1.5). Compared to the temperature excess method, the weighted temperature excess method is more stringent for light buildings. For heavy buildings, both requirements correspond rather well.

A comparable long-term evaluation criterion is included in the European standard EN ISO 7730-1996 (ISO, 1996) (see also above).

2.1.3.4.2.3 Adaptive temperature limits indicator (van der Linden et al., 2006)

The adaptive temperature limits indicator was developed in The Netherlands based on the adaptive comfort theory of de Dear and Brager (2002). Two types of buildings are distinguished, based on the definitions of de Dear and Brager (2002). The type alpha and

beta buildings can be derived from a flow chart (see Fig. 2.11) depending on the availability of operable windows and the possibility to adjust the indoor temperature and clothing. Unlike ASHRAE Standard 55-2004, adaptation is taken into account for all types of buildings.
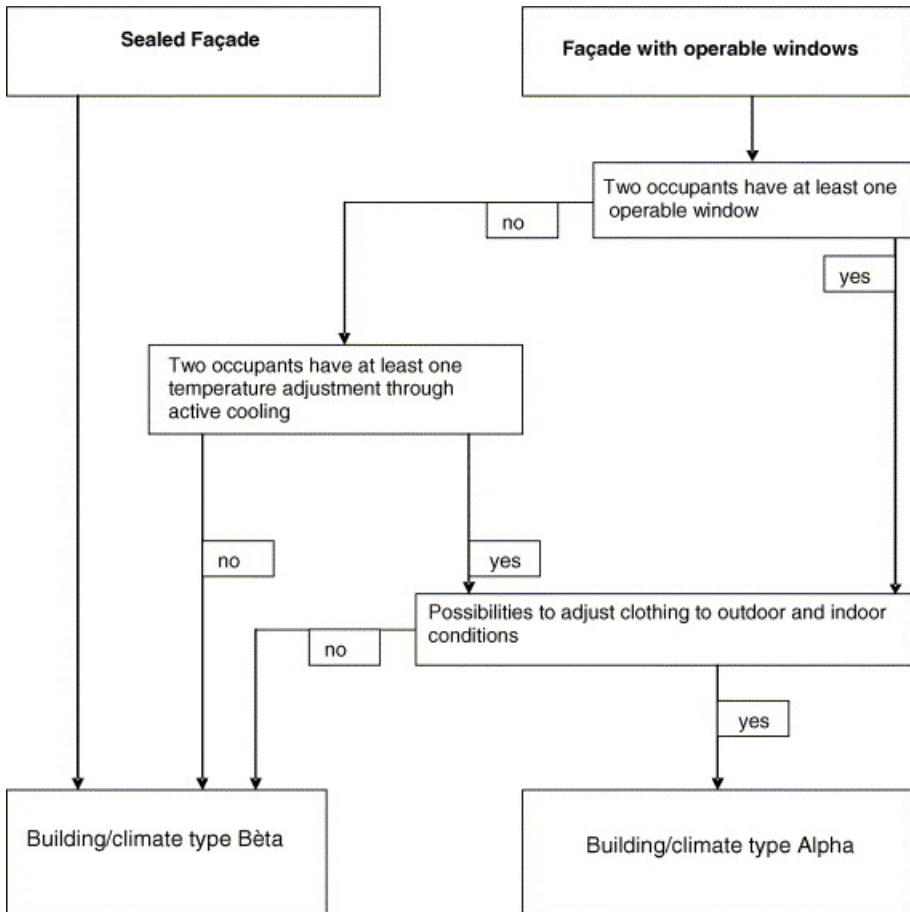
Fig. 2.11 Flow chart for determining the type of building (van der Linden et al., 2006)

Unlike ASHRAE Standard 55-2004, thermal comfort is divided into three levels. Level A corresponds to 90% thermal acceptability and is applied in buildings with high performance requirements to thermal comfort. Level B (80% thermal acceptability) means good indoor thermal comfort and is the standard level. Level C (65% thermal acceptability) finally, is only applied in temporary situations in existing buildings. This latter comfort zone was specially calculated for this Dutch guideline by de Dear and Brager. Fig. 2.12 and Fig. 2.13 show the adaptive temperature limits for respectively an alpha and a beta building. Contrary to the ASHRAE Standard 55-2004 (ASHRAE, 2004), the lower limits of the alpha building are the same as these of the beta building. This means the adaptation to lower temperatures is smaller than to higher temperature.
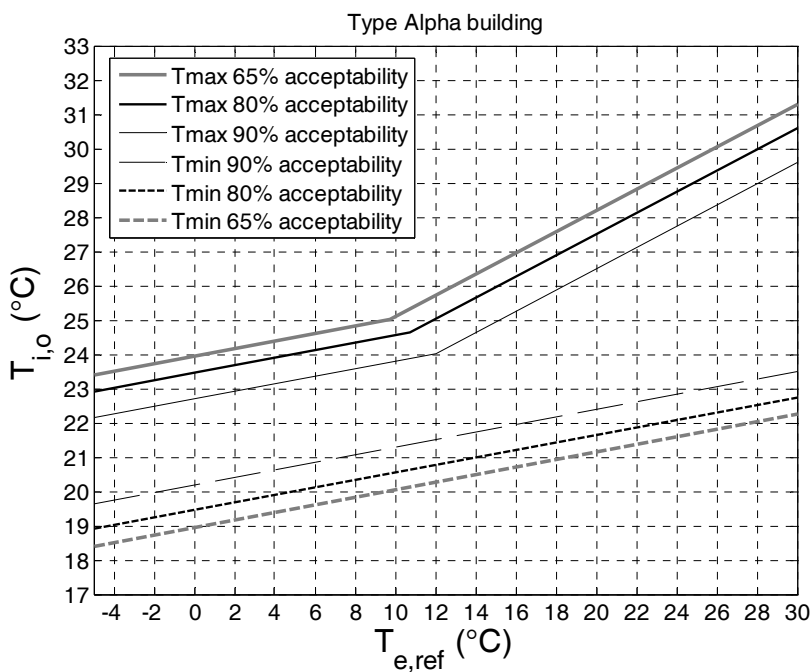
Fig. 2.12 Limits of the adaptive temperature limits indicator for an alpha building
(van der Linden et al., 2006)
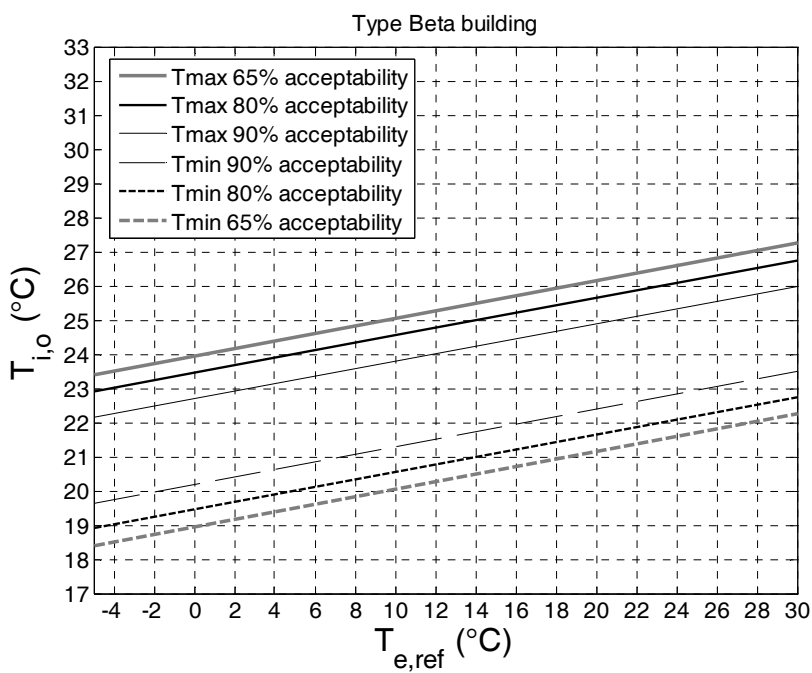
Fig. 2.13 Limits of the adaptive temperature limits indicator for a beta building
(van der Linden et al., 2006)

The equations for optimal thermal comfort in a type alpha and beta building are respectively given in Eq. 2.12 and 2.13, where the first equation corresponds to the line of neutral comfort in naturally ventilated buildings in the ASHRAE Standard 55-2004.

$$T_{i,o} = 17.8 + 0.31 \cdot T_{e,ref} \qquad \text{Eq. 2.12}$$

$$T_{i,o} = 21.45 + 0.11 \cdot T_{e,ref} \qquad \text{Eq. 2.13}$$

The minimum and maximum limiting indoor temperatures on a given day depend on the effective outdoor temperature $T_{e,ref}$, i.e. the running mean external temperature of that and the three preceding days (Eq. 2.14). The effective outdoor temperatures of 3, 9, 16 and 22°C correspond to winter, autumn/spring, summer and hot summer situations in The Netherlands respectively. In contrast with ASHRAE Standard 55-2004, the adaptive temperature limits indicator is valid for effective outdoor temperatures ranging from –5 to +30 °C. The reference weather data are taken from weather station De Bilt from both 1964 (normal year) and 1995 (warm year). Comparison of the climatological normals for Uccle (1961-1990) (RMI, 2004) and De Bilt (1971-2000) (KNMI, 2006) shows that the Dutch weather is comparable to the Belgian.

$$T_{e,ref} = \frac{\left(T_{today} + 0.8 T_{yesterday} + 0.4 T_{day\,before\,yesterday} + 0.2 T_{2\,days\,before\,yesterday}\right)}{2.4} \qquad \text{Eq. 2.14}$$

2.1.3.5 Conclusions

Two criteria are chosen to evaluate the performances of natural night ventilation based on either Fanger's (Fanger, 1972) or the adaptive theory (de Dear and Brager, 2002) of thermal comfort. Based on the comfort theory of Fanger (Fanger, 1972), the weighted temperature excess method (van der Linden et al., 2002) has been selected. This criterion takes into account the differences in thermal mass and is suited for an evaluation concerning the entire summer period. To take the adaptation into account, the adaptive temperature limits indicator (van der Linden et al., 2006) has been chosen. This method is made for a moderate (Dutch) climate, has a clear definition for the different types of buildings and does not take the adaptation to lower temperatures into account.

2.1.4 Conclusions

Natural night ventilation uses the outside air as a heat sink to cool down the building structure at night. This convective passive cooling method is driven by natural driving forces and requires a sufficient thermal heat capacity of the building structure to store the heat by day. The energy balances of a room and the internal surfaces can predict the indoor temperature. The performances of natural night ventilation are evaluated by thermal comfort criteria, based on this indoor temperature. Two suitable criteria of thermal comfort are selected: the weighted temperature excess method, based on Fanger's comfort theory, and the adaptive temperature limits indicator, based on the adaptive theory of thermal comfort.

2.2 State of the art

2.2.1 Introduction

The theoretical principles of natural night ventilation as well as the evaluation criteria are discussed in the previous section. However, how does natural night ventilation perform in practice? In addition, how are these performances predicted? What are the limitations of this technology? This section tries to answer these questions by discussing the results of international projects and research concerning natural night ventilation.

2.2.2 PASCOOL (1992-95) (Allard et al, 1996)

2.2.2.1 Aim

The PASCOOL program aimed to develop techniques, tools and design guidelines in order to promote passive cooling applications in buildings.

2.2.2.2 Results

2.2.2.2.1 Pre-design: Lesocool (Roulet et al., 1996)

LESO-PB, the Solar Energy and Building Physics Laboratory of the Swiss Federal Institute of Technology (EMPA) developed a computer program for the evaluation of the overheating risk and the cooling potential through ventilation. Lesocool is a multizonal pre-design simulation tool and can predict the internal temperatures and the cooling potential of night ventilation. This simplified model includes three components: a ventilation model, a heat storage model and a heat transfer model. The ventilation model is based on Eq. 2.1 and Eq. 2.2. The heat storage is based on the solution of the equation of dynamic heat transfer in a semi-infinite medium, submitted to a heat flow step function. In this solution, the thermal effusivity b has great importance. Energy and mass balances are solved in each zone, assuming that heat transfer between the zones occurs by airflow only. In addition, convective heat transfer occurs between the air and the walls.

As the model is based on simplified equations, two main limitations can be distinguished. Firstly, only one single airflow path without branches can be modelled. Secondly, the thermal model is only valid for infinitely thick walls. On the other hand, Lesocool is validated: a good agreement is found between simulated and experimental indoor air temperatures.

2.2.2.2.2 Analysis tool: Passport-air

Passport-air was developed to calculate the airflow rates in a naturally ventilated building. It is a network ventilation tool, similar to the tool that is used in this research (see chapter 4).

2.2.2.2.3 Cp-generator

In order to give realistic data of the wind pressure coefficient Cp in the analysis tool Passport-air, the empirical tool CPCALC+ (Grosso, 1995) was developed. Wind tunnel experiments have been used to obtain regression curves for the determination of the pressure coefficient distribution.

2.2.3 IEA Annex 28: Low-energy cooling (1993-97) (IEA, 1995, 1997, 1998)

2.2.3.1 Aim

The aim of IEA Annex 28 was to investigate the feasibility and provide design tools or guidance on the application of alternative cooling strategies to buildings. The project was divided into three main activities: description of the low-energy cooling strategies, development of design tools for both early and detailed design and illustration of the various cooling technologies in demonstration projects. Following low energy cooling technologies were investigated: night cooling by natural and mechanical ventilation, ground cooling with air and water using aquifers, slab cooling with air and water, desiccant cooling, evaporative cooling, chilled ceilings and displacement ventilation.

2.2.3.2 Results

The outputs of IEA Annex 28 include a review of the low-energy cooling strategies, selection guidance, early design guidance, detailed design tools and case study descriptions. The results concerning night ventilation in offices will be discussed.

2.2.3.2.1 Performances and limitations

Hot and moderate climates with large diurnal temperature difference over the summer are best suited for natural night ventilation. Givoni (1994), who recommended a diurnal temperature difference of approximately 10–12 °C, confirms this. Moreover, natural night ventilation is highly discouraged in humid climates. The humidity ratio of the outside air should be less than 15 g/kg dry air since this technology provides primarily sensible cooling. Natural night ventilation is also advised against when close temperature or humidity control is required. Furthermore, this passive cooling technique may only satisfy a low or moderate periodic cooling demand. As a rule of thumb, a maximum of 20-30 W/m^2 heat gains in heavy constructions is recommended. Corresponding internal peak room temperature reductions are of the order of 2-3°C. Performances will be reduced for constructions with little exposed mass.

2.2.3.2.2 Early design (Kolokotroni et al., 1997)

The pre-design tool Nitecool for night ventilation in offices was developed in IEA Annex 28 and NatVent (see paragraph 2.2.6). The program is based on a single zone ventilation model for a typical cellular office with dimensions: 10m width x 6m depth x 3m floor-to-ceiling height. It is positioned in the middle of a row of offices on the middle floor of a 3-storey office building. The input is restricted to 8 main building variables (internal heat gains, infiltration rate, orientation, glazing ratio, thermal mass, occupied period, solar protection and shading coefficient and site location), weather data, day ventilation, night ventilation and control strategies. The cooling system for day and night can be chosen independently from a list of nine different systems among which mechanical ventilation, natural ventilation and active cooling systems. The outputs of Nitecool are a weekly internal temperature profile, the maximum and minimum internal temperature during occupancy, the energy savings and peak cooling capacity savings relative to a reference system.

Kolokotroni (1997) also gives design charts, based on the same model and assumptions as in Nitecool, for determining the saved energy consumption during office hours and the internal dry resultant temperature that is exceeded in an office for 30h from June to September in Heathrow (United Kingdom). The inputs are the solar and internal heat gains, ventilation rate by day and night and thermal mass (reference or exposed mass).

Nitecool also includes the CIBSE reverse method (CIBSE, 1997) to design the openings of natural ventilation. Based on Eq. 2.1 (driving forces) and Eq. 2.2 (ventilation rate, orifice equation), CIBSE (1997) formulated design charts and worksheets to size the ventilation openings for stack-driven, wind driven and combined wind and stack driven natural ventilation if the required ventilation rate is known. Inputs are the wind speed on site, the difference in pressure coefficient across the flow path, assumptions of the temperature difference inside-outside and of the height between the opening and the neutral pressure level NPL, i.e. the height where the external and internal pressure are equal. All resistance along the flow path is assumed to be situated at the inlet and outlet.

2.2.4 Passive cooling of buildings (1996) (Santamouris and Assimakopoulos, 1996)

2.2.4.1 Aims

The aim of this book is to report the basic knowledge on passive cooling and prediction tools, to present recent progress in this field and to identify priorities for future research. Following passive cooling technologies are examined in detail: heat attenuation, natural ventilation, solar control, ground cooling, evaporative and radiative cooling. Climate and environment characteristics, thermal comfort and the cooling load of buildings are also discussed.

2.2.4.2 Results

Simplified methods to predict the cooling requirements for passive cooling applications are derived (Santamouris, 1996). The reduction in cooling load due to night ventilation is calculated based on the night degree days, derived from the mean night-time indoor temperature of the building without night ventilation. This temperature can be calculated from the steady state energy balance of the indoor air. To prevent this total energy loss due to night ventilation being overestimated, two checks are performed. The heat loss by night ventilation should be smaller than both the maximum possible stored energy and the cooling load of the building without night ventilation.

This model is validated against extensive and detailed simulation data obtained using the dynamic thermal simulation model TRNSYS 13.1 (Klein et al., 1990). A very good agreement can be noticed for both monthly and annual cooling loads (Santamouris et al., 1996). Furthermore, this calculation method is incorporated in the software tool SUMMER (Klitsikas et al., 1996).

2.2.5 AIOLOS (1995-1997) (Allard, 1998), (Santamouris et al., 1996a)

2.2.5.1 Aim

The purpose of the AIOLOS project was to create specific educational material on the efficient use of natural ventilation in buildings.

2.2.5.2 Results

The results of this project include a handbook on natural ventilation (Allard, 1998), a tool to evaluate the performances of natural ventilation and case studies on naturally ventilated buildings.

2.2.5.2.1 Handbook (Allard, 1998)

This handbook discusses the basic principles of natural ventilation (see also paragraph 2.1.2) and gives an overview of prediction methods (see chapter 4) and diagnostic techniques. Critical barriers, design guidelines, technical solutions and case studies are additionally discussed.

2.2.5.2.2 Analysis tool (Dascalaki, 1998)

The analysis tool AIOLOS was developed to calculate the airflow rates in a naturally ventilated building, based on the Passport-air tool (see above). It is a network ventilation tool, similar to the tool that is used in this research (see chapter 4).

2.2.6 NatVent (1994-1998) (NatVent, 1998)

2.2.6.1 Aims

NatVent aimed to provide solutions to barriers that prevent the uptake of natural ventilation and low-energy cooling in countries with moderate and cold climates. Countries with low winter and moderate summer temperatures where summer overheating from solar and internal gains can be significantly reduced by low-energy design and good natural ventilation were targeted. Furthermore, this project aimed to encourage and accelerate the use of natural ventilation and 'smart' controls as the main design option in new-designs and major refurbishments of office-type buildings. Solutions in urban areas with high levels of external air pollution and noise were a priority. The project was divided into three main activities. Firstly, the perceived barriers to natural ventilation were identified. Secondly, the performances of existing energy-efficient naturally ventilated buildings were evaluated. Thirdly, smart naturally ventilated technology systems and component solutions to overcome the barriers were developed.

2.2.6.2 Results

2.2.6.2.1 Barriers (Aggerholm, 1998)

The perceived barriers restricting the implementation of natural ventilation were identified by interviewing architects, consultant engineers, contractors, governmental decision makers and building owners and developers. These interviews showed a significant lack of knowledge and experience of specially designed natural ventilation in office buildings

compared to the knowledge and experience of mechanical ventilation. In addition, a lack of source and information about natural ventilation in standards, guidelines and building studies was noticed. New design tools, simple and advanced computer programmes are also necessary.

2.2.6.2.2 Performances and limitations (NatVent, 1998)

Indoor temperature, humidity and ventilation rates during both winter and summer were monitored in nineteen naturally ventilated buildings in seven countries (Bergsoe, 1998a,b), (Demeester et al., 1998a,b), (Kukadia et al., 1998), (Liem et al., 1998), (Liem and van Paassen, 1998), (White et al., 1998), (Zacceddu, 1998). The indoor air quality in most of the buildings was acceptable. On the contrary, eight of these buildings suffered of serious overheating problems particularly caused by solar gains. Two different concepts of naturally ventilated buildings were distinguished: controlling the indoor air quality (IAQ) or achieving good summer comfort. The characteristics for these systems are very different. The required airflow rates for summer comfort are much higher than for IAQ control. In addition, accessible thermal mass is required when a good summer comfort has to be achieved. The optimal solution, a building with exposed heavy ceilings, floors and walls, is often not possible for practical reasons. However, an exposed ceiling or an (half) open lowered ceiling only already achieves acceptable results. In addition, van Paassen et al. (1998) concluded from their calculations (see 2.2.6.2.3.1) that natural night ventilation is only suitable in buildings with sufficient and accessible thermal mass (75-100 kg/m^2 total internal room area). The internal gains have to be limited to 30 W/m^2 floor area.

2.2.6.2.3 Technological solutions

2.2.6.2.3.1 Sizing night ventilation openings (Van Paassen et al., 1998a)

Van Paassen et al. (1998a) developed a dynamic thermal and ventilation network simulation tool to investigate the control strategies and the required ventilation opening area of natural night ventilation for a generic office building of two single offices with dimensions 6 x 3.6 x 2.7 m^3, separated by a central corridor with a vertical chimney optionally implemented. Singled-sided, cross and stack ventilation are investigated. The thermal comfort criterion used to evaluate the performances is the temperature excess method (see paragraph 2.1.3.4.2.1). The results of this model are shown in a graphical chart (Fig. 2.14).

This chart helps to determine the effective ventilation opening area for natural night ventilation (in percentage of floor area) in an early stage of the design. The inputs are the internal heat gains, solar gains, accumulation mass and the control strategy of the night cooling. Solar gains can be easily derived from the orientation and the size of the window and the nature of the shading device. The accumulation mass is divided into three categories and has to be calculated as the sum of half the weight of the side walls, back wall, floor and ceiling and the entire weight of the façade, divided by the total inner room area. Distinction is made between open, i.e. exposed, and closed ceilings. In addition, three operation/control strategies for natural night ventilation are distinguished: no night ventilation, (predictive) control and manual control by the operator. An example is shown in Fig. 2.14. An office having low internal heat gains of 20 W/m^2 is presented. North-south orientated windows with an area of 40% of the façade are applied, i.e. 10 W/m^2 solar

gains. A medium accumulation mass with open ceiling and a predictive control of natural night ventilation are available. Summing up all the corresponding values gives 30. Filling in this result: the table of the ventilation system on the right gives the possibilities of natural night ventilation: single-sided ventilation with ventilation openings with an area of 3% of the floor area or cross ventilation with openings of 2% of the floor area or chimney ventilation with openings of 1% of the floor area.

Selection Natural Ventilation Cooling System

Internal Heat/Load W/m²

low	20
	25
	30
middle	35
	40
high	45
	50

→ 20

Ventilation System

Natural System	Single Sided			Cross			Chimney + fan **		
Effective opening in % floor	1	2	3	1	2	3	1	2	3
Vent. rate fan [ach]	-	-	-	-	-	-	2	2	2

(chart: values 27, 28, 32, 34, 38, 39, 42, 44; "not acceptable" region in red)

Solar gain W/m²

sun	window %	N/S	W/E
	20	15	17
	40	30	34
	60	46	51
	20	5	7
	40	10	14
	60	15	21
	40	20	28

+ ⊗ 30

Accumulation mass

Type *	Ceiling	Points
Heavy M = 100	open	- 7
	closed	- 5
Medium M = 75	open	0
	closed	+ 6
Light M = 50		+ 8

+ ⊗ 30

End result dimensions of vent openings (effective opening in % floor area)

Control Strategy Night Cooling	Points
No Night Cooling	+ 10
Predictive Control	0
Manual by Operator	+ 5

+ ⊗

**
No wind fan on.

*
M = the sum of half the weight of the side walls, back wall, floor, ceiling and the entire weight of the facade divided by the total inner room area. Weight of a wall should be limited to 400 kg/m².
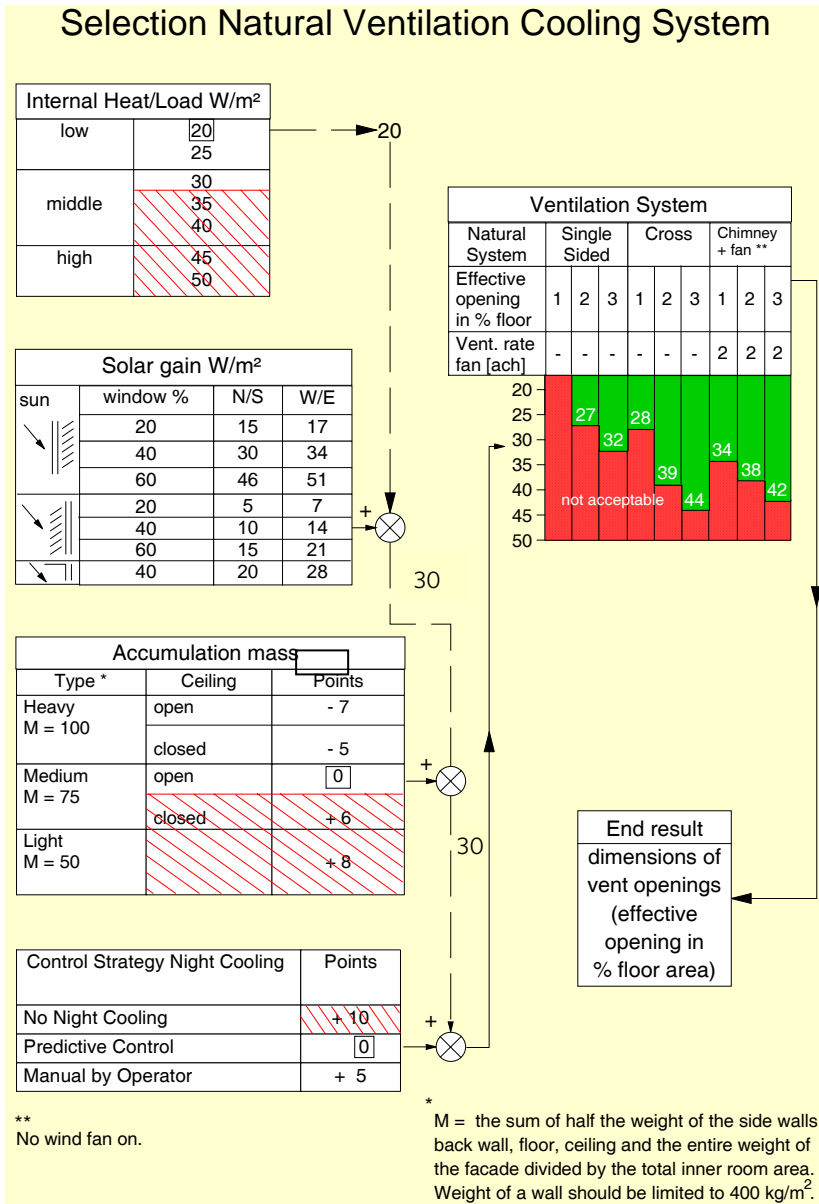
Fig. 2.14 Graphical design tool to determine the effective ventilation opening area for natural night ventilation (% of floor area) (van Paassen et al., 1998a)

2.2.6.2.3.2 Components and control system (van Paassen et al., 1998b)

A prototype of a night ventilator for cooling was designed and tested. The main objectives were controlling the supplied air and the indoor temperature. It included a normal trickle ventilator with sound attenuation for daytime ventilation, a motorised window for night ventilation and a control unit connected to the building management system. The hardware and control of a demo and an office window were tested. In addition, a field test was carried out during the summers of 1993, i.e. an average summer, and 1994, i.e. an extremely hot summer. The ventilation openings were sized by the above mentioned method. These measurements showed that the automatic control maintained comfortable indoor temperatures using the designed openings and consequently validated the design method to size the openings.

2.2.7 IEA Annex 35: HybVent (1998-2002) (Heiselberg, 2002)

2.2.7.1 Aims

HybVent is the abbreviation of hybrid ventilation systems, which were defined in this project as ventilation systems providing a comfortable internal environment by combining both natural ventilation and mechanical systems, but using different features of each system depending on the time of day or season of the year. IEA Annex 35 aimed to develop control strategies for hybrid ventilation systems for newly built and retrofitted office and educational buildings. The development of methods to predict the hybrid ventilation performance in hybrid ventilation buildings was also targeted. Finally, energy and cost-effective hybrid ventilation systems were promoted in office and educational buildings. These objectives were translated in the three main activities of the HybVent project. Firstly, integration of a natural and mechanical ventilation system requires the development of control strategies for hybrid ventilation. Secondly, analysis methods for hybrid ventilation were developed. Thirdly, pilot studies with hybrid ventilation systems were monitored to evaluate the performances and control strategies.

2.2.7.2 Results

2.2.7.2.1 Control strategies

In the state-of-the-art, Delsante and Vik (2002) present an overview of classical, advanced and complex control strategies and the implementation and integration in the building management system. Furthermore, Delsante and Aggerholm (2002) investigated the use of simulation tools to evaluate hybrid ventilation control strategies. Four coupled temperature and airflow rate simulation tools were examined for evaluating the performance of building ventilation systems and control strategies at the design stage. A preliminary study is undertaken to check if different tools will lead to the same conclusions about relative performance. The tools agree well on the effect of mechanical night cooling.

2.2.7.2.2 Analysis tools

An overview of the available analysis tools is presented in the state-of-the-art. The application, the required input data, the integration with thermal modelling and the validation with regard to hybrid ventilation are compared (Delsante and Vik, 2002). In addition, Heijmans and Wouters (2002a) investigated the impact of the uncertainty on

wind pressures on thermal comfort predictions. The wind pressures were predicted and measured on real buildings. Simulations were carried out with the predicted and measured values. To determine wind pressures around buildings, two parameters should be known: the local wind data (speed and direction) and the wind pressure coefficient C_p. They showed it was difficult to predict the local wind speed and to evaluate the wind pressure coefficient with classical tools. Nevertheless, these parameters have a large impact on the predicted thermal comfort.

2.2.7.2.3 Performances and limitations

Twelve office and educational buildings were monitored (Heijmans and Wouters, 2002b,c), (Hendriksen et al., 2002), (Meinhold and Rösler, 2002), (Principi et al., 2002), (van der Aa, 2002).

Aggerholm (2002) summarized the lessons learnt in the case studies concerning the control strategy. During non-occupancy, automatic control is necessary to cool down the building structure by night ventilation. During occupancy, a distinction is made between cellular and landscaped offices. User control functions well in cellular offices. On the contrary, in landscaped offices automatic control is also necessary by day, although it seems difficult to find an acceptable strategy for controlling the ventilation inlets. It should also be possible for the users to overrule this automatic control. In most buildings, a relatively complex control system is used to operate the hybrid ventilation system. It can be remarked that great care has to be taken in the design, implementation and maintenance of this control system.

2.2.8 Other research

Besides the international research projects in the previous paragraphs, other researchers have studied the performances of natural night ventilation in moderate and hot climates as well.

The temperature decrease and the level of thermal comfort have been measured in moderate climates. Amongst others, Pfafferott et al. (2003) monitored a new office and laboratory building in Freiburg (Germany) during the summer of 2002. It was noticed that night ventilation reduces the mean room temperature by 1.2°C during working hours. In addition, Pfafferott et al. (2004) monitored an office building in Hamm (Germany) and noticed acceptable indoor climate conditions: the operative room temperature of 25°C was exceeded 11 to 15% of the working hours. Furthermore, Blondeau et al. (1997) performed a full-scale experiment in a three level office and classroom building in La Rochelle (France) with mechanical night ventilation. They measured a diurnal temperature decrease of 1.5-2°C in the room with night ventilation compared to a reference room. With regard to the thermal comfort, the average predicted mean vote (PMV) decreases from 1.5 (warm) to 0.75 (slightly warm) when mechanical night ventilation was applied.

In addition, the reduction in cooling energy has been calculated in moderate climates. Kolokotroni and Aronis (1999) predicted 30 % reduction of the cooling energy consumption and 40 % reduction of the installed cooling capacity in a low energy office building with stack ventilation flow rate at night of 10 ach in the United Kingdom was

predicted. In addition, Gratia et al. (2004) calculated 40% reduction of the daily cooling demand in a high mass narrow office building with natural night ventilation on a sunny Belgian summer day. Blondeau et al. (1997) calculated that a night ventilation flow rate of 8 ach reduces the calculated mechanical cooling need with 12 to 54%, depending on the temperature set point.

With regard to hot climates, Givoni (1994) experimentally showed that in a hot dry climate the excess hours considerably reduce in a high mass building. Furthermore, Geros et al. (1999) studied the potential of night ventilation techniques when applied to full scaled buildings with different structure, design, ventilation and climatic characteristics. Based on measurements, calculations showed a decrease of the peak indoor temperature up to 3°C by use of high ventilation rates at night in an office building in Athens (Greece) under free-running conditions. The average reduction of the temperature in the various zones was predicted 1.8 - 3°C. When the building was air-conditioned, the average reduction of the indoor temperature was 1 - 2.8°C depending on the set point temperature.

2.2.9 Conclusions

Monitoring the performances of non-residential buildings in international projects and research has shown that hot and moderate climates with a large diurnal temperature difference are best suited for natural night ventilation. In moderate climates, good thermal comfort can be reached by combining night cooling, other passive cooling techniques and measures reducing the cooling load. In hot climates, natural night ventilation is used to reduce the energy consumption of the active cooling system. On the other hand, this cooling technique is discouraged in humid climates, i.e. with a humidity ratio of more than 15 g/kg dry air. Moreover, good performances can only be achieved in a building with low internal heat gains and sufficient exposed thermal mass.

Furthermore, the output of the research projects consists of pre-design and evaluation tools to dimension the effective ventilation opening and predict the (maximum) internal temperature, the energy savings and peak cooling capacity savings respectively. However, how accurate is the prediction of these simple tools in a particular case? In addition, what are the performances in a project with specific characteristics like e.g. a low thermal mass or a large glazing area? To answer these questions, the particular project should be analysed in detail by building simulation tools.

2.3 CONCLUSIONS

The general principles of natural night ventilation are discussed. Natural night ventilation is a convective passive cooling method, driven by natural driving forces. It uses outside air at night to cool down the exposed building structure in which the heat of the previous day is accumulated. Its performances are evaluated by thermal comfort criteria. Two suitable criteria of thermal comfort are selected: the weighted temperature excess method, based on Fanger's comfort theory, and the adaptive temperature limits indicator, based on the adaptive theory of thermal comfort.

In addition, the outputs of international projects and research concerning natural night ventilation are discussed. The measured performances, limitations, pre-design and evaluation tools are focussed on. In moderate climates, good thermal comfort can be reached by combining night cooling, other passive cooling techniques and measures reducing the cooling load. In hot climates, natural night ventilation is mostly used to reduce the cooling demand of the active cooling system. Chapter 3 discusses in detail the operation, performances and limitations of natural night ventilation in two Belgian office buildings.

Moreover, pre-design and evaluation tools to dimension the opening characteristics and to predict the indoor temperature, the energy savings and peak cooling capacity savings respectively have been derived. The accuracy of the results of these tools in a particular case is unclear. Building simulation tools offer a more detailed and accurate evaluation of the performances of a specific project with natural night ventilation. These analysis tools are discussed in the chapter 4.

3 Monitoring the performances of natural night ventilation in two Belgian office buildings

The performances of two Belgian office buildings with natural night ventilation are examined in detail to illustrate the operation of this passive cooling technique in a moderate climate. The indoor summer temperatures are monitored to evaluate the operation and the level of thermal comfort. Both office buildings use passive stack driven night ventilation. The Renson building (Waregem) is also naturally ventilated during daytime. Fans in the chimneys can be used to ensure a sufficient flow rate in summer. Mechanical supply ventilation by day is provided in the offices of SD Worx (Kortrijk).

3.1 SD Worx (Breesch et al., 2005)

3.1.1 Building description

The office building SD Worx is located in Kortrijk, Belgium and consists of two office floors on top of a limited ground floor with building services. On the south side, the floors are connected with an open vertical circulation zone. Fig. 3.1 shows a plan of the first floor and a vertical section. The plan of the second floor is very similar. The office floors and the ground floor have a floor area of respectively 497 m^2 and 198 m^2. The most important rooms on the office floor are the open plan office (n° 1), circulation zone (n° 2), conference rooms (n° 3) and other offices or an auditorium (n° 4). The vertical section indicates the open plan offices (n° 1) and the stairwell (n° 2) on both floors as well as the technical rooms (n° 5) on the ground floor. Building characteristics are shown in Table 3.1. The building design is a cooperation of amongst others architect Stramien and sustainable design consultant Cenergie.
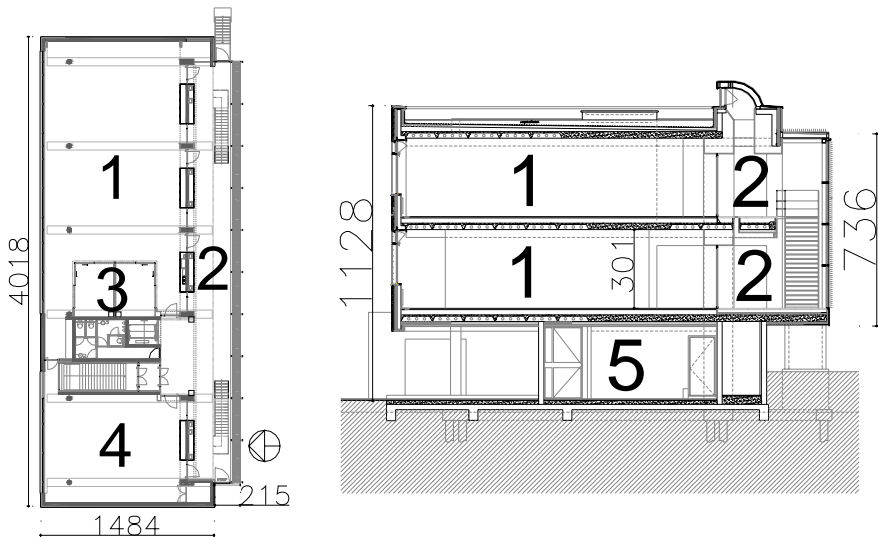

Fig. 3.1 Plan (left) and cross section (right) of the first floor of SD Worx (Kortrijk, Belgium) with open plan office (n°1), circulation zone on the first and the second floor (n°2), conference rooms (n°3), auditorium (n°4) and building services on the ground floor (n°5)

Table 3.1 Building characteristics SD Worx

Night ventilation building data							
Zone	Reference height (m)	Dimensions h/d/w (m)	Louvers				
			From	To	h (m)	A_{eff} (m^2)	C_d (-)
Office 1st floor	3.5	3/12.1/21.2	outside	office 1st	6.0	2.36	0.65
			office 1st	circulation	6.3	1.53	0.65
Office 2nd floor	7	3/12.1/21.2	outside	office 2nd	9.5	2.36	0.65
			office 2nd	circulation	9.8	1.53	0.65
Circulation zone	3.5	8.4/2.9/21.2	circulation	outside	11.4	4.44	0.65

Thermal building data					
Wall	U (W/m^{2}K)	g (-)	Wall		U (W/m^{2}K)
Glazing	1.1	0.6	External floor		0.24
Glazing, horizontal, circulation	0.6	0.28	External floor, circulation		0.15
			Internal floor		1.61
			External wall		0.28
			Internal wall		0.93
			Window frame		3.5
			Roof		0.28

Wall composition	
External wall	reinforced concrete, embedded with brick panes
Internal wall	wooden cupboards
Flat roof	hollow core concrete slabs
Internal and external floor	hollow core concrete slabs, raised floor

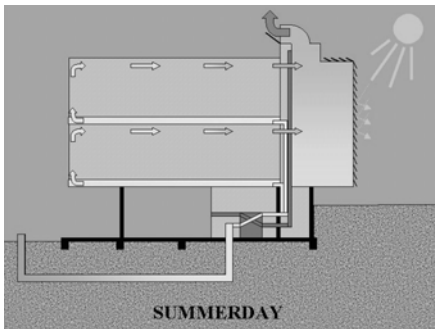| Internal heat gains per floor							
	Present	Maximum		Radiant (%)		Convective (%)	Usage diversity
People	9 pers.	24 pers.	80 W/pers.	50		50	1
PC + Screen	9 pc.	24 pc.	130 W/pc.	25		75	0.75
Laser printer	1 pc.	1 pc.	320 W/pc.	20		80	0.5
lighting	235 m^2	235 m^2	9W/m^2	25		75	0.6
Total	12.9 W/m^2	24.2 W/m^2		31	33	69	67

Fig. 3.2 Operation scheme of the earth-to-air heat exchanger in SD Worx (Cenergie, 2003)
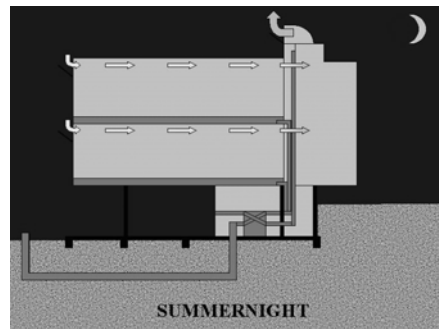

Fig. 3.3 Operation scheme of natural night ventilation in SD Worx (Cenergie, 2003)

The principles of this low-energy office building are reduction of the heating and cooling load, use of passive cooling and heating and enhanced control automation (Cenergie, 2003). Following actions are taken to achieve a good thermal summer comfort. Firstly, the cooling load is reduced. Zoning minimizes the solar heat gains because the offices face north and the circulation zone faces south. This glazed south-facing façade is finished with controllable

external sunblinds to achieve solar shading. The heat emission of lighting and office equipment is also minimized. The installed power of the lighting is limited to 9.5 W/m^2, presence detection and daylight control are applied. An exposed concrete ceiling additionally delivers a high thermal capacity, which reduces and postpones the cooling load.

Secondly, passive cooling is applied. By day, an earth-to-air heat exchanger pre-cools the supply airflow (Fig. 3.2). By night, outside air enters the office floors through bottom hung windows, located near the ceiling in the offices on the north side. The air cools down the exposed ceiling and leaves the building at the top of the circulation zone through outlet windows along the width of the building (see Fig. 3.3). This natural night ventilation system is primarily driven by thermally (stack) generated pressures. The effective area of the façade louvres is 1 % of the floor area.

Table 3.2 Control system natural night ventilation

Natural night ventilation is in operation if the conditions below are fulfilled
Previous day
$\theta_{i,max}$ > 23°C θ_i > 20°C
At that moment
22h < time < 6h θ_i > 20°C $\theta_i - \theta_e$ > 2°C φ_i < 70 % No rainfall v < 10 m/s

Thirdly, the use of these passive cooling techniques is automatically controlled to meet requirements at different climatic loads. When the temperature in every zone exceeds 23 °C during the day, the supply ventilation rate increases proportionally to the mean indoor temperature: from 5400 m^3/h at 23 °C to 8000 m^3/h at 26 °C and above. In this situation, the exhaust air leaves the building through the windows on top of the circulation zone. When the internal temperature in a zone is less than 23 °C, the ventilation rate in this zone is demand controlled and the ventilation air is mechanically extracted as in the heating season. The operation of natural night ventilation depends on multiple control parameters: the maximum inside and outside air temperature of the day before, the inside air temperature, the difference between inside and outside air temperature, the internal relative humidity, the rainfall and the wind velocity at that moment. Table 3.2 lists the settings of the control system. The control parameters were optimised after the first summer. While the inlet windows before were opened at inside air temperatures larger than 20 °C, the opening is now controlled by ceiling surface temperatures exceeding 22 °C.

3.1.2 EVALUATION OF THE PERFORMANCES

The building operation system monitors continuously (every 15 min.) the outdoor and indoor climate, the airflow rate in the mechanical ventilation system and the control parameters. Measurements from May 15 to September 30, 2002 are used to evaluate the performances of natural night ventilation in the cooling season. This was the first summer that the building was in operation.

3.1.2.1 Natural night ventilation

The monitoring (De Paepe, 2003) shows that natural night ventilation was in operation during 60 % of the nights from the end of June until the end of September 2002. Fig. 3.4 shows the outdoor temperature, the operative and surface temperatures on both floors and the operation of natural night ventilation during a warm summer period. Natural night ventilation cooled down the inside air and exposed ceiling, which had stored the heat of the previous day, from 10 p.m. until 6 a.m. As a result, excess heat accumulated in the ceiling the following day (surface temperature increased by day) and the air temperature peaks by day decreased. No humidity or condensation problems were noticed.
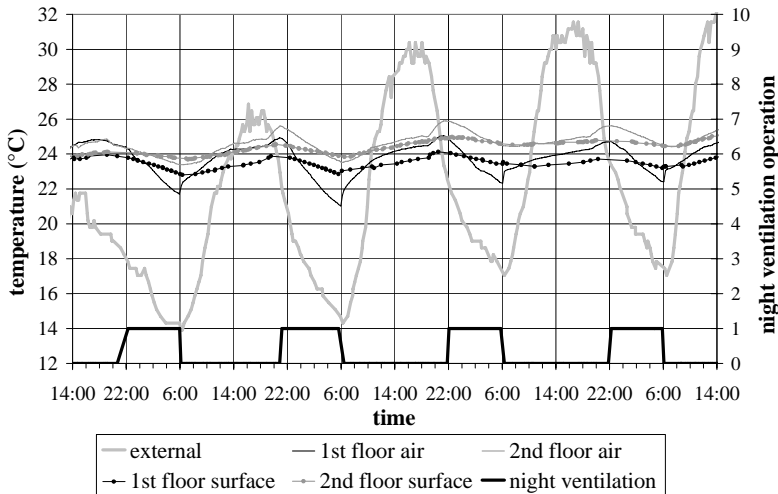

Fig. 3.4 Measured operation of natural night ventilation (August 12-16, 2002)

The performance of natural night ventilation is analysed based on the achieved operative and surface temperature drop overnight (between 10 p.m. and 6 a.m. the next day). These temperature drops were higher on the first than on the second floor because of the higher thermal stack effect (see Table 3.3). The outside temperature peak was on average postponed for 5 h. As a result, the indoor operative temperature peaks occurred after the office hours.

Table 3.3 Natural night ventilation: temperature drop overnight

		First floor	Second floor
$\Delta\theta_{a,i}$ (°C)	μ	2.0	1.3
	σ	0.8	0.6
$\Delta\theta_{s,i}$ (°C)	μ	0.7	0.5
	σ	0.3	0.2

3.1.2.2 Thermal comfort

Thermal summer comfort is evaluated by Fangers' comfort theory (Fanger, 1972). Fanger defined the conditions in which more than 10 % of the occupants are dissatisfied. The critical indoor operative temperature meeting this requirement depends on the metabolism and clothing resistance. Assuming seated office work (metabolism of 65 W/m^2) and light working clothes (0.7 Clo), a threshold temperature of 26.0 °C is found (ISSO, 1990). The temperature exceeding hours method (TO) (GBA, 1999) requires the excess hours of this threshold indoor

temperature should be limited to 100 during occupancy. Additionally, a maximum of 20 excess hours above 28°C is allowed. Fig. 3.5 shows the excess hours of the measured temperatures on both floors. An excellent thermal summer comfort was reached: 26 °C was only exceeded during 3 hours on the second floor and never on the first floor. Fig. 3.5 also proves that high temperatures were more frequently monitored on the second floor. Fig. 3.6 relates the daily maximum operative temperature on the second floor to the daily maximum outdoor temperature. The maximum operative temperature on the second floor averaged 24.6 °C. 98 % of the maximum indoor temperatures on the second floor are from 23.5 °C to 26 °C. Low present internal heat gains explain these results. In case of maximum internal heat gains, simulations predict an acceptable thermal comfort with an amount of weighted temperature excess hours somewhat larger than 150h (Breesch et al., 2005).
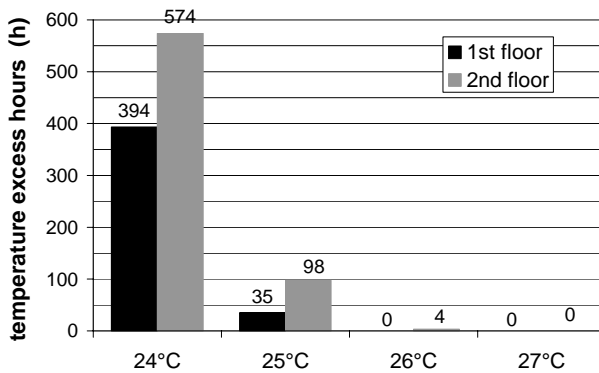

Fig. 3.5 Measured temperature excess hours on both floors during working hours
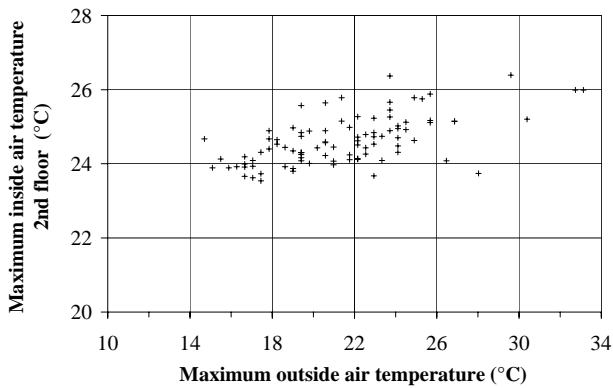(May 15 to September 30, 2002)

Fig. 3.6 Measured daily maximum inside temperature on the second floor during working hours as a function of the measured maximum outside temperature (May 15 to September 30, 2002)

De Paepe (2003) also noticed a conflict between cooling and heating at 6h in the morning during 8 working days in September 2002. Optimizing the control systems of both cooling and heating can solve this overcooling problem.

3.2 RENSON (BREESCH ET AL., 2004)

3.2.1 BUILDING DESCRIPTION

The low-energy office building of Renson, a company that develops and manufactures natural ventilation and solar shading systems, is located in Waregem (Belgium) in between the manufacture plant and the highway. The office is designed to demonstrate the so-called 'healthy building concept', which relies on natural ventilation and solar shading to achieve an indoor air quality and temperature control with limited energy consumption, by architect Jo Crepain and VK Engineering Building Services.

All offices are located on the second floor on top of a limited ground and first floor with building services. Fig. 3.7 and Fig. 3.8 show a plan of the second floor and a vertical section respectively. The office floor includes an open plan office (n°1), oriented to the north, surrounded by small offices on the south-west side (n°2 and 3), internal (n°4) and external (n°5) meeting rooms on the southeast and northeast side and lunch rooms (n°6). With exception of the external meeting rooms (n°5), which are mechanically ventilated, all the rooms are naturally ventilated. The façade is almost completely glazed. Properties of the insulating glass and other thermal building data are shown in Table 3.4. The floor consists of a raised (false) floor system. The total volume of this office floor is 8388 m^3.
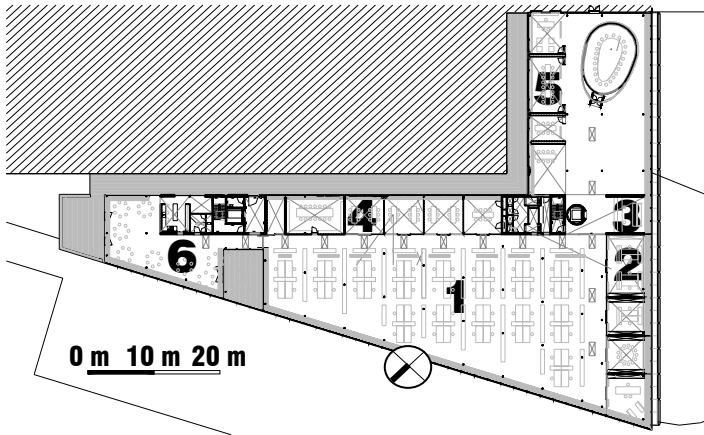

Fig. 3.7 Plan of second floor with landscape office (n°1), accounting and management section (n°2), reception desk (n°3), internal (n°4) and external (n°5) conference rooms and service rooms (n°6)
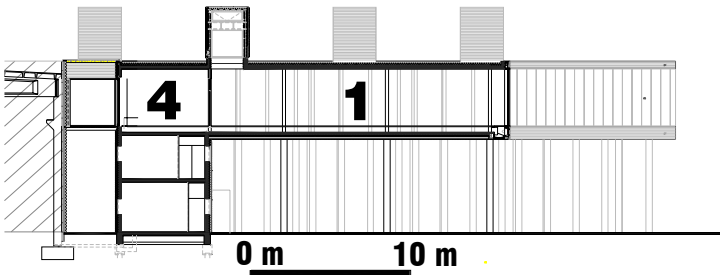

Fig. 3.8 Vertical section through landscaped office (n°1) and internal conference rooms (n°4)

A prerequisite for the feasibility of any passive cooling system is a reduced cooling load in the building. Following measures were taken: automated external sun blades at the south-west side, energy-efficient lighting and office equipment, a well-insulated roof (Table 3.4) and accessible thermal inertia of the concrete office ceilings.

Table 3.5 report the internal heat gains of some interesting rooms. In the actual occupancy, a low level of internal heat gains in the open plan office and the reception desk and a medium level of internal heat gains in the accounting offices are noticed. For this reason, the accounting offices (as well as the external meeting rooms) are the only rooms where an additional cooling system is installed: an overhead fan-coil unit is integrated in the lowered ceiling.

Table 3.4 Thermal building data

window					floor	roof
Orientation	NE (n°6)	NE(n°5)	NW	SW	-	-
A (m^2)	75	250	300	225	2330	2330
g (-)	0,61	0,61	0,53	0,53	-	-
U$_{glazing}$ (W/m^{2}K)	1,3	1,3	1,3	1,3	0,5	0,3
LTA (-)	0,76	0,76	0,74	0,74	-	-
Sun blades	no	no	no	yes	-	-

Table 3.5 Internal heat gains with actual and design occupation in some office rooms

		landscape (n°1)	Accounts 1 (n°2)	Accounts 2 (n°2)	Reception (n°3)
Area (m^2)		992	63	37	35
People	actual	50	4	2	2
	design	85	4	2	2
Office equipment	PC + monitor p.p.	1	1	1	1
	Printers	5	2	2	-
	Fax	2	-	-	1
	Copiers	2	-	-	-
Lighting (W/m^2)		8	8	8	8
Heat gains (W/m^2)	actual	15.4	22.7	23.2	18.2
	design	21.0	22.7	23.2	18.2

Table 3.6 Internal heat gains of people, office equipment and lighting (Wilkins and Hosni, 2000)

Heat gains			diversity	
			n°1	n°2 & 3
people		80 W/pers.	0.75	1
PC + screen		130 W/pc.	0.75	1
Laser printer	desk	215 W/pc.	-	0.5
	office	320 W/pc.	0.5	-
Fax machine		15 W/pc.	0.5	
Copier		1100 W/pc.	0.3	
lighting		8 W/m^2	0.75	

The natural ventilation system to control the indoor air quality includes acoustic self-regulating inlet grills and passive stack exhausts. The inlet grills are located at the bottom

of the curtain wall over the full length of the façade (see Fig. 3.9). In winter, the supply air is heated by the underfloor convector heating system. The extraction openings are located in 15 individual chimneys on top of the building (Fig. 3.10), at a height of 7.5 m above the inlet grills. In addition, the natural night ventilation system (Fig. 3.11) for temperature control consists of motorised inlet and outlet windows, located at the bottom of the curtain walls (Fig. 3.9) and in the chimneys (Fig. 3.10). In the chimney, two windows on opposing sides are available. Depending on the wind direction, the window on the leeward side is automatically opened. The outlet windows also serve a day lighting function. The area of inlet and outlet openings is 2% and 1% of total floor area. They are designed to reach a mean ventilation flow rate at night of 6 ach. This airflow allows cooling down the exposed concrete ceiling of the office floor (625 kg/m^2 thermal mass). Both inlet and outlet windows are automatically controlled. The occupants may also individually control the inlet windows if additional airing is desired by day. By night, the controls are set as follows (see Table 3.7). The system operates generally from 9 p.m. until 7 a.m. The operation time may be extended in extremely warm summer periods. The operation of natural night ventilation further depends on the maximum inside and outside temperature of the previous day, and on the inside room temperature, relative humidity, wind speed at the moment. When these conditions are fulfilled, the inlet and outlet windows are automatically opened to allow an increased ventilation rate.
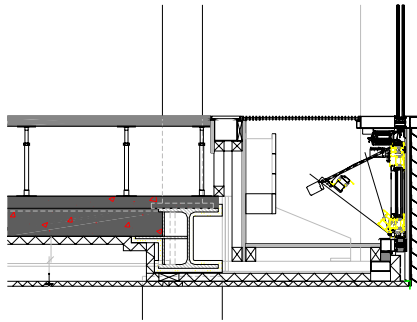

Fig. 3.9 Inlet grill and window for natural day and night ventilation at the bottom of the curtain wall.
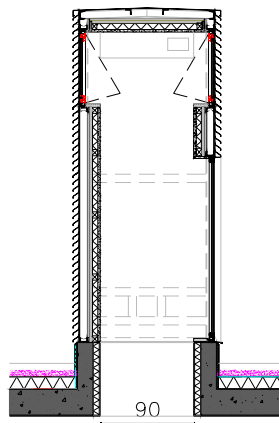

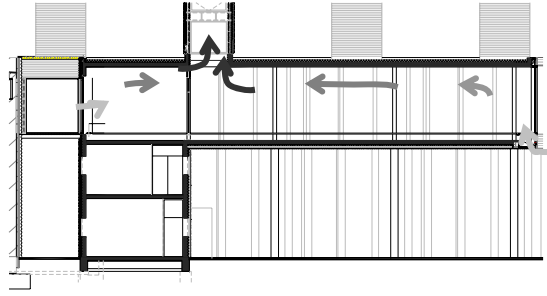Fig. 3.10 Passive stack and outlet windows for natural night ventilation

Fig. 3.11 Operation of natural night ventilation.

Table 3.7 Control system natural night ventilation Renson

Natural night ventilation is in operation if the conditions below are fulfilled
Previous day
$\theta_{i,max}$ > 23°C
$\theta_{e,max}$ > 22°C
At that moment
21h < time < 7h
θ_i > 18 or 20°C
φ_i < 70 %
No rainfall
v < 14 m/s

3.2.2 EVALUATION OF THE PERFORMANCES (DESCHEEMAEKER, 2004)

To evaluate the operation and the performances of the natural night ventilation system, continuous measurements of the temperatures from the Building Management System (BMS) (May 1 to September 30, 2003) are analysed.

3.2.2.1 NATURAL NIGHT VENTILATION

Monitoring the effective system performance shows the system was in operation every night between May 28 and August 27 and 8 days during the second half of September. Control parameters were fine-tuned in this period. Fig. 3.12 shows temperatures, relative humidity and operation of ventilation openings during the first week of the heat wave in August (see below). The highest relative humidity (between 60 and 70%) and the lowest temperatures were noticed in the morning. Inlet windows were generally opened during the whole night. Outlet windows were separately controlled and opened and closed several times a night.
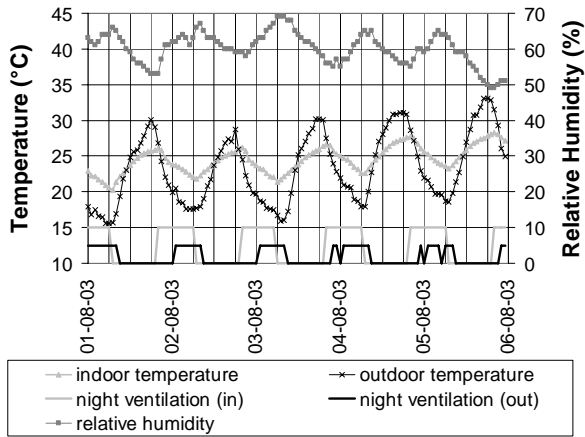
Fig. 3.12 Measured indoor and outdoor temperature, indoor relative humidity and operation of ventilation openings during a heat wave.

The performance of natural night ventilation is analysed based on the achieved temperature drop overnight (between 9 p.m. and 8 a.m. the next day). Fig. 3.13 shows that the temperature drop in the landscaped office hardly depends of the mean indoor-outdoor temperature difference during the night. Similar results are noticed in the reception and accountancy offices. This can be explained by the control system, which closes the windows when the indoor air temperature is lower than 18 or 20°C.
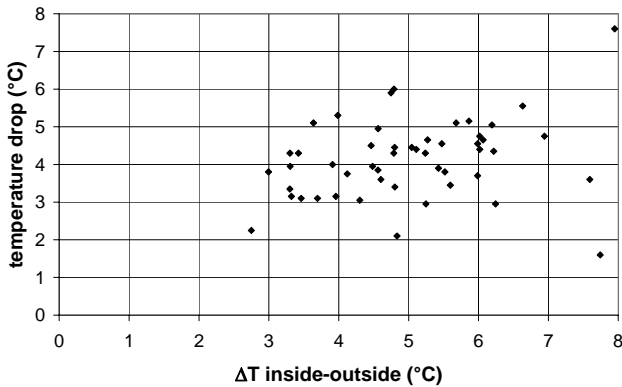

Fig. 3.13 Temperature drop in the landscaped office as a function of the mean indoor-outdoor temperature difference during the night

The average indoor-outdoor temperature difference during night when night ventilation was in operation is also measured. It can be noticed that in 95 % of the cases a temperature drop of 3°C and 2°C is exceeded in the open plan office and the reception and accountancy offices respectively.

3.2.2.2 THERMAL COMFORT

The thermal comfort, measured in the open plan office, reception desk and accountancy office are discussed and compared. Only the latter office is provided with a mechanical cooling system.

Measurements from May to September 2003 are used in this analysis. According to the Royal meteorological institute of Belgium (RMI, 2003), the summer of 2003 was extremely warm and sunny. Normal mean outside temperature was exceeded nearly every day. Furthermore, during the first two weeks of August a heat wave occurred: temperature peaks of more than 37°C were measured on 4 days. Fig. 3.14 compares the statistics from May 15 to September 30 of the daily average external temperatures measured on site to the external temperatures of test reference year (TRY) in Uccle, which are normally used in design calculations to assess thermal comfort. The comparison is in agreement with the conclusions of the RMI.
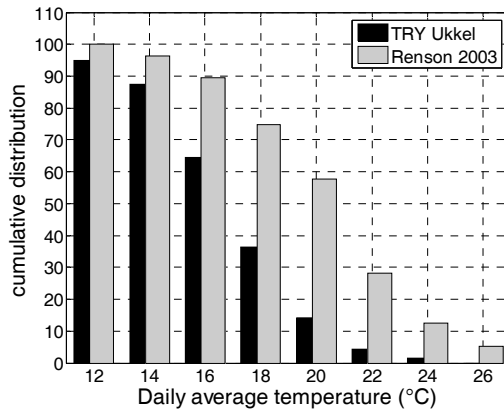

Fig. 3.14 Comparison of cumulative daily average outside temperature distributions on site versus Test Reference Year (TRY) Uccle (Belgium) (May 15 – September 30).

The temperature excess method (GBA, 1999) and the adaptive temperature limits indicator (van der Linden et al., 2006) are used to evaluate the dynamic thermal comfort. Firstly, Fig. 3.15 shows the measured temperature excess hours in the open plan, reception and accounting offices. The temperatures in the landscaped office are generally higher than in the other offices because of solar heat gains in the evening. The glazed northwest oriented façade of the landscaped office lacks sun blades. Compared to the other rooms, the exceeding hours in the accountancy offices with mechanical cooling are extremely reduced. In the open plan office, the daily maximum indoor temperature occurred in the late afternoon (at 4 or 5 p.m.). In other offices, with southwest orientation and external solar shading devices, the maximum temperatures were reached during the whole afternoon, depending on the actual weather (from 12 a.m. to 5 p.m.). The measured exceeding hours are 69h, 47h and 34h for respectively the open plan office, reception desk and accountancy office. Compared to the performance criterion of 100 exceeding hours above 26°C, the thermal comfort in all offices proves to be acceptable, especially considering the extremely warm and sunny weather. However, the additional requirement of maximum 20 exceeding hours above 28°C, is not met in the landscaped office. 25 exceeding hours were measured in this room, particularly occurring during the August heat wave. Considering the exceptional occurrence of such weather, it can be concluded that the requirement will be fulfilled in a normal summer.
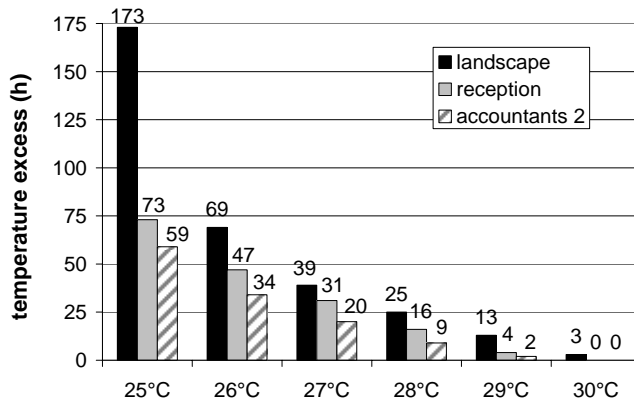
Fig. 3.15 Temperature excess in landscape office, reception and accountancy offices.

Secondly, Fig. 3.16 and Fig. 3.17 show the measured daily maximum and minimum indoor temperatures during occupancy, compared to the adaptive temperature limits indicator. The measured maximum temperatures confirm the conclusions of the temperature excess method. The observed thermal comfort is good (Level A or B) as long as the outdoor temperatures are not extremely high ($T_{e,ref} < 25°C$). Only during the August heat wave, which had a running mean outdoor temperatures above 26°C, the acceptability level of 65% is not met in the landscaped office over 3 days. Furthermore, the analysis of the measured minimum temperatures during occupancy reveals a more systematic comfort problem. The operative temperatures occurring at 8 a.m. when occupants arrive are often smaller than the 65%-acceptability limit and might cause complaints of discomfort. This is caused by an inadequate set point in the night ventilation control algorithm. During the measurements, the inside temperature set-point for closing the inlet and outlet windows was set at 20°C in the landscaped office and 19°C in reception and accountancy offices. To solve the problem and achieve a good indoor comfort this control set point should be increased.
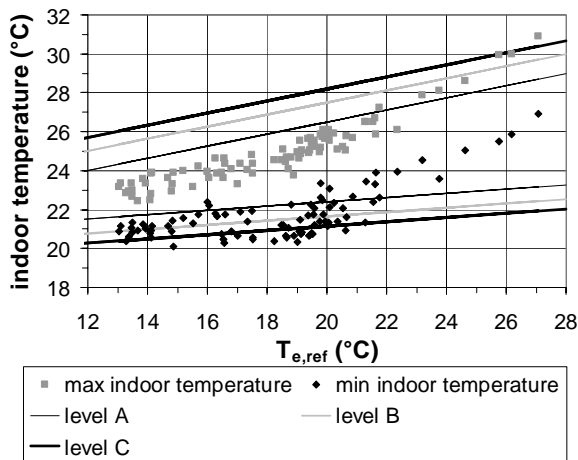

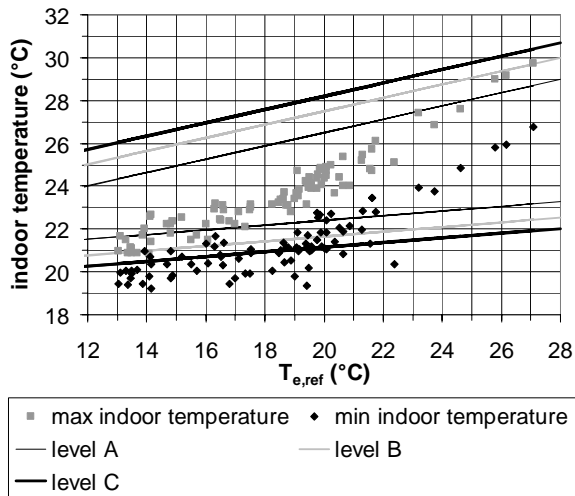Fig. 3.16 Adaptive temperature limits indicator in the landscape office

Fig. 3.17 Adaptive temperature limits indicator in the reception desk

3.3 CONCLUSIONS

Natural night ventilation is applied in the Belgian office buildings of SD Worx (Kortrijk) and Renson (Waregem). The indoor summer thermal temperatures were measured in both buildings to evaluate the performances. These two examples show that the requirements of good thermal comfort can be met in a moderate climate in case of a low cooling load. However, natural night ventilation does not perform well when the outdoor temperatures are extremely high. It can also be concluded from these office buildings that the control system has an important impact on the performances of this passive cooling technique. It determines the temperature drop overnight in the offices and can prevent overcooling in the morning. In addition, the building design has to be adapted to natural night ventilation: e.g. a low flow resistance between supply and extract openings is required, passive stacks need to be provided, acoustic adjustments to the floor or walls are an inevitable consequence of an exposed ceiling.

4 Building Simulation

This chapter discusses the methods used to evaluate the performances of natural night ventilation thereby taking the uncertainties in the input into account. Firstly, a building simulation tool to predict the thermal comfort is selected and its principles are discussed. Secondly, a method for uncertainty and sensitivity analysis is selected. Finally, the uncertainties on the input parameters are discussed. The physical background of each input parameter is discussed and the uncertainty interval is defined. For that, the input parameters are subdivided in three categories: boundary conditions, building and system characteristics.

4.1 Building simulation tool

4.1.1 Overview and selection

Chapter 2 discusses the criteria defining the performances of natural night ventilation and the related requirements. Moreover, simplified tools are presented to assess whether these requirements are fulfilled in general or in the pre-design stage. To evaluate the performances of a designed natural night ventilation system in a particular project in detail, building simulation is used. Two kinds of tools can be distinguished. Firstly, thermal building simulation tools evaluate the thermal comfort and calculate the indoor temperature and the energy consumption, given the building characteristics, outdoor climate and ventilation rates. Secondly, given the building characteristics, the outdoor climate and the indoor temperatures, ventilation (analyzing) tools predict the air flows through the building and the indoor air quality. These latter tools can be subdivided into three groups (Delsante and Vik, 2002):

- Multi-zone or network airflow models, which divide the building into zones corresponding to the rooms, assuming that the air in these zones is perfectly mixed. Stating the mass balance in each zone allows to solve the bulk flows through the whole building which are caused by wind, temperature differences and/or building operation. The advantages are a user-friendly problem definition (input) and a straightforward calculation procedure. However, these tools cannot predict the temperature and airflow distributions within a room.
- Computational Fluid Dynamics (CFD) models are suited to analyze air movement in and around buildings in great detail. Two- or three-dimensional airflow and thermal distribution patterns in a room can be predicted. The room is subdivided in a large number of small cells. In each of these cells, the equations of conservation of mass, energy and momentum are solved iteratively. The disadvantages of CFD are laborious model set-up and a large computation time.
- Zonal models might be considered as an intermediate approach between the two above-mentioned models. Zonal models provide a global indication of the airflow and temperature distributions in a room and are relatively easy for users to define the problem.

In this work, a network airflow tool is selected and consequently coupled or integrated with a thermal building model to simulate natural night ventilation because this tool can assess a whole-building and whole-year performance in a limited computation time (Delsante and Vik, 2002). Coupling or integration with a thermal model is necessary because the internal temperatures in a naturally ventilated building depend on the ventilation flow rates. And as natural night ventilation is partly temperature driven, these flow rates on their turn are

function of the indoor air temperatures (Breesch and Janssens, 2002). Moreover, airflow network tools are user-friendly and can therefore easily be used by designers and engineering companies to predict the performances of natural night ventilation.

An extended comparison of (multi-zone) thermal building simulation tools is given among others by Crawley et al. (2005). An overview of ventilation (network) models is found in Feustel and Dieris (1992), Delsante and Vik (2002) and Orme (2002). Hien et al. (2000) give an overview of all kinds of performance-based tools for building design and evaluation.

4.1.2 TRNSYS-COMIS

The existing coupling between TRNSYS (Klein et al., 2004), a transient multi-zone thermal simulation model, and COMIS (Feustel, 1999), (Dorer et al., 2001), a multi-zone infiltration and ventilation simulation model, is chosen to predict the thermal comfort in a building, cooled with natural night ventilation.

4.1.2.1 DESCRIPTION

Both TRNSYS and COMIS subdivide the building in various zones, mostly corresponding to the rooms, in which the air is assumed to be perfectly mixed.

4.1.2.1.1 TRNSYS

In TRNSYS, a zone is represented by two temperatures: the homogeneous air temperature T_i and the so-called star temperature T_{star} (Seem, 1987). Each internal surface is additionally characterized by one surface temperature T_s (see Fig. 4.1). To calculate these temperatures, equations Eq. 4.1-4.6 have to be solved. First of all, the convective heat flow balance of zone i is given by Eq. 4.1 (see also Eq. 2.3).

$$\Phi_{s,i} + \Phi_{inf,i} + \Phi_{v,i} + \Phi_{g,c,i} + \sum \Phi_{cplg,j-i} = C_i \frac{dT_{i,a}}{dt}$$

<div align="right">Eq. 4.1</div>

where $\Phi_{s,i}$ is the convective heat flow from the internal surfaces, Φ_{inf} the infiltration heat gain, $\Phi_{v,i}$ the ventilation heat gain, $\Phi_{g,c,i}$ the internal convective heat gains, $\sum \Phi_{cplg,j-i}$ the gains due to airflow from adjacent zones j to zone i and C_i the thermal capacity of zone i.

Secondly, Eq. 4.2 presents the heat balance of an internal surface m (see also Eq. 2.4):

$$q_{s,i,m} + S_{s,m} + WG_m = q_{c,s,m} + q_{r,s,m}$$

<div align="right">Eq. 4.2</div>

where $q_{s,i,m}$ is the conduction heat flux from the wall at the internal surface, $S_{s,m}$ the radiative heat gains absorbed at the internal surface m, e.g. solar and internal heat radiative gains and WG_m is a user-defined energy flow to the inside wall surface, e.g. floor heating, $q_{c,s,m}$ the convective heat flux from the internal wall m to the zone air, $q_{r,s,m}$ the net radiant heat flux from surface m to all other surfaces in the room.

Thirdly, in order to solve the convective and radiative heat flows to the wall surfaces, TRNSYS introduces the concept of the 'star network'. Fig. 4.1 shows this star network and the relations between the air, surface and star temperatures for a zone with three surfaces.

The star temperature is noticed the weighted average of the zone air temperature and the surface temperatures of the walls surrounding the zone. This star temperature differs from the operative temperature, which also is a weighted average of the air and mean radiant temperature. This latter weighting factor is user-defined, mostly 0.5.

The relations between T_{star} and T_i, and T_{star} and $T_{s,m}$ are respectively defined as follows:

$$q_{c,s,m} + q_{r,s,m} = \frac{1}{R_{equ,m} A_{s,m}} \left(T_{s,m} - T_{star} \right)$$

Eq. 4.3

$$\Phi_{s,i} = \frac{1}{R_{star}} \left(T_{star} - T_{i,a} \right)$$

Eq. 4.4

Finally, R_{star} and $R_{equ,m}$ (in K/W) are determined by minimizing following estimations for each internal surface m:

$$R_{equ,m} + R_{star} \cong R_{c,m-i}$$

Eq. 4.5

$$R_{equ,m} + R_{equ,k} \cong R_{r,m-k}$$

Eq. 4.6

where $R_{equ,m}$ is the equivalent resistance between the surface temperature and the star temperature, R_{star} the star resistance, $R_{c,m-i}$ the convective resistance between surface m and the air, $R_{r,m-k}$ the radiant resistance between the internal surfaces m and k.
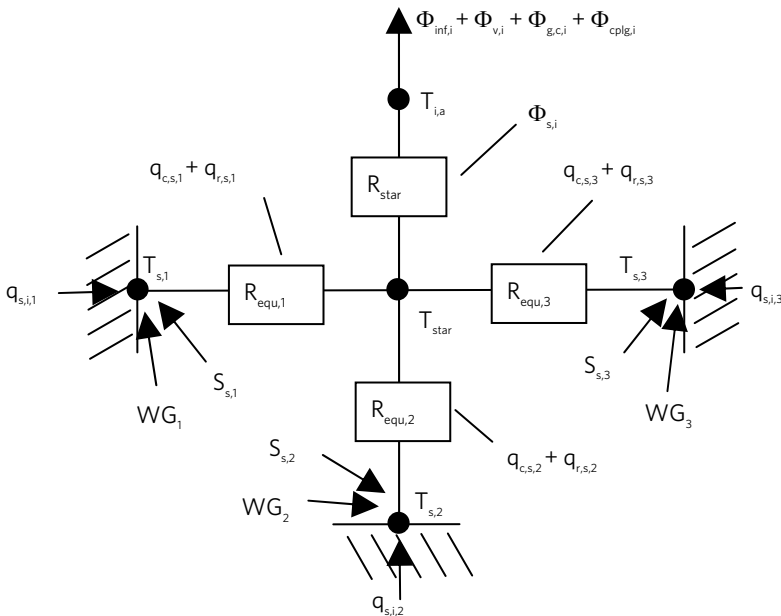

Fig. 4.1 Internal heat transfer by convection and radiation are calculated in TRNSYS by an artificial star network (Klein et al., 2004)

The star concept was introduced to facilitate the calculation of conduction heat loss over a wall. This is modelled according to transfer function relationships as follows (Klein et al., 2004):

$$q_{s,i} = \sum_{k=0}^{n_{b_s}} b_s^k T_{s,o}^k - \sum_{k=0}^{n_{c_s}} c_s^k T_{s,i}^k - \sum_{k=1}^{n_{d_s}} d_s^k q_{s,i}^k \qquad \text{Eq. 4.7}$$

$$q_{s,o} = \sum_{k=0}^{n_{a_s}} a_s^k T_{s,o}^k - \sum_{k=0}^{n_{b_s}} b_s^k T_{s,i}^k - \sum_{k=1}^{n_{d_s}} d_s^k q_{s,o}^k \qquad \text{Eq. 4.8}$$

where $q_{s,i}^k$ and $q_{s,o}^k$ are the conduction heat flux respectively from the wall to the internal surface and into the wall from the external surface at preceding calculation time steps k, $T_{s,i}^k$ and $T_{s,o}^k$ respectively the internal and external surface temperatures and a_s^k, b_s^k, c_s^k and d_s^k the transfer coefficients at current and preceding calculation time steps k. These coefficients are determined in TRNSYS from the thermophysical properties of the wall.

The transfer functions describe the heat flux at one side of the wall varying in time depending on a change of the heat flux at the other side of the wall or on a change of the surface temperature at one of both sides of the wall. In other words, they tell the 'thermal history' of a wall. The number of time steps k of the transfer coefficients shows whether the wall has a high or low thermal mass. A comparison of the transfer coefficient b_s^k, which gives the impact of the outdoor temperature on the internal heat flux, between a high and low thermal capacitive wall with the same thermal resistance is given in Fig. 4.2. It can be noticed that the influence of a variation in outdoor temperature on the internal heat flux is attenuated and postponed in the high capacitive wall compared to the wall with low capacity.
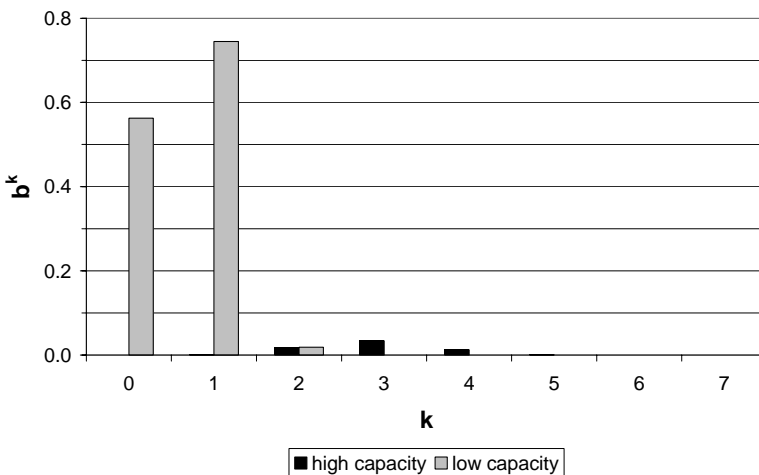

Fig. 4.2 Comparison of the transfer coefficient b^k of a high to a low capacitive wall with the same thermal resistance

The advantage of this method is that the transfer coefficients are only calculated once. However, surface temperatures and heat fluxes from previous time steps have to be stored. These transfer functions are noticed to generate problems in case of thick or capacitive walls. This disadvantage could be anticipated by numerically solving the heat conduction over a wall by the control volume method. In this method, a wall is divided in a grid of elementary elements or volumes with constant thermo physical properties. In each volume, the energy balance is formulated. This set of equations can be solved when the boundary conditions are known and results in the unknown surface temperatures (Hens, 1997). However, as in this method a large set of equations has to be solved each time step, it is more time-consuming. This method is not applied in TRNSYS.

Transmission of solar radiation is calculated by a detailed window model in TRNSYS based on the output data of the program WINDOW (LBNL, 2003), which determines in detail the thermal and solar optical properties of glazing and window systems. The distribution to the internal surfaces of the short-wave radiation entering the zone has to be specified by the user. Long-wave radiative and convective heat transfer are defined in the star network (see above). The absorbed short-wave radiation of the window panes determines the indoor surface temperature of the window. In addition, external shading devices reduce the incoming solar radiation on the glazing area of the window by a factor given in the building description in TRNSYS. In addition, a thermal resistance that reduces the heat losses of the glazing to the ambient may be specified.

4.1.2.1.2 COMIS

In COMIS, each zone is represented by single values for the air temperature and pressure and connected to other internal zones and the external environment by air flow paths. An example of this network representation is shown in Fig. 4.3.
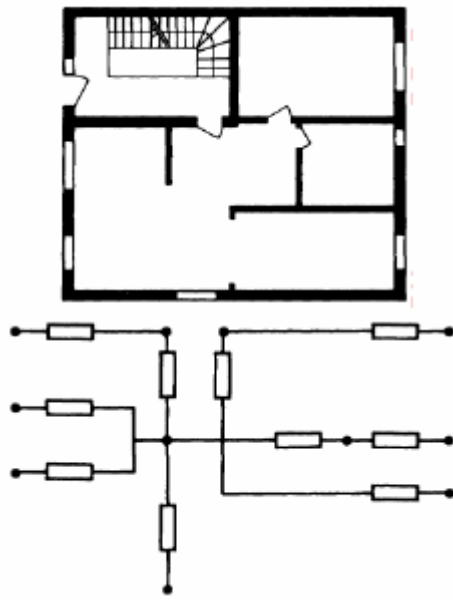

Fig. 4.3 Floor plan of a building and its representation in a nodal network (Feustel, 1999)

The pressure difference over a flow path is already defined in Eq. 2.1. A non linear equation relates the flow rate through a flow path to this pressure difference. Air leaks, air leakages in closed large openings and fans out of action are represented by the power law equation (Eq. 4.9):

$$G = C(\Delta p)^n$$

Eq. 4.9

where G is the mass flow rate (kg/s), Δp the air pressure difference inside-outside (Pa), C the flow coefficient (kg/s.Pa^n) and n the dimensionless flow exponent. These coefficients are further discussed in paragraph 4.3.3.4 and 4.3.4.1.

The airflow through large vertical openings like windows and doors is two-directional steady-state gravitational as shown in Fig. 4.4. On each side of the opening, linear density stratification is assumed. Consequently, a large vertical opening can have two, one or zero neutral pressure levels (Allard and Utsumi, 1999). Nevertheless, the solution without density gradients is applied in the simulations in the following chapters. In addition, the wind turbulence effect is not taken into account. The locations of the neutral pressure levels are given by equilibrium in pressure. The flow direction through the opening consequently changes on this level. The mass flow for each part of the opening with different flow direction, caused by density differences, is calculated as follows. The total mass flow rate is obtained by summation of these flows for the whole opening (Feustel, 1999).

$$G_i = C_d w_{eff} \int_{z_0}^{z_t} \rho_i v_i(z) dz = \frac{2}{3} C_d w_{eff} (z_t - z_0)^{3/2} \sqrt{2g\rho_i(\rho_e - \rho_i)}$$

Eq. 4.10

$$G_e = C_d w_{eff} \int_{z_b}^{z_0} \rho_e v_e(z) dz = \frac{2}{3} C_d w_{eff} (z_0 - z_b)^{3/2} \sqrt{2g\rho_e(\rho_e - \rho_i)}$$

Eq. 4.11

where G_i and G_e is the mass flow rate of the air flowing out and into the room respectively, v_i and v_e the velocity of the air flowing out and into the room respectively, ρ_i and ρ_e the density of the internal and external air respectively, z_0 the neutral pressure level, z_t and z_b the heights of the top and the bottom of the opening respectively, C_d the discharge coefficient, and w_{eff} the width related to the effective area of the opening. The effective area is defined as the geometrical permeable section of the opening. The discharge coefficient is discussed in detail in paragraph 4.3.4.1.

$$\rho_1(z) = \rho_{01} + b_1 z \qquad \rho_2(z) = \rho_{02} + b_2 z$$

$$ZN_2 \qquad ZN_1$$

$$P_{01} \qquad \rho_{01} \qquad O \qquad \rho_{02} \qquad P_{02}$$
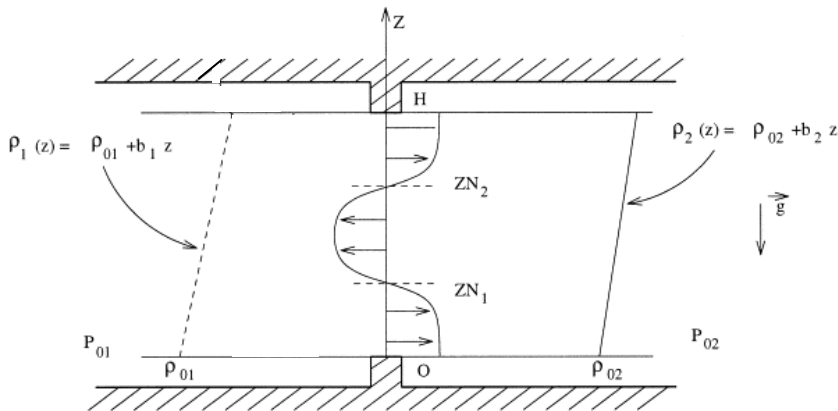
$$H \qquad \vec{g}$$

Fig. 4.4 Gravitational flow through a vertical opening (Feustel, 1999)

The steady-state mass conservation laws for each zone constitute a set of non-linear equations. The Newton-Raphson's method solves this non-linear problem by an iteration of the solutions of linear equations. The pressure of all the nodes is simultaneously updated. Relaxation is applied in order to accelerate the convergence and consequently reducing the number of iterations (Haghighat and Rao, 1991). This iterative solution defines the pressure in each zone and the air flow through every link.

The simulation code of COMIS has been integrated into TRNSYS (Dorer and Weber, 1999), (Haas et al., 2002). TRNSYS and COMIS iterate the mass and energy balance per zone, i.e. using the results from the other model, till convergence is achieved in each time step, i.e. the 'onions method' (Hensen, 1995). This default successive substitution solver can be enhanced in case of natural ventilation by adding automatically adapted relaxation to ensure convergence and find consistent solutions of the two models (Weber et al., 2003), (Klein et al., 2004).

4.1.2.2 VALIDATION

The thermal building model TRNSYS and the air flow model COMIS have been validated (Lomas et al., 1997), (Fürbringer et al., 1996), (Delsante and Aggerholm, 2002).

Lomas et al. (1997) compared 25 dynamic thermal simulation programs among which TRNSYS version 12 and 13.1 and studied their experimental validation. The predictions of heating energy demand and air temperatures were compared. Empirical data were obtained in rooms representing typical lightweight rooms in UK dwellings in terms of the level of insulation, the amount of thermal mass and the window-to-floor area ratio. Data were measured in two 10-day experiments in rooms with and without heating and with and without glazing. When no heating was applied, the peak air temperature was under predicted in the glazed room by TRNSYS, although, the minimum temperature was included in the error band of the measured value. The minimum and maximum air temperatures in the opaque room were well predicted by TRNSYS. Moreover, the predicted south-facing vertical solar irradiance was within the error bands of the measurements.

Fürbringer et al. (1996) evaluated COMIS within IEA Annex 23. A sensitivity analysis, an analytical comparison, an inter-model comparison, a comparison with experiments and a

user test were carried out. The analytical comparison showed that in a limited number of cases the solutions of COMIS correspond to what is expected. Moreover, inter-model comparison of COMIS to 14 other models showed that COMIS is able to predict the air and contaminant flows as well as many of these other models. The agreement of measurements and calculated global airflows within the range of a relative error of $\pm$ 25% has been verified. This difference is mainly caused by the description of the actual network and the determination of the boundary conditions. Furthermore, the user test showed that the user introduced uncertainty is as large as the experimental induced uncertainty.

Delsante and Aggerholm (2002) studied control strategies for hybrid ventilation systems and compared the results of TRNSYS-COMIS to those of three other tools. In terms of relative performance of the control systems, the tools are most consistent with respect to CO_2 concentrations but are less consistent regarding the heating energy in winter, because of different implementation of the heating controller. The tools agree quite well for the mean temperature in winter; the agreement is less good for the maximum temperature. The differences between maximum and mean temperatures in summer between the tools are small but consistent. The tools agree well on the effect of mechanical night cooling. Therefore, TRNSYS-COMIS seems a suitable tool to predict the performances of natural night ventilation.

4.2 Uncertainty and sensitivity analysis

To take the uncertainties on the input in the building simulation tool into account, uncertainty and sensitivity analysis are applied. Uncertainty analysis defines the variation or uncertainty in the output of a model due to the variations in the input. Sensitivity analysis is used to study qualitatively or quantitatively, how this variation in the model output is attributed to the variations in the input (Saltelli et al., 2000), (Macdonald, 2002).

4.2.1 Uncertainty and sensitivity analysis in building simulation

As already mentioned in chapter 1, designers require information on performance robustness rather than performance quantification with no account taken of uncertainty, to make effective use of simulation (Macdonald and Strachan, 2001). Moreover, a probability distribution curve gives substantially more information to decision makers than the outcome of one single simulation (Wouters, 2000). Consequently, uncertainty analysis is an interesting method to predict the performances of natural night ventilation with building simulation.

Both uncertainty and sensitivity analysis have already been applied in building simulation. With regard to uncertainty analysis, de Wit (2001) concluded that the variability in the thermal comfort performance is significant in a naturally ventilated office building. Fig. 4.5 shows the distribution of the thermal comfort performance indicator temperature excess hours (see paragraph 2.1.3.4.2.1) of a sample of 250 simulations. Furthermore, Macdonald (2002) implemented uncertainty analysis in the code of the building simulation software ESP-r (ESRU, 2005). Pietrzyk and Hagentoft (2005) developed a probabilistic model to predict the distribution of the air change rate for a naturally ventilated house based on variations in climatic conditions. Wouters et. al (2004) proposed a probabilistic approach to assess innovative systems in the regulations of the Energy Performance of Building Directive (EU, 2002). Furthermore, sensitivity analysis is widely used in model validation; see among others Borchiellini and Fürbringer (1999), Fürbringer et al. (1999), Aude et al. (2000).
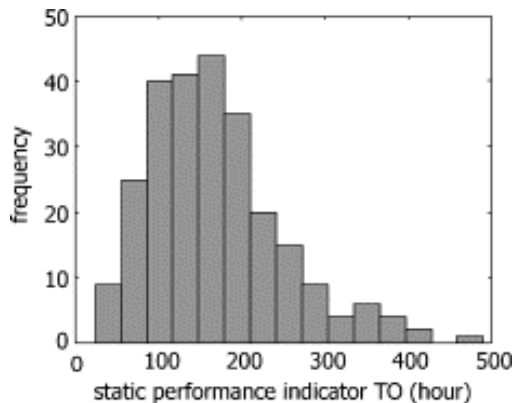

Fig. 4.5 Histogram of the thermal comfort performance indicator TO (GBA, 1999) of a sample of 250 simulations (de Wit, 2001)

Applying sensitivity analysis on the results of building simulation have shown that the following parameters have the most important impact on the prediction of thermal comfort (de Wit and Augenbroe, 2002), indoor (air) temperature (Aude et al., 2000) and ventilation flow rates (Fürbringer et al., 1999): wind related factors (wind pressure coefficients, wind reduction parameters and velocity), temperatures (outdoor and indoor gradient), characteristics of the environment (internal and external heat transfer coefficient and albedo), ventilation openings characteristics (discharge coefficient, air tightness) and glass properties (transmission coefficient and area).

4.2.2 Overview methods sensitivity analysis (Saltelli et al., 2000)

An overview of sensitivity analysis methods used in building simulation can be found in (Lomas and Eppel, 1992), (Fürbringer and Roulet, 1995), (Fürbringer and Roulet, 1999), (Purdy and Beausoleil-Morrison, 2001). Three groups can be distinguished:

- Screening methods are essentially qualitative sensitivity methods because they identify the parameter subset controlling most of the output variability and rank these input factors in order of importance. Screening is usually the first step in a sensitivity analysis when dealing with a model containing a large number of inputs.
- Local sensitivity quantitatively investigates the local impact of the input factor uncertainties on the model results. It is usually carried out by computing the partial derivates of the output functions with respect to the input variables. To compute the derivatives numerically, the input factors are varied around a nominal value within a small interval, which is usually the same for all factors. Local sensitivity is discouraged when the model is nonlinear and the input variables are affected by uncertainties of different orders of magnitude. Therefore, local sensitivity will not be discussed further.
- Global sensitivity quantitatively evaluates the effect of one parameter while all other parameters are varied as well. This method additionally incorporates the influence of the whole range of variation of the input parameters, typically described by a probability distribution.

An overview of methods for screening design and global sensitivity and their advantages and disadvantages will be discussed in the following paragraphs.

4.2.2.1 Screening designs

Screening designs are preliminary numerical experiments aiming to isolate the most important factors among a large number of influencing model parameters. Typical examples of screening designs are discussed (Saltelli et al., 2000), (Trocine and Malone, 2000).

4.2.2.1.1 One-at-a-time (OAT)

One-at-a-time (OAT) experiment evaluates the impact of each factor in turn. This method can be easily applied. No simplifying assumptions about the model are made. Moreover, the number of runs is proportional to the number of input factors. The major limitation of this method is that the interactions between input factors are not determined, i.e. only the first-order effects are defined. An example of a global approach is the OAT design proposed by Morris (1991).

4.2.2.1.2 Factorial design

Factorial design on the other hand evaluates first as well as high-order effects. Due to this, the computational cost is high and equals l^k, where k is the number of factors and l the number of possible values of these factors. Consequently, factorial design is only suitable for a small number of variables, i.e. less than 20. The number of required runs is reduced in derived methods, like fractional factorial design and systematic fractional replicate design (Cotter, 1979).

4.2.2.1.3 Iterated fractional factorial design (IFFD)

Iterated fractional factorial design (IFFD) (Saltelli et al., 1995) examines the main and quadratic effects and the two-factor interactions of the influential factors. This method requires fewer simulations than the number of factors. Therefore, it suits simulations with a large amount of parameters (> 1000). The input parameters are screened in group with fractional factorial design. IFFD requires that the effects of a few highly influential factors dominate the model output.

4.2.2.1.4 Sequential bifurcation

Sequential bifurcation (Bettonvil and Kleijnen, 1997) is also a group-screening technique suitable for a large amount of parameters (> 100) as it requires fewer runs than the number of factors. It investigates the main effects and two-factor interactions. Sequential bifurcation is a simple, efficient and effective screening design. Its major limitation is that the sign of the main effects must be known and that the model output is approximated by a polynomial. De Wit (1997) compared sequential bifurcation to Morris' OAT design to identify the important parameters in thermal building simulation. He concluded that both screening designs identified the same set of important parameters. The identification of these parameters with sequential bifurcation required only 1/5 of the number of model evaluations necessary for the Morris' design. However, sequential bifurcation could only be reliably applied after the results of Morris' OAT were known. These results revealed significant interactions, showed that a priori estimation of the signs of several parameter main effects was erroneous and supplied information to facilitate optimal clustering of parameters.

4.2.2.2 Global sensitivity

Contrary to a screening design, global sensitivity defines quantitatively the global effect of all input parameters and can be subdivided into the following methods.

4.2.2.2.1 Monte Carlo Analysis

Monte Carlo Analysis (MCA) performs multiple evaluations with randomly selected model input factors. Both sensitivity and uncertainty can be determined based on these results. Moreover, MCA can deal with correlated input parameters. The following steps are successively carried out in a Monte Carlo Analysis: (1) selection of a range and distribution for each input parameter, (2) sample generation from these distributions, (3) evaluation of the model for each element of this sample, (4) uncertainty analysis and (5) sensitivity analysis. Several indicators for sensitivity analysis are defined, based on correlation or regression analysis. They assume that the output and input factors are near-linearly or near-monotonically related. The computational cost is low and depends on the method for generating a sample (see below). In case of Latin Hypercube sampling, the minimum number of a representative sample is 1.5 x k, where k is the number of input factors.

4.2.2.2.2 Variance-based methods

Variance-based methods estimate the contribution of the input parameters in the variance of the output as an indicator of importance. Eq. 4.12 shows a suitable measure of the importance of X_i. The numerator is the variance of the conditional expectation of Y, conditioned on X_i. It expresses how well the variability in the expectation $E(Y|X_j)$ as X_i varies, mimics the total variation in y. The main drawback of the variance based measures is their computational cost as they require N*(k+2) evaluations where k is the number of factors and N is of the order of N = 500. Other variance-based methods are Sobol' Sensitivity Indices (Sobol', 1993) and Fourier amplitude sensitivity test (FAST) (Cukier et al., 1973). The computational cost is reduced to minimum 65 simulations for each (group of) input parameters but is still high.

$$\frac{Var_{X_j}\left[E(Y|X_j)\right]}{Var(y)} \qquad \text{Eq. 4.12}$$

4.2.3 Requirements and selection

The main requirement to select a method of sensitivity analysis is a low computational cost, i.e. a restricted number of simulations, taking into account that the number of parameters in a simulation of natural night ventilation is approximately 70. In addition, a quantitative method is preferred to a qualitative.

Therefore, a method for global sensitivity is chosen to calculate the sensitivity of the predicted thermal comfort of natural night ventilation. Sensitivity indicators based on Monte Carlo Analysis are chosen because their computational cost is low compared to other methods. Moreover, both uncertainty and sensitivity analysis can be performed using this same method. The assumptions of near-linearly or near-monotonically related input parameters will be checked. MCA has already been successfully implemented in building simulation (de Wit, 2001), (Macdonald, 2002), (Wouters et. al, 2004). The statistical software SIMLAB (POLIS, 2003) will be used to prepare the samples and to analyse the results. The steps included in this method are examined in detail in the following paragraphs.

4.2.3.1 Generation of a sample (Saltelli et al., 2000)

Various sampling procedures are used in MCA studies. The Latin Hypercube sampling strategy will be used in the analysis of the performances of natural night ventilation because this method ensures full coverage of the range of each variable. The sample space is exhaustively divided into a number of non-overlapping regions or strata. One value is then randomly sampled from each sub region. In particular, the range of each variable is divided into N non-overlapping intervals of equal probability 1/N. One value from each interval is randomly selected. These N values of the first input factor are step-by-step and at random combined with N randomly chosen values of each other input factor. The generation of an LHS of size N = 5 from k = 2 factors U and V is illustrated in Fig. 4.6. The ranges of U and V are subdivided in 5 intervals of equal probability. Then, random values from both intervals are sampled and combined. LHS is used when large samples are not computationally practicable. It performs better than random sampling when the output is dominated by only a few components of the input factors. Moreover, when the output is a monotonic function, LHS is better than random

sampling. The minimum number of model evaluations, required for LHS for a representative sample, is one and a half times the number of input factors k (POLIS, 2003).
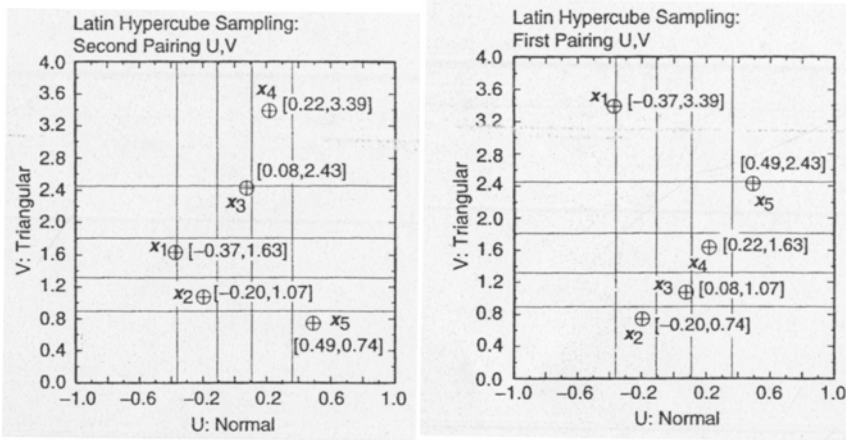

Fig. 4.6 Examples of Latin Hypercube sampling to generate a sample size of N = 5 from 2 factors U and V (Saltelli et al., 2000)

4.2.3.2 UNCERTAINTY ANALYSIS

The determination of the uncertainty analysis is straightforward. The expected average value and variance of the output y are estimated by respectively Eq. 4.13 and Eq. 4.14:

$$\hat{\mu}(Y) = \frac{1}{N} \sum_{i=1}^{N} y_i \qquad \text{Eq. 4.13}$$

$$\hat{V}ar(Y) = \frac{1}{N-1} \sum_{i=1}^{N} \left[y_i - \hat{\mu}(Y) \right]^2 \qquad \text{Eq. 4.14}$$

where y is the output, i the sample and N the total number of samples.

4.2.3.3 SENSITIVITY ANALYSIS

The Standardized regression coefficients (SRC) will be applied to determine the sensitivity of the thermal comfort in a building, cooled with natural night ventilation. This quantitative measure of sensitivity is based on regression analysis. A linear regression model is made, based on a N*k sample:

$$\hat{y}_i = b_0 + \sum_{j=1}^{k} b_j x_j \qquad \text{Eq. 4.15}$$

where $\hat{y}_i$ is the estimate of the output y_i, x the input factor, i is the sample, N the total number of samples, j the input factor, k the total number of input factors and b the regression coefficient. This regression model can be standardized by subtracting the mean value from each input and output factor and successively dividing this result by its standard deviation (see Eq. 4.16).

$$\frac{\hat{y} - \mu(y)}{\hat{\sigma}} = \sum_{j=1}^{k} \frac{b_j \hat{\sigma}_j}{\hat{\sigma}} \frac{\left(x_j - \mu(x_j)\right)}{\hat{\sigma}_j}$$

$$\text{with } \mu(y) = \sum_{i=1}^{N} \frac{y_i}{N}, \ \mu(x_j) = \sum_{i=1}^{N} \frac{x_{ij}}{N} \qquad \text{Eq. 4.16}$$

$$\hat{\sigma} = \left[\sum_{i=1}^{N} \frac{\left(y_j - \mu(y)\right)^2}{N-1}\right]^{1/2}, \ \hat{\sigma}_j = \left[\sum_{i=1}^{N} \frac{\left(x_{ij} - \mu(x_j)\right)^2}{N-1}\right]^{1/2}$$

The coefficients $\frac{b_j \hat{\sigma}_j}{\hat{\sigma}}$ in Eq. 4.16 are called standardized regression coefficients (SRCs). When the input parameters x_i are independent, the SRCs provide a measure of variable importance since SRC measures the effect of the variation of an input parameter x_i with a fixed fraction of its standard deviation on the variation of the output y, while all other input parameters equalize their expected value. Both the distribution of the input x_i and its impact on the output affect the SRC.

Using SRC, the model coefficient of determination R_y^2 (Eq. 4.17) has also to be calculated to evaluate how well the linear regression model $\hat{y}_i$ reproduces the actual output y_i. R_y^2 represents the fraction of variance on the output, explained by the regression model. For a good estimation, the model coefficient of determination has to be close to unity.

$$R_y^2 = \frac{\sum_{i=1}^{N}\left(\hat{y}_i - \mu(y_i)\right)^2}{\sum_{i=1}^{N}\left(y_i - \mu(y_i)\right)^2} \qquad \text{Eq. 4.17}$$

Since regression analysis is based on linear relationships between output and input variables, it often performs poorly for non-linear models with a low value of R_y^2 computed on the raw values. Rank transformation can be applied to avoid this problem. It is a simple procedure, which involves replacing the data by their corresponding ranks. Specifically, the smallest value of each variable is assigned rank 1, the next smallest rank 2 and so on up to the largest value rank N. The regression model is then based on these ranks. Consequently, if the model coefficient of determination R_y^{*2} based on the rank-transformed model, is higher than R_y^2, based on the raw data, the standardized rank regression coefficient (SRRC) can be used for sensitivity analysis instead of SRC. The difference between R_y^{*2} and R_y^2 is a useful indicator of the nonlinearity of the model. The performance of SRRC is shown to be very satisfactory when the model output varies monotonically with each input variable because the use of rank-transformed data results in an analysis based on the strength of monotonic rather than on linear relationships. Attention has to be paid to the fact that the resulting sensitivity measures give information on a different model. Consequently, the relative weight of the first-order terms is increased at the expense of the interactions and high-order interactions.

The linearity and the monotonicity of the model used for simulating natural night ventilation will be checked and a rank transformation will be applied when needed.

4.3 UNCERTAINTIES ON INPUT PARAMETERS

Based on the selected methods for building simulation and uncertainty and sensitivity analysis, this section will discuss the physical background and the uncertainty interval of the input parameters. Following parameters are distinguished: boundary conditions, building and system characteristics. The building model and its specific building, system and simulation characteristics are discussed in the next chapter.

Furthermore, the building use is an important source of uncertainty. However, the information about both the behaviour of the occupants and the way to simulate this use are scarce. Therefore, this research is restricted to the evaluation of the design of natural night ventilation in an office building. Nevertheless, the impact of the occupancy and the manual control of windows on the level of thermal comfort are touched upon.

4.3.1 UNCERTAINTY INTERVAL AND DISTRIBUTION

All the input parameters of building simulation model are assumed to be normally distributed. Eq. 4.19 and Fig. 4.7 show the density function of a normal distribution (Ottoy, 2002). These distributions on the input parameters will be estimated from data in the literature and standards in the following sections. The given ranges correspond to $[\mu - 2\sigma; \mu + 2\sigma]$, where μ and σ are respectively the average and standard deviation. This means a parameter is included in this interval with a probability of 0.98.

$$f(x) = \frac{1}{\sigma\sqrt{2\pi}} \exp\left[-\frac{1}{2}\left(\frac{x-\mu}{\sigma} \right)^2 \right]$$
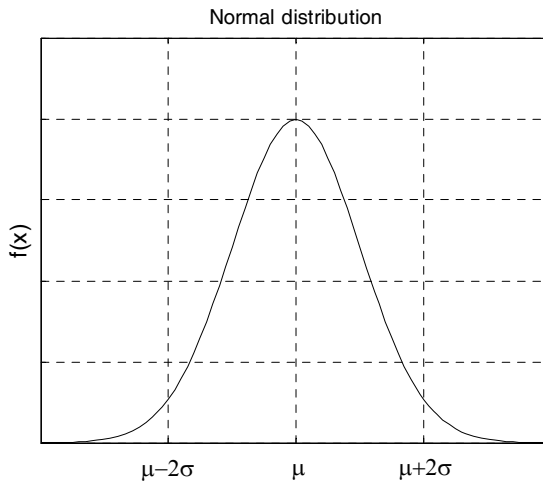
Eq. 4.19

Fig. 4.7 Density function of a normal distribution

4.3.2 BOUNDARY CONDITIONS

4.3.2.1 WEATHER DATA

The thermal comfort in a building, cooled with natural night ventilation, depends on the external weather conditions. Hence, outdoor temperature, irradiation, wind velocity and direction, are important boundary conditions in this evaluation process. Therefore, which data set is to be used has to be well thought. A measured (ISSO, 2004) or typical weather data set of 1 year with hourly values is typically used to predict the annual energy use or long-term behaviour of a building or HVAC system. Crawley (1998) recommends the use of a typical as well as a hot/sunny weather data set to evaluate the performances of passive cooling in building simulation. Measurements in the meteorological station of Ukkel support this recommendation for the outdoor temperature. The climatologically daily average value from June to August of 16.5°C is exceeded every year during the last 10 years (see Fig. 4.8). In addition, the Intergovernmental Panel on Climate Change (IPCC, 2002) noticed an increase of the global surface temperatures of 0.6 ±0.2°C since the late 19th century. Most of this increase has occurred in two distinct periods, 1910 to 1945 and since 1976. The rate of temperature increase since 1976 has been over 0.15°C/decade. Frank (2005) studied the impact of this climate change on the building heating and cooling demand in Switzerland for a climatic warm reference scenario for 2050-2100. He concluded that an increase of 4.4°C in the mean annual air temperature, relative to the 1961-1990 climatological normals, results in an increase in the annual cooling load of 223-1050% in office buildings with internal heat gains of 20-30 W/m^2. In addition, an increased air temperature is noticed in the urban environment compared to the rural where meteorological stations are located. This phenomenon has a large impact on the performances of natural night ventilation: the efficiency of this technique is significantly reduced in this urban environment (Geros et al., 2005), (Kolokotroni et al., 2005). Both phenomena cause uncertainty on the outdoor temperature. Therefore, it is important to define a weather data set including warm temperatures in addition to normal temperatures. Both weather data sets are discussed in the following paragraphs.
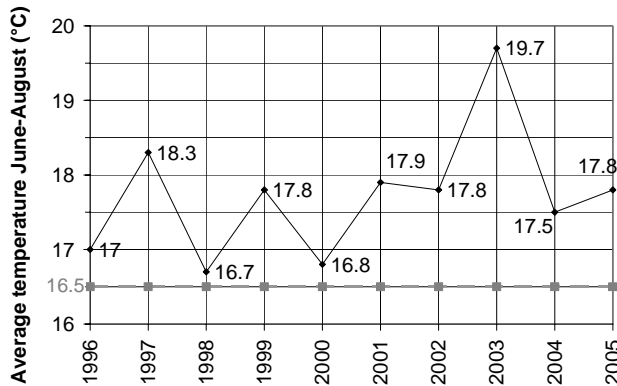

Fig. 4.8 The average summer temperature measured in the meteorological station Ukkel (based on data of RMI)

4.3.2.1.1 Typical weather data

In Belgium, the following typical weather data sets can be distinguished:

▪ TRY or Test Reference Year (EC, 1985) is a compilation of measured data of 12 separate months from years of 1958-1972 for the meteorological stations Ukkel (near Brussels, in the centre of the country), Oostende (at the coast) and Saint-Hubert (in the south of the country, i.e. the Ardennes).

▪ IWEC or International Weather Year for Energy Calculations (ASHRAE, 2001), (Thevenard and Brunger, 2002) is a compilation of 12 separate months from years between 1983-1999 for the meteorological stations Brussels, i.e. another station as Ukkel, Oostende and Saint-Hubert. However, solar radiation is not measured but estimated on an hourly basis from the earth-sun geometry and cloud amount information.

▪ Meteonorm (Meteotest, 2003) constructs the synthetic hourly weather data based on the climatological normals of 1961-1990 (RMI, 2004) of the meteorological stations Ukkel, Oostende and Saint-Hubert. These normalized values of the World Meteorological Organization include measured monthly values for air and dew point temperature, global solar radiation on a horizontal surface, sunshine duration, precipitation, and days with precipitation, wind speed and direction.

These weather data sets are only valid in a restricted region around the meteorological station. As a rule of thumb, a weather data set can be used in the area where the deviations in calculated results, caused by the geographical distance from the original location, do not exceed the standard deviation of the results caused by stochastic variations in the weather from year to year (EC, 1985).

In order to select a suitable weather data set, the data sets of TRY, IWEC and Meteonorm for a typical year in Ukkel, Brussels are compared with each other and with recent measured data of the meteorological station of Ukkel. The data of the outdoor temperature and global and beam irradiance from May 15 to September 30 will be discussed.

The daily average and maximum temperatures and the daily temperature range are compared in Table 4.1. Both daily average and maximum temperatures are almost the same in the data sets of TRY Ukkel and IWEC Brussels, and are slightly smaller in the typical year of Meteonorm. The measurements additionally show that the summers of 2001 and 2002 in Ukkel were warmer than a typical summer in all the weather data sets. Larger differences are shown in Table 4.2, which discusses the monthly average temperatures. The monthly average temperatures in the IWEC data set are generally higher than the climatological normals, used in Meteonorm, in particular in July. The TRY data set deviates from the measured average: the monthly average temperature in May and July are significant smaller, these in June and September significant larger than the measured averages. The measurements of 2001 and 2002 also disagree to the average values. May and August 2001 were extremely warm, while September 2001 was extremely cold. Moreover, June and July were warmer than normal (RMI, 2001). The summer of 2002 was relatively warm with monthly average temperatures higher than normal (RMI, 2002). These conclusions are confirmed by the comparison of the distributions of the daily average temperatures of 2001, 2002 and TRY in Fig. 4.9.

Table 4.1 Comparison daily average and maximum temperature and daily temperature range of weather data sets and measurements (May 15 – September 30)

		Weather data sets				Measurements		
		TRY Ukkel	IWEC Brussels	Meteonorm Ukkel	Meteonorm extreme Ukkel	1995	2001	2002
Daily average temperature (°C)	μ	16.1	16.1	15.6	17.1	17.8	16.5	17.0
	σ	3.1	3.3	3.4	3.3	4.9	3.7	2.9
Daily average range (°C)	μ	9.0	8.5	8.4	8.2	8.9	8.6	8.0
	σ	3.0	3.6	3.3	2.8	2.4	3.2	2.7
Daily maximum temperature (°C)	μ	20.6	20.4	19.8	21.2	22.2	20.8	21.0
	σ	3.8	4.5	3.6	3.7	4.9	4.7	3.7

Table 4.2 Comparison monthly average temperatures of weather data sets and measurements

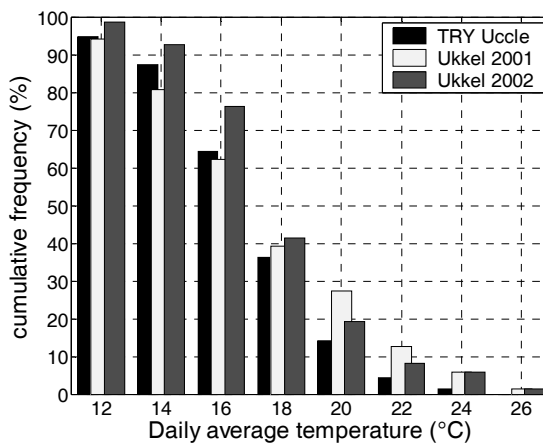|	Monthly average temperature (°C)						
	Weather data sets				Measurements		
month	TRY Ukkel	IWEC Brussels	Meteonorm Ukkel	Meteonorm extreme Ukkel	1995	2001	2002
May	11.9	12.9	12.7	14.1	14.1	14.6	13.7
June	16.7	15.6	15.5	17.0	15.4	15.4	17.0
July	16.1	18.4	17.2	18.7	21.6	18.8	18.0
August	17.1	17.4	17.0	18.4	20.7	19.2	18.6
September	16.1	14.5	14.4	15.7	14.5	12.8	15.0

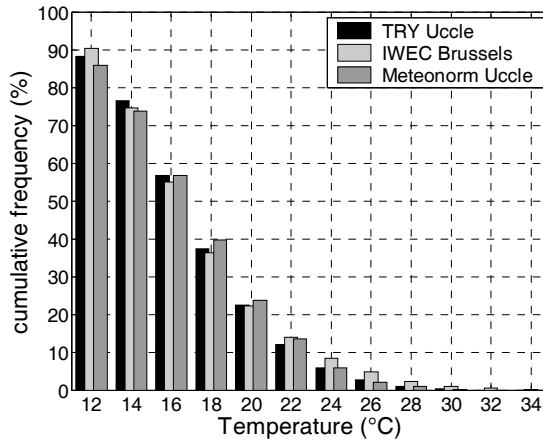Fig. 4.9 Comparison of the cumulative distribution of the daily average temperatures

Fig. 4.10 Comparison of the cumulative distributions of the hourly temperatures

Furthermore, the distributions of the hourly temperatures in the weather data sets are compared in Fig. 4.10. It can be concluded that IWEC includes a larger amount of high temperatures (from 24°C) than the other data sets.

The daily temperature range, correlated to the daily average temperature, is also of interest for the analysis of night ventilation. It is calculated as the difference between the daily maximum and minimum temperature. Fig. 4.11 shows that the daily temperature amplitude in the TRY data set is always higher than 6°C on a normal summer day, i.e. when the daily average temperature exceeds 16 °C (van der Linden et al., 2006). The correlation in the IWEC data set shows almost the same. Contrary to these latter data sets, Meteonorm shows small and large daily temperature ranges on all values of daily average temperatures. In other words, the Meteonorm data set includes nights where the cooling capacity of natural night ventilation is small, i.e. the so-called terrace nights. Measured data in the summers of 2001 and 2002 show that the combination of high average and small temperature amplitudes occurred more often (see Fig. 4.12).
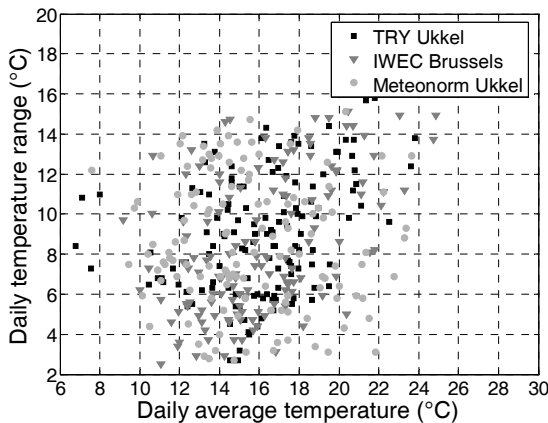

Fig. 4.11 Comparison of the daily temperature ranges of the weather data sets
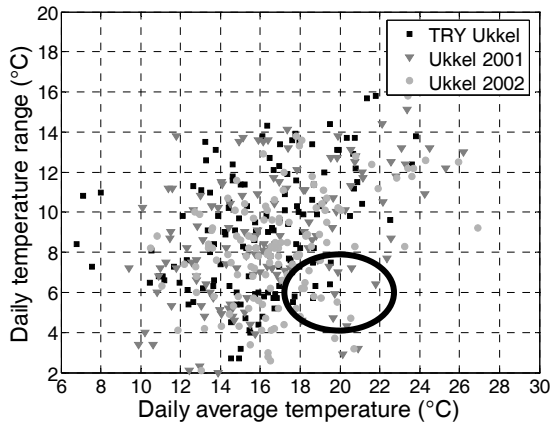
Fig. 4.12 Comparison of the daily temperature ranges of TRY to the measurements

The daily average and maximum values of the global and beam irradiance are compared in Table 4.3. The daily average global irradiation is comparable in the three weather data sets. On the other hand, the daily maximum global and daily average and maximum beam irradiance are significantly smaller in the IWEC than in the TRY and Meteonorm data set. Nevertheless, the monthly average global irradiation values (see Table 4.4) of the IWEC and Meteonorm data sets are comparable except in June where the monthly average value is smaller in IWEC than in Meteonorm. The TRY data set differ from these latter datasets concerning the monthly average global irradiation. The months May and July are on average less sunny, June and September are sunnier in TRY than in Meteonorm, i.e. the normals in Ukkel.

Table 4.3 Comparison daily average and maximum global and beam irradiation of weather data sets (May 15 – September 30)

		Weather data sets			
		TRY Ukkel	IWEC Brussels	Meteonorm Ukkel	Meteonorm extreme Ukkel
Daily average global horizontal irradiation (W/m^2)	μ	176	168	175	192
	σ	71	68	82	79
Daily maximum global horizontal irradiation (W/m^2)	μ	596	535	572	608
	σ	183	183	206	183
Daily average beam irradiation (W/m^2)	μ	118	87	120	148
	σ	100	90	120	123
Daily maximum beam irradiation (W/m^2)	μ	454	351	442	496
	σ	242	257	276	268

Table 4.4 Comparison of monthly average global irradiance in weather data sets

| month | Monthly average global irradiation (W/m²) | | | |
| | Weather data sets | | | |
	TRY Ukkel	IWEC Brussels	Meteonorm Ukkel	Meteonorm extreme Ukkel
May	176	181	188	215
June	221	181	196	224
July	173	196	191	217
August	161	168	167	186
September	136	109	117	133

Furthermore, the distributions of the global and beam irradiation are compared in Fig. 4.13 and Fig. 4.14. These graphs prove that the global and the beam irradiation in particular in the IWEC data set significantly differ from the other weather data sets. Moreover, high values of both global and beam irradiation are more frequently noticed in the Meteonorm than in the TRY data set.
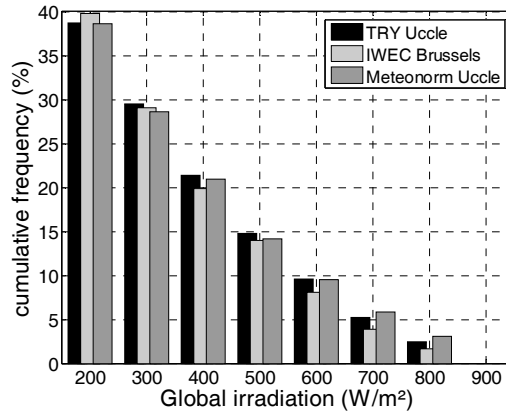

Fig. 4.13 Comparison of cumulative distribution of the hourly global irradiation data
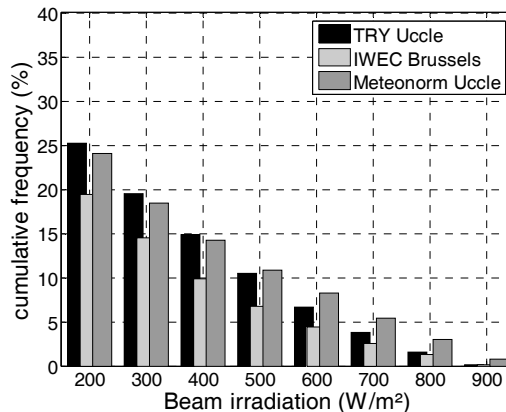

Fig. 4.14 Comparison of cumulative distribution of the hourly beam irradiation data

4.3.2.1.2 Extreme weather data

Meteonorm (Meteotest, 2003) can create an extreme warm and/or sunny weather data set, i.e. temperatures or irradiation occurring once every 10 year. This extreme weather data set for Ukkel is compared to the Meteonorm data set of a typical year and to measurements of the meteorological station. Data of the outdoor temperature and global and beam irradiance from May 15 to September 30 will be discussed.

Table 4.1 and Table 4.2 show respectively the daily and monthly average temperature of the extreme Meteonorm data set. The absolute values of temperature are significantly higher compared to the values of a typical Meteonorm data set. However, the daily temperature range is comparable in both data sets. This is also shown on Fig. 4.16, which compares the relation of the daily temperature range to the daily average temperature. Fig. 4.15 compares the cumulative distributions of the daily average temperature of the extreme Meteonorm data set to measurements of 2002 and 1995. The latter is an extraordinary warm summer used as extreme weather data set in the Dutch regulations (ISSO, 2004), (van der Linden et al., 2006). It is shown that the temperature distribution of the extreme weather data of Meteonorm is comparable to the measurements of 2002 rather than to these of 1995. This conclusion is also shown on Fig. 4.17, which compares the correlation of the daily temperature range to the daily average temperature of the extreme Meteonorm data set to the measured correlation of 2002 and 1995.

In addition, the daily and monthly average values of the global and beam irradiation of an extreme Meteonorm data set are shown in Table 4.1. The distributions of hourly values of a typical and extreme Meteonorm data set are compared with each other in Fig. 4.18 and Fig. 4.19. Despite the solar radiation is on average higher in the extreme than in the typical weather data set, the peak values of both global and beam irradiance have the same probability.
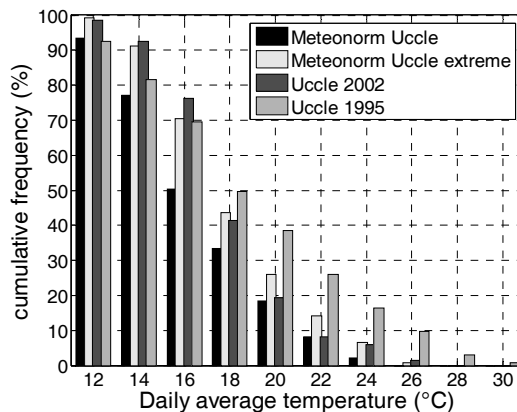

Fig. 4.15 Comparison of the cumulative distribution of the daily average temperatures extreme, typical weather data set and measurements
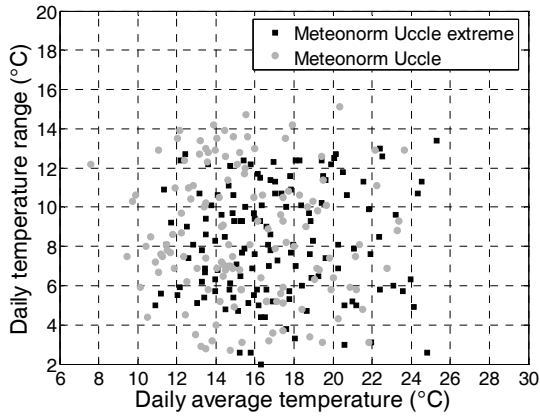
Fig. 4.16 Comparison of the daily temperature ranges of extreme to typical weather data set
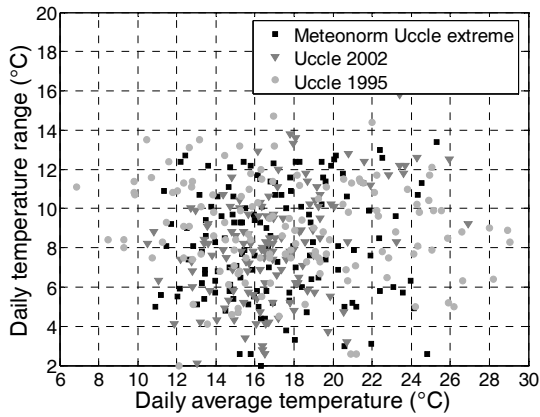

Fig. 4.17 Comparison of the daily temperature ranges of extreme weather data to measurements
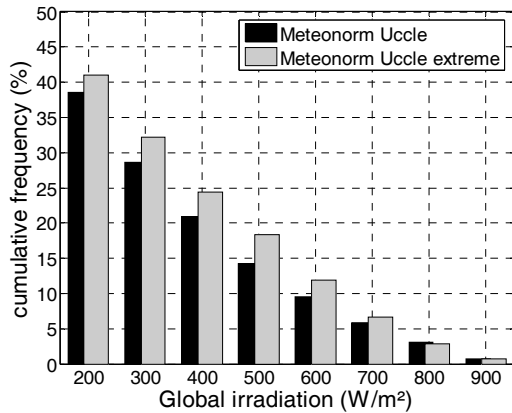

Fig. 4.18 Comparison of cumulative distribution of the hourly global irradiance in typical and extreme Meteonorm data set
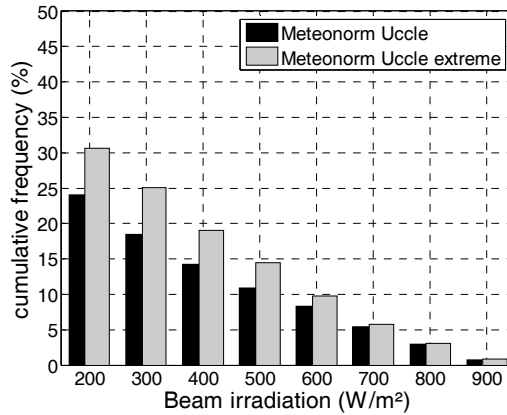
Fig. 4.19 Comparison of cumulative distribution of the hourly beam irradiance in typical and extreme Meteonorm data set

4.3.2.1.3 Conclusions

In conclusion, the data set of IWEC will not be used in the simulations of natural night ventilation because the calculated data of the irradiation significantly differ from the data in the other weather data sets. The data sets of TRY and Meteonorm are comparable. Because Meteonorm can create extreme weather data and takes into account small daily temperature ranges on warm days, this weather data set will be used in the simulations. The impact of the uncertainty on the outdoor temperature will be defined by comparing the thermal comfort reached in normal and extremely warm outdoor temperatures.

4.3.2.2 Wind

Wind is a highly variable and irregular physical phenomenon (Allard and Alvarez, 1998) and causes uncertainty on the prediction of the airflows of natural ventilation. In a multi-zone ventilation model, the wind pressures on buildings are calculated from the wind characteristics of meteorological measurements via the following parameters:

- wind reduction: conversion of the average meteorological wind velocity to the wind velocity on site
- wind pressure coefficient Cp: calculation of the local wind pressure on buildings from this wind velocity on site

These parameters are examined in detail in the following paragraphs.

4.3.2.2.1 Wind reduction

Several models exist to convert the wind velocity, measured on a meteorological station in standard conditions, to the wind velocity on a homogeneous site depending on the height and the nature of the site. They can be classified into two wind profiles:

- Logarithmic wind profile (Allard and Alvarez, 1998): analysis of the physical background of wind shows that the wind velocity is a logarithmic function of the height above the ground. Eq. 4.20 expresses the relationship between the wind velocity on site $\overline{v_z}$ and the reference wind velocity $\overline{v_{ref}}$, i.e. the mean velocity measured at a height of 10m on a meteorological site having a homogeneous roughness height of 0.05m. The velocity of the geotropic wind is assumed to be identical above the two sites.

$$\overline{v}_z = \lambda(z_0)\ \overline{v}_{ref}\ \ln\left(\frac{z}{z_0}\right)$$

<div align="right">Eq. 4.20</div>

where z is the height above the ground, z_0 the roughness height and $\lambda(z_0)$ an empirical coefficient. The roughness height is an aerodynamic characteristic of the ground surfaces and thus a function of the nature of the ground and of the geometry of the existing obstacles. Table 4.5 presents a range of experimental values of roughness heights obtained on homogeneous sites of large horizontal extension (Wieringa, 1992) and values of the coefficient $\lambda(z_0)$ for different types of terrain roughness (ESDU 82026, 1982).

<div align="center">Table 4.5 Roughness class, height z_0 and $\lambda(z_0)$</div>

Type of surface	Roughness height z_0	$\lambda(z_0)$	Roughness class
Sea, snow, sand	0.0005	0.14	I
Sea with very strong wind	0.005	0.15	II
Short grass	0.01	0.17	III
Cultivated open fields	0.05	0.19	IV
High plants, open country	0.10	0.20	V
Countryside and spread habitat	0.25	0.21	VI
Peripheral urban zone	0.50	0.22	VII
Mean city centre, forest	1.00	0.24	VIII
Metropolitan centre, tropical forest	4.00	0.25	IX

- Power law wind profile: The wind velocity is in this empirical relationship a power function of the height above the ground. Eq. 4.21 shows the relationship between the wind velocity on site $\overline{v}_z$ and the reference meteorological wind velocity $\overline{v}_{ref}$ (Orme and Leksmono, 2002).

$$\overline{v}_z = \overline{v}_{ref}\, K\, z^a$$

<div align="right">Eq. 4.21</div>

where z is the height above the ground and K and a parameters depending on the roughness of the site (see Table 4.6). Eq. 4.22 shows another empirical relationship between the wind velocity on site $\overline{v}_z$ and the reference meteorological wind velocity $\overline{v}_{ref}$ (Feustel et al., 1999).

$$\overline{v}_z = \overline{v}_{ref}\left(\frac{z}{z_{bound}}\right)^{a_0}\left(\frac{z_{bound}}{10}\right)^{a_m}$$

<div align="right">Eq. 4.22</div>

where z is the height above the ground, z_{bound} is the height of the boundary layer above which the wind velocity is assumed identical at the two sites, a_0 and a_m are wind velocity profile exponents at building location and meteo station respectively depending on nature of the site. Values for a_0 and a_m can be found in the COMIS' user's guide (Dorer et al., 2001).

An important remark can be made upon the assumptions in this wind conversion. The site environment is rarely homogeneous but characterized by its position in the relief (hill, valley, etc.), the nature of the terrain (geographical distribution of urban zones, extended area of water, etc.) and the presence of nearby obstacles (hedges, trees, houses, etc.) (Allard and Alvarez, 1998). These site characteristics affect the local wind velocity on site. As a consequence, the presented wind profiles are only valid for heights between ($20 \times z_0 + d$) and 60-100m. The boundary layer below this band is referred to as the urban canopy for which the wind is mostly dependent on obstacles and will require wind tunnel tests or detailed CFD simulations for an accurate estimation. Therefore, care must be taken using this wind profile in the urban canopy (Clarke, 2001). Table 4.6 shows the height z_{min} of this urban canopy for some natures of sites for a 10m high building. It can be concluded that the presented wind profiles are not valid on terrains where most buildings are built (roughness class VII and higher). This is a source of uncertainty. Although, the choice of roughness class by the user in the input is the most important source of uncertainty in wind conversion. Therefore, a variation of 1 roughness class is assumed for the roughness class on site. The range of the roughness height z_0 for a building in an industrial zone is assumed [0.125 – 0.25 – 0.50], which corresponds to variation of roughness classes V – VI – VII. When the building is located in the city, a roughness height of [1 – 2 - 4] is assumed, corresponding to the variation between roughness classes VIII and IX. The variation of the roughness height of the meteorological station is assumed to be much smaller: [0.03 – 0.04 – 0.053].

Table 4.4.6 Rougness parameters K,a, z_0 and height z_{min} of the urban canopy for h = 10m (BS5925:1991)

terrain	K	a	z_0	d	z_{min}
open flat country	0.68	0.17	0.03	0	0.6
country, scattered wind breaks	0.52	0.2	0.1	0	2
rural	-	-	0.5	0.7 h	17
urban	0.35	0.25	1	0.8 h	28
city	0.21	0.33	2	0.9 h	49

4.3.2.2.2 Wind pressure coefficient Cp

Given the local wind velocity, the wind effect on the building is calculated in a multi-zone ventilation model using the wind pressure coefficient Cp. This coefficient is the ratio of the wind pressure on the building surface Δp_w to the dynamic pressure of the wind velocity on site $\overline{v_z}$ at building height (Eq. 4.23). The wind pressure on a building surface is additionally defined as the difference between the local pressure on the surface and the static pressure in the undisturbed wind on the same height. The relationship between velocity and related pressure is obtained from Bernoulli's equation with the assumption of a constant density along the streamline.

$$Cp = \frac{\Delta p_w}{\frac{\rho}{2}\left(\overline{v_z}\right)^2} \qquad \text{Eq. 4.23}$$

Values of the pressure coefficient depend on the building shape, the wind direction, the environment (nearby buildings and vegetation) and the specific location on the building surface (height and distance from the middle) (ASHRAE, 2005). These Cp coefficients can be determined by wind tunnel experiments and CFD simulations. These methods are usually too expensive and time-consuming for building simulation. Therefore, the easier but less reliable methods of Cp generators (Grosso, 1995), (Knoll et al., 1995), (Swami and Chandra, 1988), (Allen, 1984) and tables and figures (Orme and Leksmono, 2002), (ASHRAE, 2005) are used. They rely on inter- or extrapolation of generic knowledge and previously measured data in wind tunnel studies and full-scale experiments. Heijmans and Wouters (2002a) noticed that the correlation between the monitored and predicted Cp values with the method of respectively Knoll et al. (1995) and Orme and Leksmono (2002) is excellent, except in the zone with obstacles. The impact of these obstacles is underestimated.

Due to the complexity of the underlying physics of the wind pressure, these Cp generators and tables may introduce considerable uncertainty (de Wit, 2001). Moreover, the use of these models is an important source of uncertainty. Therefore, the uncertainty on the Cp values is derived as follows. When no information of the local environment of the building is provided, the simplified tables of Orme and Leksmono (2002) are used for low-rise buildings as shown in Fig. 4.20. The uncertainty is assumed as the difference between two successive classes in the tables. This means a variation for the pressure coefficient on the façade and flat roof of respectively ± 0.2 and ± 0.15 (see Table 4.7). The Cp coefficients on a building and its variations are assumed to be correlated. When the local environment of the building is known, the use of a Cp generator is recommended. The uncertainty interval is then derived from values on different positions on the building façade (see chapter 7 Design application).
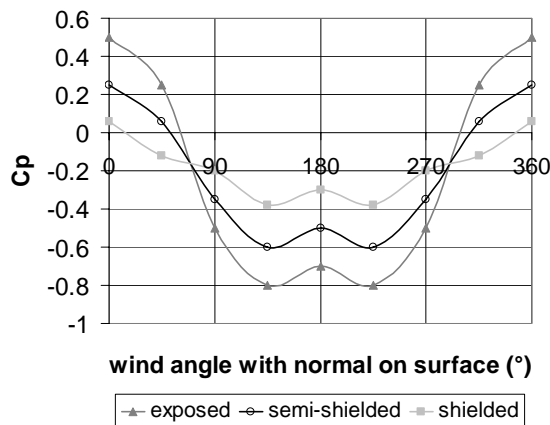

Fig. 4.20 Comparison of wind pressure coefficient Cp on the façade for a low-rise building with different shielding conditions (Orme and Leksmono, 2002)

Table 4.7 Wind pressure coefficient Cp for a building surrounded by obstructions equivalent to half the height of the building (Orme and Leksmono, 2002)

Cp		Wind direction (°) (angle with normal on surface)							
		0	45	90	135	180	225	270	315
façade	μ	0.25	0.06	-0.35	-0.60	-0.50	-0.6	-0.35	0.06
	σ	0.10							
flat roof	μ	-0.60	-0.60	-0.60	-0.60	-0.60	-0.60	-0.60	-0.60
	σ	0.08							

4.3.3 Building characteristics

Dimensions, thermophysical properties, convective heat transfer coefficients and air tightness are understood by building characteristics.

4.3.3.1 Dimensions

The geometrical properties of each component, i.e. width and height, are measured from the internal surfaces as laid down in the standard prEN ISO 13791:2004 (CEN, 2004), which calculates the internal temperature of a room without mechanical cooling.

Nevertheless, the Belgian standard NBN B62-003 (BIN, 1986) requires the use of external dimensions to calculate the heat losses in buildings. ISSO (1994) recommends the use of axis-to-axis dimensions in building simulation. However, in case of natural night ventilation, it can be expected that the choice of dimensions of the external walls would have a larger impact on the amount of exposed thermal mass than on the transmission losses. This influence is investigated in section 5.3.1.2, which discusses the impact of thermal mass on the probability of good thermal comfort.

Furthermore, due to irregularities in the construction process, the realized geometry may slightly deviate from the geometry given in the design specifications. The range of possible deviations has been estimated at [-0.02, 0.02] m (de Wit, 2001) and is considered in the results of the uncertainty and sensitivity analyses in sections 5.2.3 and 5.2.4.

4.3.3.2 Thermophysical properties

The thermophysical properties of interest are the thermal conductivity λ, the density ρ, the specific heat capacity c, the thickness of the layer d and the solar absorption coefficient of the surface material a. These properties define the heat transfer and storage in the particular material layer. In addition, the solar heat gain coefficient of glass and external sunblinds are discussed.

The mean thermophysical properties (μ) are assumed for dry materials, listed in the Belgian standard NBN B62-002/A1 (BIN, 2001). The uncertainties on the thermal conductivity, density and specific heat capacity are caused by variations in temperature and moisture content. Uncertainty is also caused by heterogeneity of products. A moisture content for each material in particular, determined by EN 12524 (CEN, 2000), and a temperature variation of 10°C are assumed. ISO 10456 (ISO, 1999) calculates the influence of temperature and moisture on the thermal conductivity as follows (Eq. 4.24):

$$\lambda' = \lambda\, F_T F_m \qquad\qquad \text{Eq. 4.24}$$

where F_T en F_m are respectively the temperature and moisture conversion factor, defined as follows:

$$F_T = e^{f_T(\Delta T)} \qquad\qquad \text{Eq. 4.25}$$

$$F_m = e^{f_u(\Delta u)} \qquad\qquad \text{Eq. 4.26}$$

where f_T en f_u are respectively temperature and moisture conversion coefficients and given in ISO 10456 (ISO, 1999) and EN 12524 (CEN, 2000). Eq. 4.27 determines consequently the standard deviation on the thermal conductivity:

$$\sigma(\lambda) = \frac{\lambda' - \lambda}{2} = \frac{\lambda}{2}\left(F_T F_m - 1\right) \qquad\qquad \text{Eq. 4.27}$$

The influence of moisture on the specific heat capacity is defined as follows (IEA, 1991):

$$c' = c + 4187u = c + 4187\frac{1000\Psi}{\rho} \qquad\qquad \text{Eq. 4.28}$$

where u is the moisture content mass by mass (kg/kg) and Ψ the moisture content volume by volume (m^3/m^3). The standard deviation is defined in Eq. 4.29.

$$\sigma(c) = \frac{c' - c}{2} = 4187\frac{u}{2} = 4187\frac{1000\Psi}{2\rho} \qquad\qquad \text{Eq. 4.29}$$

The influence on the density is assumed 2% of the mean value, based on measurements of the thermophysical properties of bricks in Janssens et al. (1998). The standard deviation consequently equals 1% of the mean value. The calculated values in Table 4.8 are comparable to the estimations of Macdonald (2002). Besides, the variation in thickness is caused by lack of information on the exact properties (de Wit, 2001) and is derived from the sensitivity analysis of building thermal modeling of Pinney et al. (1991). Furthermore, Macdonald (2002) derived for every material an average value and a standard deviation of the solar absorption coefficient from Clarke et al. (1990), which collected data of thermophysical properties from standards, measurements from different research projects and product information. Small standard deviations can be noticed because this coefficient can be measured with good accuracy (Macdonald, 2002).

Table 4.8 shows the mean value (μ) and standard deviation (σ) of the thermal conductivity λ, the density ρ, the specific heat capacity c, the thickness of the layer d and the solar absorption coefficient of the surface material a of the materials of interest. The thermophysical properties of glazing are not varied: a fixed thermal resistance is assumed 0.74 m^2K/W. In addition, spacers are not included in this glazing.

Table 4.8 Uncertainties on the thermophysical properties

material		λ (W/mK)	ρ (kg/m³)	a (-)	c (J/kgK)	d (m)
Façade brick	μ	0.90	2000	0.49	1000	0.090
	σ	0.06	20	0.06	13	0.001
Internal brick	μ	0.54	1500	0.49	1000	0.140
	σ	0.04	15	0.06	17	0.001
Reinforced concrete	μ	1.70	2400	0.72	1000	0.030
	σ	0.11	24	0.04	38	0.002
Light concrete (screed)	μ	0.24	850	0.72	1000	0.030
	σ	0.02	9	0.04	84	0.004
Hollow core concrete slab	μ	1.09	1800	0.72	1000	0.130
	σ	0.10	18	0.04	47	0.010
bitumen	μ	0.23	1100	0.88	1000	0.0050
	σ	0	0	0.01	0	0.0003
Insulation (mineral wool)	μ	0.040	50	-	1000	0.080
	σ	0.001	0.5	-	10	0.004
Gypsum board	μ	0.25	900	0.40	1050	0.0100
	σ	0.03	9	0.05	86	0.0005
carpet	μ	0.06	200	0.60	1300	0.004
	σ	0.008	2	0.03	51	0.001
Plywood	μ	0.24	850		1880	0.018
	σ	0.03	9		335	0.001
Air cavity: R (m²K/W)	μ	0.16	-	-	-	-
	σ	0.01	-	-	-	-
Aluminum window frame: U (W/m²K)	μ	3.8	-	0.53	-	-
	σ	0.2	-	0.06	-	-

In addition, the solar heat gain coefficient of a window g is the fraction of incident irradiance that enters and includes both the directly transmitted and the absorbed and reemitted portion (ASHRAE, 2005). Therefore, the g-value depends on the optical glass properties, i.e. the solar transmission, absorption and reflection coefficient of the glass pane and the heat transfer coefficients on the surfaces. In case of double or triple glass the heat transfer characteristics of the cavity, i.e. its thickness, the conductivity of the fluid and the long-wave emission coefficient of glass, also determine the solar heat gain coefficient. In this research low-emission double glass with a Krypton filled cavity will be used. This type of glass has a typical g-value of 0.60 (Hens, 1999). An uncertainty of ± 0.02 is estimated form product information (Glaverbel, 2005). A variation of corresponding glass systems is chosen in the program WINDOW (LBNL, 2003) assuming fixed combined heat transfer coefficients of 8 and 25 W/m²K (BIN, 1996). This program consequently calculates the solar absorption, reflection and transmission coefficients of the glass panes, which are used in TRNSYS for the calculation of the transmission of solar radiation. In addition, the heat transfer coefficients on the window surfaces also vary (see next paragraph), causing uncertainty on the solar heat gain coefficient as well. This uncertainty is not included in the uncertainty interval of ± 0.02.

The most effective way to reduce the solar load on a window is to intercept the direct radiation from the sun before it reaches the glass. Therefore, exterior sunblinds are added: moveable awnings are chosen. The solar heat gain coefficient for the combined system of glass and sunblinds varies from 0.10 to 0.20 (Hens, 1998). This assumption is also justified by the simplified simulation of external shading devices in TRNSYS (see paragraph 4.1.2.1.1). The reduction factor, i.e. the ratio of the area of the non-transparent shading device to the whole window area, is calculated from the ratio of the solar heat gain coefficients of glass and the combination of shading device and glass.

4.3.3.3 CONVECTIVE HEAT TRANSFER COEFFICIENT

Convective heat transfer can be classified by the nature of the driving force of the flow. Natural convection is driven by a density difference because of a temperature difference in the fluid. Forced convection is driven by an external forced pressure difference or flow e.g. the wind, a fan, etc (Beausoleil-Morisson, 2002a). Moreover, the convective heat transfer is defined as follows (Eq. 4.30):

$$q_c = \alpha_c \left(\theta_f - \theta_s \right)$$
<div align="right">Eq. 4.30</div>

where α_c is the convective heat transfer coefficient (CHTC) defining the relationship between the heat transfer q_c and the temperature difference between the fluid and the surface $\theta_f - \theta_s$. This CHTC is an input in the multi-zone building simulation tool.

4.3.3.3.1 External

The convective heat transfer coefficient on external surfaces α_{ce} depends on the local wind velocity on site v (Eq. 4.31) (ASHRAE, 2005).

$$\alpha_{ce} = 5.6 + 3.9\,v \quad \text{when} \ v \leq 5\,\text{m/s}$$
$$\alpha_{ce} = 7.2\,v^{0.78} \quad \text{when} \ v > 5\,\text{m/s}$$
<div align="right">Eq. 4.31</div>

This equation agrees well to the equation in the standard prEN ISO 13791:2004 (CEN, 2004a), which determines the indoor temperature in a room without mechanical cooling. Furthermore, applying Eq. 4.31 on the weather data of TRY Ukkel from May 15 to September 30, i.e. the cooling season in Belgium, on a terrain with 0.1 roughness height, results in an average external convective heat transfer coefficient of 17 W/m^{2}K and a standard deviation of 5 W/m^{2}K.

The uncertainty on the external convective heat transfer coefficient is determined by the variation in the wind velocity on site on its turn defined by the variations in the meteorological wind velocity in the weather data and in the roughness heights on site an at the meteo site (see paragraph 4.3.2.2.1).

4.3.3.3.2 Internal

The internal convective heat transfer coefficient by natural convection is function of the temperature difference between the concerned surface and the air ($\Delta\theta$):

$$\alpha_{ci} = C\left(\Delta\theta\right)^n$$
<div align="right">Eq. 4.32</div>

where C and n are semi-empirical coefficients which were determined amongst others by Awbi and Hatton (1999), ASHRAE (2005), Alamdari and Hammond (1983), Khalifa and Marshall (1990), Khalifa (2001) (see Table 4.9). Beausoleil-Morisson (2002a) discusses and compares the results of these researches. Experiments with heated walls in full-size rooms were carried out. The internal CHTCs were calculated from temperatures measurements and averaged over the surface.

The internal convective heat transfer coefficient varies from surface to surface in the building, as well as with the time and the flow regime (Beausoleil-Morisson, 2002a). Fig. 4.21 and Fig. 4.22 show the convective heat transfer coefficient for respectively a vertical and a horizontal surface with a buoyant, i.e. an upward, and a stably stratified flow based on the equations in Table 4.9, assuming a hydraulic diameter of 4.3 m^{-1} and a height of 2.5 m. Both flow regimes may range from laminar to turbulent flow, as shown by the semi-empirical exponent n, which varies from approximately 0.25 to 0.33. The CHTC on a horizontal surface (buoyant flow) and a vertical surface are comparable. The CHTC on a horizontal surface (stably stratified) is significantly smaller. The difference between the model predictions is significant and equals up to respectively 1 and 0.3 W/m^2K for the CHTC on a vertical or horizontal surface (buoyant flow) and a horizontal surface (stably stratified flow).

Table 4.9 The internal convective heat transfer by natural convection

α_{ci}	vertical	horizontal	
		Buoyant	Stably stratified
ASHRAE	$\alpha_{ci} = 1.31(\Delta\theta)^{0.33}$	$\alpha_{ci} = 1.52(\Delta\theta)^{0.33}$	$\alpha_{ci} = 0.6(\Delta\theta)^{0.25}$
Awbi & Hatton	$\alpha_{ci} = \dfrac{1.823}{D_h^{0.121}}(\Delta\theta)^{0.293}$	$\alpha_{ci} = \dfrac{2.175}{D_h^{0.076}}(\Delta\theta)^{0.308}$	$\alpha_{ci} = \dfrac{0.704}{D_h^{0.601}}(\Delta\theta)^{0.133}$
Khalifa & Marshall	$\alpha_{ci} = 2.30(\Delta\theta)^{0.24}$	$\alpha_{ci} = 2.27(\Delta\theta)^{0.24}$	-
Alamdari & Hammond	$\alpha_{ci} = \left\{ \left[1.5\left(\dfrac{\Delta\theta}{H}\right)^{1/4} \right]^6 + \left[1.23(\Delta\theta)^{1/3} \right]^6 \right\}^{1/6}$	$\alpha_{ci} = \left\{ \left[1.4\left(\dfrac{\Delta\theta}{D_h}\right)^{1/4} \right]^6 + \left[1.63(\Delta\theta)^{1/3} \right]^6 \right\}^{1/6}$	$\alpha_{ci} = 0.6\left(\dfrac{\Delta\theta}{D_h^2}\right)^{1/5}$

where D_h is the hydraulic diameter of horizontal surfaces, defined as follows (Eq. 4.33):

$$D_h = \frac{4P}{A} \qquad \text{Eq. 4.33}$$

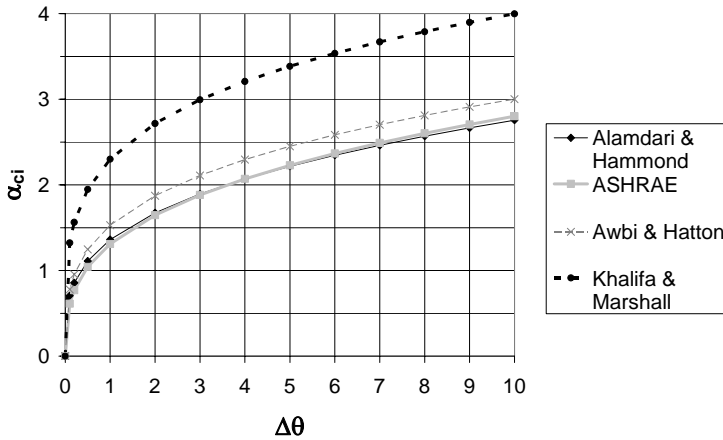where P is the perimeter and A the area of the surface.

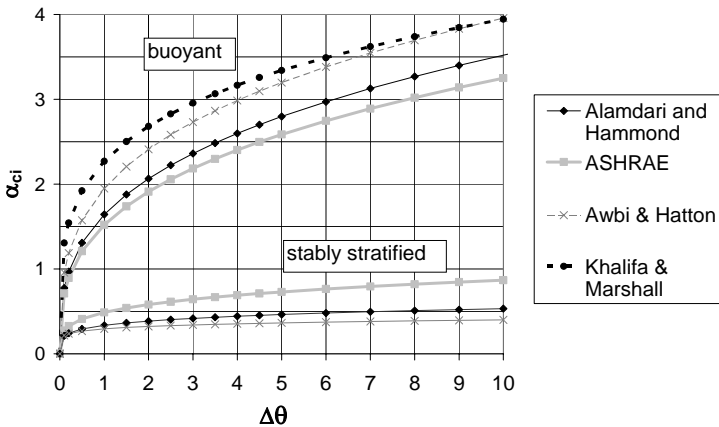Fig. 4.21 Convective heat transfer coefficient on a vertical surface

Fig. 4.22 Convective heat transfer coefficient on a horizontal surface

The semi-empirical coefficients C and n will be taken as input for the calculation of the convective heat transfer instead of fixed values of the CHTC, provided in standards and regulations, see e.g. prEN ISO 13791 (CEN, 2004a) in Table 4.10. The uncertainty on C and n is derived from the difference between the maximum and minimum value in the models presented in Table 4.9. For a vertical and a horizontal surface (buoyant flow) e.g., ASHRAE (2005) and Khalifa and Marshall (1990) respectively estimate the lowest and highest value of the internal CHTC. These uncertainty intervals of C and n are shown in Table 4.11 for various flow regimes of natural convection.

Table 4.10 Fixed values for the internal convective heat transfer in prEN ISO 13791 (CEN, 2004)

α_{ci}	vertical	horizontal	
		Buoyant	Stably stratified
W/m^{2}K	2.5	5.0	0.7

Table 4.11 Semi-empirical coefficients C and n defining internal convective heat transfer coefficient

α_{ci}	vertical	horizontal	
		Buoyant	Stably stratified
C	(1.31; 2.30)	(1.52; 2.27)	(0.29; 0.6)
n	(0.33; 0.24)	(0.33; 0.24)	(0.13; 0.25)

An important remark has to be made on this approach. When natural night ventilation is in operation, the convective heat transfer is driven by a mixed flow, i.e. by natural and forced convection. Beausoleil-Morisson (2002) proposed a combination of the equations of Alamdari and Hammond (1983), i.e. a temperature driven, and Fisher (1995), i.e. a mechanical driven heat transfer, to describe this mixed convective heat transfer, e.g. for a stably stratified flow at a ceiling (Eq. 4.34):

$$(\alpha_{ci})^3 = (\alpha_{cn})^3 + \left(\frac{\theta_s - \theta_{diff}}{\Delta\theta}\right)^3 (\alpha_{cf})^3 = \left(0.6\left(\frac{\Delta\theta}{D_h^2}\right)^{1/5}\right)^3 + \left(\left(\frac{\theta_s - \theta_{diff}}{\Delta\theta}\right)\left(-0.166 + 0.484\, n^{0.8}\right)\right)^3 \qquad \text{Eq. 4.34}$$

where α_{cn} and α_{cf} respectively are the natural and forced convection coefficient, θ_s-θ_{diff} is the temperature difference between the surface and the incoming airflow and n is the ventilation rate (h^{-1}). This CHTC for mixed flow consequently depends on the air flow rate, the geometry of the surface and the temperature differences between respectively surface-air and surface-incoming ventilation air. The difference between the CHTC for mixed and natural convection is significant when the surface to air temperature difference is small. This mixed flow model is applicable for mechanically ventilated rooms which are heated or cooled with air supplied through ceiling diffusers. Furthermore, Awbi and Hatton (2000) measured the mixed convection from heated surfaces in an office-sized test room. A floor, ceiling and wall were subjected to an air jet partially covering each surface to represent this mixed convection. Equations to calculate the CHTC were proposed, e.g. for a heated ceiling (Eq. 4.35):

$$(\alpha_{ci})^{3.2} = (\alpha_{cn})^{3.2} + (\alpha_{cf})^{3.2} = \left(\frac{0.704}{D_h^{0.601}}(\Delta\theta)^{0.133}\right)^{3.2} + \left(1.35W^{0.074}v^{0.772}\right)^{3.2} \qquad \text{Eq. 4.35}$$

where W is the width of and U the velocity at the nozzle opening. The CHTC for mixed convection depends on the surface to air temperature difference, the width of and the velocity at the nozzle opening. These last two variables are unknown in case of natural ventilation. Awbi and Hatton (2000) concluded that the effect of the jet velocity on the convective heat transfer coefficient is significant in all cases. The largest effect was measured when a jet acts on a heated ceiling or a stably stratified flow, i.e. the case of a ceiling cooled by natural night ventilation at night. As a consequence, the heat transfer from the surface to the air, when natural night ventilation operates, will be underestimated assuming natural convection. However, these two models for mixed convection are derived for mechanical ventilation and require related inputs which are unknown in the case of natural ventilation. Application of these models will thus include uncertainty on the CHTC. Moreover, the implementation of a user-defined equation for the CHTC only during the operation of natural night ventilation results in convergence problems in the building simulation tool TRNSYS-COMIS. Therefore, natural convection is assumed in the simulation of natural night ventilation.

4.3.3.4 Airtightness

Unintentional gaps or cracks in the building envelope cause uncontrolled airflow through this envelope. Potential locations for these gaps are the joints of building components, penetration of e.g. pipes and ducts, windows and doors. The way of construction has an important impact on the type of cracks. The rate of air infiltration or exfiltration depends on the porosity of the building envelope and the magnitude of the natural driving forces of wind and temperature difference. Insufficient airtightness may consequently cause building energy loss, condensation problems, increasing noise level and air pollution. In addition, the intended airflow pattern of the ventilation system may be distorted (Dorer et al., 2004).

Airtightness can be quantified by a measured leakage flow, normalized to a reference pressure difference and to a factor that takes the building size into account. Amongst other things, the n_{50}-value is the measured leakage flow rate at 50 Pa pressure difference across the envelope divided by the volume of the building. In addition, many countries express the leakage airflow rates as airflow per envelope area, related to a reference pressure difference of e.g. 4 Pa in France and Switzerland. Moreover, the effective leakage area (ELA) is the flow rate related to an orifice equation at a reference pressure corresponding to the measured leakage volume flow rate at the same pressure difference, e.g. 4 Pa in the US (Limb, 2001). These values for airtightness can be obtained by measurements, i.e. pressurization tests or leakage distribution measurements, or derived from databases, see amongst others (Orme and Leksmono, 2002), (Sherman and Chan, 2004).

Requirements or recommendations for the airtightness of the building envelope are included in most national building standards and guidelines (Limb, 2001). The European ventilation standard for non-residential buildings EN 13779 (CEN, 2004b) makes no demands, only recommendations for buildings with balanced mechanical ventilation systems. The n_{50}-value should be below 1.0 h^{-1} and 2.0 h^{-1} in case of buildings with respectively more or less than three stories. In addition, dwellings in Belgium with a balanced mechanical ventilation system are advised in the Belgian ventilation standard NBN D50-001 (BIN, 1991) to have an n_{50}-value smaller than 3.0 h^{-1}.

Air infiltration or exfiltration is characterized in a multi-zone model as a one-dimensional flow or a crack by the power law (Eq. 4.40). The uncertainty on the flow coefficient C is derived from measurements of the airtightness in flats in France (Litvak et al., 2000a,b), (Orme and Leksmono, 2002) and Belgium (BBRI, 1999), (Bossaer et al., 1998). The geometry of a flat agrees well to this of a cross section of two offices, separated by a central corridor.

Litvak et al. (2000a,b) measured 26 multi-family and 38 single-family dwellings of less than 5 years old with different types of construction and thermal insulation. The leakage parameters n and C were determined from the collected data (Δp, Q) of the pressurization test. These parameters were used to define the infiltration airflow rates at 4 (Q_4) and 10 Pa (Q_{10}) and consequently the airtightness indicators I_4 and τ_{10}, related to respectively the unheated surface and the heated volume. The average flow exponent n in multi-family dwellings equals 0.68, which agrees well to the normalized value. No uncertainty is assumed on this flow exponent in the simulations of natural night ventilation. The average and standard deviation of the flow coefficient C are calculated from the infiltration flow rates Q_4 at 4Pa in the multi-family buildings, given the average flow exponent n, using external dimensions: $\mu_C = 4.0 \times 10^{-4}$ kg/s.m^2.Pa^n and $\sigma_C = 3.9 \times 10^{-4}$ kg/s. m^2.Pa^n.

This corresponds to an average and standard deviation of the n_{50}-value of respectively 3.9 and 3.8 h^{-1} in a cross section with a volume of 100 m^3, i.e. approximately the volume of the generic office model in paragraph 5.1.2. This corresponds on its turn to the measured global airtightness in nine new Belgian apartments in the SENVIVV study (BBRI, 1999), (Bossaer et al., 1998). The average n_{50} in flats is 4.1 h^{-1}, a wide variation is noticed from less than 2 h^{-1} to more than 8 h^{-1}. This study investigated the insulation, ventilation and heating in 200 newly built dwellings in Belgium. Amongst other things, a method was developed to estimate visually the minimum level of the airtightness of a dwelling.

These values also correspond in the generic building model to an average and standard deviation of the v_{50}-value of respectively 17.2 and 16.7 $m^3/h.m^2$ external area of the external walls. This average value corresponds to the average measured airtightness in 12 office buildings in the United Kingdom, i.e. 20.4 $m^3/h.m^2$ as well (CMHC, 2001). This means that the assumed air tightness is larger than the default value in the calculations of the heating energy consumption in the energy performance regulations of 12 $m^3/h.m^2$ (Flemish Government, 2005b). However, the leakage flow rate v_{50} is in this case only related to the area of the two façades. When the n_{50}-value is related to the area of the external walls of the whole office building, i.e. including also roof, floor and side walls, the v_{50}-value will be lowered. For example, in an office building with 2 floors of 20 offices each (12.2 x 32.7 x 7.4 m^3), n_{50}-value of 3.9 corresponds to a v_{50}-value of 7.8 $m^3/h.m^2$.

Furthermore, it has to be remarked that physically unrealistic, i.e. negative, values of the flow coefficient in the Latin Hypercube samples are replaced with zero.

4.3.4 SYSTEM CHARACTERISTICS

Night ventilation opening characteristics and control parameters of the building management system are understood by systems characteristics.

4.3.4.1 CHARACTERISTICS OF NIGHT VENTILATION OPENINGS

To ensure intensive natural ventilation at night, top or bottom-hung windows, louvres, etc. are provided. The airflow through these envelope openings is derived from the relationship between the pressure and the velocity along a streamline, i.e. Bernoulli equation, and usually written as follows, i.e. the orifice equation:

$$Q = C_d A_{eff} \sqrt{\frac{2\Delta p}{\rho}}$$

Eq. 4.36

where C_d is the discharge coefficient, A_{eff} the effective area of the opening, ρ the density of the incoming air and Δp the air pressure difference inside-outside.

The discharge coefficient C_d is defined as the product of the contraction coefficient C_c, which indicates that the flow section (the vena contracta) is smaller than the geometrical section of the opening, and the velocity coefficient C_v, which depends on the friction in the opening. The contraction coefficient depends on the shape of the flow and of the opening. For a flow directly through a sharp-edged opening, C_c is close to 0.6. For an opening with smooth rounded edges, the coefficient will be close to 1. Furthermore, the friction loss of a flow through a short opening, i.e. short in the direction of the flow, is small compared to the

loss in a pipe. Therefore, the velocity coefficient is assumed to be 0.95 for a ventilation opening (Heiselberg, 2003).

Measurements have been carried out to define the value of this discharge coefficient. A wide variation of values has been found for envelope openings: 0.65 (small openings), 0.9 (large openings) (Santamouris, 1992), 0.67-0.73 (Limam et al., 1991), 0.49-0.58 (Mahajan and Hill, 1986), 0.6 ± 0.2 (Allard et al., 1992). Heiselberg et al. (2001) monitored the airflow through different types of windows in laboratory. They concluded that the discharge coefficient depends on the type of window, the area of the opening and the temperature difference. C_d varies from 0.6 (large) to 1 (small opening) for a side hung window and from 0.8 (large) to 1 (small opening) for a bottom hung window. Favarolo and Manz (2005) studied the temperature driven single-sided ventilation through a large rectangular opening by CFD simulations. These results were validated by experimental data. They investigated the impact of the dimensions and position of a large rectangular opening and of the inside-outside temperature difference on the air flow rate. They concluded that the vertical position of the opening has the greatest impact on the discharge coefficient. The C_d is also influenced by the opening width and wall thickness. The area and the horizontal distance of the opening from the wall are of minor importance. An asymptotic value is reached when the temperature difference is larger than 6°C. Calculated values for the C_d coefficient vary from 0.48 to 0.73. Flourentzou et al. (1998) measured the discharge coefficient in a real naturally ventilated three-level office building where the staircase acted as exhaust chimney. They concluded a discharge coefficient of 0.6 ± 0.1. The average value of the discharge coefficient is assumed 0.6 for a sharp-edged opening. In addition, an uncertainty of ± 0.1 is assumed.

The effective area of an open window equals the total area. Besides, the effective area of a bottom-hung window is calculated according to van Paassen et al. (1998):

$$A_{eff} = \sqrt{\dfrac{1}{\dfrac{1}{A^2} + \dfrac{1}{\left(2A \sin\left(\dfrac{\varphi}{2}\right) + h^2 \sin(\varphi)\right)^2}}} \qquad \text{Eq. 4.37}$$

where h, φ and A are respectively the height, opening angle and total area of the window as shown in Fig. 4.23. The factor $\left(2A \sin\left(\dfrac{\varphi}{2}\right) + h^2 \sin(\varphi)\right)$ corresponds to the sum of the areas marked in grey. In other words, Eq. 4.37 means that the flow resistance of the bottom-hung window is the sum of the resistances of the fully opened window and the opened parts (see also Eq. 4.38 and 4.39).
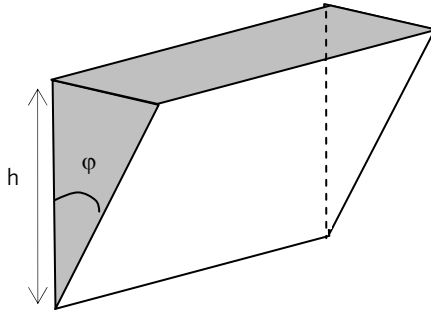
Fig. 4.23 Definition of the effective area of a bottom-hung window

In case of a combination of ventilation components, e.g. a window and a louvre, the total area can be derived from Eq. 4.38 from the required effective area and the total flow resistance coefficient, which is defined in Eq. 4.39 as the sum of the flow resistance coefficients of its components.

$$\frac{A}{A_{eff}} = C_d \sqrt{\xi}$$

Eq. 4.38

$$\xi_{tot} = \xi_{louvre} + \xi_{window}$$

Eq. 4.39

Furthermore, the airflow through closed internal ventilation openings is characterized in a multi-zone model by the power law (Eq. 4.40).

$$G = C(\Delta p)^n$$

Eq. 4.40

where Δp is the pressure difference over the opening, C the flow coefficient (kg/s.Pa^n) and n the dimensionless flow exponent which has a normalized value of 0.65 but varies from 0.5 (turbulent flow) to 1.0 (laminar flow). The average value and the uncertainty on the flow coefficient C for the internal door are derived from Orme and Leksmono (2002): 1.3 ± 0.6 dm^3/s.m.Pa.

4.3.4.2 Ventilation by day

The European ventilation standard EN 13779 (CEN, 2004b) determines a classification for indoor air quality (IDA) in non-residential buildings (see Table 4.12). The Energy Performance Regulations in Flanders requires a minimum flow rate of 22 m^3/h.pers, i.e. IDA 3 (Flemish Government, 2005). The design value of the ventilation system is 36 m^3/h and corresponds to the border value between the typical ranges of IDA 2 and IDA 3, i.e. medium and moderate indoor air quality respectively. An increased airflow of 72 m^3/h corresponds to the default value of IDA 1, i.e. high indoor air quality. The variation on these airflows is assumed 10%.

Table 4.12 Classification of indoor air quality with corresponding CO_2-levels in rooms and rates of outdoor air per person (CEN, 2004b)

category	Description	CO_2-level above outdoor air (ppm)	Outdoor air in a non-smoking area	
			Typical range (m³/h.pers)	Default value (m³/h.pers)
IDA 1	High indoor air quality	< 400	> 54	72
IDA 2	Medium indoor air quality	400 - 600	36 - 54	45
IDA 3	Moderate indoor air quality	600 - 1000	22 - 36	29
IDA 4	Low indoor air quality	>1000	< 22	18

4.3.4.3 Control systems

Ventilation by night and the sunblinds in an office building need to be controlled. These items are examined in detail in the following paragraphs.

4.3.4.3.1 Natural night ventilation

The case studies in chapter 3 prove that the control system of natural night ventilation has a large impact on the thermal comfort. Overcooling in the morning e.g. can be avoided by adequately controlling the operation of the passive cooling.

Table 4.13 proposes an automatical control system, based on the research of Martin and Fletcher (1996). Four office buildings with natural and mechanical night ventilation in the United Kingdom were monitored. This monitoring study showed that complex algorithms were no more beneficial than simpler systems. In addition, the control setpoints to initiate night ventilation have to be carefully selected. During summer months, i.e. July and August, all control strategies in the monitored buildings operated for the maximum amount of time. It was during the marginal summer monthts, i.e. May, June, September and October, that the different control strategies resulted in a wide variation regarding utilisation because of the differences in daytime conditions to permit night ventilation.

A minimum zone setpoint should be specified to prevent overcooling. This value should be related to the heating setpoint to avoid the situation where overcooling is followed by heating. The monitoring results also showed that during peak conditions, the external air temperature remained higher than the internal temperature until late into the evening. Therefore, night ventilation should only be permitted when the zone temperature exceeds the external temperature. Furthermore, night ventilation at weekends is recommended, particularly for peak ambient conditions.

The uncertainty on the temperatures in this control system are assumed the average accuracy of the temperature loggers, used in the monitoring of the building management system (Onset, 2005).

Table 4.13 Controlling natural night ventilation

Natural night ventilation is in operation if the conditions below are fulfilled
Previous day
$\theta_{i,max}$ > 23°C [22.5 – 23.0 – 23.5]°C
At that moment
22h < time < 6h $\theta_{s,ceiling}$ > 22°C [21.5 – 22.0 – 22.5]°C (= heating set point + 1°C) θ_i - θ_e > 2°C [1.5 – 2.0 – 2.5]°C v < 7 m/s

4.3.4.3.2 Sunblinds

The external sunblinds on the façade are automatically controlled. They are lowered from an incident solar radiation on the particular façade of 150 W/m² (ISSO, 1994). The uncertainty is estimated 10% of this value.

4.3.5 BUILDING USE

4.3.5.1 INTERNAL HEAT GAINS

Internal heat in an office is emitted by the people, lighting and office equipment (PC, monitor, printer, fax, copier, etc.). For non-dehumidified buildings, only sensible heat is important. These heat gains are partly convective and radiant. The convective heat gains result in an instantaneous cooling load in the air point. The radiant heat gains however, are first absorbed by the room surfaces before being re-emitted to the air (CIBSE, 1999).

Values for the internal heat gains are listed by standards and regulations (see Table 4.14), among others (ASHRAE, 2005), (CIBSE, 1999), (ISSO, 1994), (CEN, 2004a). The heat production of people depends on the activity, clothing resistance and characteristics of the indoor environment. In an office in the cooling season, seated and light to moderate work is executed in light clothing. 40 to 60% of the total heat gain of people is convective. Moreover, 70 to 80% of the gains of lighting, personal computer and monitor are convective.

The actual power consumption of office equipment is assumed equal to the total heat gain (ASHRAE, 2005). The power consumption of monitors (CRT and LCD) and computers (desktop and laptop) was measured by Roberson et al. (2002). This equipment was manufactured in 2000 and 2001. The power levels when the equipment was on, off and in sleep power, i.e. the lowest power level between on and off, were monitored. The average and the values corresponding to the 25th and 75th percentile are shown in

Table 4.15. It can be noticed that LCD-monitors consume significantly less power than CRT-monitors of similar size when on, i.e. 30 to 51%. In addition, desktop computers consume significantly more power when on than laptops.

The heat gains of computers, monitors, printers and lighting are multiplied by a diversity factor. This factor takes into account that not all equipment is in use all the time or is emitting its actual peak heat gain (Wilkins and Hosni, 2000). Continuous measurements

during one workweek showed a diversity ranging from 37% to 78% with an average of 46% (Wilkins and McGaffin, 1994). However, the diversity will vary significantly for spaces with different occupants (Wilkins and Hosni, 2000). This uncertain nature of building use mainly causes the uncertainty on the internal heat gains. In addition, small variations in standards and guidelines are taken into account.

In conclusion, three scenarios of internal heat gains are made depending on the use and heat production, based on the scenario's proposed by Wilkins and Hosni (2000). The diversity is assumed equal in case of people, equipment and lighting. Table 4.16 shows that the total heat gains (including diversity) vary from 17.8 to 28.1 W/m^2 for a single office of 15 m^2 occupied by one person. In case of two persons, the total heat gains are increased with approximately 60%. Moreover, the convective-radiant ratio is not varied: 70% of the total internal heat gains are emitted by convection. In addition, no variation is assumed on the internal heat gains in the corridor. ISSO (1994) suggests 6 W/m^2. These values are assumed constant during working hours, i.e. from 9h to 18h daylight savings time.

Table 4.14 Summary of assumptions for internal heat gains in standards and regulations

Internal heat gains		ASHRAE (2005)	CIBSE (1999)	ISSO (1994)	CEN (2004a)
People	W/pers.	70-75	63-90	80-100	80
PC + screen	(W/pc.)	110-155	116-187	130	96
Lighting	W/m^2	-	8-18	15	15
Laser printer	W/pc.	130-215	98-150	300	-

Table 4.15 Power consumption of office equipment (W): average, 25th and 75th percentile value (Roberson et al., 2002)

Power level	On (W)	Sleep (W)	Off (W)
monitor	55 (33-74)	30 (9-54)	1 (0-2)
Desktop computer	70 (50-94)	9 (3-15)	3 (2-4)
Laptop computer	19 (15-20)	3 (2-3)	2 (1-3)

Table 4.16 Internal heat gains in a single office (15 m^2) with one or two persons

Internal heat gains		low	medium	high
People	W/pers.	75	80	85
	Diversity	0.67	0.75	1
PC + screen	(W/pc.)	110	135	135
	Diversity	0.67	0.75	1.00
Lighting	W/m^2	10	10	10
	Diversity	0.67	0.75	1.00
Laser printer	W/pc.	130	130	130
	Diversity	0.33	0.4	0.4
Total (including diversity) (W/m^2)	1 pers.	17.8	21.7	28.1
	2 pers.	26.0	32.5	42.8
Total convection (W/m^2)	1 pers	12.5	15.2	19.5
	2 pers	17.6	22.2	28.9

4.3.5.2 Manual controls of windows

The adaptive temperature limits indicator is selected to evaluate the thermal comfort in an office building considering adaptation (see paragraph 2.1.3.4.2.3). Two types of office buildings are distinguished, based on, amongst other things, the availability of operable windows in the façade. The control of these windows by users has an important impact on the achieved comfort level. However, how can this manual control be simulated?

Following models for manual control of windows have been derived based on field measurements. Herkel et al. (2005) developed a preliminary stochastic model to characterize the user behaviour in one building in Germany. Inkarojrit and Paliaga (2004) derived relationships between the percentage of open windows and operative temperature in a naturally ventilated office building in California (USA). Raja et al. (2001) analysed that the use of controls is related to the thermal sensation in naturally ventilated office buildings in the UK. Nicol and Humphreys (2004) developed a probability algorithm to relate the window opening by occupants to the indoor temperature in office buildings based on field measurements in UK, Europe and Pakistan. Their model for offices in the UK is used in this research (Eq. 4.41).

$$p = \frac{\exp(-13.55 + 0.531\theta_{i,o})}{1 + \exp(-13.55 + 0.531\theta_{i,o})} \qquad \text{Eq. 4.41}$$

Window opening by users in offices in the UK has an estimated probability of 0.5 at an indoor temperature of 25.5°C (Nicol and Humphreys, 2004). This threshold temperature is used to simulate the opening of the windows by the users to cool down their office. The windows are assumed to be closed when the internal operative temperature drops below 24.5°C or at the end of the working day.

4.3.6 Overview

Table 4.17 summarizes the uncertainties on all the input parameters, except these on the thermophysical properties which are given in Table 4.8. The average (μ) and standard deviation (σ) of the uncertainty interval of each input parameter are shown.

Table 4.17 Uncertainty on all input parameters

| Input parameter			μ	σ
Weather data			Meteonorm normal temperature	Meteonorm extreme temperature
Wind reduction	On site	$\ln(z_0)$	-1.39	0.35
	meteo	$\ln(z_0)$	-3.22	0.14
Wind pressure coefficient	façade	Cp (0°)	0.25	0.10
	roof	Cp (0°)	-0.60	0.08
Dimensions	Length, width, height		-	0.01 m
External convective heat transfer coefficient		α_{ce}	5.6 +3.9v	
Internal convective heat transfer coefficient	Vertical	C	1.80	0.25
		n	0.285	0.022
	Horizontal buoyant	C	1.90	0.19
		n	0.285	0.022
	Horizontal stably stratified	C	0.44	0.08
		n	0.19	0.03
Discharge coefficient		C_d	0.60	0.05
Closed internal door	Flow coefficient	C	1.3 dm^3/s.m.Pa	0.3 dm^3/s.m.Pa
	Flow exponent	n	0.65	-
Air tightness	Flow coefficient	C	4.0 x 10^{-4} kg/s.m^2.Pa	3.9 x 10^{-4} kg/s.m^2.Pa
Total internal heat gains	1 pers.		21.7 W/m^2	2.6 W/m^2
	2 pers.		32.5 W/m^2	4.2 W/m^{2}K
Controlling temperatures		θ	-	0.25 °C
Ventilation flow rate by day	normal		36 m^3/h	1.8 m^3/h
	increased		72 m^3/h	3.6 m^3/h
Lowering sunblinds	irradiance	I_s	150 W/m^2	7.5 W/m^2
solar heat gain coefficient	window	g	0.60	0.01
	Window + sunblinds	g	0.15	0.025

4.4 CONCLUSIONS

Fig. 4.24 summarizes the implementation of the uncertainty and sensitivity analysis of the predicted performances of natural night ventilation. The existing coupling of the multi-zone building simulation tool TRNSYS (Klein et al., 2004), a transient thermal simulation model, and COMIS (Feustel, 1999), (Dorer et al., 2001), an infiltration and ventilation simulation model, is chosen to predict the thermal comfort. Uncertainty and sensitivity analysis is used to take into account the uncertainties in the input of this building simulation tool. A Monte Carlo Analysis (MCA) with a Latin Hypercube sampling (LHS) design is used to investigate the uncertainty on the output. To relate the sensitivity of the output to the uncertainties in the input, the Standardized Regression coefficient (SRC), based on the global sensitivity MCA, is selected. The statistical software SIMLAB (POLIS, 2003) is used to prepare the samples and to analyse the results. These samples are further processed by the computational software Matlab (MathWorks, 2004). Furthermore, the uncertainties on the input parameters of the simulation of natural night ventilation are defined. These distributions are the input for the uncertainty and sensitivity analysis in the next chapter.
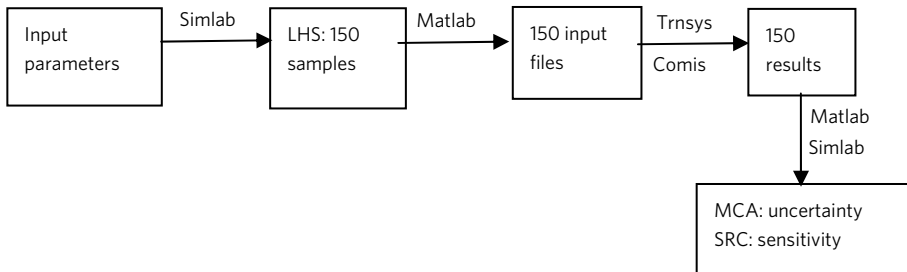
Fig. 4.24 Implementation scheme of the uncertainty and sensitivity analysis of the predicted performances of natural night ventilation

5   Uncertainty and sensitivity analysis

This chapter studies the uncertainty and sensitivity of thermal comfort achieved in a building cooled by natural night ventilation. The first section discusses the selection of a representative domain for building simulation and presents the model for single-sided, cross and stack ventilation used in the building simulation tool to predict the degree of thermal comfort. The second section discusses the simulation results. The uncertainty on and the sensitivity of thermal comfort in these three natural night ventilation strategies are compared. The surplus of the uncertainty analysis with respect to one simulation is focussed upon. In the third section, the results of this sensitivity analysis are used to increase the reliability of good thermal comfort by optimizing the building and system design. Moreover, the impact of the weather data and boundary conditions on these optimized designs are investigated. In the last section, practical use of uncertainty and sensitivity analysis in building simulation is studied. The prediction of the probability and distribution of good thermal comfort through three simulations is aimed for.

5.1 Building model and characteristics

5.1.1 Creating a building model

5.1.1.1 General rules

To evaluate the performances of a building using building simulation, a model has to be created. This means the building has to be idealised or simplified by dividing the building into zones. A zone is an air volume at a uniform temperature including the bounding surfaces. This zone does not always correspond to a room. The objective is to define as few zones as possible without significantly compromising the integrity of the simulation. The appropriate number of zones depends on the aim of the simulation, e.g. evaluating the level of thermal comfort requires a higher resolution than predicting the energy consumption for heating.

Following general rules can be applied to evaluate the level of thermal comfort in the building. Firstly, characterising the whole building by taking a building section has to be under serious consideration. This section can be a symmetrical or identical repeating part of the building. Secondly, the first assumption is a one-zone model of a characteristic room of this building (section). Thirdly, different orientations or internal heat gains of this characteristic room make expansion of this one-zone model necessary. If these rooms are directly connected, i.e. by an airflow or a conducting wall, a multi-zone model of this floor has to be made. On the other hand, if these rooms are hardly connected, several one-zone models have to be evaluated. Fourth, in case of natural ventilation by passive stack, differences in driving forces between the floors cause further expansion of the model. If the airflows on the various floors are connected, a multi-zone model including all these floors has to be made. On the contrary, the existing multi-zone floor model is sufficient.

5.1.1.2 Example (Breesch and Janssens, 2005)

An example of modeling a naturally ventilated office building is discussed to understand the impact of the modeling decisions. The examined office buildings "Sint-Pietersnieuwstraat" are situated on the west and the east side of a courtyard and are part of large complex of offices, laboratories and an auditorium in the city centre of Ghent. Architect of this complex is the temporary partnership Beel-De Geyter-SWK, the concept of natural night ventilation is

made by the company Cenergie. Both buildings include three office floors on top of a foyer and two underground service floors. Fig. 5.1 and Fig. 5.2 respectively show a floor plan and a cross section. Furthermore, Fig. 5.3 shows the design scheme of the natural ventilation system (by day and night) on a floor plan. Outside air enters the offices on each floor through top hung windows, cools down the exposed floor by night, flows through the lowered ceiling to the corridor and continues its way to the central stairwell on the south side of the courtyard where the air leaves on top of the building through outlet windows on both sides.
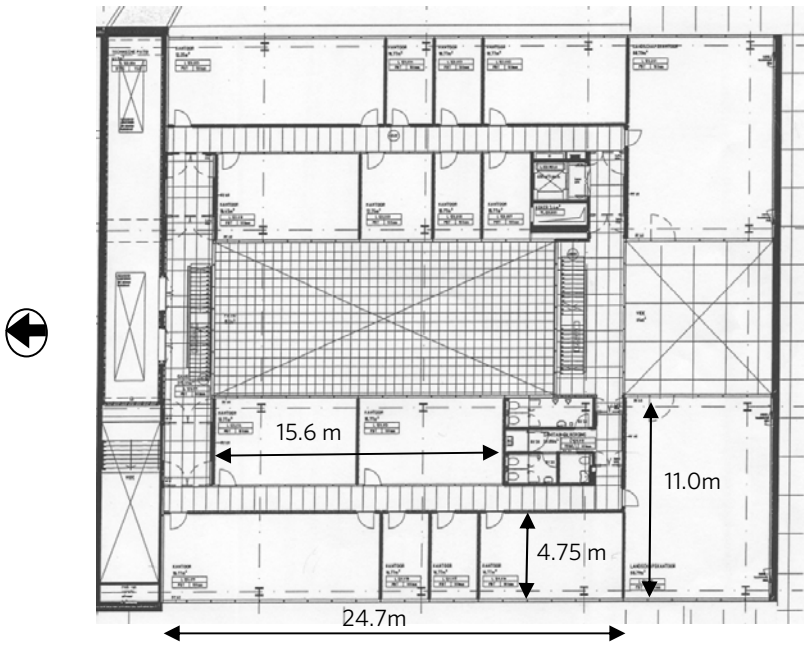
Fig. 5.1 Floor plan of the new office buildings "Sint-Pietersnieuwstraat" (Ghent University)
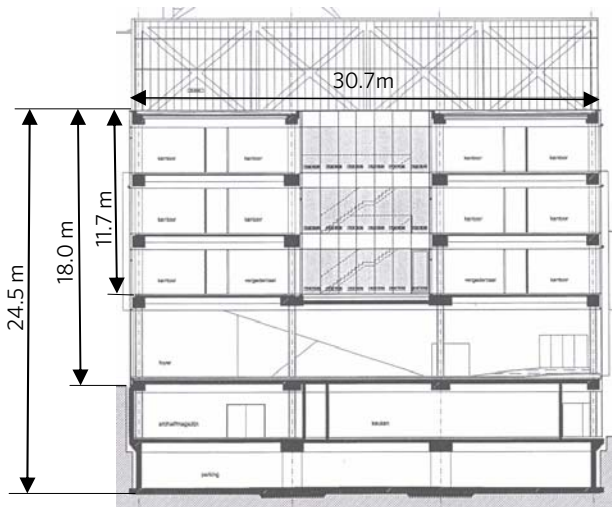
Fig. 5.2 Cross section of the new office buildings "Sint-Pietersnieuwstraat" (Ghent University)
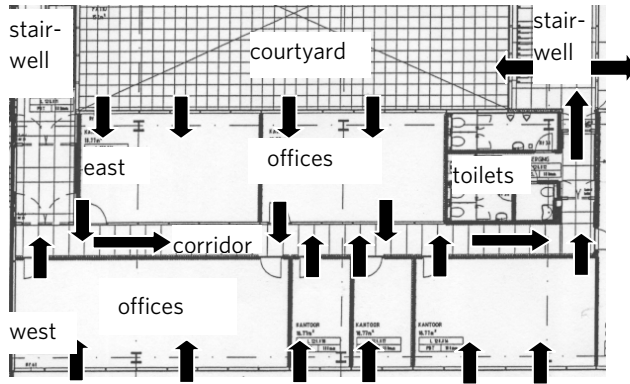
Fig. 5.3 Design scheme of natural night ventilation in the new office building "Sint-Pietersnieuwstraat" of the Ghent University

A 3-zone model of each floor connected to the stairwell (see Fig. 5.4) was created to design the ventilation openings. This model assumes a neutral pressure plane on each floor between the supply openings in the façade and the exhaust opening in the stairwell. The openings are designed to create an air change rate of 10/h when an indoor-outdoor temperature difference of 7°C and no wind are assumed. The resulting effective leakage area (C_d*A_{eff}) of the supply and circulation openings in 1 office module of 2.6m wide on each floor is given in Table 5.1. The effective leakage area of the exhaust openings in the stairwell is 4.6m^2 or 70% of the total area of the inlet openings.
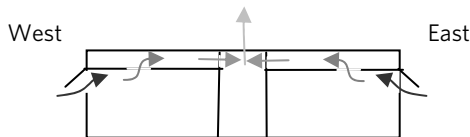
Fig. 5.4 3-zone model of the third floor

Table 5.1 Characteristics of natural night ventilation in the new office building "Sint-Pietersnieuwstraat" of the Ghent University

Characteristics of night ventilation openings in 1 office module				
floor	supply		circulation	
	C_d*A_{eff} (m^2)	A_{eff}/A_{floor} (%)	C_d*A_{eff} (m^2)	A_{eff}/A_{floor} (%)
first	0.08	1.1	0.16	2.4
second	0.10	1.3	0.17	2.6
third	0.24	3.2	0.18	2.7

The impact of using this simplified 3 zone model to design the ventilation openings is shown in Fig. 5.5. A mass balance is applied in a single-zone building model to estimate the neutral pressure level and the ventilation rates under design boundary conditions, i.e. an indoor-outdoor temperature difference of 7°C and a wind velocity of 0 m/s. An inflow of 10 h^{-1} or more is noticed on the first and the second floor, as designed with the simplified model. However, the impact of the assumptions of this simplified model is clear on the

ventilation rates of the third floor. The air is noticed to be flowing out on this floor because the neutral pressure level of this building is situated between the openings of the second and the third floor. This is caused by a difference in height of only 0.5m between the supply openings on the third floor and the exhaust openings on top of the stairwell. The 3-zone model of each office floor on the other hand, assumes a neutral pressure plane on each floor between the supply and the exhaust openings. As a consequence, an inflow is predicted on each floor. It can be concluded that this 3-zone model is not a correct representation.
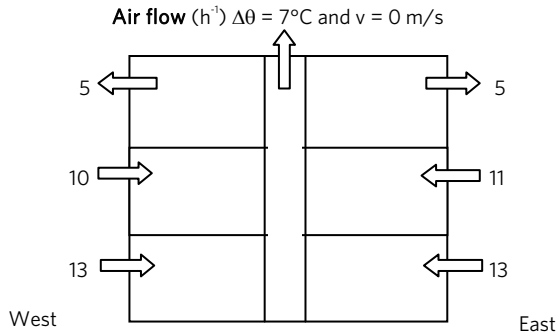
Fig. 5.5 Resulting air flows at design conditions by night

According to the design rules, a 7-zone building model should be used instead. The west and east orientated offices are connected by an airflow. As the stack driven force differs on each floor, the three office floors have to be taken into account in the model. Because the door between the corridor on each floor and the stairwell is always open to ensure the ventilation flow, the corridors on the various floors are connected. Therefore, the corridors and the stairwell are assumed to be presented by one zone. Fig. 5.6 shows this resulting 7-zone model including one office zone on the west and the east side on each floor, connected by one circulation zone.
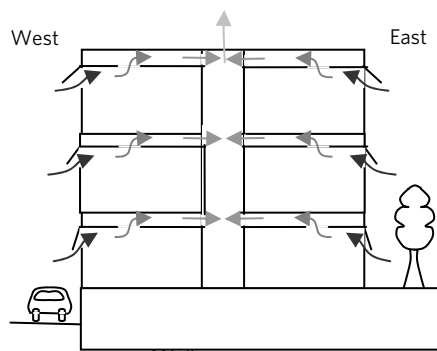
Fig. 5.6 7-zone building model of the new office building "Sint-Pietersnieuwstraat" of the Ghent University

In conclusion, this example has shown that creating an appropriate building model is important in the design and simulation of natural night ventilation. This design and evaluation considering the uncertainties are further discussed in chapter 7.

5.1.2 Generic building model

A building model has to be made to predict the generic performances of natural night ventilation by the building simulation tool TRNSYS-COMIS. A typical office building is taken into consideration: a two- (or more) storey building with identical small offices on both sides of a central corridor. As a consequence, the building is simplified by taking only the cross-section into account. In addition, the floors are connected by stairwells on both sides of the building. The corridors and the stairwells are assumed to be disconnected, e.g. separated by fire proof doors because of fire regulations. As a consequence, the floors can be analyzed separately. The resulting building models for cross, passive stack and single-sided night ventilation are respectively shown in Fig. 5.7, Fig. 5.8 and Fig. 5.9. In addition, Fig. 5.10 shows a nodal network of the cross ventilation case, used in the simulations in COMIS. This model includes 3 zones: two identical offices separated by a central corridor. The offices are situated on an intermediate floor, in this case the lowest floor of a two-storey office building. The orientation can be chosen: north-south or east-west. A passive stack can be added to the corridor. Internal separations between the concerned office and adjacent offices are assumed adiabatic. A similar model is also used by van Paassen et al. (1998) and Kolokotroni et al. (1997) in their pre-design tools for natural night ventilation.
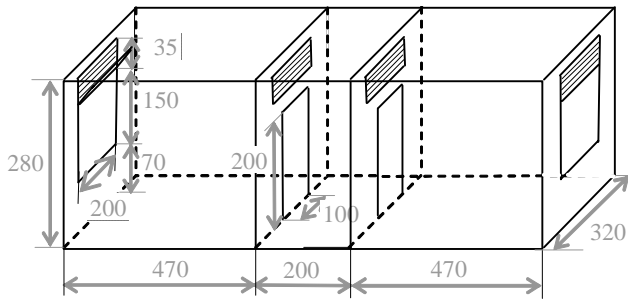
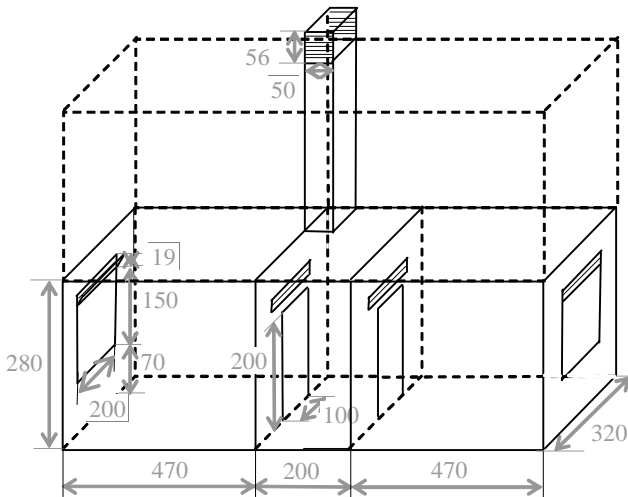Fig. 5.7 3-zone office model provided with cross ventilation openings

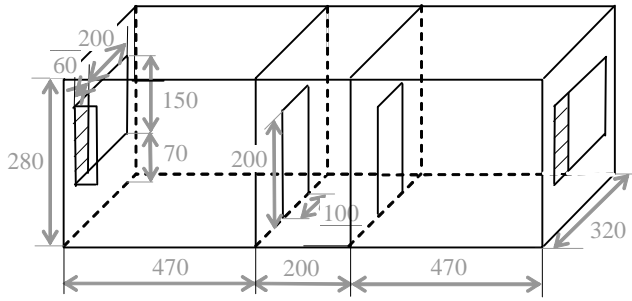Fig. 5.8 3-zone model for passive stack ventilation

Fig. 5.9 3-zone office model for single-sided night ventilation

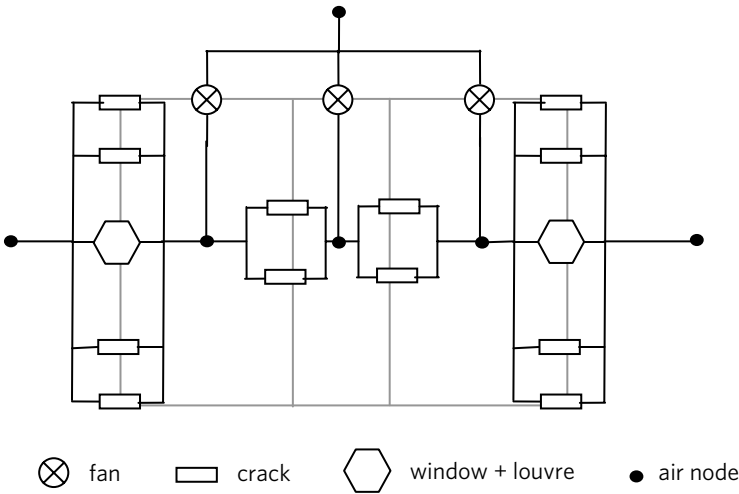fan   crack   window + louvre   air node

Fig. 5.10 Nodal network in COMIS for cross night ventilation case

5.1.3 INPUT PARAMETERS

Most input parameters of the building simulation and their uncertainties are already determined in the previous chapter. Therefore, the discussion in this paragraph is restricted to boundary conditions, building, system and simulation characteristics specific to the building model defined in the previous paragraph and properties of the performance indicators.

5.1.3.1 BOUNDARY CONDITIONS

The wind pressure coefficients on top of the passive stack are calculated using the Cp generator of Knoll et al. (1995). Fig. 5.11 shows the variation of the wind pressure coefficient on the exhaust opening on the north side of the passive stack. This variation is derived from values calculated on various positions on the stack.
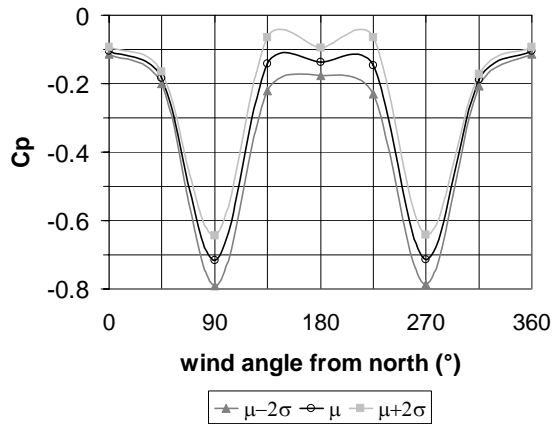
Fig. 5.11 Variation on the wind pressure coefficients on the exhaust opening on the north side of the passive stack

5.1.3.2 Building characteristics

Fig. 5.7 to Fig. 5.9 show the average internal dimensions of the concerned offices: an internal floor area of $15m^2$ is assumed, i.e. the design occupancy for offices in the requirements for ventilation in non-residential buildings (Flemish Government, 2005a). The area of the other walls is given in Table 5.4. These internal dimensions are taken into account in the simulations for heat transfer and storage. Moreover, exterior shading devices are provided on all orientations. The total window area including the aluminium frame can be varied as shown in Table 5.2. In the basic case, an area of 25% of the external area of the façade is provided. The area of the aluminium frame is assumed 25% of the total window area as mentioned as a default value in the Belgian standard to calculate the thermal transmittance coefficient of walls (BIN, 2001). This results in a glazing area of 25% of the internal façade area.

Table 5.2 Characteristics of windows and natural night ventilation louvres

window			louvre						
			supply					exhaust	
				cross/stack		single-sided		stack	
A (%)	w (m)	h (m)	A_{eff} louvre (%)	w (m)	h (m)	w (m)	h (m)	w (m)	h (m)
20	2.00	1.20	2	2.00	0.35	-	-	-	-
			3	2.00	0.50	0.73	1.20	-	-
25	2.00	1.50	1	2.00	0.19	-	-	0.50	0.56
			2	2.00	0.35	-	-	0.50	1.05
			3	2.00	0.50	0.60	1.50	-	-
30	2.40	1.50	2	2.40	0.30	-	-	-	-
			3	2.40	0.45	0.60	1.50	-	-

The air tightness is modelled by four cracks in each office façade: at floor and ceiling height and at the bottom and the top of the window. Schild (2003) states that the façade should

be subdivided in horizontal strips to model the leakage due to stack-effect properly. An even number of strips is recommended. Four horizontal strips create a discretisation error of 2% of the infiltration flow. This error decreases with increasing number of horizontal strips.

The composition and thermal transmittance of the walls are additionally shown in Table 5.3 and Table 5.4 respectively. The basic office includes an exposed ceiling, a raised floor, a heavy façade and light internal walls. The thermophysical properties of the layers and their corresponding uncertainties can be found in Table 4.8. For the adiabatic internal separations, only half the wall is considered. This means that the model of the exposed ceiling is made of the hollow core concrete slabs and the raised floor includes the other layers listed in Table 5.3. The lowered ceiling is divided in the same way: the model of the exposed floor includes the reinforced and light concrete layers, the lowered ceiling the other layers. In addition, the internal wall dividing the considered office from the adjacent offices is modelled as a gypsum board and half the insulation layer.

Table 5.3 Wall composition

Raised floor		Heavy façade		Light internal wall	
Layer	d (cm)	Layer	d (cm)	Layer	d (cm)
Hollow core concrete slabs	13	Façade brick	9	Gypsum board	1
Reinforced concrete	3	Air cavity	2	Insulation	5
Light concrete	5	Insulation	8	Gypsum board	1
Air cavity	50	Internal brick	14		
Plywood	1.8				
Carpet	0.5				
Lowered ceiling		Light façade		Heavy internal wall	
Layer	d (cm)	Layer	d (cm)	Layer	d (cm)
Gypsum board	1	Aluminium	0.5	Internal brick	9
Insulation	5	Insulation	10		
Air cavity	50	Gypsum board	1		
Hollow core concrete slabs	13				
Reinforced concrete	3				
Light concrete	5				

Table 5.4 Thermal transmittance and area of the walls for a 15m^2 office

wall	A (m^2)	U (W/m^{2}K)
Raised floor*	15.00	1.00
Lowered ceiling	15.00	0.49
Heavy façade*	5.96	0.37
Light façade	5.96	0.37
Light internal walls (office + corridor)*	35.28 (26.32 + 8.96)	0.63
Heavy internal walls (office + corridor)	35.28 (26.32 + 8.96)	2.40

 * base case

5.1.3.3 System characteristics

External louvres are provided in the façade to ensure natural night ventilation flow rates. In case of cross and passive stack ventilation, horizontal louvres are situated above the windows and internal doors as shown in respectively Fig. 5.7 and Fig. 5.8. The external louvres are automatically opened and closed by bottom-hung windows. In case of single-sided ventilation, a vertical louvre is provided on one side of each window, protected by a side-hung window as shown in Fig. 5.9. No internal louvres are additionally provided. Furthermore, in case of passive stack night ventilation a chimney with top hung extract windows on two sides is placed on top of the roof. This means a stack height of 3.89 m for the basic office on the lowest floor.

The effective area of all these louvres, i.e. external and internal, is determined as a proportion of the floor area using the design rules of van Paassen et al. (1998) (see Fig 2.14). Assuming medium internal gains for 1 person, i.e. 22 W/m^2 (see Table 4.14), a west-east orientation and 25% windows with external sunblinds, i.e. + 14 points, a heavy accumulation mass (M = 124 kg/m^2) with an open ceiling, i.e. -7 points, and a predictive control, i.e. +0 points results in a total of 29 points. This means an effective opening of 3% and 2% of the floor area for single-sided and cross ventilation respectively. In addition, an opening of only 1% is required for mechanically supported stack ventilation.

The corresponding total area and dimensions of these louvres, as shown in Table 5.2, are derived from Eq. 4.37 – 4.39 as follows. In case of single-sided ventilation, an open window and a louvre are combined. The flow resistance coefficients of both components are calculated from Eq. 4.38, considering a discharge coefficient of 0.6 and assuming the effective area of the louvre 60% of the window area. The flow resistance coefficient for the open window and louvre are 2.8 and 7.7 respectively. Consequently, the ratio of the total to the effective area of this combination equals 1.94. In case of cross and stack ventilation, a bottom-hung window is used instead of an open window. The effective area of this combination is estimated by evaluating Eq. 4.37, in which the total area is estimated by the effective area of the louvre, i.e. 60% of the window area.

A mechanical ventilation system by day is provided. The flow rates are directly supplied to the office and extracted from the corridor. Moreover, a heating system is implemented to ensure good thermal comfort during office hours at the beginning and the end of the simulation period, where low morning temperatures occur. When the internal air temperature in the previous time step drops below the heating set point minus 0.8°C, both the mechanical supplied ventilation flow is preheated to the set point temperature and the radiator heating with unlimited heating power is started in the current time step. The heating is stopped when the internal air temperature is increased to the heating set point plus 0.2°C in the previous time step. This heating set point equals to the set point of night ventilation minus 2°C. The heating is started up 1h before occupancy and stopped at the end of the working day.

5.1.3.4 Performance indicators

5.1.3.4.1 Weighted temperature excess method

The method of the weighted temperature excess requires the input of both environmental and personal characteristics. Apart from the air and mean radiant temperature, which are

part of the simulation results, the air velocity, internal vapour pressure, metabolism and clothing resistance are demanded. The Dutch government (GBA, 1999) determines a metabolism of 1.2 met or 70 W/m^2 body's area and a clothing resistance of 0.7 Clo, i.e. light working clothes and a chair. This latter value is specified as 0.66, i.e. the average value of the clothing resistance of people including the chair in naturally ventilated buildings in the analysis of de Dear and Brager (1997). The air velocity is assumed 0.1 m /s (ISSO, 1994). This value corresponds to the measured mean air velocity corresponding to an operative temperature of 21.6°C in naturally ventilated buildings in de Dear and Brager (1997). The internal vapour pressure $p_{v,i}$ is calculated from the weekly-mean weather data in Eq. 5.1 (Hens, 1992). This is the maximum vapour pressure difference for a building of internal condensation class 2 (BBRI, 1982), i.e. a building with low vapour production or a ventilation system.

$$p_{v,i} - p_{v,e} = 436 - 22\theta_e \qquad \text{Eq. 5.1}$$

5.1.3.4.2 Adaptive temperature limits indicator

A type alpha building with an operable window in each office is assumed (see paragraph 2.1.3.4.2.3). Moreover, the evaluation of the thermal comfort by the adaptive temperature limits indicator is only based on the temperature excess of the upper limits. Therefore, the results can be compared to those of the weighted temperature excess method, which also only considers the temperature excess.

5.1.3.4.3 Saved cooling demand

Furthermore, the savings in cooling load, compared to the case without natural night ventilation, is predicted based on the adaptive temperature limits indicator as follows. A good internal comfort, i.e. level B, is aimed. Two simulation models are created respectively with and without natural night ventilation. In both cases, the adaptive temperature limit B, i.e. 80% thermal acceptability, is used as a set point for cooling during office hours. The cooling system is 100% convective and ideally controlled. The cooling demand to prevent the operative indoor temperatures to exceed the limits of 80% thermal acceptability is calculated in both cases. Consequently, the savings in cooling demand are estimated as the difference between the cooling demand in the case without and with natural night ventilation.

5.1.3.5 Simulation characteristics

Simulations are carried out during the Belgian summer from May 21 to September 15 preceded by a 3-week dynamic start up. The Meteonorm normal weather data set of Uccle (Belgium) is used. A time step of 15 min is chosen. The offices are assumed to be occupied during working hours from 8h to 17h. The total building height averages 7.3m. The floor and internal walls are assumed to absorb 60% and 40% of the direct solar radiation entering the office respectively.

The characteristics of the uncertainty and sensitivity analysis are also defined. For the Monte Carlo analysis, 150 independent Latin Hypercube samples are developed using Simlab software (POLIS, 2003). This number largely exceeds the minimum of 1.5 x 72 = 108 factors (Saltelli et al., 2000) and is checked in the analysis.

5.2 Simulation results

5.2.1 Average performances

Before discussing the results of the uncertainty and sensitivity analysis, the results of the building simulation of the office model with average properties is examined. Consequently, a clear understanding in the surplus of the results of the uncertainty and sensitivity analysis is gained.

5.2.1.1 Thermal comfort

Table 5.5 compares the results of the building simulation of the office model of the previous section with average building and boundary characteristics for different natural night ventilation strategies and effective louvre areas. Thermal comfort is evaluated by both selected criteria, i.e. the weighted excess hours (GTO) and the adaptive temperature limits (ATG). For the adaptive temperature limits method, in addition to the level of comfort the amount of hours in either the lower or the upper interval of each level is given in Table 5.5. Cases with a good thermal comfort according to GTO are marked in grey. Moreover, Fig. 5.12 and Fig. 5.13 present the results of the adaptive temperature limits method for a cross ventilated office with a louvre area of 3% on the east side with and without natural night ventilation. The results for the other orientations and strategies are similar.

Table 5.5 Results of building simulation with average properties

strategy	Louvre area (%)	Orientation	GTO (h)	ATG (h)								Saved cooling demand (kWh/m².year)
				level	-	-C	-B	A	+B	+C	-	
Single-sided	3	W	313	-	0	3	11	521	163	40	18	6.2
		E	398	-	0	0	2	443	209	74	28	7.9
		N	354	-	0	0	8	498	180	46	24	7.2
		S	306	-	0	2	23	533	146	37	15	6.3
Cross	2	W	147	-	1	7	33	599	98	12	6	6.5
		E	286	-	0	3	16	484	178	62	13	8.0
		N	219	-	0	2	25	561	137	28	3	7.5
		S	185	-	6	11	45	553	122	16	3	6.5
	3	W	111	-	1	8	36	625	76	9	1	6.5
		E	199	-	0	5	18	544	158	27	4	8.3
		N	162	-	0	2	29	599	110	15	1	7.6
		S	129	-	6	10	42	594	98	5	1	6.6
stack	1	W	137	-	2	5	40	609	89	10	1	6.5
		E	263	-	0	4	14	504	178	41	15	8.1
		N	202	-	0	3	28	571	128	20	6	7.6
		S	157	-	8	11	45	591	90	10	1	6.6
	2	W	99	C	1	7	44	632	64	8	0	6.6
		E	164	-	0	5	14	570	143	19	5	8.3
		N	126	C	0	4	32	617	95	8	0	7.6
		S	91	C	3	11	55	627	57	3	0	6.6
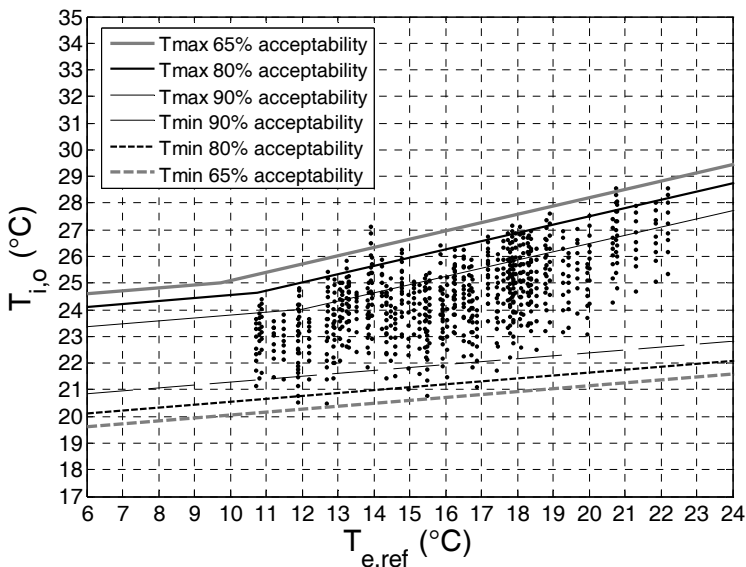
Fig. 5.12 Result of adaptive temperature limits method in an office on the east side with cross natural night ventilation and an effective area of 3%
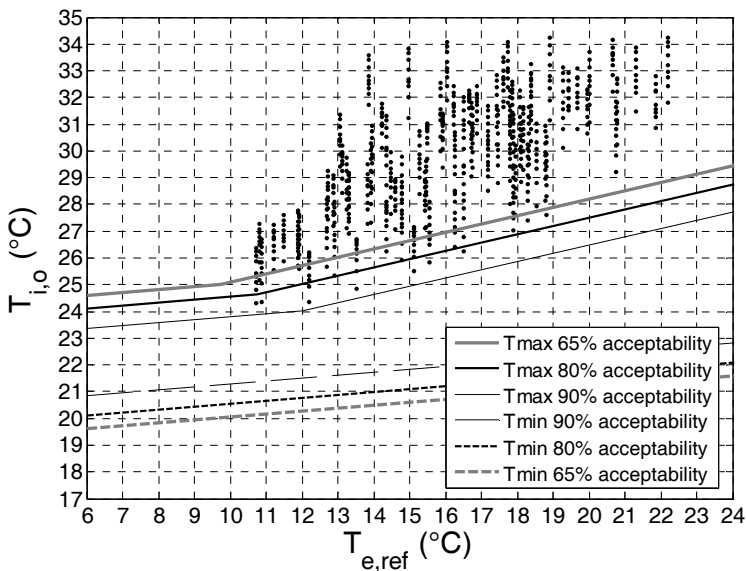

Fig. 5.13 Result of adaptive temperature limits method in an office on the east side without natural night ventilation

This table shows that the office on the south side has best thermal comfort in case of single-sided ventilation while an office on the west has best thermal comfort in case of passive stack and cross ventilation. The east orientation always has the worst result, followed by the north orientation. These differences are explained by differences in wind direction and moment of incident solar radiation. Both phenomena are unfavourable for the east orientation because solar heat gains are large in the morning and the main wind

direction in Belgium is south-west. Consequently, the outside air cooling down the building structure at night is mostly warmer and less infiltration is noticed in the east than in the west office. Moreover, when the west office has been cooled down, the bottom hung windows in this office consequently close and the night ventilation in the east office has to continue in the less performing single-side mode. In case of north orientation, differences in both wind direction and the moment of lowering the exterior shading explains the difference in thermal comfort.

Furthermore, these results show that thermal comfort is insufficient in case the louvre area is sized according to the dimensioning method of van Paassen et al. (1998). This can be explained by differences in the input data. The weather data differs and the assumptions of amongst other things the air tightness, ventilation by day and internal convective heat transfer coefficient are not mentioned in the paper. Therefore, the effective area is increased to 3% and 2% in the case of cross and stack ventilation respectively. This measure improves thermal comfort: the weighted excess hours vary between 91 and 199, i.e. good to acceptable thermal comfort. However, according to the temperature limits method, the degree of thermal comfort still does not meet the requirements. The difference between these criteria is further investigated in paragraph 5.2.5. Moreover, in case of single-sided ventilation additional measures are needed to ensure good thermal comfort. These measures are discussed in the next section.

In addition, single-sided ventilation can be noticed to lead up to the worst thermal comfort. Passive stack and cross ventilation strategies result in comparable comfort. Differences are related to the different flow rates during night ventilation. Fig. 5.14 shows that these night ventilation flow rates in single-sided ventilation are low in comparison to the other cases because the stack driving force is low as a result of the small height difference between the supply and extract opening. In addition, a wide distribution of the flow rates in cross ventilation can be noticed in Fig. 5.14. On the contrary, the passive stack guarantees a more stable flow rate, even when the wind velocity is low or the wind direction reverse.

The distribution of the corresponding indoor-outdoor temperature differences during nighttime ventilation are compared in Fig. 5.15. It is shown that an indoor-outdoor temperature difference of 5 and 4°C is probable in respectively single-sided and both cross and stack ventilation. This temperature difference is decreased to 3°C in case of cross and stack ventilation when the louvre area is increased with 1%. In addition, Fig. 5.16 discusses the minimum duration of the opening of the windows for natural night ventilation. A minimum opening duration of 6 and 5h is probable for single-sided and both stack and cross ventilation respectively. This time decreases with 1h when the louvre area increases with 1% in case of cross and stack ventilation.

Besides, Fig. 5.17 to Fig. 5.19 relate the night flow rates to the indoor-outdoor temperature differences in case of single-sided, cross and stack ventilation respectively. It can be noticed that the flow rates in cross and passive stack ventilation, unlike single-sided ventilation, are strongly influenced by wind effects.
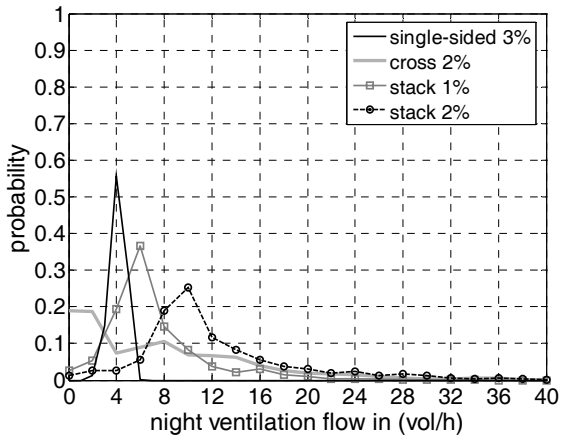
Fig. 5.14 Comparison of the distributions of the night ventilation flows between the various strategies in an office on the south side
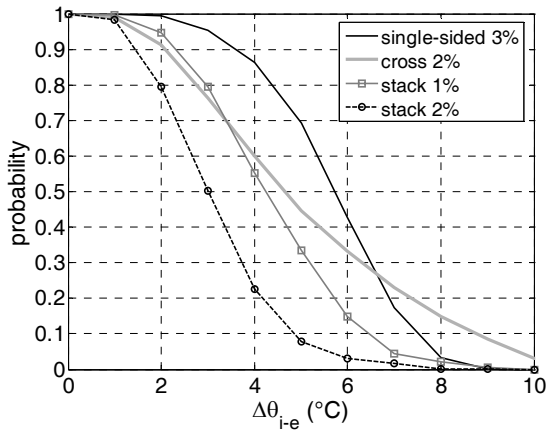

Fig. 5.15 Comparison of distributions of the indoor-outdoor temperature difference during night ventilation in an office on the south side
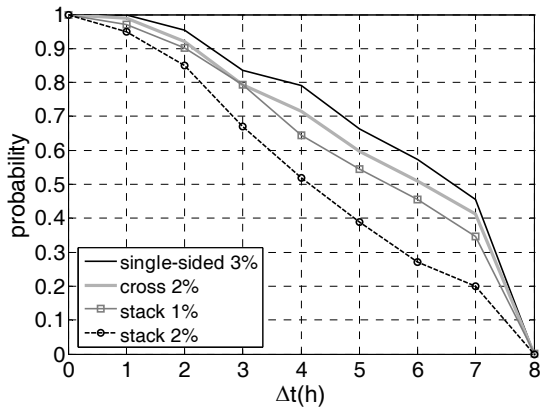

Fig. 5.16 Comparison of distributions of the minimum opening duration (h) of the windows for night ventilation in an office on the south side
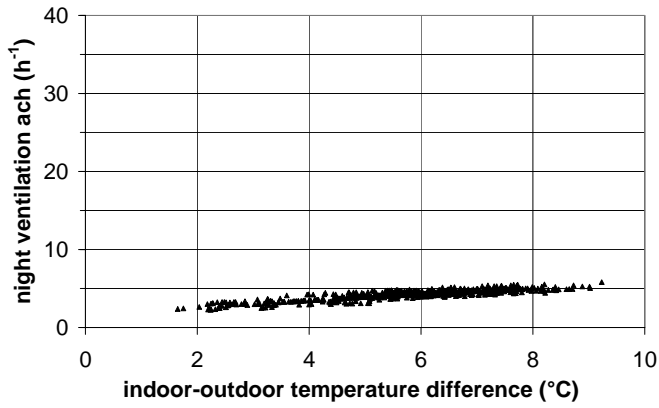
Fig. 5.17 Relationship of the night ventilation flow rates to indoor-outdoor temperature differences in an office on the south side in case of single-sided ventilation (3% louvre area)
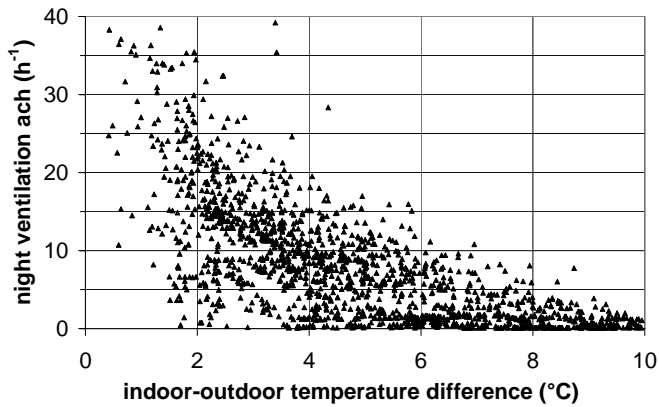
Fig. 5.18 Relationship of night ventilation flow rates to indoor-outdoor temperature differences in an office on the south side in case of cross ventilation (2% louvre area)
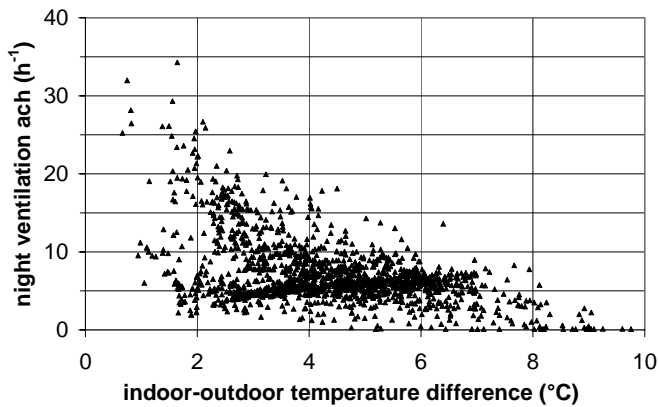
Fig. 5.19 Relationship of night ventilation flow rates to indoor-outdoor temperature differences in an office on the south side in case of stack ventilation (1% louvre area)

Table 5.5 also shows the saved cooling demand (in kWh/m^2.year) to reach a thermal comfort level B according to the adaptive temperature limits method (see Fig. 2.12 and Fig. 2.13). This savings is defined as the difference in cooling demand in the office without and with natural night ventilation respectively as shown in Table 5.6.

Table 5.6 Comparison of cooling demand to reach ATG-level B

Necessary cooling demand to reach level B (kWh/m^2.year)					
Ventilation strategy	Louvre area (%)	North	East	South	West
Without night ventilation	-	7.7	8.5	6.6	6.6
Single-sided	3	0.4	0.6	0.3	0.4
Cross	2	0.2	0.5	0.1	0.1
Cross	3	0.1	0.2	0.0	0.1
Stack	1	0.1	0.4	0.0	0.1
Stack	2	0.1	0.2	0.0	0.0

The saved cooling demand is comparable in all strategies and orientations. This conclusion is explained by comparable cooling demands in all orientations to reach ATG-level B in the case without night ventilation. Moreover, these savings are noticed to be small. A low cooling load (in W/m^2) in the office without natural night ventilation due to low internal and solar heat gains and an exposed thermal mass explains this. This cooling load is shown in Table 5.7 for a single office on a hot day in July and September ensuring an indoor air temperature of 24°C. These values are calculated according to the German standard VDI 2078 (1996) including heat storage and checked for the whole summer period by simulations in TRNSYS-COMIS. These cooling loads are small compared to the rule of thumb of BSRIA (Pavey, 1995) of 125 W/m^2 or 1 kW/occupant cooling load in offices.

Table 5.7 Calculated cooling load in 1 office (W/m^2) according to VDI 2078 (1996)

Cooling load to keep $\theta_{i,a}$ = 24°C (W/m^2)	North	East	South	West
Time	12h	9h	12h	16h
July	31	36	35	41
September	26	30	38	35

Furthermore, Fig. 5.20 shows the saved cooling demand of cross night ventilation as a function of the internal heat gains. This figure indicates the absolute and relative savings in cooling demand that can be reached by applying natural night ventilation in case of a medium or high exposed thermal mass Aρd$_{penetration}$, i.e. 3885 kg and 6871 kg respectively (see paragraph 5.3.1.2). The latter case includes an exposed ceiling, façade and internal walls. In addition, the peak cooling capacity that can be saved by applying cross night ventilation in a west office is shown in Fig. 5.21. Minimum 13 W/m^2 peak cooling capacity can be saved by cross ventilation in case of medium exposed mass.
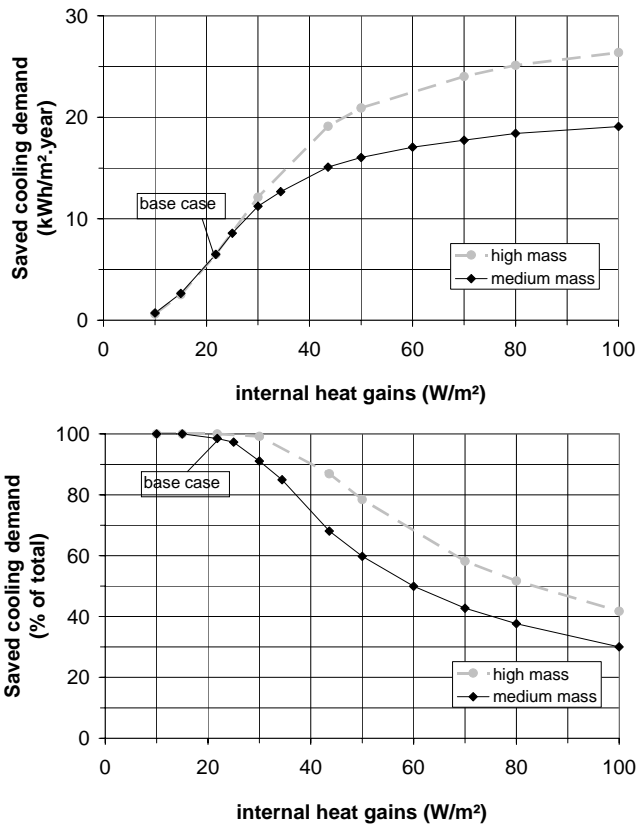
Fig. 5.20 Saved cooling demand (in kWh/m².year and % of total cooling demand) of cross night ventilation in a west office as a function of the internal heat gains
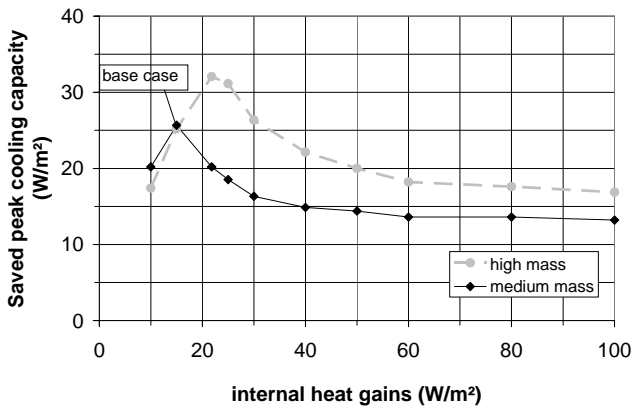

Fig. 5.21 Saved peak cooling capacity (W/m²) of cross night ventilation in a west office as a function of the internal heat gains

Moreover, the savings in electrical consumption in comparison with a fully air conditioned office, are calculated in Table 5.8. The total savings in electrical consumption amounts to 6.5 – 7.4 kWh/m².year, i.e. approximately 10% of the total electrical consumption of a

typical office building in Belgium (VITO, 2002). Furthermore, Fig. 5.22 shows the saved electrical consumption of cross night ventilation in a west office as a function of the internal heat gains in case of a medium or high exposed thermal mass (see above). These savings are the sum of the electrical savings in cooling demand and fan energy and are calculated as follows.

Table 5.8 Calculated saved electrical consumption (kWh/m^2.year)

Saved electrical consumption (kWh/m^2.year)	North	East	South	West
Cooling demand	3.0	3.3	2.6	2.6
Fan energy	3.5	4.1	4.4	4.8
total	6.5	7.4	7.0	7.4
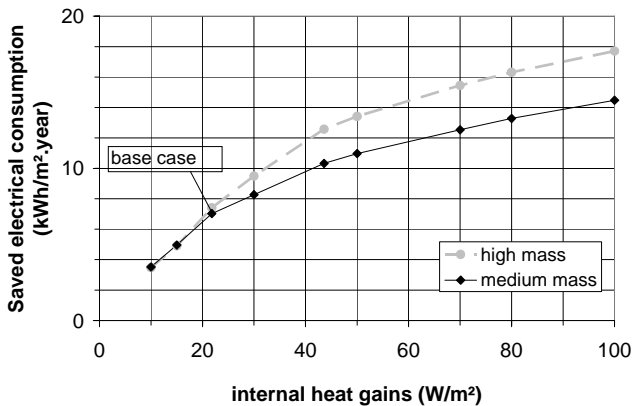
Fig. 5.22 Saved electrical consumption (kWh/m^2.year) of cross night ventilation in a west office as a function of the internal heat gains

Assuming a COP of 2.5, i.e. also considering the losses in the pipework, the calculated savings in cooling demand in Table 5.5 corresponds to a savings in electrical cooling energy of 2.6 to 3.3 kWh/m^2.year. Besides, the saving in fan energy is calculated as the difference in electrical consumptions of the fan. This electrical consumption is proportional to the flow rate and calculated according to the Flemish energy performance regulation for utility buildings (Flemish Government, 2005) (Eq. 5.2).

$$W = c_{sys} \dot{V}_{supply} f_{fan} \frac{t_m}{3.6}$$

Eq. 5.2

where W is the electrical consumption of the fans (kWh), $\dot{V}_{supply}$ the supply design flow rate (m^3/h), f_{fan} the time fraction the fan is in use, t_m the duration of the considered period (Ms) and c_{sys} a coefficient depending on the HVAC system (Wh/m^3). In case of balanced ventilation without cooling, c_{sys} equals 0.55 Wh/m^3. This value increases to 0.85 Wh/m^3 in case of balanced ventilation with cooling.

An operation time of 60 days, i.e. 3 summer months, with 9 working hours a day is assumed. The supply design flow rate in the office with natural night ventilation equals 36

m^3/h. In case of the air-conditioned reference office, the supply design flow rate is estimated from the cooling load in Table 5.7 as follows, assuming a temperature difference between the internal and supply air of 10°C. This results in a design flow rate of 137 to 181 m^3/h.

$$\Phi_{cool} = 0.34\dot{V}_{supply}\left(\theta_i - \theta_{supply}\right)$$

In addition, the saved electrical consumption in Fig. 5.22 is determined assuming an air-conditioning to cool down the heat gains which cannot be cooled by natural night ventilation. The supply design flow rate is calculated from Eq. 5.3, considering a cooling load equal to the sum of the internal and solar heat gains minus the saved peak cooling capacity by natural night ventilation, which can be derived from Fig. 5.21.

5.2.1.3 Conclusions

The results of the simulations with average properties show that applying natural night ventilation significantly improves the level of thermal comfort. The largest probability of thermal comfort can be noticed in case of cross and stack ventilation, followed by single-sided ventilation. The office on the east side always has the worst thermal comfort, followed by the office on the north side. The office on the west side has the best thermal comfort, followed by the south side.

Moreover, these results show that thermal comfort is insufficient in case the louvre area is sized according to the dimensioning method of van Paassen et al. (1998). This can be explained by differences in ventilation system by day. Unlike the assumptions in this research, van Paassen et al. (1998) assumed a natural ventilation system and opening of windows in the façade. Paragraph 5.3.1.3 will show that these conditions cause a better thermal comfort.

The expected flow rates, indoor-outdoor temperature difference when night ventilation is in operation and opening duration are derived from these results as well. The night ventilation flow rates in single-sided ventilation are low in comparison to the other cases. A wide distribution of the flow rates in cross ventilation can be noticed whereas the passive stack guarantees a more stable flow rate, even when the wind velocity is low or the wind direction reverse. In addition, in case of respectively single-sided and both cross and stack ventilation a minimum indoor-outdoor temperature difference of 5 and 4°C and a minimum opening duration of 6 and 5h are probable. These assumptions can be used to pre-design the effective area of the night ventilation openings (see Eq. 2.1 and 2.2).

Furthermore, the saved cooling demand compared to the case without natural night ventilation is calculated. Small differences can be noticed between the various strategies and orientations. Both saved cooling demand and peak cooling capacity of cross night ventilation are related to the internal heat gains. Minimum 13 W/m^2 peak cooling capacity can be saved in case of medium exposed mass. Moreover, the savings in electrical consumption in comparison with a fully air conditioned office, are calculated. These savings are the sum of the electrical savings in cooling demand and fan energy. The total savings in electrical consumption amounts to 6.5 – 7.4 kWh/m^2.year, i.e. approximately 10% of the total electrical consumption of a typical office building in Belgium.

5.2.2 Control of the sample size

For the uncertainty and sensitivity analysis, 150 independent Latin Hypercube samples are developed. Before discussing the results of these analyses, this paragraph checks whether this sample size is sufficient. For this reason, another sample set is randomly generated and the results of both sets are compared to each other.

5.2.2.1 Uncertainty analysis

Fig. 5.23 and Fig. 5.24 compare the cumulative probability of thermal comfort between two sets of samples. The impact of the sample set on the probability is negligible for both comfort criteria. Consequently, it can be concluded that a sample size of 150 is sufficient with regard to the uncertainty.
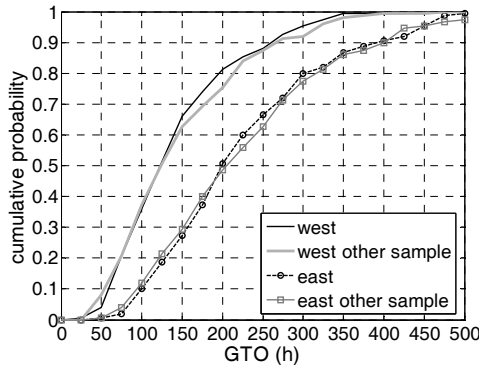
Fig. 5.23 Impact of a sample set on the probability of thermal comfort based on GTO
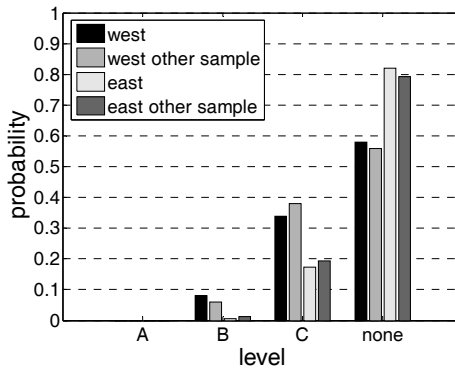
Fig. 5.24 Impact of a sample set on the probability of thermal comfort based on ATG

5.2.2.2 Sensitivity analysis

Fig. 5.25 compares the sensitivity of the thermal comfort between both sample sets. Although the order of importance slightly differs, the same list of important parameters is shown. Therefore, it can be concluded that a sample size of 150 is sufficient.
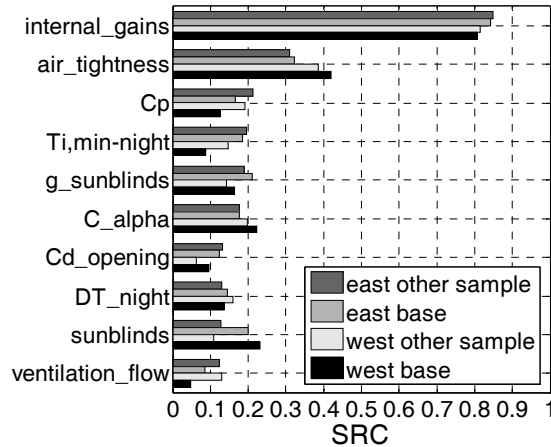
Fig. 5.25 Impact of sample set on the sensitivity of thermal comfort based on GTO

5.2.2.3 Conclusions

The results of the uncertainty and sensitivity analysis of two sample sets are compared. Because only small differences are noticed, it can be concluded that the chosen sample size is sufficient.

5.2.3 Uncertainty analysis

The uncertainty analysis discusses and compares the probability of good thermal comfort in case of natural night ventilation. These distributions give more reliable information on the predicted thermal comfort than the result of one single simulation in the previous paragraph. Firstly, the uncertainty of the comfort level reached by various strategies of natural night ventilation are compared with one another for each orientation. Afterwards, differences in orientation are discussed for each strategy.

5.2.3.1 Comparison of strategies

Thermal comfort in case of single-sided, cross and passive stack ventilation is compared to the case without natural night ventilation. These results are summarized in Table 5.9, where cases with a probability on good thermal comfort of more than 0.5 are marked in grey. The cumulative distributions of the weighted temperature excess hours, the level of the adaptive temperature limits method and the savings in cooling demand are shown for an office on the south side in Fig. 5.26, Fig. 5.27 and Fig. 5.28 respectively.

Table 5.9 Comparison of probabilities of good thermal comfort

strategy	Louvre area (%)	p(GTO <150)				p(ATG A or B)			
		West	East	North	South	West	East	North	South
No night ventilation	-	0.00	0.00	0.00	0.00	0.00	0.00	0.00	0.00
Single-sided	3	0.05	0.01	0.03	0.07	0.00	0.01	0.01	0.01
Cross	2	0.48	0.09	0.21	0.31	0.01	0.00	0.03	0.02
	3	0.66	0.27	0.43	0.53	0.08	0.01	0.08	0.05
Stack	1	0.55	0.15	0.25	0.44	0.07	0.00	0.02	0.05
	2	0.76	0.49	0.41	0.57	0.09	0.01	0.03	0.07

The results of the uncertainty analysis confirm the conclusions of the building simulation in the previous paragraph. However, these results are expressed as probabilities. A significant improvement in thermal comfort is made by natural night ventilation. Thermal comfort is also shown to be least probable in case of single-sided ventilation. In addition, the difference in probability between cross and stack ventilation is small. A GTO-value less than 150 has a probability of 0.09-0.66, compared to a probability of 0.15-0.76 for stack and less than 0.1 for single-sided ventilation. Moreover, a probability of 0.01-0.08 for an A or B level of adaptive comfort is noticed for cross ventilation versus 0.00-0.09 for stack ventilation and quasi 0.00 for single-sided ventilation. The differences in saved cooling demand for the various strategies are small as explained in the previous paragraph.

In addition to the average performances predicted in the previous paragraph, uncertainty is added to these results. This uncertainty can be derived from the steepness of the curves in Fig. 5.26. It can be concluded that the uncertainty is largest in case of single-sided night ventilation too. The uncertainty in case of passive stack and cross ventilation is comparable. This is also shown in Fig. 5.27, which compares the distributions of the GTO. In addition, the distributions of the levels of the adaptive temperature limits method in Fig. 5.28 also show that the uncertainty on thermal comfort for cross and passive stack ventilation is comparable. Moreover, similar uncertainties on saved cooling demand can be noticed for all strategies in Fig. 5.29.
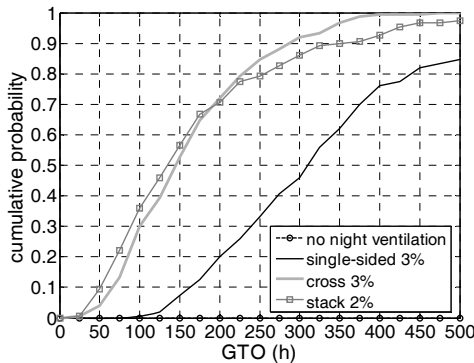

Fig. 5.26 Cumulative probability of the weighted excess hours of various strategies compared in an office on the south side
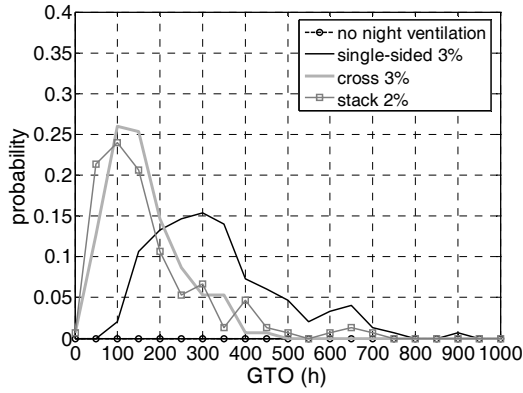
Fig. 5.27 Distribution of the weighted excess hours of various strategies compared in an office on the south side
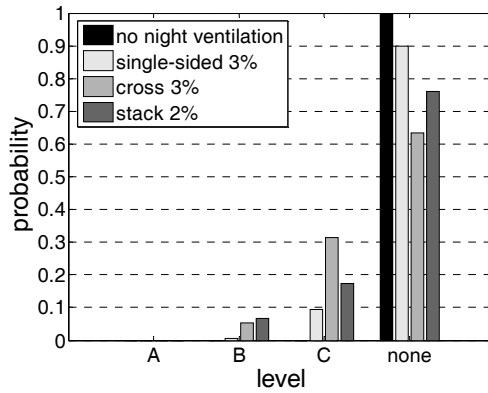

Fig. 5.28 Distribution of the levels of the adaptive temperature limits method of various strategies compared in an office on the south side
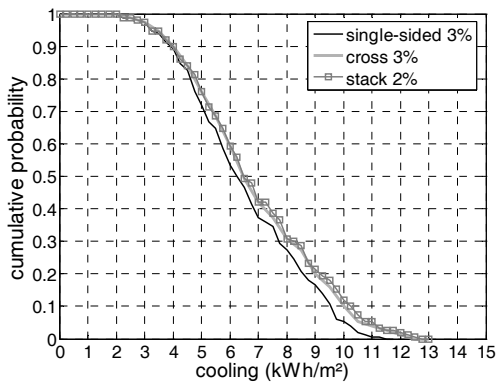

Fig. 5.29 Cumulative probability of saved cooling demand of various strategies compared in an office on the south side

5.2.3.2 COMPARISON OF ORIENTATIONS

The influence of the orientation on the probability of the predicted thermal comfort and the saved cooling demand is discussed in a cross ventilated office in Fig. 5.30 to Fig. 5.32 and Fig. 5.33 respectively. These graphs confirm the conclusions of the deterministic performance prediction. However, differences in comfort evaluation can be noticed in the office on the north side. Unlike the weighted excess temperature method, the adaptive temperature limits indicator predicts a probability of good comfort on the north side comparable to the probability on the west and south side. This evaluation difference can be explained by the difference in comfort criteria (see paragraph 5.2.5). The weighted excess hours method evaluates the average comfort while the level in the adaptive temperature limits method can be determined by occasional temperature excess.

The uncertainty intervals are calculated for each orientation as well. It is shown that the uncertainty is the largest in the east office. The uncertainties for the other orientations are similar. Furthermore, comparable savings in cooling demand are noticed for all orientations as explained above.
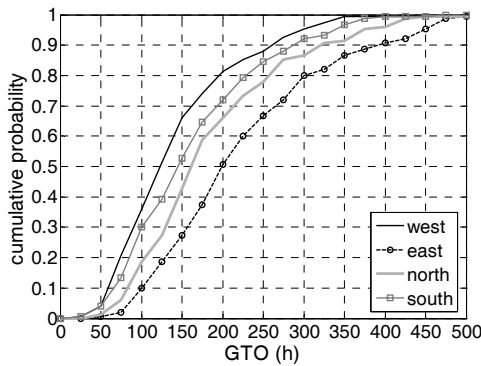
Fig. 5.30 Comparison of weighted excess hours in a cross ventilated office with different orientations
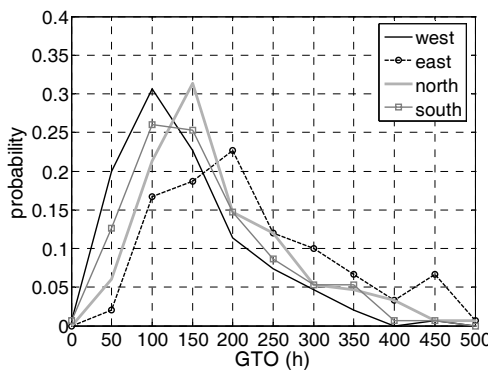

Fig. 5.31 Distribution of the weighted excess hours in a cross ventilated office with different orientations
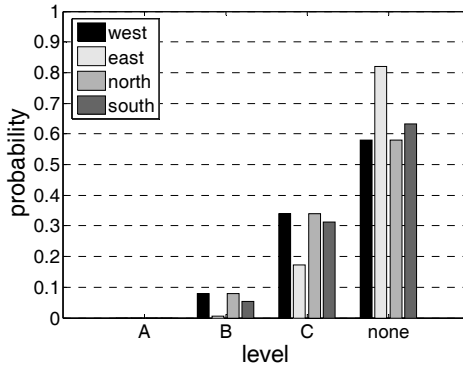
Fig. 5.32 Comparison of levels of the adaptive temperature limits method in a cross ventilated office with different orientations
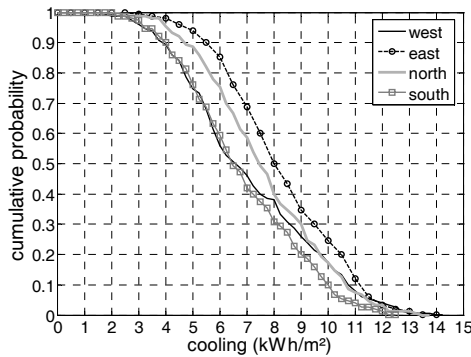

Fig. 5.33 Comparison of savings in cooling demand in a cross ventilated office with different orientations

5.2.3.3 Conclusions

The results of the uncertainty analysis confirm the conclusions of one simulation with average properties. A significant improvement in thermal comfort is made by natural night ventilation. Thermal comfort is shown to have the largest probability in case of cross and stack ventilation. The office on the west side has the best thermal comfort, followed by the south side. Moreover, small differences in saved cooling demand are noticed between the various strategies and orientations.

In the uncertainty analysis, uncertainty is added to the evaluation with average properties. In other words, the result is a distribution of the thermal comfort level. It is concluded that the uncertainty is also the largest in case of single-sided night ventilation and in the office on the east side. The uncertainties on thermal comfort in case of passive stack and cross ventilation, as well as in the offices on the north, south and west side, are similar.

5.2.4 Sensitivity analysis

The sensitivity analysis discusses the input parameters causing the uncertainty on the thermal comfort level. Differences in strategies and orientations are discussed by comparing the standardized regression coefficients (SRCs) based on the weighted temperatures excess method.

5.2.4.1 Most influential input parameters

The standardized regression coefficients (SRCs) of the input parameters of single-sided, cross and stack natural night ventilation are calculated for various orientations based on the weighted temperature excess method. The regression model approaches the real output very well as the model coefficient of determination varies from 0.91 to 0.97. This means that the regression model can explain 91 to 97 % of the uncertainty. The SRCs of most influential parameters in case of cross ventilation on the south side are summarized in Table 5.10. Besides, the regression coefficient b and the SRC (%), defined as the ratio to the sum of the absolute values of the SRCs of all the parameters, are shown. The entire list can be found in appendix A.

Table 5.10 Most influential parameters on thermal comfort with cross night ventilation on the south side: standardized regression coefficient SRC and regression coefficient b

Nr.	parameter	SRC	SRC (%)	b
1	Internal heat gains	0.84	20.6	0.72
2	Air tightness	-0.35	8.5	-3323.39
3	Solar heat gain coefficient of sunblinds (g_sunblinds)	0.27	6.7	960.92
4	Internal convective heat transfer coefficient (C_alpha)	-0.21	5.1	-93.48
5	Wind pressure coefficient Cp	-0.15	3.7	-135.69
6	Controlling night ventilation (DT_night)	0.14	3.5	49.77
7	Irradiance controlling sunblinds (sunblinds)	0.11	2.6	1.26
8	Cd,opening	-0.10	2.6	-186.90
9	Controlling night ventilation (Ti,min-night)	0.10	2.3	33.60
10	Thermophysical properties (d_plywood)	-0.07	1.8	-5652.11
11	Ventilation flow	-0.07	1.7	-3.51
12	Thermophysical properties (lambda_int._brick)	-0.07	1.7	-147.85
13	Thermophysical properties (c_plywood)	-0.07	1.7	-0.02
14	Thermophysical properties (lamba_concrete)	-0.07	1.6	-56.21

The standardized GTO, i.e. the deviation from the average divided by the standard deviation, can be written as a function of these standardized input variables:

$$\Delta GTO = 0.84 \, \Delta IHG - 0.35 \Delta C_{air\,tightness} + 0.27 \Delta g_{sunblinds} - 0.21 \Delta C_{\alpha} - 0.15 \Delta Cp$$
$$+ 0.14 \, \Delta \left(\Delta T_{night} \right) + 0.11 \Delta I_{sunblinds} - 0.10 \, \Delta C_{d,opening} + 0.10 \, \Delta T_{i,min-night} - 0.07 \Delta d_{plywood} \quad \text{Eq. 5.4}$$
$$- 0.07 \Delta Q_{vent} - 0.07 \Delta \lambda_{int.brick} - 0.07 \Delta c_{plywood} - 0.07 \Delta \lambda_{concrete}$$

with:

- IHG the convective internal heat gains (kJ/h)
- $C_{airtightness}$ the flow coefficient of the cracks in the two façades, corresponding to the characteristic n_{50}-value (kg/s.Pa^n)
- C_α the coefficient of the internal convective heat transfer coefficient
- ΔT_{night} the indoor-outdoor temperature difference by night that has to be exceeded to continue the natural night ventilation (°C)
- $I_{sunblinds}$ the irradiance on the façade controlling the sunblinds (W/m^2)
- $T_{i,min-night}$ the internal temperature controlling the closing of the bottom-hung windows at night (°C)
- Q_{vent} the ventilation flow by day (m^3/h)
- $c_{plywood}$ the specific heat capacity of the plywood layer in the raised floor (kg/m^3)
- $\lambda_{int.brick}$ the thermal conductivity of the internal brick cavity wall (W/m.K)
- $\lambda_{concrete}$ the thermal conductivity of the hollow core concrete slabs (W/m.K).

These parameters define 65% of the output. However, the sensitivity analysis based on another sample set in paragraph 5.2.2.2 reproduces only the list of the first nine parameters of Table 5.10. In addition, the impact of the number of varied input parameters on the uncertainty interval is investigated in paragraph 5.4.2. Small differences can be noticed between the results of varying nine or eleven parameters. Therefore, only the nine most important parameters are concluded to have a significant influence on the level of thermal comfort. This result agrees rather well with the list of important factors influencing thermal comfort in a naturally ventilated office, determined by de Wit (2001).

In addition, Table 5.10 gives the portion and the sign of each input parameter in particular. A positive sign means decreasing the concerned parameter improves the thermal comfort and vice versa. Moreover, the regression coefficients b are added for the most influential input parameters. These coefficients give the variation of the output caused by a unit variation in the input.

In addition, this regression model can predict the weighted temperature excess for each set of input parameters. Table 5.11 shows the results for various strategies and orientations in case of average properties. These predictions should be compared to the weighted temperature excess evaluated by one simulation in TRNSYS-COMIS with average properties in Table 5.5. The predictions with the regression model agree rather well with these simulation results. The ranking of the orientations and strategies is the same, except in the offices on the north and the south side in case of single-sided and stack ventilation with a louvre area of 2% of the floor area. In this latter case, the linear regression model reproduces the output worse than in the other cases. The model coefficient of determination R^2_y equals 0.91-0.92, compared to 0.95-0.97 in the other strategies and orientations.

Nevertheless, the predicted GTOs are always larger than those simulated are.

Table 5.11 Prediction by the regression model of weighted temperature excess with average properties

strategy	Louvre area (%)	GTO			
		West	East	North	South
Single-sided	3	273	379	295	337
Cross	2	181	312	258	224
	3	140	223	184	159
Stack	1	160	272	223	176
	2	116	171	171	215

5.2.4.2 COMPARISON OF STRATEGIES

The SRCs of the input parameters of the various strategies are compared with each other and to the case without natural night ventilation in an office on the east side in Fig. 5.34. The comparisons for other orientations are similar.
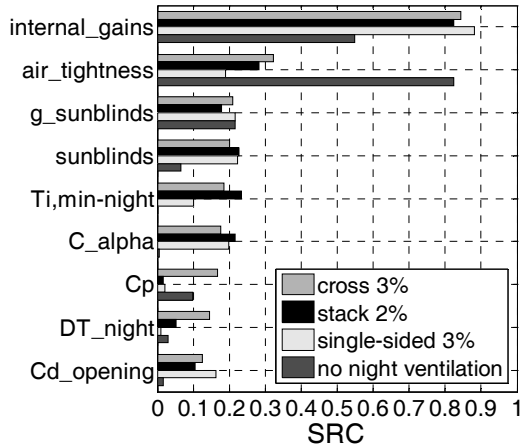
Fig. 5.34 Comparison of SRCs of input parameters in an office on the east side cooled by various strategies of natural night ventilation

In essence, the same input parameters have an important effect on thermal comfort when natural night ventilation is applied. The internal heat gains and the air tightness are noticed to have the greatest impact by far. In addition, the solar heat gain coefficient of the sunblinds (g_sunblinds), the solar radiation controlling the sunblinds (sunblinds), the internal heat transfer (C_alpha, i.e. the coefficient C of the convective heat transfer coefficient), the discharge coefficient Cd of the night ventilation opening and the internal temperature controlling the opening of the bottom-hung windows at night (Ti,min-night) are important. Nevertheless, the indoor-outdoor temperature difference by night controlling the night ventilation (DT_night) and the wind pressure coefficient Cp only have an important impact on thermal comfort in cross ventilation.

The differences between the strategies are caused by differences in the airflow rates and in the nature of the driving force. Because cross ventilation is wind driven the impact of the wind pressure coefficient is more remarkable than in the other strategies. Moreover, large driving forces in this strategy cause the greater impact of the indoor-outdoor temperature

difference controlling the operation of the night ventilation (DT_night). Due to these large flow rates, the indoor temperature decrease fast causing the indoor-outdoor temperature difference to reach the threshold temperature and close the bottom-hung windows.

Furthermore, large differences are noticed between an office with or without natural night ventilation. Because the internal temperatures are very high in the latter case (see Fig. 5.13), the parameters directly influencing the heat gains or cooling are important. These parameters include the internal heat gains, solar heat gain coefficient, solar radiation from which the sunblinds are lowered, air tightness, ventilation flow and wind pressure coefficient. Moreover, the order of importance is changed.

5.2.4.3 COMPARISON OF ORIENTATIONS

Fig. 5.35 shows that the SRCs of the input parameters are comparable for all orientations in case of cross ventilation. Similar results are noticed for single-sided and stack ventilation.
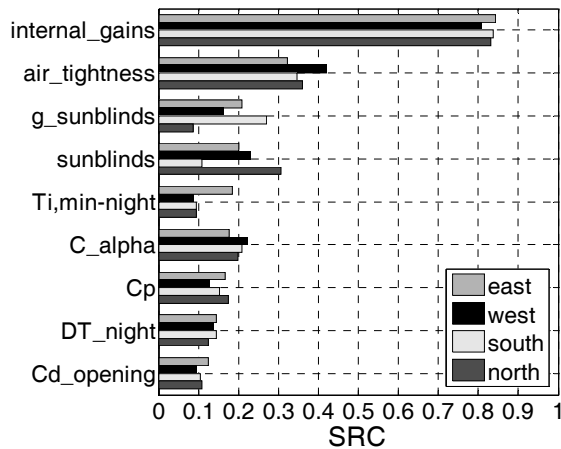
Fig. 5.35 Comparison of the SRCs in a cross ventilation case with various orientations

5.2.4.4 CONCLUSIONS

The sensitivity analysis discusses the input parameters causing the uncertainty on the predicted thermal comfort. The impacts of the natural ventilation strategy and the orientation are investigated. In essence, the same input parameters have an important effect on the thermal comfort when natural night ventilation is applied. Differences are noticed in the absolute value of the standardized regression coefficients and in the order of importance.

The internal heat gains and the air tightness can be noticed to have the greatest impact by far. In addition, the solar heat gain coefficient of the sunblinds, the solar radiation controlling the sunblinds and the internal convective heat transfer coefficient are important. Moreover, the temperatures controlling the natural night ventilation at night influence the variation of the thermal comfort. In addition, the wind pressure coefficient Cp and the discharge coefficient C_d of the night ventilation opening have a large effect on the thermal comfort.

This list of influential input parameters is used as a starting point to optimize the building and system design in the next section increasing the reliability of good thermal comfort in case of natural night ventilation. Moreover, this list is used to develop an easy-to-use method to predict the uncertainty on the predicted thermal comfort.

5.2.5 COMPARISON OF THERMAL COMFORT CRITERIA

The previous paragraphs discussed the uncertainty of the predicted thermal comfort and the input parameters causing this uncertainty, based on the weighted temperature excess method. This paragraph compares these results to the results of the uncertainty and sensitivity analysis based on the adaptive temperature limits method. Because the levels of this latter method are not suitable for calculating the SRCs, the sum of following weighted hours are taken into account. Each hour when the temperature is exceeding the neutral comfort temperature (see Eq. 2.12 and 2.13), is multiplied by its extent of temperature excess.

5.2.5.1 UNCERTAINTY ANALYSIS

Although it is assumed that the criteria of thermal comfort correspond (van der Linden, 2006), large difference in the predicted comfort is noticed. The weighted excess hours method predict a probability of good thermal comfort of e.g. 0.66 in case of cross ventilation with 3% effective area while this probability only equals 0.08 in the adaptive temperature limits method. Fig. 5.36 compares the distribution of the predicted comfort by both criteria in a cross ventilated case on the east and west side. The results for other orientations and strategies are similar. Both comfort criteria agree upon the cases with a good thermal comfort according to the adaptive temperature limits method. Cases with a level A or B also have a GTO smaller than 150. In addition, the corresponding weighted excess hours of most cases without a comfort level are noticed to exceed this limit. Nevertheless, most cases with a level C in the west, east, south and north office respectively have a GTO smaller than 150.
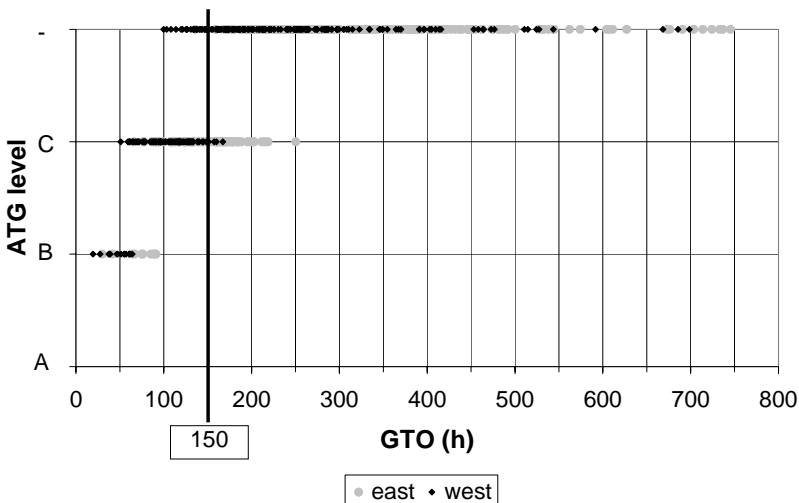

Fig. 5.36 Criteria of thermal comfort compared in a cross ventilated case

Following observations explain the difference between both comfort criteria. Firstly, the definition of both comfort criteria differs. The threshold for good thermal comfort in the weighted excess hours method does not depend on the external temperature. This means the adaptive temperature limits method is more severe when evaluating temperature excess on cooler summer days. This is illustrated in Fig. 5.12 where temperature excesses on days with a running mean outdoor temperature of 14°C determines the evaluation of thermal comfort in the office on the east side.

Secondly, the evaluation of both criteria corresponds over the entire period but not at each moment. The weighted temperature excess method is based on a satisfaction of 90% of the people during minimum 90% of the time (see paragraph 2.1.3.4.2), i.e. an average satisfaction of 80%. Contrary to the adaptive temperature limits method, this satisfaction does not have to be met all the time, i.e. temperature excesses are allowed but limited in total. The adaptive temperature limits method, on the other hand, does not tolerate any temperature excess of 80% of thermal acceptability and is therefore more stringent than the weighted excess hours method. This is illustrated in Fig. 5.37, which compares the probability of a GTO smaller than 150 to the probability of a level A or B when excess hours are tolerated in the classification of level B. It is shown that the results of the adaptive temperature limits indicator tolerating excess hours have more similarity to these of the weighted excess hours method.
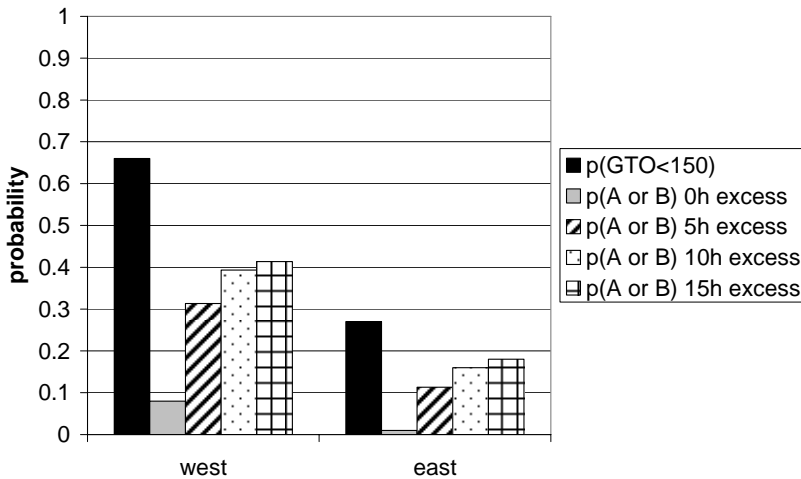

Fig. 5.37 Influence of tolerating excess hours in level B on the probability of good thermal comfort based on the adaptive temperature limits indicator

5.2.5.2 SENSITIVITY ANALYSIS

Fig. 5.38 compares the standardized regression coefficients (SRCs) based on either the adaptive temperature limits or the weighted temperature excess method in an office with cross ventilation on the east and west side respectively. The comparisons for other orientations and strategies are similar. The model coefficient of determination varies in case of adaptive temperature limits method from 0.96 to 0.99. Both sensitivity analyses result in the same list of important input parameters. Difference can be noticed in the absolute value of the SRCs and in the order of importance.

The nature of the comfort criteria used in the sensitivity analysis explains these small differences. The sum of the weighted hours exceeding the neutral temperature in the adaptive temperature limits method is comparable to the sum of the weighted hours exceeding the temperature corresponding to a PMV of 0.5.
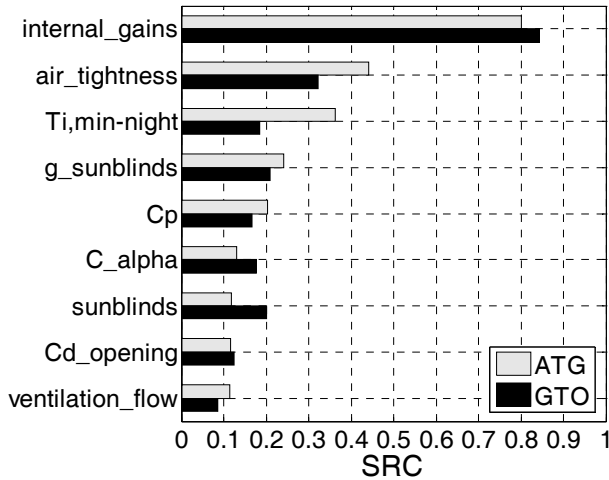

Fig. 5.38 Comparison of SRC in a cross ventilation case on the east side based on either ATG or GTO thermal comfort criteria

5.2.5.3 REMARK ON THE USE OF ATG

In the evaluation of the thermal comfort by the adaptive temperature limits indicator a type Alpha building is assumed. Consequently, operable windows are required (see Fig. 2.13). This means that the users opening these windows have to be taken into account in the simulations. However, this is not included in the simulations discussed in the previous sections because insufficient information exists to model this manual control of windows. Moreover, the ATG method does not provide guidelines to simulate this opening. However, the use of a type Alpha building is justified because the users are assumed to open the windows at high internal temperatures, i.e. show behavioural adaptation.

5.2.5.4 CONCLUSIONS

Although the criteria of thermal comfort are assumed to correspond, large differences in the predicted comfort by GTO and ATG are noticed. Firstly, difference in definition causes this disagreement: contrary to GTO, ATG considers adaptation. Secondly, the evaluation of both criteria is in agreement over the entire summer period but not at each moment. This difference can be diminished by tolerating excess hours in the determination of the comfort level B.

Furthermore, both sensitivity analyses conclude the same list of important input parameters.

5.3 Optimizing building and systems design to increase the reliability of thermal comfort

The previous section discussed the results of the uncertainty and sensitivity analysis of the thermal comfort in one particular office design with natural night ventilation. The aim of this section is to increase the reliability of this thermal comfort by optimizing the building and systems design. The results of the sensitivity analysis are used to reach this purpose. Design decisions influencing the heat gains, thermal mass and ventilation are discussed. Moreover, the impact of weather data and boundary conditions on these optimized designs is investigated. These measures are applied on a cross ventilation case in a west and east oriented office. The results for other strategies and orientations are similar except when mentioned otherwise.

5.3.1 Design decisions

The following design decisions to increase the probability of good thermal comfort in a cross ventilated office are discussed:
- heat gains
- thermal mass
- measures with regard to day and night ventilation

5.3.1.1 Heat gains

Fig. 5.39 to Fig. 5.40 show the impact of the window area and the occupancy on the probability of good thermal comfort based on the weighted temperature excess and the adaptive temperature limits method respectively. A window area of respectively 20% and 30% instead of 25% of the façade area in the base case is considered. Moreover, the impact of two occupants instead of one occupant in the base case is shown. The probability of good comfort with respect to the base case decreases by implementing a larger heat gain. The impact of the occupancy is the largest. It is unlikely to have good thermal comfort in this case.
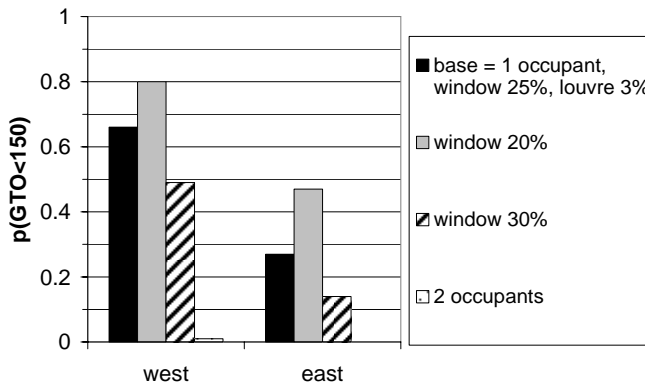

Fig. 5.39 Comparison of the impact of window area and occupancy on the probability of thermal comfort based on GTO

Fig. 5.40 Comparison of the impact of window area and occupancy on the uncertainty of thermal comfort based on ATG

5.3.1.2 THERMAL MASS

The impact of the exposed thermal mass on the probability of good thermal comfort based on the weighted temperature excess is investigated in Fig. 5.41 and Fig. 5.42 for a west and east office respectively. In addition, Fig. 5.43 and Fig. 5.44 show this impact on the probability of good thermal comfort based on the adaptive temperature limits indicator.

Following conclusions can be drawn. Firstly, these graphs show that a minimum exposed thermal mass of 3500-4500 kg, depending on the orientation and night flow rate, is required to reach a probability of more than 0.5 for GTO < 150 in an office with exposed ceiling. To reach the same probability of good comfort, based on the adaptive temperature limits indicator, an exposed thermal mass of 5300 – 6600 kg is required. This value can be explained by comparing the heat that can be stored in this thermal mass $Q_{storage}$ to the internal and solar heat that is released in the office during working hours Q_p.

$$Q_{storage} = \sum \rho c A d_{penetration} \left(\theta_{s,17h} - \theta_{s,9h} \right)$$
Eq. 5.5

$$Q_p = \int_{8}^{17} \Phi_{cool}(t) dt$$
Eq. 5.6

The penetration depth is restricted to 10 cm as defined in the standard NBN EN ISO 13790 for diurnal heat storage (CEN, 2004c). In addition, a surface temperature difference between the end and the beginning of the working day of 4°C is assumed. Furthermore, the daily progress of the total radiation on an external surface on July 23 from VDI 2078 (1996) is assumed. This means that an exposed thermal mass of 3880 kg is required to store the heat that is released during working hours. Fig. 5.45 shows that this value of exposed thermal mass in this office model corresponds to a specific working mass (SWM) of 37 kg/m², i.e. a light to medium thermal mass (ISSO, 1994).

Besides, applying axis-to-axis dimensions, as specified in the recommendations for building simulation of ISSO (1994), instead of internal dimensions for the walls significantly

increases the probability of good thermal comfort with regard to the base case. This can be explained by the assumed increase in thermal mass. Therefore, dimensions have to be carefully dealt with in simulations of natural night ventilation.
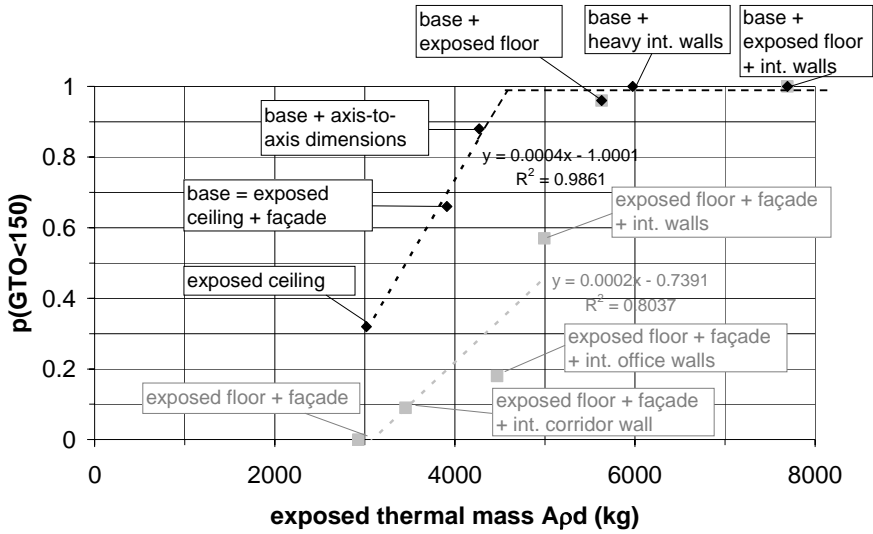

Fig. 5.41 Impact of exposed thermal mass on probability of GTO < 150 in a cross ventilated west office
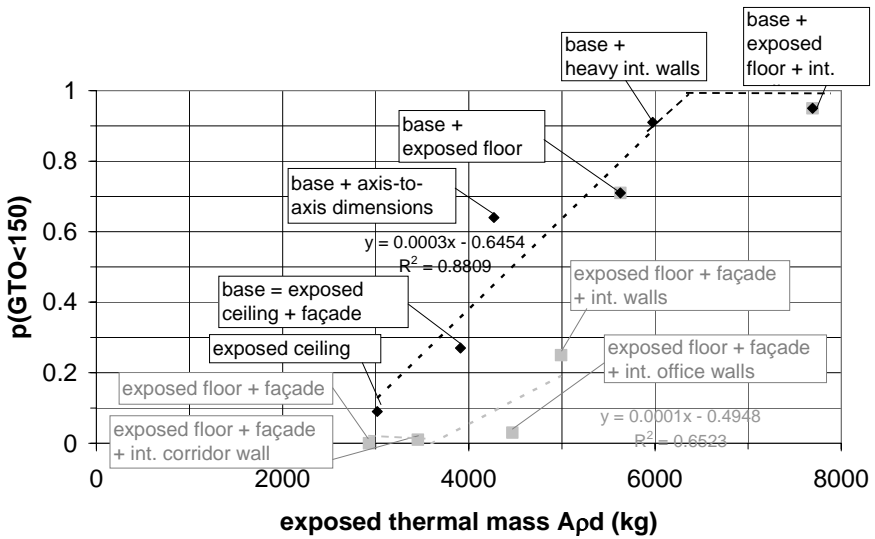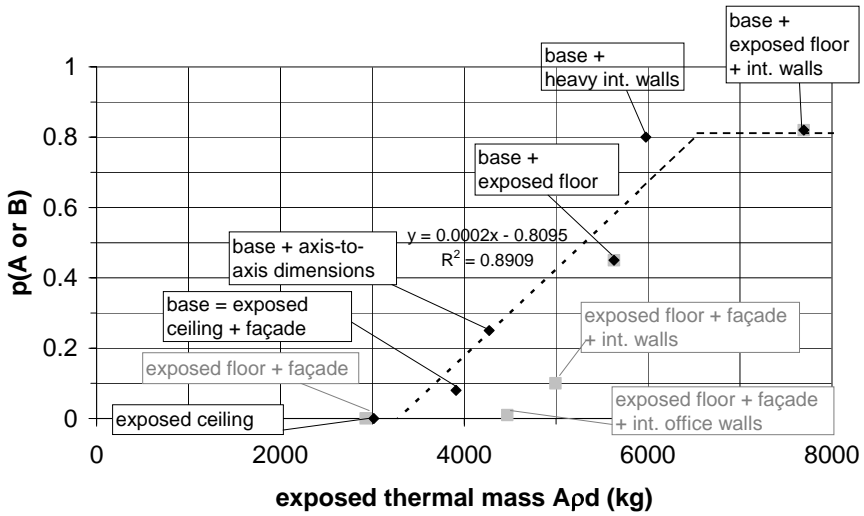

Fig. 5.42 Impact of exposed thermal mass on probability of GTO < 150 in a cross ventilated east office

Fig. 5.43 Impact of exposed thermal mass on probability of level A or B in a cross ventilated west office
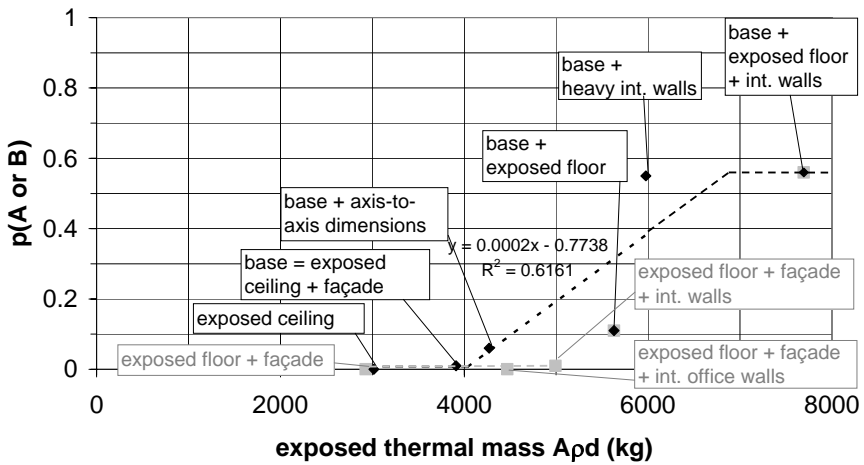

Fig. 5.44 Impact of exposed thermal mass on probability of level A or B in a cross ventilated east office
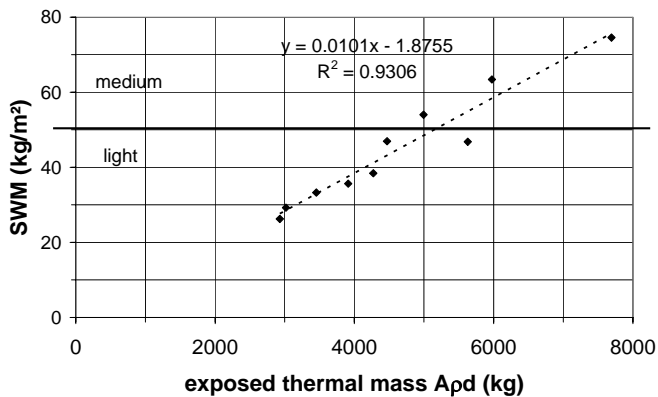
Fig. 5.45 Comparison of the exposed thermal mass Aρd (kg) with the specific working mass (SWM) (kg/m^2)

Furthermore, Fig. 5.41 and Fig. 5.42 show that good thermal comfort is less probable in an office with an exposed floor than an exposed ceiling. The exchanged convective heat transfer between the air and an exposed floor is smaller than between the air and an exposed ceiling. This is shown in Fig. 5.46, which compares the convective heat transfer on a floor and a ceiling in the case with exposed ceiling and floor. A positive sign means that heat is transferred from the air to the surface. It can be noticed that the convective heat transfer to the surface by day is significantly larger in case of an exposed ceiling. Conversely, the heat transfer from the surface to the air by night, when night ventilation is in operation, is larger on the floor but is still sufficiently large on the ceiling. This can be explained by the difference in internal convective heat transfer coefficient between a buoyant and stably stratified flow (see paragraph 4.3.3.3).
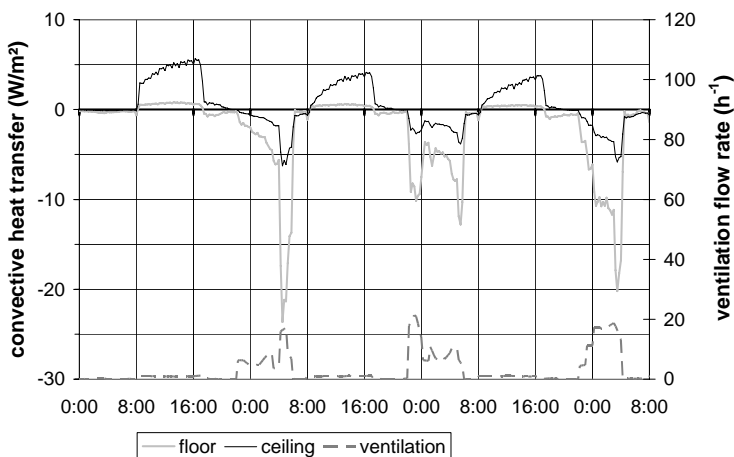

Fig. 5.46 Comparison of the convective heat transfer (W/m^2) on an exposed floor and ceiling in a cross ventilated office on the west side

5.3.1.3 Ventilation

Five different variations in the ventilation system and their impact on the probability of good thermal comfort are investigated:
- Top cooling
- Increased ventilation flow by day
- Manual control of the windows
- Different louvre area
- Other stack height

Top cooling means that the ventilation flow rate by day is cooled down to the set point of night ventilation -6°C, i.e. 15.5 to 16.5, when the operative internal temperature exceeds the set point of night ventilation + 3°C, i.e. an indoor temperature between 24 and 25 °C. In addition, the ventilation capacity by day can be increased from 36 m^3/h.pers in the base case to 72 m^3/h.pers. This airflow rate corresponds to the required flow rate of IDA 1, i.e. the best indoor air quality category in the European ventilation standard EN 13779 (CEN, 2004b), see chapter 4. The amount of extra energy used for top cooling is calculated in a west and east office with cross ventilation, i.e. 0.9 and 1.2 kWh/m^2.year respectively.

Moreover, the effect of manual control of the windows is studied. The opening of the bottom-hung window provided for night ventilation is focussed on. It is assumed that the users open this window to cool down from an internal operative temperature of 25.5°C and close it when the operative temperature drops below 24.5°C or at the end of the working day (see paragraph 4.3.5.2). In addition, the window is closed when the local wind velocity exceeds 7 m/s. The effective area of this window equals 0.5% of the floor area.

Besides, a louvre area of 2% instead of 3% is considered.

Fig. 5.47 and Fig. 5.48 show the probability of good thermal comfort in case of top cooling, increased ventilation capacity, manual control of the windows and decreased louvre area. The application of top cooling, an increased ventilation flow rate by day or the opening of windows by users improves the probability of good thermal comfort with regard to the base case. However, a significant improvement of the thermal comfort, evaluated by the adaptive temperature limits method, is only found in case of top cooling. Unlike the measures causing an extra airflow by day, top cooling can cool down the office even when high outdoor temperatures occur. This is shown on June 19 on Fig. 5.49. Additionally, the windows are assumed to be opened by users when an internal operative temperature of 25.5°C occurs. This threshold has a strong influence on the maximum indoor temperatures and especially on the temperature excesses of the comfort level B at low outdoor temperatures.
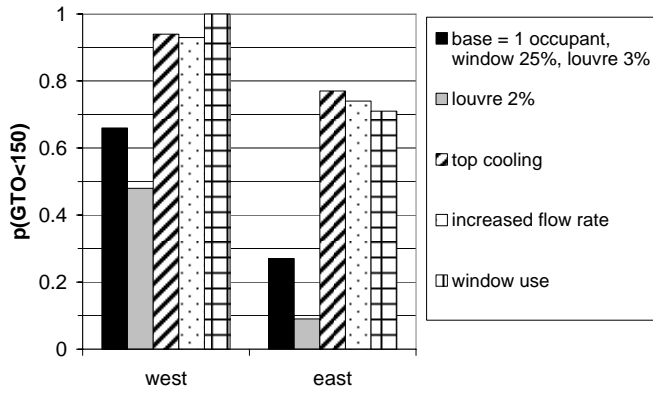
Fig. 5.47 Comparison of the impact of internal doors, top cooling, increased ventilation and window opening on the uncertainty of thermal comfort based on GTO in case of cross ventilation
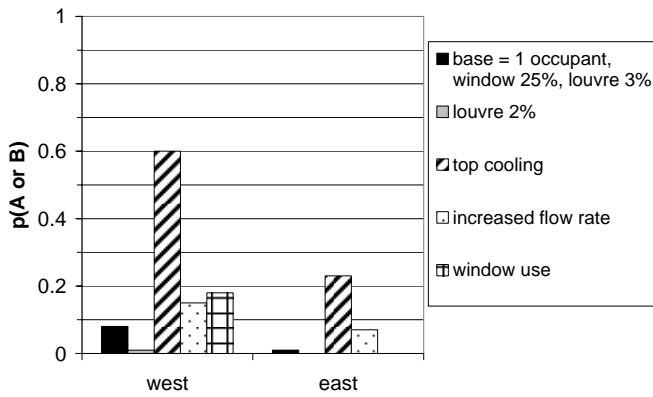

Fig. 5.48 Comparison of the impact of top cooling, increased ventilation and window opening on the uncertainty of thermal comfort based on ATG in case of cross ventilation
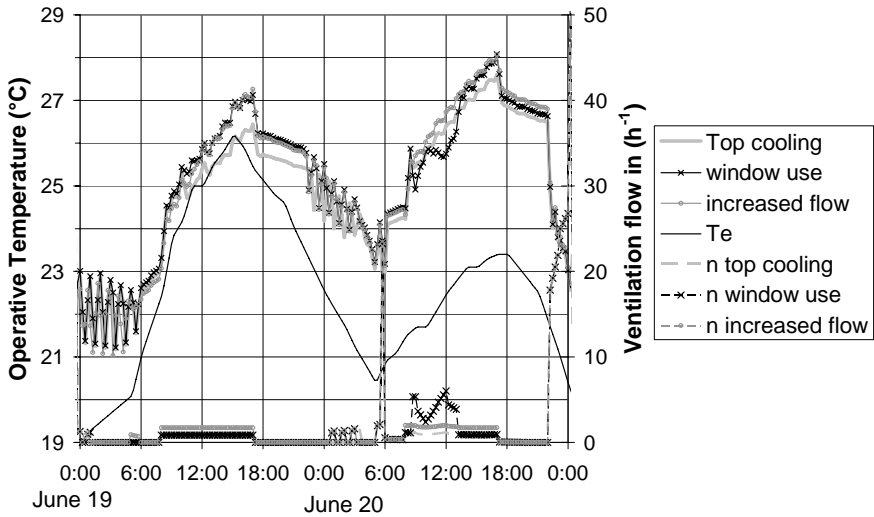
Fig. 5.49 Comparison of the internal operative temperature in the east office with cross night ventilation in case of top cooling, increased ventilation and window use

Furthermore, the impact of the stack height is investigated in Fig. 5.50 and Fig. 5.51. The resulting thermal comfort in an office on the first and the ground floor with a stack height of respectively 0.38m and 3.89m is compared. Good comfort is significantly more probable on the ground floor because of the larger stack height. To ensure a larger probability of good thermal comfort on the first floor, a greater louvre area for both supply and exhaust has to be provided.
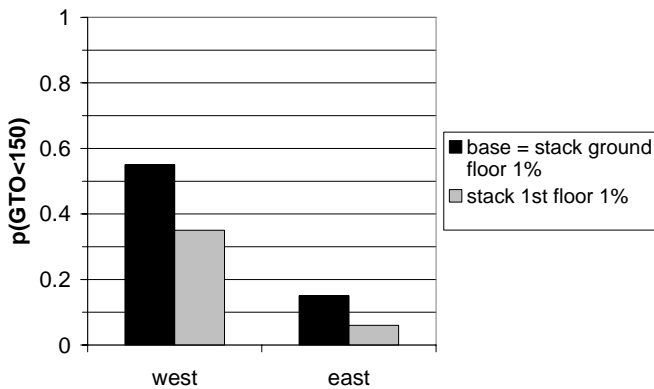

Fig. 5.50 Impact of stack height on the probability of good thermal comfort based on GTO
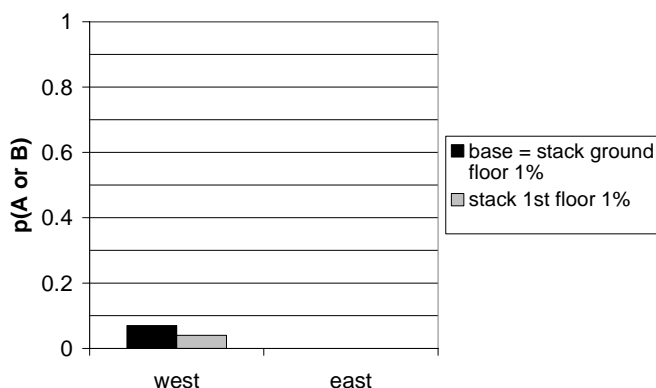
Fig. 5.51 Impact of stack height on the probability of good thermal comfort based on ATG

5.3.1.4 CONCLUSIONS

To ensure a high probability of thermal comfort, following measures have a positive effect. First of all, the internal and solar heat gains have to be restricted. Secondly, sufficient exposed thermal mass has to be provided. In addition, an exposed ceiling is preferred to an exposed floor. Moreover, the ventilation openings, i.e. louvers, windows and stacks, have to be carefully dimensioned to ensure a high flow rate at night. Furthermore, additional cooling techniques, like top cooling, increased ventilation flow rate, opening windows by users have to be provided.

5.3.2 WEATHER DATA

This paragraph investigates which weather data are preferred to predict the performances of natural night ventilation. Fig. 5.52 and Fig. 5.53 compare the influence of the weather data on the probability of good thermal comfort based on either GTO or ATG. These simulation results are compared for the base case and for an optimized design of natural night ventilation, i.e. with top cooling.

The data of Meteonorm Uccle, i.e. used in the base case, TRY Uccle and Meteonorm Uccle with different starting day are concerned. The two first data sets are already discussed in chapter 4. The latter data set differs from the standard Meteonorm weather data by starting on January 1st on a Wednesday instead of a Monday. As a consequence, more warm summer days are included in the working week in this weather data than in the standard Meteonorm data set.
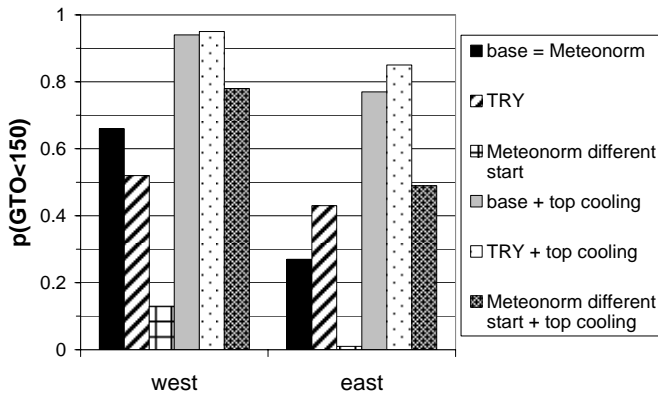
Fig. 5.52 Impact of weather data on the uncertainty of thermal comfort based on GTO in case of cross ventilation
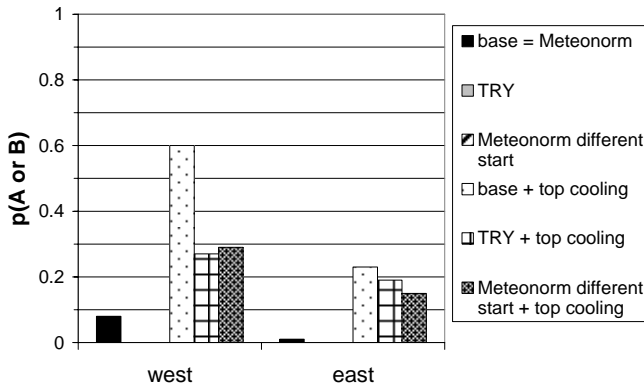

Fig. 5.53 Impact of weather data on the uncertainty of thermal comfort based on ATG in case of cross ventilation

The following difference in probability of good thermal comfort is noticed between the use of TRY and Meteonorm weather data: contrary to Meteonorm, using TRY weather data results in a comparable thermal comfort in the offices on the east and west side. This can be explained by the difference in average solar radiation on these façades during working hours, which is smaller in TRY than in Meteonorm as shown in Table 5.12.

Table 5.12 Comparison of average solar radiation in TRY and Meteonorm weather data

Average solar radiation during working hours (1 May – 30 September) (W/m²)	West	East
Meteonorm Ukkel	48	57
TRY Ukkel	51	55

However, these differences are reduced when top cooling is applied. Similar probabilities of good thermal comfort are noticed for TRY and Meteonorm in case of a reliable design, except on the west side when the comfort is evaluated by the adaptive temperature limits

method. This difference is caused by some successive extremely warm summer days in TRY that cannot be cooled by top cooling and are shown for average properties in Fig. 5.54 and Fig. 5.55. These warm summer days are taken into account in the Meteonorm extreme warm weather data in the next paragraph.

Fig. 5.54 Result of adaptive temperature limits method in an office on the west side with cross natural night ventilation and top cooling using Meteonorm weather data
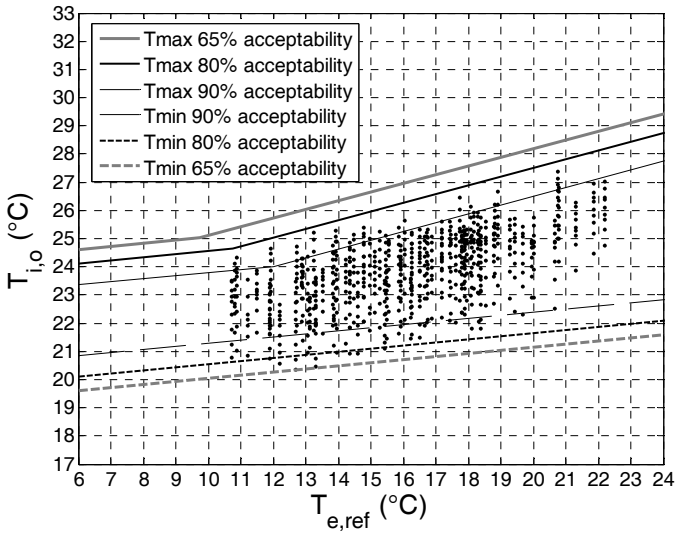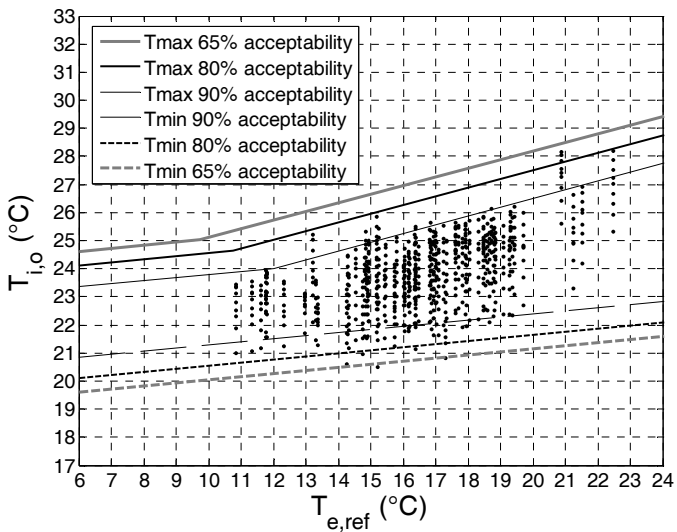

Fig. 5.55 Result of adaptive temperature limits method in an office on the west side with cross natural night ventilation and top cooling using TRY weather data

An even larger difference is noticed between the results of Meteonorm data with different starting weekdays in Fig. 5.52 and Fig. 5.53. This difference is reduced in a reliable design of natural night ventilation but remains significant.

In conclusion, the choice of weather data and in particular that of the starting weekday has an important impact on the predicted probability of good thermal comfort. However, the predicted performances of a reliable design of natural night ventilation, like the case with top cooling, are less sensitive than the base case for the choice of weather data.

5.3.3 Boundary conditions

The impact of assumptions in boundary conditions on the probability of good thermal comfort is studied in this paragraph: sheltering the building from the wind and using extreme warm outdoor temperatures. Moreover, this section tries to answer the question 'How to improve natural night ventilation systems to create good thermal comfort in this extreme warm weather?'

To investigate the influence of the wind shelter, the building is located in the city centre instead of in a half open field in the base case, i.e. a roughness height z_0 of 2.0 in stead of 0.25. Fig. 5.56 shows that sheltering the building from the wind has a significant impact on the probability of good thermal comfort in a cross and stack ventilated case because the wind is an important driving force in both cases. Therefore, caution is needed when applying wind based natural night ventilation in an environment that shelters the building from the wind.
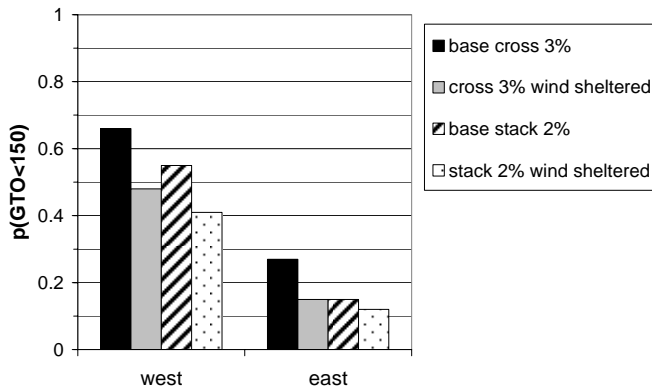
Fig. 5.56 The impact of sheltering the building from the wind on the uncertainty of thermal comfort in a cross (3%) and stack (2%) ventilated office based on GTO

In addition, a weather data set for Uccle with extremely warm outdoor temperatures, i.e. temperatures occurring once every 10 years, are implemented using Meteonorm and compared to standard weather data of Meteonorm Uccle.

Fig. 5.57 and Fig. 5.58 show that these weather data have a very large impact in an office on the west side cooled with cross night ventilation: good thermal comfort is unlikely to occur. The same conclusion can be drawn for other orientations and night ventilation strategies.

Consequently, extra measures should be added in order to reach a high probability of good thermal comfort in an extremely warm summer. Paragraph 5.3.1 already shows that top cooling, increased ventilation capacity, extra thermal mass and the opening of windows by users are adequate measures to increase the probability of good thermal comfort. Therefore, the impact of these measures is investigated in an extremely warm summer. The thermal mass is increased by providing heavy instead of light internal walls. The probability of good thermal comfort is studied in a cross ventilated office on the west side. The results for an east office are similar.

Fig. 5.57 and Fig. 5.58 compare the impacts of these measures on the probability of good thermal comfort in extremely warm weather to normal weather. It is shown that these measures result in a probability of good thermal comfort of approximately or lower than 0.6. Consequently, to achieve a high probability of good thermal comfort during extremely warm outdoor temperatures, two of these measures should be combined. In addition, Fig. 5.57 shows a large difference in probability of GTO < 150 during extreme warm temperatures between the cases with increased flow rate and manual control of windows. This is explained by differences in flow rates as shown in Fig. 5.59: window opening can create a larger airflow rate than 1.7 h^{-1}, i.e. the increased airflow rate.

Fig. 5.57 Impact of measures compared on the probability of good thermal comfort based on GTO between normal and extremely warm weather in a cross ventilated office on the west side
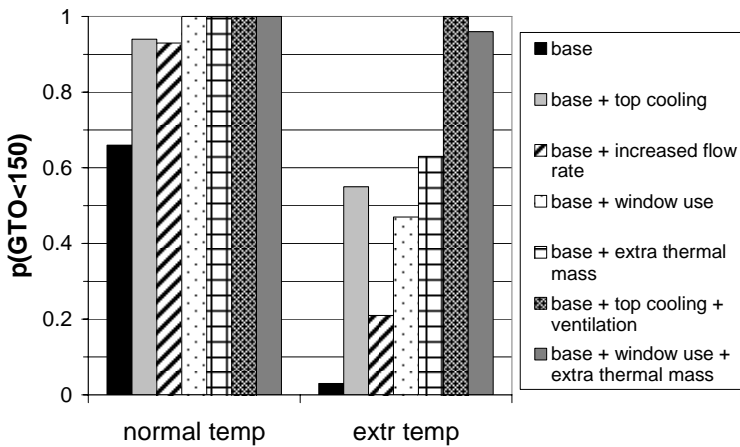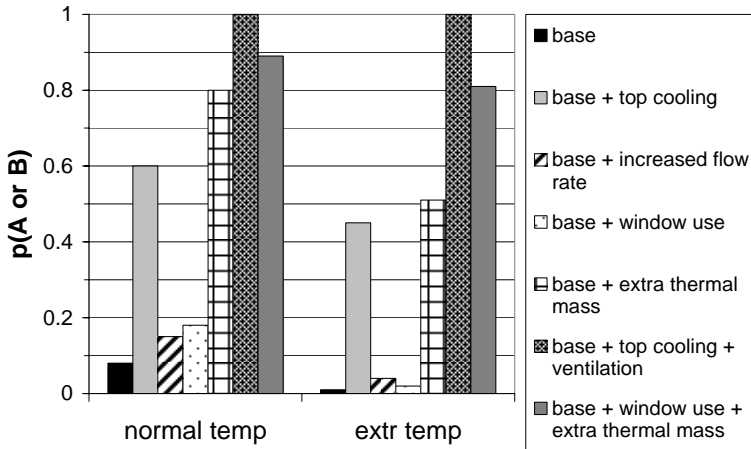
Fig. 5.58 Impact of measures compared on the probability of good thermal comfort based on ATG between normal and extremely warm weather in a cross ventilated office on the west side
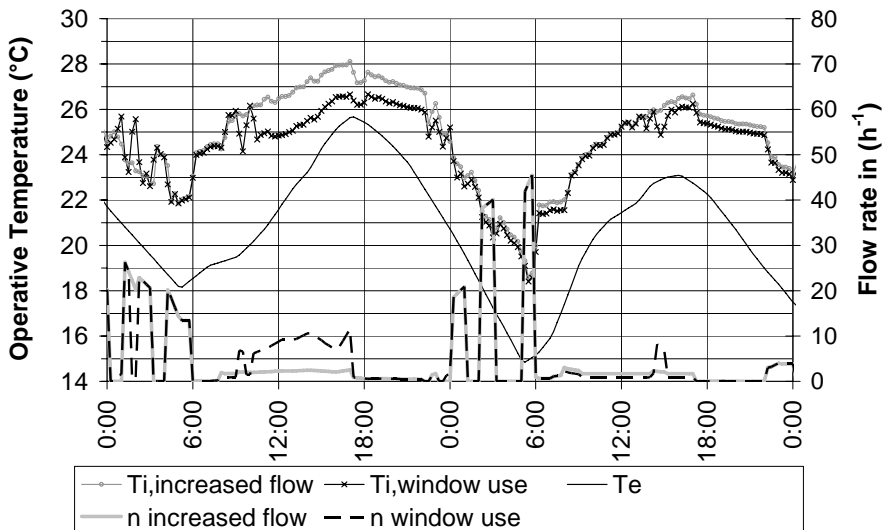
Fig. 5.59 Comparison of the flow rates and internal operative temperatures in the west office with cross night ventilation in case of increased ventilation and window use for Meteonorm extreme weather data

5.3.4 Conclusions

To ensure a high probability of good thermal comfort, two conditions have to be fulfilled. Natural night ventilation has to be applied in a low energy office building with restricted fenestration and internal heat gains and sufficient exposed thermal mass. In addition, a properly sized natural night ventilation has to be combined with additional cooling techniques like top cooling, increased ventilation flow by day or window opening by day.

With regard to the exposed thermal mass, following conclusions can be drawn. Exposed mass should be related to the cooling load. Good thermal comfort is less probable in an

office with an exposed floor than an exposed ceiling. In addition, dimensions have to be carefully dealt with in simulations of natural night ventilation as they cause a difference of exposed thermal mass. The use of internal dimensions are on the safe side.

Furthermore, the choice of weather data has an important impact on the predicted probability of good thermal comfort. However, the predicted performances of a reliable design of natural night ventilation are less sensitive to this choice.

Moreover, in extremely warm weather data, the probability of good thermal comfort of an optimized design of natural night ventilation can be significantly reduced. Consequently, the combination of the standard and extremely warm weather data sets of Meteonorm Uccle is preferred to evaluate the performances of a natural night ventilation design.

5.4 Practical use of uncertainty and sensitivity analysis

The previous sections discuss the advantages of the uncertainty and sensitivity analysis. A distribution of thermal comfort gives more reliable information than one single simulation. The most influencing input parameters are defined. Nevertheless, uncertainty and sensitivity analysis require a large amount of simulations. This prevents building engineers from using uncertainty and sensitivity analysis in the design of natural night ventilation. Therefore, this section aims to derive a method to predict the probability of good comfort and to estimate the distribution of thermal comfort using a limited number simulations.

5.4.1 Prediction of the probability of good thermal comfort

The results of the uncertainty analysis in paragraph 5.2.3, i.e. the probability of good thermal comfort, confirm the prediction of thermal comfort of one building simulation using average properties. Therefore, the aim of this section is to find a way to predict the probability of good thermal comfort based on the result of one simulation. Fig. 5.60 and Fig. 5.61 show the relation between the thermal comfort in an office with average properties and the probability of good thermal comfort, based on respectively the weighted temperature excess and the adaptive temperature limits method. These results are a summary of the comfort evaluations of the cases with a different design in the previous paragraphs.

When evaluating the level of thermal comfort using GTO, Eq. 5.7 gives the correlation between the predicted probability of good thermal comfort and the GTO of one building simulation with average properties. It can be noticed that a GTO of 150 coincides with a probability of 0.52.

$$
\begin{aligned}
&GTO \leq 50 \Rightarrow p\big(GTO < 150\big) = 1 \\
&50 < GTO < 300 \Rightarrow p\big(GTO < 150\big) = 1.06 - 0.0036 * GTO \\
&GTO \geq 300 \Rightarrow p\big(GTO < 150\big) \approx 0
\end{aligned}
\qquad \text{Eq. 5.7}
$$

The ATG-level of the simulation with average properties correlates with the predicted probability of good thermal comfort, i.e. level A or B, as follows:

$$
\begin{aligned}
&ATG\ A \Rightarrow p\big(A\,or\,B\big) = 1 \\
&ATG\ B \Rightarrow p\big(A\,or\,B\big) > 0.7 \\
&ATG\ C \Rightarrow p\big(A\,or\,B\big) < 0.3 \\
&ATG\ - \Rightarrow p\big(A\,or\,B\big) < 0.15
\end{aligned}
\qquad \text{Eq. 5.8}
$$

Nevertheless, some exceptions to the rules in Eq. 5.8 can be noticed due to exceptional temperature excess, in particular, when the thermal comfort is evaluated as 'level C'.
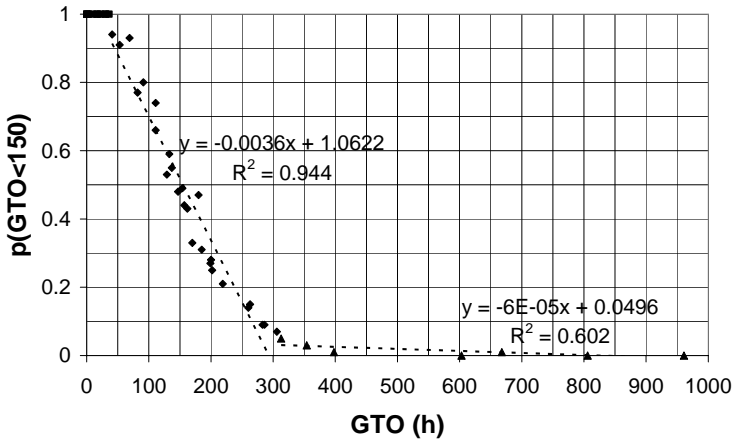
Fig. 5.60 Relationship between the thermal comfort in an office with average properties and the probability of good thermal comfort based on GTO
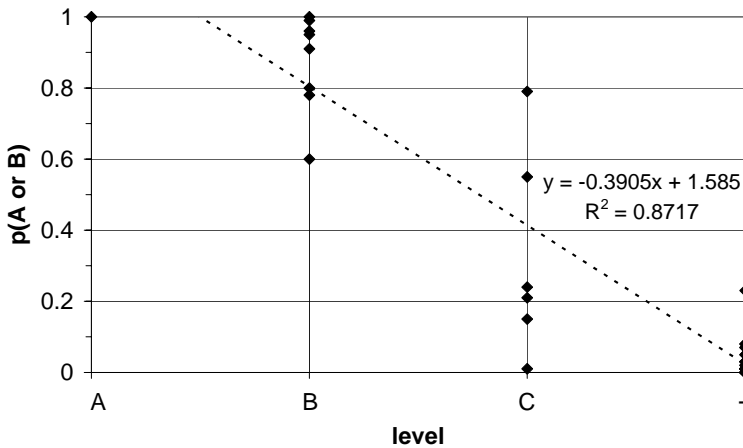
Fig. 5.61 Relationship between the thermal comfort in an office with average properties and the probability of good thermal comfort based on ATG

5.4.2 PREDICTION OF THE DISTRIBUTION OF THERMAL COMFORT

It was concluded that the surplus of the uncertainty analysis is the distribution of the thermal comfort. This distribution gives more reliable information on the predicted thermal comfort than the result of one single simulation. Nevertheless, an uncertainty analysis requires many simulations, e.g. the computational time of 150 simulations of the generic 3-zone model is approximately 4.5h on a PC with a 3.0 GHz processor and 512 Mb RAM.

Therefore, the width of this distribution is estimated based on the simulation with average properties. Fig. 5.62 shows the correlation between the standard deviation of the GTO and the GTO in case of average properties. It is noticed that the standard deviation of the distribution of the GTOs proportionally varies along with the GTO of the simulation with average properties. The standard deviation can be estimated by 50% of this latter value.

This relationship explains the difference in uncertainty interval of thermal comfort between the cases with both cross and stack and single-sided ventilation. Thermal comfort is worse

in this latter case, while comparable comfort can be noticed when cross and stack ventilation are applied.

Fig. 5.62 Relationship between the thermal comfort in an office with average properties and the uncertainty of good thermal comfort based on GTO
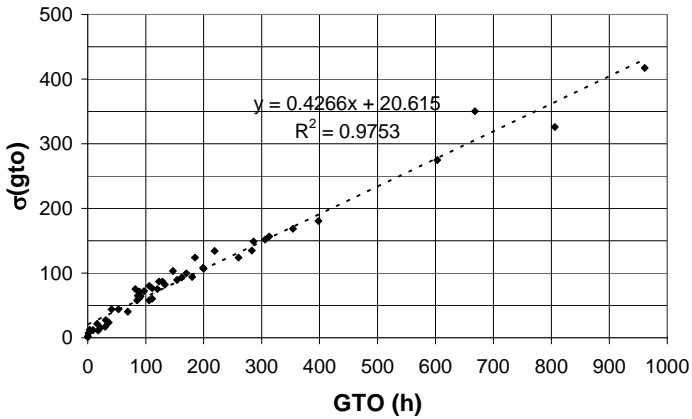
However, the distribution of the weighted temperature excess hours is not always symmetrical. Moreover, the average, minimum and maximum values of this distribution are interesting. Therefore, it is investigated to predict the range of the distribution based on three discrete simulations in which only the most important input parameters are varied. The list of most important parameters is based on the results of the sensitivity analysis in paragraph 5.2.4 and is summarized in Table 5.13. The sets of input parameters for these three simulations are generally determined as follows:

- Average: average values for all input parameters
- Minimum: values smaller than the average for the most important parameters, average values for the remaining parameters
- Maximum: values larger than the average for the most important parameters, average values for the remaining parameters

Table 5.13 Most important parameters influencing thermal comfort in naturally night ventilated office

Nr.	parameter
1	Internal heat gains
2	Air tightness
3	Solar heat gain coefficient of sunblinds (g_sunblinds)
4	Controlling sunblinds (sunblinds)
5	Convective heat transfer coefficient (C_alpha)
6	Wind pressure coefficient Cp
7	Controlling night ventilation (DT_night)
8	Controlling night ventilation ($T_{i,min-night}$)
9	$C_{d,opening}$
10	Thermophysical properties (lambda_int._brick)
11	Thermophysical properties (c_int_brick)

The impact of the variation from the average value is studied in Fig. 5.63 for a cross ventilated office on the south side. The impact for other orientations and strategies is similar. The input parameters equal to the average value decreased or increased by two times the standard deviation, i.e. $\mu \pm 2\sigma$, are noticed to overpredict distribution of the weighted temperature excess. A variation of one time the standard deviation from the average gives a better agreement with the results of the uncertainty analysis.
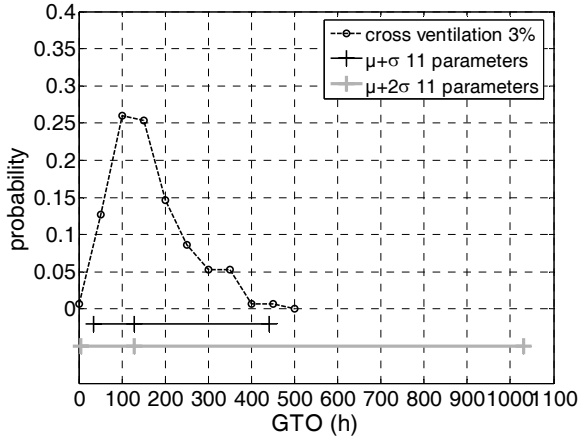
Fig. 5.63 Impact of the variation of the input parameters on the predicted distributions in a cross ventilated office on the south side

In addition, Fig. 5.64 discusses the impact of the amount of input parameters that are varied in these 3 simulations. Only varying the 5 most important parameters from Table 5.13 predicts the thermal comfort distribution rather well. No difference is noticed between the results when varying 9 or 11 input parameters. As a consequence, variations in the 9 most important parameters are taken into account in the prediction of the distribution by 3 simulations.
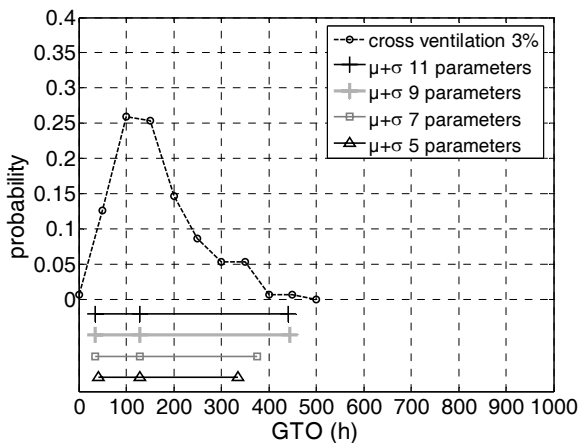
Fig. 5.64 Impact of the amount of input parameters on the predicted distributions in a cross ventilated office on the south side

The results of these predictions for an office on the south side are shown in Fig. 5.65 for the weighted temperature excess and in Fig. 5.66 for the adaptive temperature limits method respectively. These predictions are added to the particular distribution as a line with 3 dots. An excellent agreement is noticed between the uncertainty interval predicted by 3 discrete simulations and the results of the Monte Carlo analysis. However, this prediction gives more information in case of comfort evaluation by GTO than ATG because a wider range of values are possible. This is shown in Fig. 5.66 where the average and maximum levels are equal.
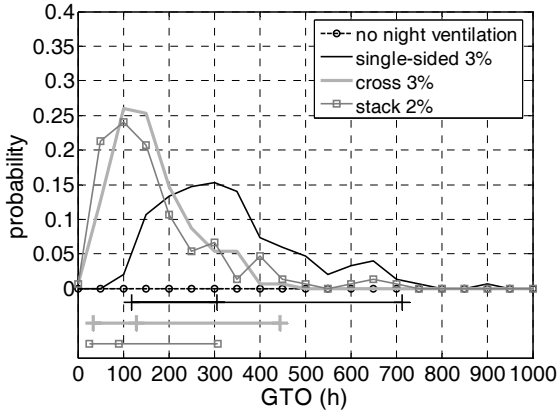
Fig. 5.65 Prediction of the distribution of the weighted excess hours in an office on the south side
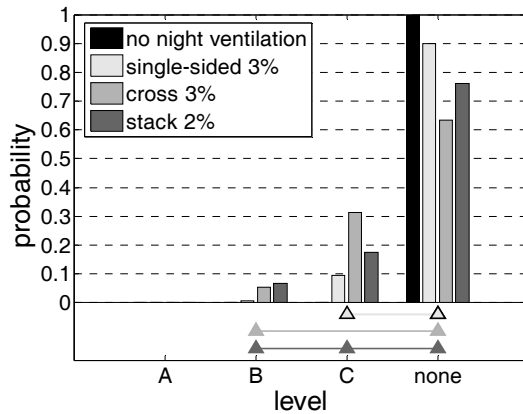
Fig. 5.66 Prediction of the distribution of the levels of the adaptive temperature limits method in an office on the south side

5.5 Conclusions

In the evaluation of the design of natural night ventilation using building simulation, many uncertainties come across. Uncertainty analysis is a methodology to deal with the uncertainties in the input. This method allows to predict the probability of good thermal comfort and the thermal comfort distribution. This distribution gives more reliable information on the predicted thermal comfort than the result of one single simulation.

To ensure a high probability of good thermal comfort in a naturally night ventilated office, two conditions have to be fulfilled. Natural night ventilation has to be properly sized and applied in a low energy office building with restricted glazing and internal heat gains and sufficiently exposed thermal mass. In addition, to increase the reliability, natural night ventilation may be combined with additional cooling techniques like top cooling, increased ventilation flow by day or opening windows by the users by day.

To evaluate the performances of a natural night ventilation design properly extremely warm weather data have to be taken into account. The combination of a normal and extremely warm weather data set is preferred.

A methodology to design natural night ventilation is derived from the results of the simulations. In the pre-design, the internal and solar heat gains define the cooling load. The simulations show that the amount of exposed thermal mass can be derived from this cooling load. The heat that can be stored in this thermal mass approximately equals the heat that is released in the office during working hours. Besides, the expected flow rates, indoor-outdoor temperature difference when night ventilation is in operation and opening duration are derived from these simulations as well. These assumptions can be used to (pre-)design the effective area of the night ventilation openings. Simulations of the naturally night ventilated office building can subsequently evaluate and adjust this (pre-) designed effective area. This methodology is applied in chapter 7 to design the office building "Sint-Pietersnieuwstraat" and subsequently evaluate this design.
The results show that thermal comfort is insufficient in case the louvre area is sized according to the dimensioning method of van Paassen et al. (1998).

Although both criteria of thermal comfort are assumed to correspond, large differences in the predicted thermal comfort by GTO and ATG are noticed. The weighted temperature excess method (GTO) gives a global evaluation of the comfort over the summer period, while the evaluation of the adaptive temperature limits method (ATG) is highly influenced by – sometimes limited - temperature excesses. This difference can be significantly diminished by tolerating excess hours in the determination of the comfort levels.

Sensitivity analysis studies how the variation in the thermal comfort is attributed to the variations in the input parameters of the building model. In other words, sensitivity analysis results in the following list of input parameters which have the most important impact on the predicted thermal comfort in a naturally night ventilated office:

- internal heat gains
- air tightness
- internal convective heat transfer coefficient
- wind pressure coefficient
- control parameters of natural night ventilation: minimum indoor-outdoor temperature difference and minimum internal temperature difference by night
- properties of the sunblinds: solar heat gain coefficient and the irradiance lowering the sunblinds
- discharge coefficient of the louvre(s)

The uncertainty on these input parameters have to be taken into account to predict the reliability of the natural night ventilation design using building simulation. In addition, a methodology is developed to predict the uncertainty interval of thermal comfort based on only three simulations in which only these input parameters are varied. Moreover, the correlation between the probability of good thermal comfort, the standard deviation of the distribution and the result of one simulation are established. A relationship is derived between the thermal comfort in an office with average properties and the probability of good thermal comfort and the standard deviation of the distribution of thermal comfort respectively.

In the next chapter, the uncertainty and sensitivity analysis and the developed simplified method to predict the uncertainty are applied on the thermal comfort in a case study.

6 Case Study: PROBE office building

The aim of this chapter is to evaluate the design of natural night ventilation in the office building of PROBE (Belgium) (Heijmans and Wouters, 2002b), (BBRI, 2002), (Demeester et al., 1998b) using the developed methodology from the previous chapters. The results for a single-sided and cross ventilation strategy in a single office on the first floor are discussed and compared to the measured performances. In addition, the distribution of thermal comfort is estimated by means of the simplified method including only three simulations. Additional information on the performances is available in Breesch and Janssens (2006).

6.1 Building model characteristics

6.1.1 Building model

The PROBE office building is located on the test site of the Belgian Building Research institute in Limelette, 30 km southeast of Brussels (Belgium). The building was completed in 1975 and pragmatically renovated from 1994 to 1998 designed by BBRI. PROBE stands for Pragmatic Renovation of Office Buildings for a Better Environment. The main objectives of this renovation were improving the thermal and visual comfort, guaranteeing a good indoor air quality and limiting the energy use.

The building includes two identical office floors on top of a ground floor with an archive room. The two floors have a total area of 1120 m^2 and contain 36 offices (672 m^2) for about 50 employees. Fig. 6.2 and Fig. 6.1 show a plan and a model of a section of the first floor with offices on the west (n°1) and the east (n°2) side, a central corridor (n°3) and a stairwell (n°4) on each side of the building. This building model includes 3 zones: a small office on the west, a large office on the east side and a central corridor separating both offices. These offices are situated on the second floor of a two-storey office building.
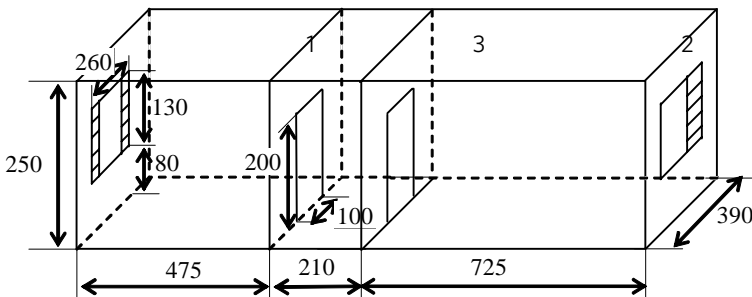

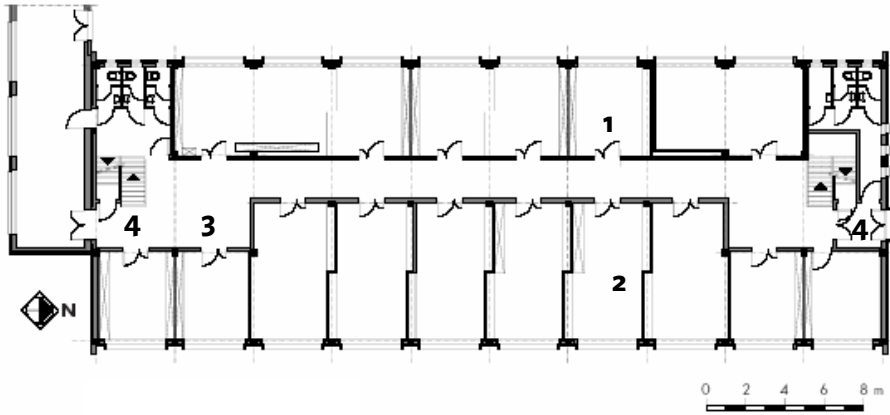Fig. 6.1 Building model of a section of the PROBE building

Fig. 6.2 Plan of the ground floor of the PROBE building with offices on the west (n°1) and the east (n°2) side, central corridor (n°3) and stairwells (n°4) on each side

6.1.2 Input parameters

As most input parameters of the building simulation and their uncertainties are already determined in chapter 4, the discussion in this paragraph is restricted to the characteristics specific to the building model of the PROBE building.

6.1.2.1 Boundary conditions

The wind velocity on site at building height is calculated from the meteorological wind velocity $\overline{v}_{ref}$ using the power law wind profile in Eq. 3.23. The boundary heights z_{bound}, the roughness parameters on site a_0 and at the meteorological station a_m and their corresponding roughness heights z_0 are given in Table 6.1 (Dorer et al., 2001). It can be noticed that the uncertainty interval on these roughness heights is somewhat wider than assumed in chapter 4.

Table 6.1 Roughness parameter a, boundary height z_{bound} and corresponding roughness height z_0 at meteo station and on site

location	Terrain description	z_{bound} (m)	a (-)	z_0 (m)
Meteo station	Cultivated open fields	60	(0.149;0.171)	(0.03;0.07)
On site	Countryside and spread habitat	60	(0.182;0.257)	(0.10;0.50)

6.1.2.2 Building characteristics

The average thermal building data are shown in Table 6.2. In addition, the solar transmission coefficient of the glass with external sunblinds varies from 0.10 to 0.20 on the west (screens) and from 0.17 to 0.27 on the east side (awnings). The airtightness is characterised by a n_{50}-value of 2 to 8 h^{-1} (BBRI, 1999) and modelled by cracks in the office façades at floor and ceiling height and at the bottom and the top of the window.

Furthermore, small (n°1 on Fig. 6.2) and large offices (n°2) are provided to be occupied by respectively 1 and 2 persons from 8h to 17u30. Heijmans and Wouters (2002c) measured the real average occupancy during office hours during 1 year. At least one person occupies

an office for respectively one and two persons during only 47% and 71% of the time. The occupancy of two persons was not registred because the results were based on the presence detection of the hygienic ventilation system. The average installed power of the lighting is 11 W/m^2 in the offices. The monitored internal gains of the office equipment amount 30.3 kWh/m^2.year, which correspond to 15 W/m^2 during 2000 office hours.

The total internal heat gains in the PROBE building vary from 15.4 to 24.4 W/m^2 in the west office (1 person), 17.3 to 27.3 W/m^2 in the east office (2 persons), 12.2 to 19.1 W/m^2 in the east office (1 person) and equals 6 W/m^2 in the corridor.

Table 6.2 Thermal building data PROBE (Heijmans and Wouters, 2002b)

wall	composition	U (W/m^{2}K)
Floor	Reinforced concrete	1.95
External wall	Uninsulated brick cavity wall (including thermal bridges)	1.95
Roof	Reinforced concrete + 11.5 cm insulation	0.33
Internal wall offices	Gypsum board	1.72
Internal wall corridor	Brick wall	2.40
Window	Glazing: double glass with low-e coating, cavity filled with argon (g = 0.6) Frame: aluminium (west) and wooden (east) Shading: movable screen (west) and awning (east)	1.45 (east) 1.79 (west)

6.1.2.3 System characteristics

The sunblinds are automatically controlled to be lowered from an irradiation on the façade of 180 to 220 W/m^2. In addition, during working hours 22.5 to 27.5 m^3/h.pers of ventilation air is mechanically supplied in the offices and a quarter thereof is mechanically extracted in the corridor. The average values of these properties can be found in Heijmans and Wouters (2002b).

External louvres for natural night ventilation are provided in the façades (see Fig. 6.1). On the east side, the louvre is placed in front of the hinged part of the window, can be removed during the heating season and has an effective area of 1.7% of the floor area. On the west side, each window is equipped with two fixed and well insulated louvres on both sides. The effective area is 2.0 % of the floor area. The opening of the windows of these façade louvres is user controlled. Measurements in the PROBE building from June to August 2001 (based on data received from the BBRI) show in Fig. 6.3 that the users start opening the windows at the end of the working day from 23°C. Nicol and Humphreys (2004) confirm this conclusion: window opening by users in offices in the UK has a measured probability of 0.21 at an indoor temperature of 23°C. Opening of windows by users from an outdoor temperature of 19°C is additionally shown to be probable (p=0.64) (Nicol and Humphreys, 2004). Based on these experimental data, the windows are assumed to be closed during working hours and left open after working hours from Monday to Thursday night when the maximum indoor operative and outdoor temperature respectively exceeds (22.5;23.5)°C and (18.5;19.5)°C (Martin and Fletcher, 1996). The assumption of the outdoor temperature is necessary to prevent window opening outside the cooling period. Table 6.3 describes the characteristics of the natural night ventilation openings (Florentzou et al., 1998, Orme et al., 1994). The internal doors are assumed to be closed in case of single-sided ventilation and to be opened in case of cross ventilation at night.
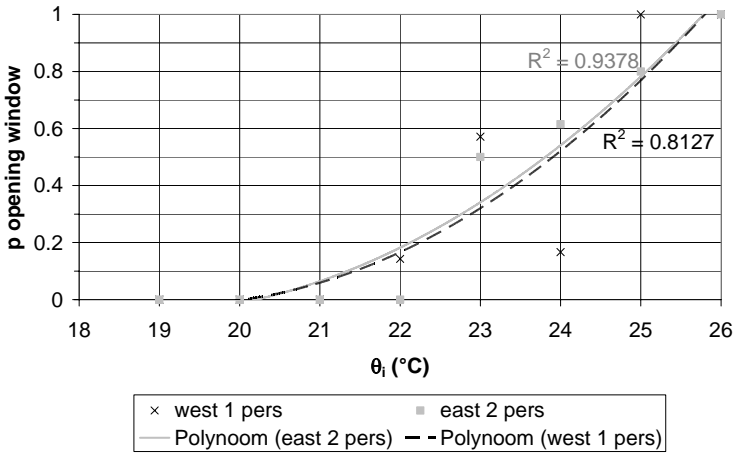
Fig. 6.3 Opening of windows by users in PROBE building (Belgium) in relation to the operative indoor temperature (based on data received from the BBRI)

Table 6.3 Natural ventilation opening characteristics

opening	bxh (m²)	A_{eff} (m²)	C_d (-)	L (m)	C (kg/s.m.Pa)	n (-)
Vertical louvre west	(0.30 x 1.15) x 2	0.38	(0.4;0.8)	-	0	0.6
Vertical louvre east	0.73 x 1.19	0.48	(0.4;0.8)	-	0	0.6
Internal door	1.00 x 2.00	2.0	(0.5;0.7)	6.00	(0.0008;0.0024)	0.6
Crack façade	-	-	-	1.00	(0.0011;0.0044)	0.6

6.1.2.4 SIMULATION CHARACTERISTICS

Simulations are carried out from May 21 to September 15. A time step of 15 min is chosen. The offices are assumed to be occupied during working hours from 8h to 17h. Internal separations between the concerned office and other offices are assumed adiabatic. The characteristics of the uncertainty and sensitivity analysis are also defined. For these analyses, 300 independent Latin Hypercube samples are developed using SIMLAB software (POLIS, 2003). This number largely exceeds the minimum of 1.5 x 72 = 108 factors. The standardized rank regression coefficient (SRRC) is used to rank and quantify the effect of the input parameters on the thermal comfort in a naturally night ventilated office. The standardized rank regression coefficient is selected because the model coefficient of determination of the ranked data exceeds the coefficient of the rough data.

6.2 Discussion

Thermal summer comfort in a single-sided and cross night ventilated office in the PROBE building is examined by uncertainty analysis. These results are compared to the measured thermal comfort. Moreover, the distribution of thermal comfort is estimated using three simulations. Firstly, the simulated and measured airflow rates of natural night ventilation are compared.

6.2.1 Airflow rates

Fig. 6.4 shows the distribution of the night ventilation flow rates in case of single-sided (turned window) and cross ventilation respectively. These airflows are the maximum of supply from and exhaust to outdoors and are averaged over the night. The average flow amounted to 3.2 and 21.4 h^{-1} respectively. These results are compared to the measured ventilation rate reached by natural night ventilation in the small offices on the west side of the first floor from July 24 to August 18, 1998 (Heijmans and Wouters, 2002b). Fig. 6.5 shows that cross ventilation creates larger airflow rates than single-sided ventilation: 13 h^{-1} on average versus 2.2 h^{-1} (tumbled window) and 3.7 h^{-1} (turned window).
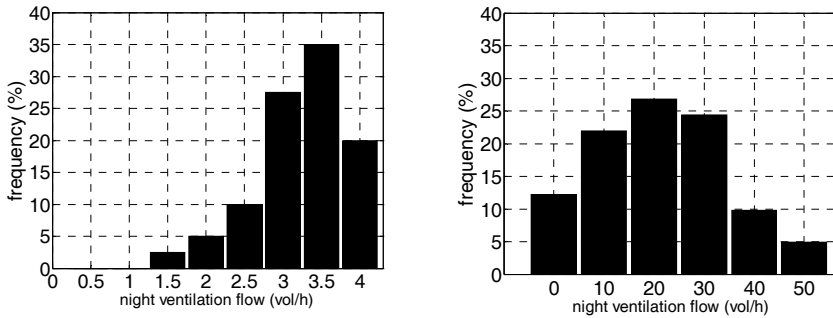
Fig. 6.4 Simulated flow rates of single-sided (left) and cross (right) natural night ventilation
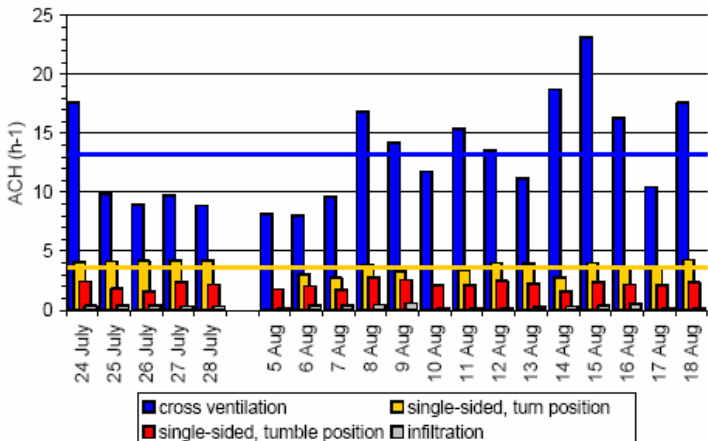
Fig. 6.5 Measured airflow rate of natural night ventilation depending on ventilation strategy in the PROBE building (July 24 – August 18, 1998) (Heijmans and Wouters, 2002b)

In case of single-sided ventilation, a good agreement is noticed between the simulations and measurements. This can be explained by comparable outdoor temperatures in the occurring weather and the typical weather data set. The Belgian meteorological institute (RMI, 1998) measured normal outdoor temperatures in July and August 1998.

However, the simulated airflow rates are significantly larger than the measured flow rates in case of cross ventilation. An overestimation of the Cp-values on the west façade when the wind blows from 180° to 315°, i.e. south to northwest, explains this difference as shown in Fig. 6.6 (Heijmans and Wouters, 2002a). The wind pressure coefficients, assumed in the simulations, do not consider the obstacles enclosing the office building as shown in Fig. 6.7 (Heijmans and Wouters, 2002a). This conclusion has to be considered when interpreting the predicted thermal comfort in the cross ventilated case.

Fig. 6.6 ΔCp-values (west-east) of PROBE office building compared between AIVC tables, used in the simulations, and measurements on site (Heijmans and Wouters, 2002a)

Fig. 6.7 Plan of the PROBE office buildings and its surroundings (Heijmans and Wouters, 2002a)

6.2.2 Uncertainty analysis

6.2.2.1 Simulation results

Fig. 6.8 and Fig. 6.9 show the results of the uncertainty analysis for a single-sided and cross night ventilated office on respectively the west and the east side. The probabilities of a good thermal comfort, i.e. level A or B, are additionally summarized in Table 6.4.

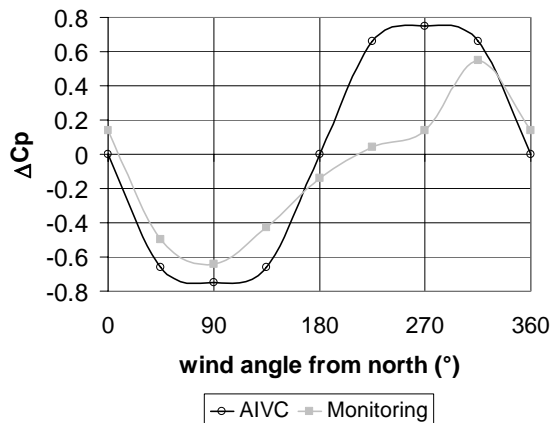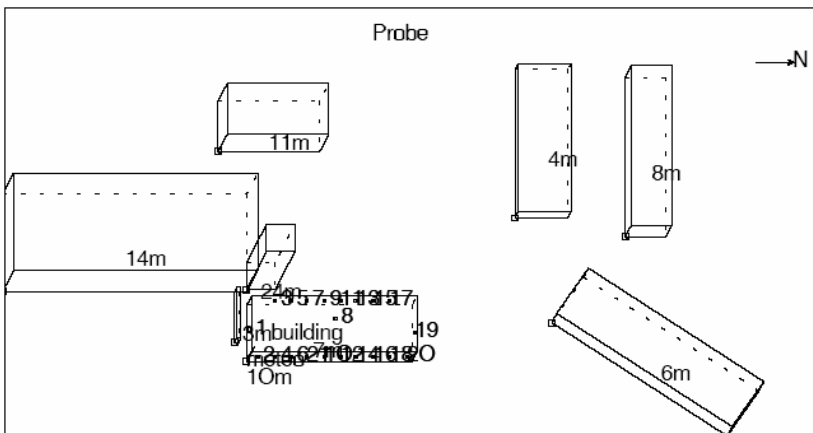Good thermal comfort is found in the west office with a probability of 0.43 and 0.95 in case of respectively single-sided and cross ventilation. These probabilities even increase when only one person occupies the east office. The ventilation rate, which is much higher when the doors are left open at night (see also Fig. 6.4), creates this difference between single-sided and cross ventilation. The same conclusion can be drawn for the east office when one person occupies it. Conversely, large differences in thermal comfort exist in the office on the east with two persons. Good thermal comfort in case of single-sided night ventilation is unlikely. This is caused by higher internal and solar heat gains in the east office and by a smaller relative area of the night cooling opening: 1.7% (east) and 2.0% (west). In case of cross ventilation, the probability of good thermal comfort in the east office is more than 0.5. Nevertheless, as the prevailing wind in Belgium is from the west, the thermal comfort in the cross ventilated case is poorer in the east than in the west office.

In conclusion, the predicted likelihood of good thermal comfort in the east office highly depends on the internal heat gains and the opening of the internal doors. The predicted comfort in the west office is less sensitive to the use of internal doors. Moreover, when ventilation system design is based on a cross ventilation strategy, it is important to prescribe fixed internal ventilation openings.

Table 6.4 Summary of the results of the uncertainty analysis in PROBE building

p(A or B)	1 person in east		2 persons in east	
	West	East	West	East
Single-sided	0.60	0.42	0.43	0.03
cross	0.99	0.98	0.95	0.69
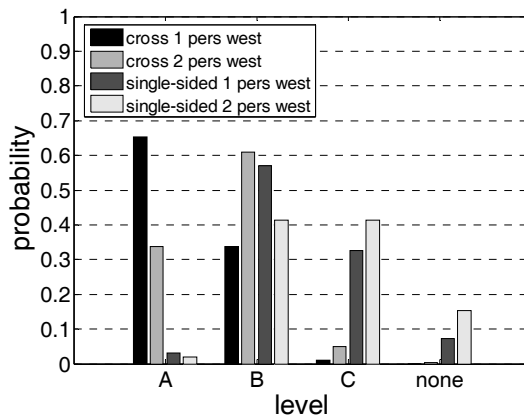
Fig. 6.8 Distribution of thermal comfort of single-sided and cross night ventilation in a west office
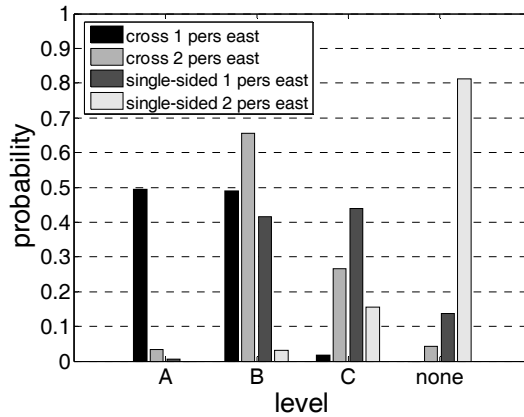
Fig. 6.9 Distribution of thermal comfort of single-sided and cross night ventilation in an east office

Furthermore, having a look at the simulated indoor operative temperatures in the cross ventilation case in the west (Fig. 6.10) and the east office with two persons (Fig. 6.11), overcooling in the morning is predicted. This is the disadvantage of user controlled supply windows. This problem can be solved by automatically controlling the inlets of the night ventilation. In addition, low indoor temperatures are noticed on cool summer days ($T_{e,ref}$ < 14°C) because of the lack of heating in the summer. Temperature excess above level A in the east office are noticed on normal ($T_{e,ref}$ = 16°C) summer days.
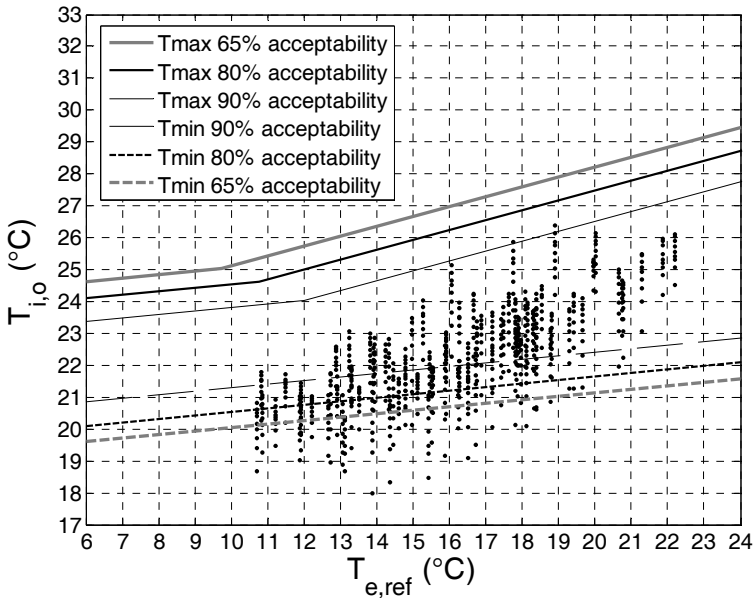
Fig. 6.10 ATG-method for the simulated thermal comfort in an average west office with cross ventilation (21 May – 15 September)
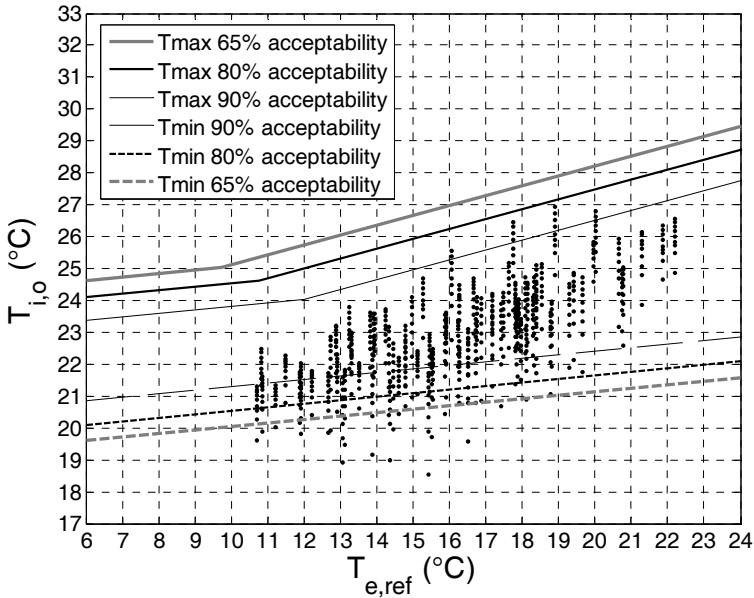
Fig. 6.11 ATG-method for the simulated thermal comfort in an average east office with cross ventilation (21 May – 15 September)

6.2.2.2 Measuring results

The thermal comfort on the first floor of the PROBE building was measured from June to August 2001 (Heijmans and Wouters, 2002d). Temperature measurements were carried out in eight offices on the west (with one person) and six offices on the east side (with two persons). The outdoor temperature in 2001 in Belgium was higher than the average, used in the simulations, especially in July and August. The irradiance in the summer had an average level, except for August when the irradiance was higher than the average (RMI, 2001) as shown in Table 4.2. Fig. 6.12 shows the distribution of the measured thermal comfort, only considering the temperature excess (based on data received from the BBRI).

Good thermal comfort is measured in all the offices on the west side. This corresponds to the predictions which indicate a probability of 0.43 (single-sided ventilation, 2 persons in east office) to 0.99 (cross ventilation, 1 person in east office) of good thermal comfort. In reality a mixture of single-sided and cross ventilation occurred because cross ventilation only happened when the users decided to leave the internal doors open overnight. Contrary to the simulations, the thermal comfort in most offices is labelled 'level A'. Furthermore, large dispersion of the levels of thermal comfort exists in the east offices as predicted (see Fig. 6.9). This is mostly caused by differences in office occupancy (see above).
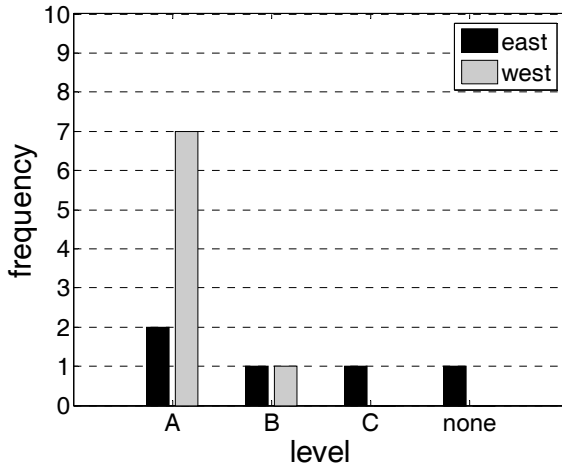
Fig. 6.12 Distribution of measured thermal comfort (based on data received from the BBRI)

In addition, Fig. 6.13 and Fig. 6.14 show the measured indoor temperatures in a typical west and east office respectively. Overcooling in the morning is noticed in the west office as predicted, especially when Te,ref < 16°C. Unlike the simulations, temperature excesses in the east office are mostly measured during warm summer days ($T_{e,ref}$ = 22°C).
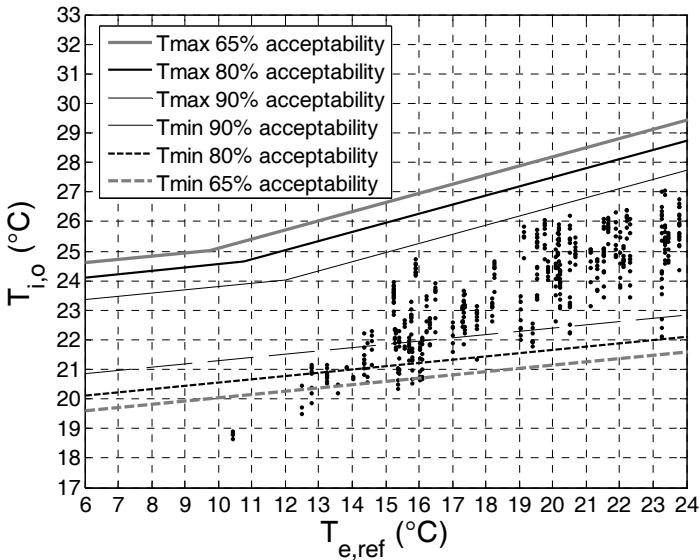
Fig. 6.13 ATG-method for the measured thermal comfort in a west office (1 June – 31 August 2001),
(based on data received from the BBRI)
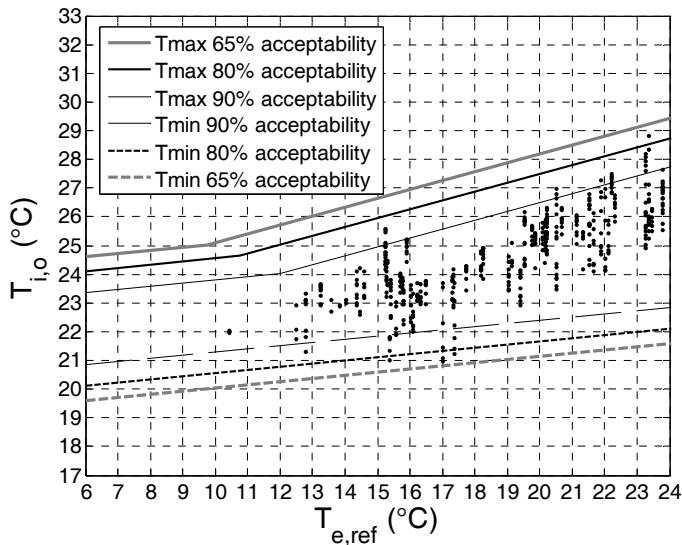
Fig. 6.14 ATG-method for the measured thermal comfort in an east office (1 June – 31 August 2001), (based on data received from the BBRI)

6.2.3 PREDICTION OF DISTRIBUTION

The distribution of the ATG-levels is estimated using three simulations in which the most important parameters of chapter 5 are varied:
- internal heat gains
- air tightness
- internal convective heat transfer coefficient
- wind pressure coefficient
- properties of the sunblinds: solar heat gain coefficient and the control parameter
- discharge coefficient of the louvre

The sets of input parameters for these three simulations are determined as follows:
- Average: average values for all input parameters
- Minimum: the average minus the standard deviation for the most important parameters, average values for the remaining parameters
- Maximum: the average plus the standard deviation for the most important parameters, average values for the remaining parameters

The results of these predictions for various combinations of strategies and internal heat gains are added to the distributions of the ATG-levels in Fig. 6.15 and Fig. 6.16 for the west and east office respectively. A good agreement is noticed between the prediction using three simulations and the distributions of the levels of the adaptive temperature limits method. Only probabilities smaller than 0.05, are not detected. This is explained by the agreement of the results of the sensitivity analyses of both cases. The input parameters having the largest impact on the thermal comfort in the PROBE building (see Table 6.5), are included in the list of the most important parameters of chapter 5 varied in these 3 simulations. The roughness on site and the external solar absorption coefficient are more important in PROBE than in the generic office building in chapter 5 because of the uninsulated façade.
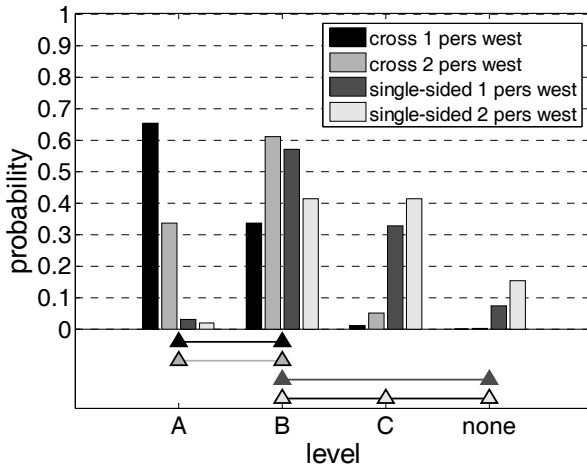
Fig. 6.15 Prediction of distribution of the levels of the adaptive temperature limits method in the west office
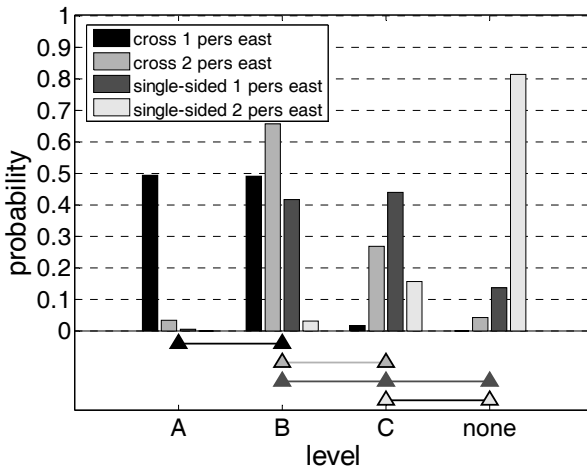
Fig. 6.16 Prediction of distribution of the levels of the adaptive temperature limits method in the east office

Table 6.5 Most influential parameters on thermal comfort with cross night ventilation in a west office

parameter	SRRC
Internal heat gains	0.76
Wind pressure coefficient (Cp)	-0.33
$C_{d,opening}$	-0.30
Controlling night ventilation ($T_{e,min}$ by day)	0.23
Airtightness: n_{50}	-0.15
Roughness on site (a_site), defines wind local speed and external convective heat transfer coefficient	0.15
External solar absorption	0.12

6.3 Conclusions

Temperature measurements in the PROBE office building confirm the predicted uncertainty on the level of thermal comfort. Moreover, this case study shows that the distribution of thermal comfort can be well predicted using three simulations in which the most important parameters of chapter 5 are varied. The correspondence of the list of important input parameters in this case study with the list of chapter 5 explains this conclusion.

7 DESIGN APPLICATION: OFFICE BUILDING "SINT-PIETERSNIEUWSTRAAT"

The rules to (pre-)design a natural night ventilation system, derived in chapter 5, are applied in the office building "Sint-Pietersnieuwstraat" of the Ghent University (Belgium). Simulations in TRNSYS-COMIS evaluate the performances of this design. As advised in chapter 5, the average value and the uncertainty interval of good thermal comfort in normal and extremely warm weather are discussed.

7.1 BUILDING MODEL

The office building "Sint-Pietersnieuwstraat" is located in the city centre of Ghent (Belgium) and consists of two buildings separated by a courtyard. Each building includes three office floors on top of a foyer and two underground service floors. The office building on the west side of the courtyard is discussed. A 7-zone building model including one office zone on the west and east side on each floor connected by a circulation zone, is already determined in paragraph 5.1.1.2. In addition, a floor plan and a cross section are shown in Fig. 5.1 and Fig. 5.2 respectively.

The total area of an office floor is 24.7 x 11 m^2 of which the offices on the west and the east side occupy 24.7 x 4.75 m^2 and 15.6 x 4.75 m^2 respectively. The height between floor and ceiling is 2.88m and between two floors 3.91m. The total height of the office building is 18m.

The curtain wall façade of the offices is composed of sandwich (63%) and glass (37%) panes; the stairwell is completely finished with glass. The composition and thermal transmittance of the walls are shown in Table 7.1 and Table 7.2 respectively. The thermophysical properties of the layers can be found in Table 4.8. The transmittance coefficient U of glass equals 1.1 W/m^{2}K, the solar transmission coefficient 0.6. External sunblinds are provided on all windows with a g-value (glass included) of 0.15. These curtains are automatically controlled to be lowered from a solar radiation of 150 W/m^2.

The offices are assumed to be occupied from Monday to Friday from 9h to 18h. The design occupancy in the west and east office is 10 and 6 persons respectively, i.e. approximately 12 m^2/pers. Each office is equipped with a PC and screen for every employee, one copier and one laser printer for each five persons. The value and the diversity of these internal heat gains are given in Table 4.14. In addition, the heat gain of a desktop copier is 85 W when operating 1 page/min (Wilkins and Hosni, 2000). The total internal heat gains in the offices average 25.1 W/m^2 of which 69% is convectively emitted. In the corridor, 6 W/m^2 of internal heat gains are assumed.

Table 7.1 Wall composition of the office building "Sint-Pietersnieuwstraat"

In between ceiling/floor	d (cm)	Roof	d (cm)	Façade	d (cm)
Layer	d (cm)	Layer	d (cm)	Layer	d (cm)
Reinforced concrete	20	Reinforced concrete	20	Gypsum board	1
Light concrete	5	Insulation	12	Insulation	9
Air cavity	76	Bitumen	0.5	Aluminium	0.5
Plywood	1.8				
Carpet	0.4				
Light internal wall		Heavy internal wall			
Layer	d (cm)	Layer	d (cm)		
Gypsum board	1	Reinforced concrete	10		
Insulation	5				
Gypsum board	1				

Table 7.2 Thermal transmittance and area of the walls of west and east offices of the office building "Sint-Pietersnieuwstraat"

wall	A (m^2)		U (W/m^{2}K)
	West	East	
In between ceiling/floor	117.3	74.1	1.26
Roof	117.3	74.1	0.30
Façade	96.6	61.0	0.41
Light internal walls (office)	37.1	27.4	0.63
Heavy internal walls (corridor)	71.1	44.9	4.37

7.2 DESIGN NATURAL NIGHT VENTILATION

The (pre-)design rules, derived from the simulations in chapter 5, define the amount of exposed thermal mass and the effective area of the openings for natural night ventilation. The scheme of natural ventilation by day and night in the "Sint-Pietersnieuwstraat" office building is already determined in Fig. 5.3. Outside air enters the offices though top-hung windows near the ceiling on each floor, flows to the corridor and leaves the building through outlet windows on top of the central stairwell.

7.2.1 DESIGN EXPOSED THERMAL MASS

Simulations in chapter 5 show that the amount of exposed thermal mass can be derived from the cooling load. The heat that can be stored in this thermal mass is equated with the heat that is released during working hours.

Eq. 5.5 and Eq. 5.6 define the stored and released heat respectively. The maximum cooling load is calculated for an office on the west and east according to the German standard VDI 2078 (1996) in Table 7.3. These values are 50 to 60% higher than the maximum cooling loads in the generic offices as shown in Table 5.7. Larger window ratio in the façade, i.e. 37% instead of 25%, and higher internal heat gains, i.e. 25 W/m^2 instead of 22 W/m^2, explain this difference. To calculate the released heat Q_p in Eq. 5.6, the daily progress of the total radiation on an external surface are assumed for July 23 from VDI 2078 (1996). Moreover, a maximum penetration depth of 10cm, a surface temperature difference between the end and the beginning of the working day of 4°C and exposed reinforced concrete walls are assumed to determine the stored heat in Eq. 5.5.

This means that an area of 162 and 100 m^2 exposed thermal mass is required in a west and an east office respectively. In addition, an exposed ceiling is advised in paragraph 5.3.1.2. The area of the ceiling in the offices in Table 7.2 does not meet the required amount of thermal mass. The internal wall separating the office from the corridor needs to be constructed in reinforced concrete as well.

Furthermore, the required night ventilation flow rate can be estimated by comparing the heat that can be removed by ventilation at night Q_v in Eq. 7.1 with the heat that is released in the office during working hours Q_p in Eq. 5.6. An indoor-outdoor temperature difference of 4°C is assumed from Fig. 5.15. This results in a design night flow rate of approximately 12h^{-1} (see Table 7.3). Due to a larger maximum cooling load in the "Sint-Pietersnieuwstraat", the required flow rate exceeds the flow rate found in the generic office with stack ventilation, as shown in Fig. 5.14.

$$Q_v = \int_{22}^{6} 0.34 nV(\theta_i - \theta_e) dt \qquad \text{Eq. 7.1}$$

Table 7.3 Calculated maximum cooling load in an office on the west and east side according to VDI 2078 (1996), design area of exposed thermal mass and design night flow rate

Orientation	Maximum cooling load to keep $\theta_{i,a}$ = 24°C (W/m^2)			Design area exposed thermal mass (m^2)	Design night flow rate (h^{-1})
	Time	July	September		
west	16h	65	53	162	11.7
east	9h	56	44	100	11.5

7.2.2 Design ventilation openings

7.2.2.1 Natural night ventilation

The supply and exhaust windows of the natural night ventilation system are provided in the façade on each floor and on top of the stairwell respectively. Fig. 7.1 shows the heights of these ventilation openings. To create an inflow on all floors, the neutral pressure plane is required in between the supply opening on the third floor and the exhaust opening. As shown in Fig. 7.1, a limited height difference can be noticed between these two windows. In addition, the total area of the exhaust windows in the "Sint-Pietersnieuwstraat" office building is restricted to 2 x 4.55m x 1m, i.e. an effective area of 6.97 m^2 assuming a opening angle of 60° in Eq. 4.37. Considering these constraints, the effective areas of the supply windows have to be designed ensuring incoming flows on all floors.

The effective area of the ventilation openings can be derived from Eq. 4.36 and Eq. 2.1. The design night ventilation flow rates determined in the previous section require unrealistically large areas of both supply windows on the third floor and exhaust openings in the stairwell. Therefore, various possible combinations of indoor-outdoor temperature difference and related expected flow rates, derived from Fig. 5.15 and Fig. 5.14 respectively, are examined. A ventilation flow rate of 3.5 h^{-1} combined to an indoor-outdoor temperature difference of 5.5°C corresponds to an exhaust window area that approximately equals the maximum.

Table 7.4 shows the corresponding designed effective leakage area ($C_d{}^*A_{eff}$) of the supply and circulation openings in one office module of 2.6m wide with a supply window of 1.3m x 0.45m on each floor. A discharge coefficient C_d of 0.6 is assumed. In addition, the ratio of the effective area of the supply window to the floor area is presented in Table 7.4. Due to the design constraints, the designed effective area of the supply windows in the offices in the "Sint-Pietersnieuwstraat" are noticed to be smaller than in the generic offices with stack ventilation (see Table 5.5).
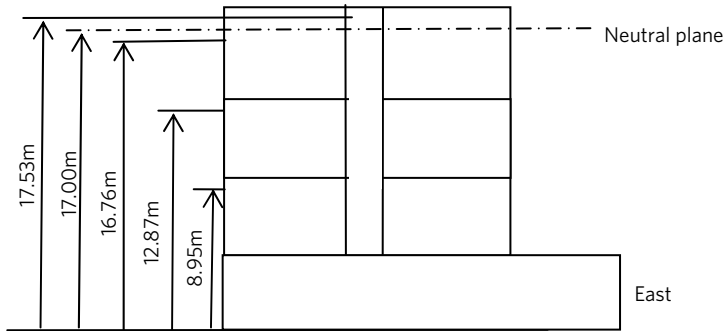
Fig. 7.1 Heights of supply and exhaust openings, measured from the ground to the middle of the opening

Table 7.4 Characteristics of night ventilation openings in one office module

floor	supply		circulation
	$C_d{}^*A_{eff}$ (m²)	A_{eff}/A_{floor} (%)	$C_d{}^*A_{eff}$ (m²)
first	0.02	0.3	0.16
second	0.03	0.4	0.17
third	0.14	1.8	0.18

7.2.2.2 HYGIENIC VENTILATION

The hygienic ventilation is a natural ventilation system as well. This ventilation by day is designed to 30 m²/h.pers, i.e. approximately 0.9 h^{-1}. This flow rate is increased to 2 h^{-1} when the indoor operative temperature exceeds 22°C.

Table 7.5 Characteristics hygienic ventilation openings in one office module

floor	$C_d{}^*A_{eff}$ supply (m²)	
	n = 0.9 h^{-1}	n = 2 h^{-1}
first	0.006	0.013
second	0.008	0.019
third	0.035	0.078

The openings for the hygienic ventilation system are designed similar to these of the natural night ventilation system. An indoor-outdoor temperature difference of 5.5 °C is assumed. Table 7.5 shows the characteristics of the hygienic ventilation openings in one office module to ensure an airflow rate of 0.9 and 2.0 h^{-1}. The designed effective leakage area ($C_d{}^*A_{eff}$) of the exhaust openings is 1.12 m² and 2.51 m² respectively. The effective area of the circulation openings is the same by day as by night. The effective area of the inlet and outlet openings is controlled to restrict the ventilation flow to the designed flow rate.

7.3 Uncertainties on building model characteristics

Most uncertainty intervals of the building model characteristics are already determined in chapter 4. Therefore, the discussion in this paragraph is restricted to the uncertainties on the boundary conditions, building, system and simulation characteristics specific to the building model of the "Sint-Pietersnieuwstraat" office building.

7.3.1 Boundary conditions

In a city centre, where the office building "Sint-Pietersnieuwstraat" is located, wind causes significant uncertainty on the airflows of natural ventilation. This uncertainty can be limited by calculating the wind pressure coefficients Cp in detail with the Cp generator of Knoll et al. (1995). These calculations are based on a plan of the concerned office building and its neighbourhood in Fig. 7.2. The calculated wind pressure coefficients Cp on the various façades, influenced by the enclosed buildings, are shown in Fig. 7.3. The variation on these Cp coefficients is derived from values calculated on various positions on the façade. Fig. 7.4 and Fig. 7.5 show the variation for the wind pressure coefficient on the west façade and on top of the south side of the stairwell respectively. Furthermore, the roughness height z_0 on site, i.e. mean city centre, is assumed 2m and varies from 1 to 4m.

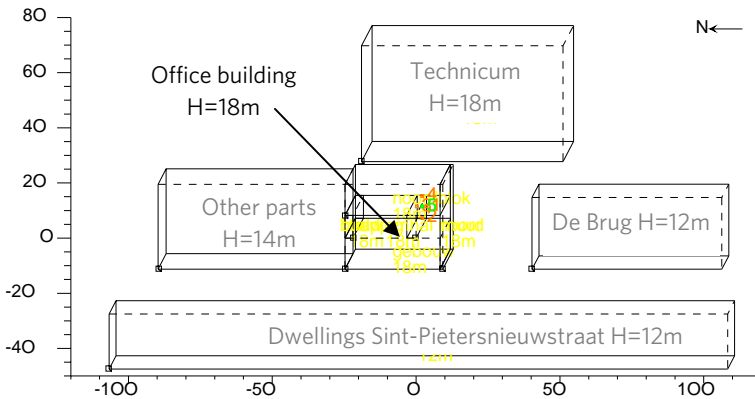Fig. 7.2 Plan of the buildings enclosing the "Sint-Pietersnieuwstraat" office building
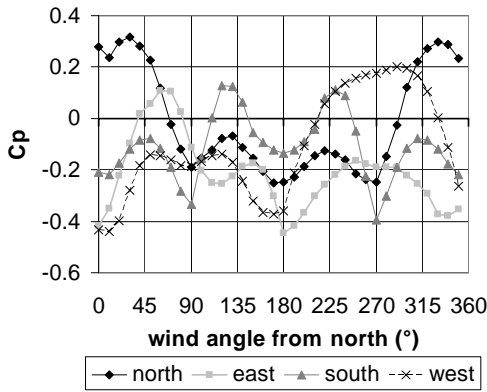
Fig. 7.3 Wind pressure coefficients in the new office building "Sint-Pietersnieuwstraat" of the Ghent University, calculated with Cp generator (Knoll et al., 1995)
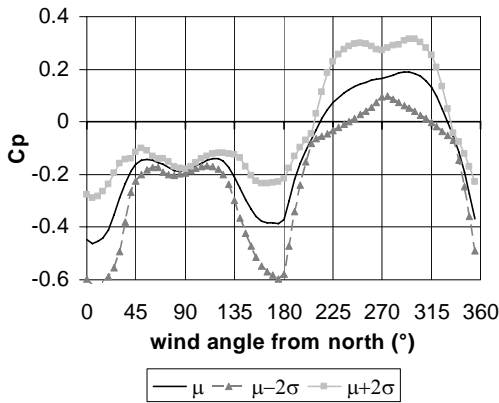
Fig. 7.4 Variation on the wind pressure coefficient Cp on the west side
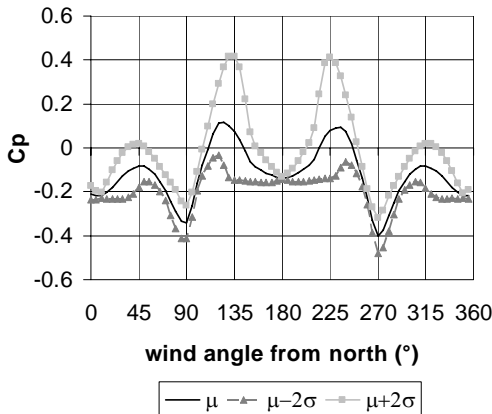
Fig. 7.5 Variation on the wind pressure coefficient Cp on the outlet windows on the south side

7.3.2 Building characteristics

The air tightness of the façade is characterised by an air mass flow coefficient C varying from 6 to $14*10^{-5}$ kg/(s.Pa^n.m^2) (Tamura and Shaw, 1976) and is modelled by cracks on office floor and ceiling height. In addition, the total internal heat gains vary from 20.3 to 31.5 W/m^2.

7.3.3 System characteristics

The openings of the natural night ventilation system are automatically controlled as described in Table 4.13. Furthermore, heating is not considered in the simulations.

7.3.4 Simulation characteristics

Simulations are carried out from May 21 to September 15. Normal and extremely warm weather data of Uccle, generated by Meteonorm are used. A time step of 15 min is chosen. Internal separations between the concerned office and the rest of the building are assumed adiabatic.

7.4 Performance evaluation

Simulations in TRNSYS-COMIS are carried out to evaluate the performances of the designed natural night ventilation system in the "Sint-Pietersnieuwstraat" office building. The average value and the uncertainty interval of good thermal comfort in normal and extreme warm weather are successively discussed.

7.4.1 Average performance

Thermal comfort is evaluated by the weighted excess hours (GTO) and the adaptive temperature limits (ATG) methods. Table 7.6 summarizes the results of the simulations with average properties. In addition, Fig. 7.6 and Fig. 7.7 show the results of the ATG-method in the west office on the second floor and in the east office on the third floor respectively.

Table 7.6 Average thermal comfort in the "Sint-Pietersnieuwstraat" office building

Orientation	Floor	GTO (h)	ATG (h)							
			level	-	-C	-B	A	+B	+C	-
west	First	139	-	5	9	83	589	66	3	1
	Second	154	-	1	5	36	617	87	9	1
	Third	161	-	11	9	38	580	101	14	3
east	First	143	C	1	12	60	596	84	3	0
	Second	170	C	0	0	15	627	102	12	0
	Third	200	-	0	0	8	591	133	17	7
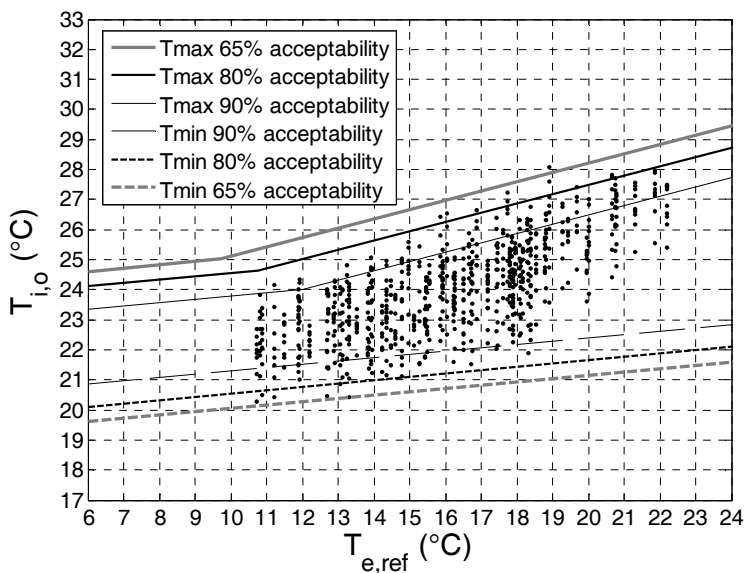
Fig. 7.6 Result of the ATG-method in the west office on the second floor
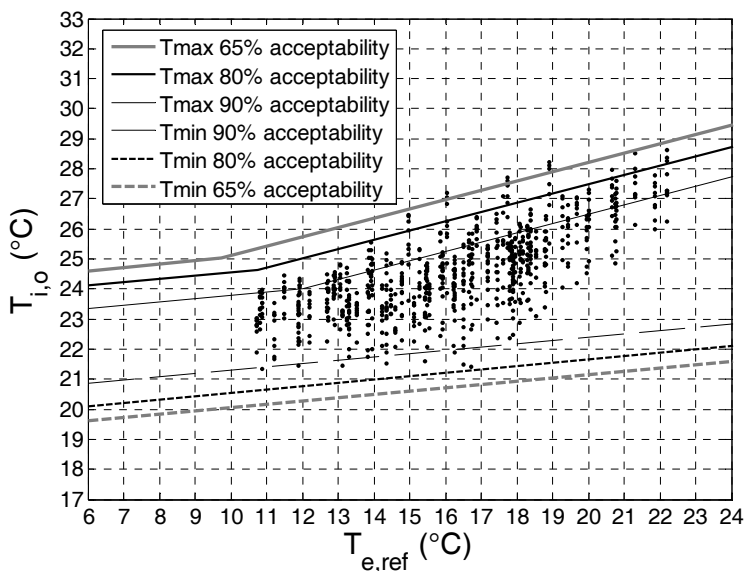
Fig. 7.7 Result of the ATG-method in the east office on the third floor

It can be concluded that moderate thermal comfort is noticed in the office building "Sint-Pietersnieuwstraat" when applying natural night ventilation. Nevertheless, thermal comfort is worse on the east than on the west side and on the third floor than on the lower floor due to the impact of the wind, which is not considered in the pre-design rules. Because the

7 DESIGN APPLICATION: OFFICE BUILDING "SINT-PIETERSNIEUWSTRAAT"

main wind direction in summer in Belgium is south-west, it is more probable that the air is flowing in on the west than on the east side (see Fig. 7.3). This impact is more obvious on the third floor where the wind velocity is higher and the wind pressure consequently exceeds the stack pressure more frequently than on the lower floors.

This is shown in Fig. 7.8 and Fig. 7.9, which compares the incoming ventilation flows between the offices when the windows are opened by day and night respectively. The distributions of the airflows on the first and second floor are similar. Significant difference between the incoming flow rates on the second and the third floor can be noticed. In addition, an exhaust flow rate has a larger probability in an office on the east than on the west side on the same floor. Furthermore, the incoming ventilation flow rates by night on the second floor are smaller than the flow rate in the stack ventilation case in the generic office, as shown in Fig. 5.12, because of smaller supply windows.
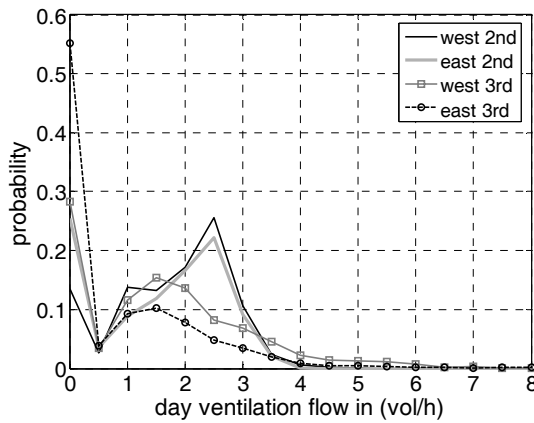
Fig. 7.8 Comparison of incoming outside ventilation flows by day
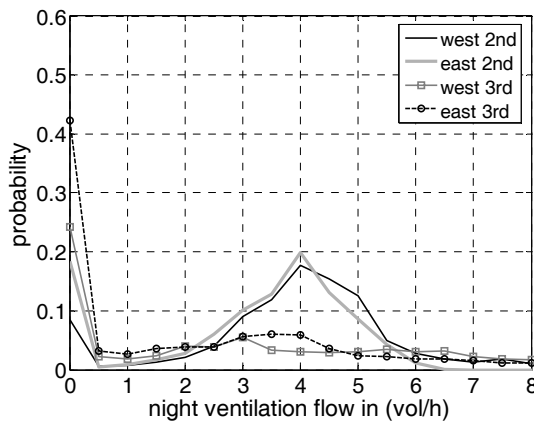
Fig. 7.9 Comparison of incoming outside ventilation flows by night when windows are opened

7.4.2 Uncertainty interval of the performances

Chapter 5 concludes that the uncertainty on the input parameters have to be considered to predict the reliability of the natural night ventilation design using building simulation. The uncertainty interval of the weighted temperature excess in all offices is estimated using three simulations in which the most important parameters of chapter 5 are varied:

- internal heat gains
- air tightness
- internal convective heat transfer coefficient
- wind pressure coefficient
- control parameters of natural night ventilation: minimum indoor-outdoor temperature difference and minimum internal temperature difference by night
- properties of the sunblinds: solar heat gain coefficient and the irradiance lowering the sunblinds
- discharge coefficient of the windows

The sets of input parameters for these three simulations are determined as follows:

- Average: average values for all input parameters
- Minimum: average minus standard deviation for the most important parameters, average values for the remaining parameters
- Maximum: average plus standard deviation for the most important parameters, average values for the remaining parameters

Fig. 7.10 compares the predicted uncertainty intervals of thermal comfort in the offices of the "Sint-Pietersnieuwstraat" office building. Large variation in the weighted excess hours can be noticed in all offices mainly caused by the predicted variation in internal heat gains. Moreover, the uncertainty is larger in the east than in the west office on the same floor.
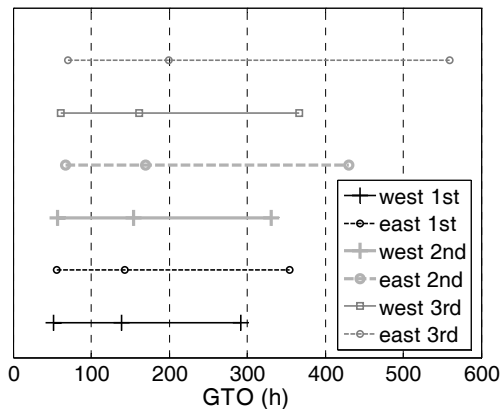
Fig. 7.10 Comparison of uncertainty intervals on GTO

7.4.3 Performance in extremely warm weather

Chapter 5 concludes that both normal and extremely warm weather data have to be taken into account to evaluate the performances of a designed natural night ventilation system properly. Fig. 7.11 shows the weighted temperature excess hours using both weather data sets. In addition, the result of the adaptive temperature limits method in a west office on the second floor and an east office on the third floor is illustrated in Fig. 7.12 and Fig. 7.13 respectively.

None of the floors meets the criteria for good thermal comfort in extreme warm weather. This is contrary to Fig. 5.57, which shows that good thermal comfort has a probability of approximately 0.5 in the generic office with manual control of the windows in extreme warm weather. A larger cooling load and smaller ventilation rates by night and day in the offices of the "Sint-Pietersnieuwstraat" explain this difference.

Nevertheless, the high GTO-values on the west side and the lowest two floors on the east side can be put into perspective by the results of the adaptive temperature limits method. The criterion of maximum 150-200 weighted temperature excess hours for good thermal comfort is determined for normal weather data. the evaluation of the adaptive temperature limits method is more weather independent. In addition, only small temperature excesses of level C during warm weather are noticed on the mentioned floors.

Moreover, differences in comfort between offices with different orientation or on different floors are more pronounced than using normal weather data.
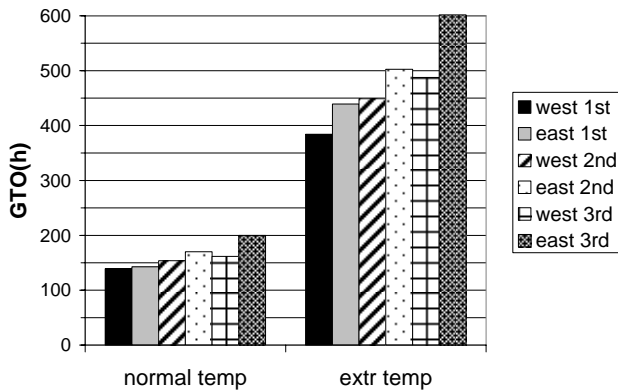
Fig. 7.11 Weighted temperature excess hours in normal and extremely warm weather
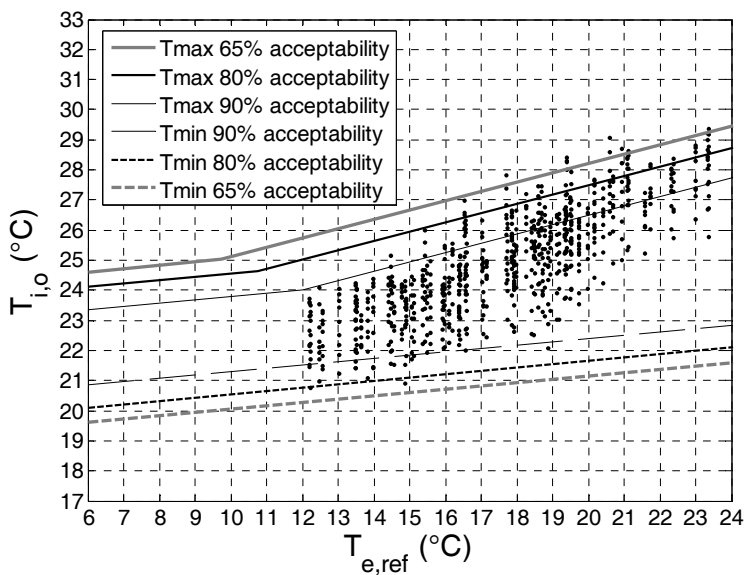
Fig. 7.12 Result of the ATG-method in the west office on the second floor in extremely warm weather
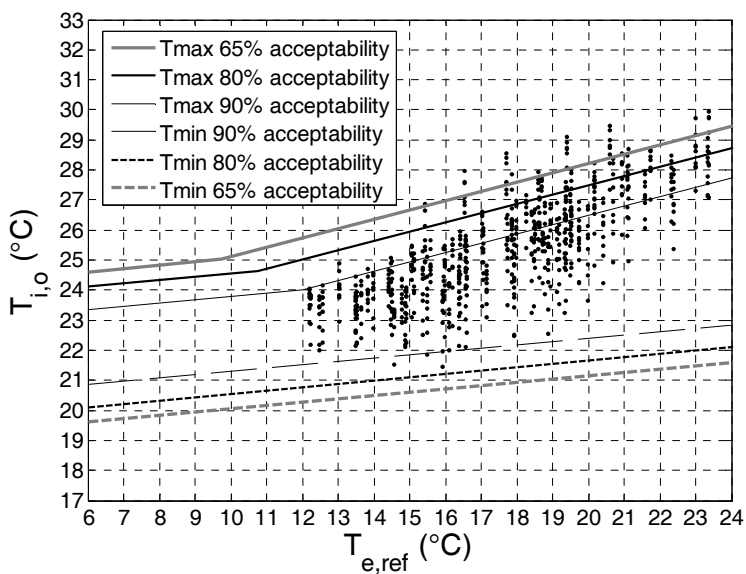
Fig. 7.13 Result of the ATG-method in the east office on the third floor in extremely warm weather

7 Design application: office building "Sint-Pietersnieuwstraat"

7.5 Conclusions

The rules to (pre-)design a natural night ventilation system, derived in chapter 5, are applied in the office building "Sint-Pietersnieuwstraat" (Belgium). Simulations in TRNSYS-COMIS evaluate the performances of this design. An acceptable average thermal comfort level can be noticed on all floors. Nevertheless, thermal comfort has a large uncertainty interval, especially in the offices on the east side. In addition, none of the floors meets the criteria for good thermal comfort in extremely warm weather. It can be concluded that the designed natural night ventilation system cannot ensure reliable thermal comfort in the office building "Sint-Pietersnieuwstraat".

Furthermore, these simulations show that it is important to investigate the interaction between the different floors of a building and to consider the impact of the wind in the design of natural night ventilation as well.

8 Conclusions and Perspectives

8.1 Conclusions

Natural night ventilation is a convective passive cooling method, driven by natural driving forces. It uses outside air at night to cool down the exposed building structure in which the heat of the previous day is accumulated. Case studies show that this cooling technique can be applied to achieve a good thermal comfort in moderate climates. The performances and potential energy savings of natural night ventilation can be predicted by building simulation. Nevertheless, in this performance evaluation, many uncertainties come across. Therefore, a methodology has been developed in this research to predict the performances of natural night ventilation by building simulation taking into account the uncertainties in the input.

To evaluate the performances of natural night ventilation, two suitable criteria of thermal comfort have been selected: the weighted temperature excess method, based on Fanger's comfort theory, and the adaptive temperature limits indicator, based on the adaptive theory of thermal comfort. Furthermore, the savings in cooling load, compared to the case without natural night ventilation, has been predicted based on the adaptive temperature limits indicator. To predict thermal comfort, the existing coupling between the multi-zone thermal simulation software TRNSYS and the infiltration and ventilation simulation software COMIS has been chosen.

Uncertainty and sensitivity analysis has been used to take into account the uncertainties in the input of the building simulation tool. Uncertainty analysis defines the variation on the predicted thermal comfort as a result of the variations in the input. Sensitivity analysis studies quantitatively and qualitatively how this variation in thermal comfort is attributed to the variations in the input parameters. A Monte Carlo Analysis (MCA) with a Latin Hypercube sampling (LHS) design has been used to investigate the uncertainty on the output. To characterize the sensitivity of the output to the uncertainties in the input, the Standardized Regression coefficient (SRC), based on the global sensitivity MCA, has been selected. The statistical software SIMLAB has been used to prepare the samples. The computational software Matlab has further processed these samples. The uncertainties on the model parameters of office building with natural night ventilation have been estimated from data in literature and standards.

The uncertainty on and sensitivity of the thermal comfort have been studied within a wide range of natural ventilation strategies, orientations, design decisions and boundary conditions. For this purpose, a representative office building model has been created and its characteristics have been defined.

The result of the uncertainty analysis is the distribution of thermal comfort and the probability of good thermal comfort in each of these cases. This distribution gives more reliable information on the predicted thermal comfort than the result of one single simulation. Thermal comfort is shown to have the largest probability in case of cross and stack ventilation, followed by single-sided ventilation considering realistic opening dimensions. The uncertainty on the thermal comfort in this latter strategy is also the largest because the uncertainty interval is related to the average value of thermal comfort.

Therefore, the uncertainties on passive stack and cross ventilation are similar.

Sensitivity analysis results in a list of input parameters which have the most important impact on thermal comfort in a naturally night ventilated office. The internal heat gains and the air tightness are noticed to have by far the greatest impact. In addition, the solar heat gain coefficient of the sunblinds, the solar radiation controlling the sunblinds and the internal convective heat transfer coefficient are important. Moreover, the controlling set-points of the natural night ventilation influence the variation of the thermal comfort. Finally, the wind pressure coefficient Cp and the discharge coefficient C_d of the night ventilation opening have a large effect on the thermal comfort.

This list of influencing input parameters has been a start to optimize the building and system design to increase the reliability of thermal comfort when natural night ventilation is applied. To ensure a high probability of good thermal comfort in a naturally night ventilated office, two conditions have to be fulfilled. A properly sized natural night ventilation has to be applied in a low energy office building with restricted fenestration and internal heat gains and sufficiently exposed thermal mass. An exposed ceiling is preferred to an exposed floor because the exchanged convective heat transfer between the air and an exposed floor is smaller than between the air and an exposed ceiling. In addition, to increase the reliability, natural night ventilation may be combined with additional cooling techniques like top cooling, increased ventilation flow by day or window opening by the users by day.

To evaluate the performances of a natural night ventilation design properly extremely warm weather data have to be taken into account. The combination of a normal and extremely warm weather data set is preferred.

Practical guidelines to pre-design natural night ventilation are derived from the results of the simulations. The cooling load defines the amount of exposed thermal mass. The heat that can be stored and the heat that is released in the office during working hours are assumed of the same size. Besides, the expected flow rates, indoor-outdoor temperature difference when night ventilation is in operation and opening duration are derived from these simulations as well. These assumptions can be used to (pre-)design the effective area of the night ventilation openings. These pre-design rules are applied to design the natural night ventilation system in the office building "Sint-Pietersnieuwstraat" (Belgium).

Although both criteria of thermal comfort are assumed to correspond, large differences in the predicted thermal comfort by GTO and ATG are noticed. The weighted temperature excess method (GTO) gives a global evaluation of the comfort over the summer period, while the evaluation of the adaptive temperature limits indicator (ATG) is highly influenced by – sometimes limited - temperature excesses. This difference can be significantly diminished by tolerating excess hours in the determination of the comfort levels in the adaptive temperature limits indicator.

The main disadvantage of the uncertainty and sensitivity analysis is the huge computational cost. These analyses require a large amount of simulations and thus prevents building engineers to use uncertainty and sensitivity in the evaluation of the performances of natural night ventilation. Therefore, practical guidelines have been derived

to take uncertainty into account in the design of natural night ventilation. Design engineers are recommended to analyse the uncertainty interval of thermal comfort instead of one single value when predicting the performances of natural night ventilation by building simulation. For this purpose, two easy-to-use methods have been developed. The probability of good thermal comfort and the distribution are predicted from the result of one simulation. The correlation is established between the thermal comfort in an office with average properties and the probability of good thermal comfort and the standard deviation of the distribution of thermal comfort respectively. In addition, a method is developed to predict the uncertainty interval of thermal comfort based on three discrete simulations in which only the most important input parameters from the sensitivity analysis are varied.

This latter simplified method has been applied on the evaluation of the comfort in the PROBE and "Sint-Pietersnieuwstraat" office building (Belgium). It has been concluded that these three simulations could very well predict the distribution of the thermal comfort in the first case study because the list of important input parameters in this office building corresponds rather well with the list mentioned above. Furthermore, although an acceptable average thermal comfort level can be noticed on all floors in the latter case study, thermal comfort has a large uncertainty interval, especially in the offices on the east side.

8.2 Perspectives

Following recommendations to further research can be identified. The convective heat transfer coefficient in case of natural night ventilation, i.e. under mixed flow conditions, may be further investigated. The heat storage in an exposed mass also may be studied in more detail. Measurements and simulations by CFD can focus on these physical phenomena. Their results should be implemented in the network simulation models.

The user behaviour and the way to simulate it may be further documented. Opening of windows and internal doors and occupancy schedules in office buildings are of particular interest.

The simplified regression model based on the results of sensitivity analysis may be further evaluated and generalized to estimate the thermal comfort in each design.

The developed methodology of dealing with uncertainties in the input may be further applied on predicting the performances of other passive (cooling) techniques like natural ventilation, earth-to-air heat exchangers, slab cooling, etc. This methodology also can lay the foundation of implementing natural night ventilation in the energy performance of building regulations. Wouters et al. (2004) already have proposed a probabilistic performance prediction as a framework to assess innovative systems in the EPBD.

Appendix A:
Standardized regression (SRC) and regression coefficients (b)

Strategy: cross ventilation
Orientation: south
Louvre area: 3%
Thermal comfort method: GTO
$R_y^2 = 0.95$

parameter	SRC	b
internal_gains	0.84	0.7
air_tightness	-0.35	-3323.4
g_sunblinds	0.27	960.9
C_alpha	-0.21	-93.5
Cp	-0.15	-135.7
DT_night	0.14	49.8
sunblinds	0.11	1.3
Cd_opening	-0.10	-186.9
Ti,min-night	0.10	33.6
d_plywood	-0.07	-5652.1
ventilation_flow	-0.07	-3.5
lambda_int._brick	-0.07	-147.9
c_plywood	-0.07	0.0
lambda_concrete	-0.07	-56.2
c_int_brick	-0.06	-0.3
rho_plywood	-0.06	-0.6
a_brick	0.05	69.1
b_window	0.05	493.2
lambda_gypsum_board	0.05	164.7
c_gypsum_board	-0.05	-0.1
lambda_light_concrete	0.05	223.9
d_heavy_concrete	0.05	2134.0
g_glass	0.05	419.2
lambda_plywood	-0.05	-123.9
h_window	0.05	364.0
building_height	0.04	116.0
c_insulation	0.04	0.3
rho_carpet	0.04	0.1
lambda_carpet	-0.04	-391.8
h	-0.04	-376.2
d_concrete	-0.04	-445.4
lambda_facing_brick	0.03	48.4
lambda_insulation	-0.03	-1691.1
Ti,min-day	0.03	9.3
d_int._brick	0.03	2185.0

parameter	SRC	b
A_frame	0.03	483.7
rho_light_concrete	0.03	0.3
c_heavy_concrete	0.02	0.1
rho_insulation	0.02	5.0
rho_facing_brick	0.02	0.1
rho_gypsum_board	-0.02	-0.2
C_door	0.02	6.1
lambda_heavy_concrete	-0.02	-16.3
d_insulation	0.02	378.1
d	-0.02	-130.1
rho_carpet	-0.02	-0.7
d_gypsum_board	-0.02	-4242.8
n_alpha	-0.02	-108.0
z0_meteo	0.02	11.9
c_concrete	-0.02	0.0
b_door	-0.02	-155.5
rho_concrete	-0.02	-0.1
rho_int._brick	0.02	0.1
R_cavity	-0.01	-128.1
Te,min-day	0.01	5.6
h_door	-0.01	-135.1
d_light_concrete	-0.01	-377.9
a_concrete	0.01	23.1
d_carpet	0.01	1157.4
z0_site	0.01	4.9
a_gypsum_board	-0.01	-17.9
c_light_concrete	-0.01	0.0
rho_heavy_concrete	-0.01	0.0
start_height_opening	0.01	40.5
h_opening	0.00	-20.2
a_carpet	0.00	31.7
d_ext._brick	0.00	-649.6
Cd_door	0.00	9.7
b	0.00	-7.9
U_frame	0.00	2.5
a_Al	0.00	12.8
c_facing_brick	0.00	0.0
reference_height	0.00	-126.7

$b_0 = -1739.2$

Nomenclature

abbreviation	parameter	dimensions
a_Al	solar absorption aluminium	-
a_brick	solar absorption brick	-
a_carpet	solar absorption carpet	-
a_concrete	Solar absorption concrete	-
a_gypsum_board	Solar absorption gypsum board	-
A_frame	Area window frame	%
air_tightness	Air tightness	$kg/s.Pa^n$
b	Width	m
b_door	Door width	m
b_window	Width of the window	m
building_height	Building height	m
C_alpha	Convective heat transfer coefficient	W/m^2K^{n+1}
C_door	Flow coefficient door	$kg/s.Pa^n$
c_concrete	Specific heat capacity hollow core concrete slabs	J/kgK
c_facing_brick	Specific heat capacity facing_brick	J/kgK
c_gypsum_board	Specific heat capacity gypsum board	J/kgK
c_heavy_concrete	Specific heat capacity heavy concrete	J/kgK
c_insulation	Specific heat capacity insulation	J/kgK
c_int_brick	Specific heat capacity internal brick	J/kgK
c_light_concrete	Specific heat capacity light concrete	J/kgK
c_plywood	Specific heat capacity plywood	J/kgK
Cd_door	Discharge coefficient door	-
Cd_opening	$C_{d,opening}$	-
Cp	Wind pressure coefficient Cp	-
d	Depth	m
d_carpet	Thickness carpet	m
d_concrete	Thickness concrete	m
d_ext._brick	Thickness external brick	m
d_gypsum_board	Thickness gypsum board	m
d_heavy_concrete	Thickness heavyconcrete	m
d_insulation	Thickness insulation	m
d_int._brick	Thickness internal brick	m
d_light_concrete	Thickness light concrete	m
d_plywood	Thickness plywood	m
DT_night	Indoor-outdoor temperature difference controlling night ventilation	°C
g_glass	Solar heat gain coefficient glass	-
g_sunblinds	Solar heat gain coefficient of sunblinds	-
h	Height	m
h_door	Door height	m
h_opening	Height external louvre	m
h_window	Window height	m
internal_gains	Internal heat gains	kJ/h
lambda_carpet	Thermal conductivity carpet	W/mK

abbreviation	parameter	dimensions
lambda_concrete	Thermal conductivity hollow core concrete slabs	W/mK
lambda_facing_brick	Thermal conductivity facing brick	W/mK
lambda_gypsum_board	Thermal conductivity gypsum board	W/mK
lambda_heavy_concrete	Thermal conductivity heavy concrete	W/mK
lambda_insulation	Thermal conductivity insulation	W/mK
lambda_int._brick	Thermal conductivity internal brick	W/mK
lambda_light_concrete	Lambda light concrete	W/mK
lambda_plywood	Thermal conductivity plywood	W/mK
n_alpha	n_α	-
R_cavity	Thermal resistance air cavity	m^2K/W
reference_height	Reference height	m
rho_carpet	Density carpet	kg/m^3
rho_carpet	Density carpet	kg/m^3
rho_concrete	Density concrete	kg/m^3
rho_facing_brick	Density facing brick	kg/m^3
rho_gypsum_board	Density gypsum board	kg/m^3
rho_heavy_concrete	Density heavy concrete	kg/m^3
rho_insulation	Density insulation	kg/m^3
rho_int._brick	Density internal brick	kg/m^3
rho_light_concrete	Density light concrete	kg/m^3
rho_plywood	Density plywood	kg/m^3
start_height_opening	Start height ventilation opening	m
sunblinds	Solar radiation controling lowering sunblinds	W/m^2
Te,min-day	External temperature by day controlling night ventilation	°C
Ti,min-day	Internal temperature by day controlling night ventilation	°C
Ti,min-night	Internal ceiling temperature at night controlling night ventilation	°C
U_frame	U window frame	W/m^2K
ventilation_flow	Ventilation flow	m^3/h
z0_meteo	Roughness at meteo site z_0	m
z0_site	Roughness on site z_0	m

Bibliography

Aggerholm, S. (1998). *Percieved barriers to natural ventilation design of office buildings.* Danisch building research institute, http://projects.bre.co.uk/natvent/index.html

Aggerholm, S. (2002). Hybrid ventilation and control strategies in the Annex 35 case studies, technical report. *In: Principles of Hybrid Ventilation.* Heiselberg, P. (Ed.) Aalborg, Denmark, Hybrid Ventilation Centre, Aalborg University, http://hybvent.civil.auc.dk

Alamdari, F., Hammond, G.P. (1983). Improved Data Correlations for Buoyancy-Driven Convection in Rooms. *Building Services Engineering Research and Technology* **4**(3): 106-112.

Allard, F., Haghighat, F., Liébecq, G., Pelletret, R., Bienfait, D., Vandaele, L., Eds. (1992). *Airflow through large openings in buildings.* Technical report of IEA Annex 20: Air flow patterns within buildings. Lausanne, Switzerland, EPFL/LESO-PB.

Allard, F., Utsumi, Y. (1992). Air-flow through large openings. *Energy and Buildings* **18**(2):133-145

Allard, F., Dascalaki, E., Limam, K., Santamouris, M. (1996). Natural ventilation studies within the EC Pascool Joule II project. *Air Infiltration Review* **17**(4): 1-4.

Allard, F., Ed. (1998). *Natural ventilation in buildings: a design handbook.* London, UK, James & James.

Allard, F., Alvarez, S. (1998). Fundamentals of natural ventilation. *In*: *Natural ventilation in buildings: a design handbook.* Allard, F. (Ed.), London, UK, James & James**:** 9-62.

Allen, C. (1984). AIVC Technical Note 13: Wind pressure data requirements for air infiltration calculations. Coventry, UK, AIVC.

Ashrae (1992). ASHRAE Standard 55 - thermal environmental conditions for human occupancy. Atlanta, USA, ASHRAE.

Ashrae (2001). International weather for energy calculations (IWEC weather files). User's manual and CD-rom. Atlanta, USA, ASHRAE.

Ashrae (2004). ASHRAE Standard 55-2004 - thermal environmental conditions for human occupancy. Atlanta, USA.

Ashrae (2005). *Fundamentals Handbook (SI).* Atlanta, USA, American Society of Heating, Refrigerating and Air Conditioning Engineers.

Aude, P., Tabary, L., Depecker, P. (2000). Sensitivity analysis and validation of buildings' thermal model using adjoint-code method. *Energy And Buildings* **31**: 267-283.

Awbi, H.B., Hatton, A. (1999). Natural convection from heated room surfaces. *Energy And Buildings* **30**: 233-244.

Awbi, H.B., Hatton, A. (2000). Mixed convection from heated room surfaces. *Energy And Buildings* **32**: 153-166.

Balaras, C. (1996). Heat attenuation. *Passive cooling in buildings.* Santamouris, M. and Asimakopoulos, D. London, United Kingdom, James & James**:** 185-219.

BBRI (1982). Moisture performance of building components (in Dutch). WTCB-tijdschrift **1**(1).

BBRI (1999). Insulation, ventilation and heating in newly built dwellings: results of a survey (in Dutch). BBRI, Brussels, Belgium.

BBRI (2002). Step by step renovation of office buildings: A better indoor climate with less energy (in Dutch). BBRI, Brussels, Belgium.

Beausoleil-Morrison, I. (2002a). The adaptive coupling of heat and air flow modelling within dynamic whole-building simulation. Glasgow, United Kingdom, University of Strathclyde. **Ph D**.

Beausoleil-Morrison, I. (2002b). The adaptive simulation of convective heat transfer at internal building surfaces. *Building And Environment* **37**: 791-806.

Bergsoe, N.C. (1998a). *Detailed monitoring report: BRF-kredit Headquarters*. Danish Building Research Institute, SBI.

Bergsoe, N.C. (1998b). *Detailed monitoring report: E. Phil & Son Headquarters*. Danish Building Research Institute, SBI.

Bettonvil, B., KLeijnen, J.P.C. (1997). Searching for important factors in simulation models with many factors: sequential bifurcation. *European Journal of Operational Research* **96**(1): 180-194.

BIN (1986). NBN B 62-003, Calculation of heat losses in buildings (in Dutch). BIN, Brussels, Belgium.

BIN (1991). NBN D50-001, Ventilation in residential buildings (in Dutch). BIN, Brussels, Belgium

BIN (1996). NBN EN ISO 6946, *Building components and building elements -- Thermal resistance and thermal transmittance - Calculation method*. BIN, Brussels, Belgium

BIN (2001). NBN B 62-002/A1, Calculation of thermal transmittance coefficients of walls and buildings (in Dutch). BIN, Brussels, Belgium.

Blondeau, P., Sperandio, M., Allard, F. (1997). Night ventilation for building cooling in summer. *Solar Energy* **61**: 327-335.

Borchiellini, R., Fürbringer, J.-M. (1999). An evaluation exercise of a multizone air flow model. *Energy And Buildings* **30**(1): 35-51.

Bossaer, A., Demeester, J., Wouters, P., Vandermarcke, B., Vangroenweghe, W. (1998). *Airtightness performances in new Belgian dwellings*. 19th Annual AIVC Conference, Oslo, Norway, 77-84.

Brager, G.S., de Dear, R.J. (2000). A standard for natural ventilation. *Ashrae Journal* **42**(10): 21-28.

BRE (1994). Digest 399: Natural ventilation in non-domestic buildings, Building Research Establishment.

Breesch, H., Bossaer, A., Janssens, A. (2005). Passive cooling in a low-energy office building. *Solar Energy* **79**(6): 682-696.

Breesch, H., Descheemaeker, K., Janssens, A., Willems, L. (2004). *Evaluation of natural ventilation systems in a landscaped office*. 21th PLEA Conference, Eindhoven, The Netherlands, 157-162.

Breesch, H., Janssens, A. (2001). *Natural ventilation: theory and simulation*. 2nd PhD symposium of the Faculty of Applied Sciences (Ghent University), Ghent, Belgium.

Breesch, H., Janssens, A. (2002). *Simulating natural ventilation: coupling thermal and ventilation model*. 3th EPIC and 23th AIVC conference, Lyon, France, 741-746.

Breesch, H., Janssens, A. (2005). Uncertainty and sensitivity analysis to evaluate natural night ventilation design in an office building. 26th AIVC Conference, Brussels, Belgium, 3-8.

Breesch, H., Janssens, A. (2006). Building simulation to predict the performances of natural night ventilation: uncertainty and sensitivity analysis. *Building and Environment, submitted*.

BS5925:1991 (1991). Code of practice for ventilation principles and designing for natural ventilation, British Standards Institute, United Kingdom.

CEN (1998). CR 1752: Ventilation for buildings: design criteria for indoor environment. Brussels, Belgium.

CEN (2000). Building materials and products - Energy related properties - Tabulated design values, EN 12524.

CEN (2004a). prEN ISO 13791:2004: Thermal performance of buildings - internal temperatures in summer of a room without mechanical cooling - general criteria and calculation procedures. Brussels, Belgium.

CEN (2004b). EN 13779 Ventilation for non-residential buildings - Performance requirements for ventilation and room-conditioning systems. Brussels, Belgium.

CEN (2004c). NBN EN ISO 13790:2004: Thermal performance of buildings – Calculation of energy use for heating. Brussels, Belgium.

Cenergie (2003). www.cenergie.be

CIBSE (1997). *Natural ventilation in non-domestic buildings: CIBSE Application Manual AM10:1997*. London, United Kingdom, The Chartered Institute of Building Services Engineering.

CIBSE (1999). *Guide A: Environmental design*. London, UK, The Chartered Institution of Building Services Engineers London.

Clarke, J.A., Yanneske, P.P., Pinney, A.A. (1990). *The Harmonisation of Thermal Properties of Building Materials*. United Kingdom.

Clarke, J.A. (2001). *Energy simulation in building design (2n ed.)*. Oxford, UK, Butterworth-Heinemann.

CMHC (2001). Air leakage characteristics, test methods and specifications for large buildings, *CMHC Research Highlights* 01-123, www.cmhc-shcl.gc.ca

Cotter, S.C. (1979). A screening design for factorial experiments with interactions. *Biometrika* **66**(2): 317-320.

Crawley, D.B. (1998). Which weather data should you use for energy simulations of commercial buildings. *ASHRAE Transactions* **104**(2).

Crawley, D.B, Hand, J.W., Kummert, M., Griffith, B.T. (2005). *Contrasting the capabilities of building energy performance simulation programs.* http://www.energytoolsdirectory.gov/pdfs/contrastingthecapabilitiesofbuildingenergyperformancesimulationprogramsv1.0.pdf

Cukier, R.I., Fortuin, C.M., Schuler, K.E., Petschek, A.G., Schaibly, J.H. (1973). Study of the sensitivity of coupled reaction systems to uncertainties in rate coefficients. I Theory. *J. Chem. Phys.* **59**: 3873-3878.

Dascalaki, E. (Ed.) (1998). The AIOLOS software. *In: Natural ventilation in buildings: a design handbook*. Allard, F. (Ed.), London, UK, James & James

D'haeseleer, W. (2005). The energy issue in a nutshell (in Dutch). *Energy today and tomorrow (in Dutch)*. D'haeseleer, W. Leuven, Belgium, Acco**:** 13-46.

de Dear, R., Brager, G.S., Cooper, D. (1997). Final report ASHRAE RP-884: Developing an Adaptive Model of Thermal Comfort and Preference.

de Dear, R.J., Brager, G.S. (2002). Thermal comfort in naturally ventilated buildings: revisions to ASHRAE Standard 55. *Energy And Buildings* **34**(6): 549-561.

De Paepe, K. (2003). Low-energy techniques in office buildings: discussion of the measurements (in Dutch). *Department of Architecture and Urban Planning*. Ghent, Belgium, Ghent University. **M Sc**.

de Wit, M. (1997). Identification of the important parameters in thermal building simulation models. *J. Statist. Comput. Simul.* **57**: 305-320.

de Wit, M.S. (2001). Uncertainty in predictions of thermal comfort in buildings, Technical University Delft, The Netherlands. **PhD**.

de Wit, M.S., Augenbroe, G. (2002). Analysis of uncertainty in building design evaluations and its implications. *Energy And Buildings* **34**(9): 951-958.

Delsante, A., Aggerholm, S. (2002). The use of simulation tools to evaluate hybrid ventilation control strategies. *in: Principles of Hybrid Ventilation*. Heiselberg, P. (Ed.), Aalborg, Denmark, Hybrid Ventilation Centre, Aalborg University. http://hybvent.civil.auc.dk

Delsante, A., Vik, T.A. (2002). Hybrid Ventilation: state of the art review. *In: Principles of Hybrid Ventilation*. Heiselberg, P. (Ed.), Aalborg, Denmark, Hybrid Ventilation Centre, Aalborg University.

Demeester, J., Wouters, P., Ducarme, D. (1998a). *Detailed Monitoring Report: PROBE-building*. Belgian Building Research Institute, http://projects.bre.co.uk/natvent/index.html

Demeester, J., Wouters, P., Ducarme, D. (1998b). *Detailed Monitoring Report: The Kepperkouter project*. Belgian Building Research Institute, http://projects.bre.co.uk/natvent/index.html

Descheemaeker, K. (2004). Performance of natural ventilation systems in offices (in Dutch). Brussels, Belgium, VUB, **M Sc**.

Dorer, V., Weber, A. (1999). Air, Contaminant and heat transport models: integration and application. *Energy And Buildings* **30**: 97-104.

Dorer, V., Haas, A., Weber, A., Feustel, H.E., Smith, B.V. (2001). *COMIS 3.1 - User's guide*.

Dorer, V., Tanner, C., Weber, A. (2004). Airtightness of buildings. *AIVC Ventilation information paper* **8**.

EC2000 (1998). *Natural ventilation and cooling strategies in new office designs.* European Commission - DG TREN - Thermie Programme, http://erg.ucd.ie/EC2000/ec2000_hp.html

EC (1985). Test Reference Years TRY, Weather data sets for computer simulations of solar energy systems and energy consumption in buildings. Commission of the European Communities, Directorate General XII for Science, Research and Development, Brussels, Belgium.

EC (2003). *European energy and transport - Trends to 2030*. European Commission - Directorate-General for Energy and Transport.

EC (2005). Green paper on energy efficiency or doing more with less, COM(2005). European Commission.

ESDU82026 (1982). Strong winds in the atmospheric boundary layer - part 1: mean hourly wind speeds. Engineering Sciences data.

ESRU (2005). ESP-r: a building and plant energy simulation environment. University of Strathclyde, Glasgow, UK.

EU (2002). Directive 2002/91/EC of the European parliament and of the council of 16 December 2002 on the energy performance of buildings. http://europa.eu.int/eur-lex/pri/en/oj/dat/2003/l_001/l_00120030104en00650071.pdf

EU (2005). *The Kyoto protocol - A brief summary*. http://www.eu.int/comm/environment/climat/kyoto.htm

Fanger, P.O. (1972). Thermal comfort: Analysis and applications in environmental engineering. London, New York, McGraw-Hill.

Favarolo, P.A., Manz, H. (2005). Temperature-driven single-sided ventilation through a large rectangular opening. *Building And Environment* **40**(5): 689-699.

Feustel, H.E., Dieris, J. (1992). A survey of airflow models for multizone structures. *Energy and Buildings* **18**(2): 79-100.

Feustel, H.E. (1999). COMIS - an international multizone air-flow and contaminant transport model. *Energy and Buildings* **30**(1): 3-18.

Fisher, D.E. (1995). An experimental investigation of mixed convection heat transfer in a rectangular enclosure. Urbana, USA, University of Illinois. **PhD**.

Flemish Government (2005a). Order of the Flemisch Government to assess the requirements according to the energy performance and the indoor climate in buildings of 11 March 2005, Annex VI: ventilation in non-residential buildings: determination and requirements (in Dutch). Brussels, Belgium. www.energiesparen.be/energieprestatie

Flemish Government (2005b). Order of the Flemisch Government to assess the requirements according to the energy performance and the indoor climate in buildings of 11 March 2005, Annex II: Determination of the level of primary energy consumption in office and school buildings (in Dutch). Brussels, Belgium. www.energiesparen.be/energieprestatie

Flourentzou, F., Van der Maas, J., Roulet, C.A. (1998). Natural ventilation for passive cooling: measurement of discharge coefficients. *Energy And Buildings* **27**(3): 283-292.

Frank, T. (2005). Climate change impacts on building heating and cooling energy demand in Switzerland. *Energy And Buildings* **37**(11): 1175-1185.

Fürbringer, J.-M., Roulet, C.A. (1995). Comparison and combination of factorial and Monte-Carlo design in sensitivity analysis. *Building And Environment* **30**(4): 505-519.

Fürbringer, J.-M., Roulet, C.A., Borchiellini, R. (1996). *Evaluation of COMIS*. Swiss Federal Institute of Technology, Lausanne, Switzerland.

Fürbringer, J.-M., Roulet, C.A. (1999). Confidence of simulation results: put a sensitivity analysis module in your model. The IEA-ECBCS Annex 23 experience of model evaluation. *Energy And Buildings* **30**(1): 61-71.

Fürbringer, J.-M., Roulet, C.A., Borchiellini, R. (1999). An overview of the evaluation activities of IEA ACBCS Annex 23. *Energy And Buildings* **30**(1): 19-33.

GBA (1999). *Building physical quality of state housing (in Dutch).*
http://www.rijksgebouwendienst.nl/bouwfys/Bouwfysica.htm

Geros, V., Santamouris, M., Tsangrasoulis, A., Guarracino, G. (1999). Experimental
evaluation of night ventilation phenomena. *Energy And Buildings* **29**: 141-154.

Geros, V., Santamouris, M., Karatasou, S., Tsangrassoulis, A., Papanikolaou, N. (2005). On
the cooling potential of night ventilation techniques in the urban environment. *Energy
And Buildings* **37**(3): 243-257.

Givoni, B. (1994). *Passive and low energy cooling of buildings.* New York, USA, Van Nostrand
Reinhold.

Givoni, B. (1998). Effectiveness of mass and night ventilation in lowering the indoor
daytime temperatures. Part I: 1993 experimental periods. *Energy And Buildings* **28**: 25-
32.

Glaverbel (2005). *Product information.* www.glaverbel.com

Gratia, E., Bruyère, I., De Herde, A. (2004). How to use natural ventilation to cool narrow
office buildings. *Energy And Buildings* **39**: 1157-1170.

Grosso, M. (1995). CpCalc+: calculation of wind pressure coefficients on buildings: user's
manual.

Haas, A., Weber, A., Dorer, V., Keilholz, W., Pelletret, R. (2002). COMIS v3.1 simulation
environment for multizone air flow and pollutant transport modelling. *Energy And
Buildings* **34**: 873-882.

Haghighat, F., Rao, J. (1991). Computer-aided building ventilation system design - a
system-theoretic approach. *Energy and Buildings* **17**(2): 147-155.

Heijmans, N., Wouters, P. (2002a). Impact of the uncertainty of wind pressures on the
prediction of thermal comfort performances, technical report. *In: Principles of Hybrid
Ventilation.* Heiselberg, P. (Ed.), Aalborg, Denmark, Hybrid Ventilation Centre, Aalborg
University. http://hybvent.civil.auc.dk

Heijmans, N., Wouters, P. (2002b). Pilot study report: Probe, Limelette, Belgium. *In:
Principles of Hybrid Ventilation.* Heiselberg, P. (Ed.), Aalborg, Denmark, Hybrid
Ventilation Centre, Aalborg University. http://hybvent.civil.auc.dk

Heijmans, N., Wouters, P., Eds. (2002c). Pilot study report: IVEG, Hoboken, Belgium. *In:
Principles of Hybrid Ventilation.* Heiselberg, P. (Ed.), Aalborg, Denmark, Hybrid
Ventilation Centre, Aalborg University. http://hybvent.civil.auc.dk

Heijmans, N., Wouters, P. (2002d). *An innovative hybrid ventilation system in the PROBE
building.* BBRI, Division of Building Physics and Indoor Climate, Brussels, Belgium.

Heiselberg, P., Svidt, K., Nielsen, P.V. (2001). Characteristics of airflow from open windows.
Building And Environment **36**(7): 859-869.

Heiselberg, P., Ed. (2002). *Principles of hybrid ventilation.* Aalborg, Denmark, Hybrid
Ventilation Centre, Aalborg University. http://hybvent.civil.auc.dk

Heiselberg, P. (2003). *Natural and hybrid ventilation course notes.* Aalborg University,
Aalborg, Denmark.

Hendriksen, O.J., Brohus, H., Frier, C., Heiselberg, P. (2002). Pilot study report: Bang &
Olufsen Head Quarter, Struer, Denmark. *Principles of Hybrid Ventilation.* Heiselberg, P.
Aalborg, Denmark, Hybrid Ventilation Centre, Aalborg University.

Hens, H. (1992). Air-wind tightness of pitched roofs - their real behaviour (in German). *Bauphysik* **14**(6): 161-174.

Hens, H. (1997). Building physics 1: heat and mass transport (in Dutch). Leuven, Belgium, Acco.

Hens, H. (1999). Applied building physics 2: components (in Dutch). Leuven, Belgium, Acco.

Hensen, J.L. (1995). *Modeling coupled heat and air flow: ping-pong vs onions.* 16th AIVC conference: Implementing the results of ventilation research, Palm Springs, USA.

Herkel, S., Knapp, U., Pfafferott, J. (2005). *A preliminary model of user behaviour regarding the manual control of windows in office buildings.* Building Simulation 2005, 9th IBPSA Conference, Montréal, Canada, 403-410.

Hien, W.N., Poh, L.K., Feriadi, H. (2000). The use of performance-based simulation tools for building design and evaluation - a Singapore perspective. *Building and Environment* **35**(8): 709-736.

Humphreys, M.A. (1976). Field studies of thermal comfort compared and applied. *Building Services Engineer* **44**: 5-27.

IEA (1991). Annex XIV: Condensation and energy.

IEA (1995). *Annex 28: Review of low energy cooling technologies.* United Kingdom, IEA ECBCS Programme.

IEA (1997). Annex 28: Selection guidance for low energy cooling technologies. United Kingdom, IEA ECBCS Programme.

IEA (1998). Annex 28: Low energy cooling: Case study buildings, IEA ECBCS Programme.

IEA (2004). *World Energy Outlook 2004.* Paris, France, OECD/IEA International Energy Agency.

IEA (2005). *World Energy Outlook 2005: Middle East and North Africa - Insights.* Paris, France, OECD/IEA International Energy Agency.

Inkarojrit, V., Paliaga, G. (2004). Indoor climatic influences on the operation of windows in a naturally ventilated building. 21th PLEA Conference, Eindhoven, The Netherlands.

Innova (2002). *Thermal Comfort*, Innova, Denmark.

IPCC (2002). Climate change 2001: synthesis report, Third assesment report. http://www.ipcc.ch/pub/reports.htm

ISO (1996). Standard 7730: Moderate thermal environments - determination of the PMV and PPD indices and specification of the conditions for thermal comfort. Geneva, Switserland, International Organisation for Standardisation.

ISO (1999). Building materials and products - Procedures for determining declared and design thermal values, ISO 10456, final draft.

ISSO (1990). Research rapport 5: Design of indoor conditions and good thermal comfort in buildings (in Dutch). Rotterdam, The Netherlands.

ISSO (1994). research rapport 32: Uitgangspunten temperatuursimulatieberekeningen. Rotterdam, The Netherlands.

ISSO (2004). Thermal comfort as performance (in Dutch), ISSO Research rapport 74. Rotterdam, The Netherlands.

Janssens, A., Depraetere, W., Morel, A., Hens, H. (1998). (in Dutch), VLIET test building: 3rd yearly report, KULeuven Laboratorium Bouwfysica, Leuven, Belgium

JRAIA (2005). *Estimates of world demand for air conditioners (2000-2008)*. http://www.jraia.or.jp/english/est/index.html

Khalifa, A.J.N., Marshall, R.H. (1990). Validation of Heat Transfer Coefficients on Interior Building Surfaces Using a Real-Sized Indoor Test Cell. *Int. J. Heat Mass Transfer* **33**(10): 2219-2236.

Khalifa, A.J.N. (2001). Natural convective heat transfer coefficients - a review I. Isolated vertical and horizontal surfaces. *Energy Conversion and Management* **42**: 491-504.

Klein, S.A., Beckman, W.A., Mitchell, J.W., Duffie, J.A., Duffie, N.A., Freeman, T.L., Mitchel, J.C., Braun, J.E., Evans, B.L., Krummer, J.P., Urban, R.E., Fiksel, A., Thornton, J.W., Blair, N.J., Williams, P.M., Bradley, D.E., McDowell, T.P., Kummert, M. (2004). *TRNSYS 16: a transient system simulation program, user manual*. Solar Energy Laboratory, University of Wisconsin, Madison, USA.

Klitsikas, N., Geros, V., Santamouris, M., Dascalaki, E., Kontoyiannididis, S., Argirou, A. (1996). *Summer version 2.0: A tool for passive cooling of buidings*. University of Athens, Athens, Greece.

KNMI (2006). *Normals for De Bilt 1971-2000 (in Dutch)*. http://www.knmi.nl/klimatologie/normalen1971-2000/per_station/stn260/4-normalen/260_debilt.pdf

Knoll, B., Phaff, J.C., de Gids, W.F. (1995). *Pressure simulation program*. 16th AIVC conference 'Implementing the results of ventilation research', Palm Springs, USA.

Kolokotroni, M. (1995). Night ventilation in commercial buildings. *Annex 28: Low Energy Cooling, Subtask 1*. IEA. United Kingdom**:** 7-11.

Kolokotroni, M. (1997). Night cooling ventilation in commercial buildings. *IEA Annex 28: Low Energy Cooling: Early design guidance for low energy cooling*. IEA. Ottawa, Canada, CANMET.

Kolokotroni, M., Tindale, A., Irving, S.J. (1997). *Office night ventilation pre-design tool*. 'Ventilation and Cooling', 18th Annual AIVC Conference, Athens, Greece, 213-224.

Kolokotroni, M., Aronis, A. (1999). Cooling-energy reduction in air-conditioned offices by using night ventilation. *Applied Energy* **63**: 241-253.

Kolokotroni, M., Giannitsaris, I., Watkins, R. (2005). The effect of the London urban heat island on building summer cooling demand and night ventilation strategies. *Solar Energy* in press.

Kukadia, V., Pike, J., White, M. (1998). *Detailed Monitoring report: Canning Crescent Centre*. Building Research Establishment, http://projects.bre.co.uk/natvent/index.html

LBNL (2003), *Window 5.2*, Lawrence Berkeley National Laboratory, http://windows.lbl.gov/software/window/window.html

Liddament, M.W. (1996). *A guide to energy efficient ventilation*. Coventry, UK, AIVC.

Liem, S.H., van Paassen, A.H.C. (1998). *Detailed Monitoring Report: The Tax Office of Enschede*. Delft University of Technology, The Netherlands, http://projects.bre.co.uk/natvent/index.html

Liem, S.H., van Paassen, A.H.C., Verwaal, M., Broekhuizen, H.F. (1998). *Detailed Monitoring Report: The town hall of Zevenhuizen*. Delft University of Technology, The Netherlands, http://projects.bre.co.uk/natvent/index.html

Limam, K., Innard, C., Allard, F. (1991). *Etude experimentale des transferts de masse et de chaleur a travers les grandes ouvertures verticales*. Conference groupe d'étude de la ventilation et du renouvellement d'air, INSA, Lyon, France, 98-111.

Limb, M.J. (2001). AIVC TN 55: A review of international ventilation, airtightness, thermal insulation and indoor air quality criteria. Coventry, UK, AIVC.

Litvak, A., Guillot, K., Kilberger, M., Boze, D. (2000). *Airtightness of French dwelllings: results from field measurement studies*. 21th AIVC Annual Conference, The Hague, The Netherlands.

Litvak, A., Kilberger, M., Guillot, K. (2000). *Field measurement results of the airtightness of 64 French dwellings*. Roomvent 2000, Reading, UK.

Lomas, K.J., Eppel, H. (1992). Sensitivity analysis techniques for building simulation program. *Energy And Buildings* **19**(1): 21-44.

Lomas, K.J., Eppel, H., Martin, C.J., Bloomfield, D.P. (1997). Empirical validation of building energy simulation programs. *Energy And Buildings* **26**: 253-275.

Macdonald, I., Strachan, P. (2001). Practical application of uncertainty analysis. *Energy And Buildings* **33**(3): 219-227.

Macdonald, I. (2002). Quantifying the Effects of Uncertainty in Building Simulation. *Department of Mechanical Engineering*. Glasgow, UK, University of Strathclyde. **Ph D**.

Mahajan, B.A., Hill, D.D. (1986). *Interzonal natural convection for various aperture configurations*. ASME Winter annual meeting, Anaheim, CA, USA.

Martin, A., Fletcher, J. (1996). *Night cooling strategies: Final report 11621/4*. BSRIA, Berkshire, United Kingdom.

MathWorks (2004). *Matlab 7.0.1*.

McCartney, K.J., Nicol, J.F. (2002). Developing an adaptive control algorithm for Europe. *Energy And Buildings*(34): 623-635.

Meinhold, U., Rösler, M. (2002). Pilot study report: Bertolt-Brecht-Gymnasium. *Principles of Hybrid Ventilation*. Heiselberg, P. Aalborg, Denmark, Hybrid Ventilation Centre, Aalborg University.

Meteotest (2003). Meteonorm: global meteorological database for engineers, planners and education version 5.0., Bern, Switzerland.

Morris, M.D. (1991). Factorial Sampling Plans For Preliminary Computational Experiments. *Technometrics* **33**(2): 161-174.

NatVent (1998). *Final Monitoring Report*. http://projects.bre.co.uk/natvent/index.html

Nicol, J.F., Humphreys, M.A. (2002). Adaptive thermal comfort and sustainable thermal standard for buildings. *Energy And Buildings* **34**: 563-572.

Nicol, J.F., Humphreys, M.A. (2004). A stochastic approach to thermal comfort - Occupant behavior and energy use in buildings. ASHRAE Annual Meeting, Nashville, USA, 1-15.

Olesen, B.W., Parsons, K.C. (2002). Introduction to thermal comfort standards and to the proposed new version of EN ISO 7730. *Energy And Buildings* **34**(6): 537-548.

Onset (2005). *HOBO® Temperature Data Logger Guide*. www.onsetcomp.com

Orme, M., Leksmono, N. (2002). *AIVC Guide 5: Ventilation Modelling Data Guide*. Brussels, Belgium, INIVe eeig.

Ottoy, J.P. (2002). *Biometry: course notes*. Ghent, Belgium, Faculty of Bioscience engineering, Ghent University.

Pavey, N. (1995). *Technical note TN 17/95: Rules of thumb*. BSRIA, Berkshire.

Pfafferott, J., Herkel, S., Jäschke, M. (2003). Design of passive cooling by night ventilation: evaluation of a parametric model and building simulation with measurements. *Energy And Buildings* **35**: 1129-1143.

Pfafferott, J., Herkel, S., Wambsganss, M. (2004a). Design, monitoring and evaluation. *Energy And Buildings* **35**: 1129-1143.

Pfafferott, J., Herkel, S., Wambsganss, M. (2004b). Design, monitoring and evaluation of a low energy office building with passive cooling by night ventilation. *Energy And Buildings* **36**(5): 455-465.

Pietrzyk, K., Hagentoft, C.-E. (2005). *Probabilistic model PROMO for evaluation of air change rate distribution*. 26th AIVC conference, Brussels, Belgium, 329-334.

Pinney, A.A., Parand, F., Lomas, K.J., Bland, B.H., Eppel, H. (1991). The choice of uncertainty limits on program input parameters within the applicability study 1 project, Research report 18 for the Energy Technology Support Unit of the Department of Energy, UK. Environmental Design Unit, School of the Built Environment, Leicester Polytechnic, Leicester, UK.

POLIS (2003). *Simlab 2.2: Reference Manual*. Ispra, Italy, Joint Research Centre, Institute for Systems, Informatics and Safety.

Principi, P., Di Perna, C., Ruffini, E. (2002). Pilot study report: I Guzzini Illuminazione office building, Macerata, Italy. *In: Principles of Hybrid Ventilation*. Heiselberg, P. (Ed.), Aalborg, Denmark, Hybrid Ventilation Centre, Aalborg University.

Purdy, J., Beausoleil-Morrison, I. (2001). *The significant factors in modelling residential buildings*. 7th International IBPSA Conference: Building Simulation, Rio de Janeiro, Brazil, 207-214.

Raja, I.A., Nicol, J.F., McCartney, K.J., Humphreys, M.A. (2001). Thermal comfort: use of controls in naturally ventilated buildings. *Energy And Buildings* **33**: 235-244.

RMI (1998). *Climatological summary of 1998 (in Dutch)*. http://www.kmi.be

RMI (2001). *Climatological summary of 2001 (in Dutch)*. http://www.kmi.be

RMI (2002). *Climatological summary of 2002 (in Dutch)*. http://www.kmi.be

RMI (2003). *Climatological overview of 2003 (in Dutch or French)*. http://www.kmi.be

RMI (2004). *Normals for Uccle 1961-1990 (in Dutch)*. http://www.kmi.be

Roberson, J.A., Homan, G.K., Mahajan, A., Webber, C.A., Nordman, B., Brown, R.E., McWhinney, M.C., Koomey, J.G. (2002). Energy Use and Power Management in New Personal Computers and Monitors. LBNL-48581. Lawrence Berkeley National Lab, Berkeley, CA, USA, http://enduse.lbl.gov/info/LBNL-48581.pdf

Roulet, C.A., Van der Maas, J., Flourentzou, F. (1996). *A planning tool for passive cooling of buildings*. Indoor Air '96, Nagoya, Japan.

Saltelli, A., Andres, T.H., Homma, T. (1995). Sensitivity analysis of model output. Performance of the iterated fractional factorial design method. *Computational Statistics & Data Analysis* **20**(4): 387-407.

Saltelli, A., Chan, K., Scott, E.M., Eds. (2000). *Sensitivity Analysis*. Chichester, UK, John Wiley and Sons.

Santamouris, M. (1992). Natural convection heat and mass transfer through large openings. Internal report. Pascal research program, European commission DGX11.

Santamouris, M., Asimakopoulos, D., Eds. (1996). *Passive cooling of buildings*. London, United Kingdom, James & James.

Santamouris, M., Dascalaki, E., Priolo, C., Vandaele, L., Wouters, P., Alvarez, S., Allard, F., Limam, K., Maldonado, E., Guarracino, G., Bruant, M. (1996a). *AIOLOS: creation of an educational structure on the use of passive cooling ventilation techniques for buildings*. 17th AIVC Conference "Optimum ventilation and air flow control in buildings", Gothenburg, Sweden, 97-102.

Santamouris, M., Mihalakakou, G., Argirou, A., Asimakopoulos, D. (1996b). The efficiency of night ventilation techniques for thermostatically controlled buildings. *Solar Energy* **56**(6): 479-483.

Santamouris, M. (1996). Simplified methods for passive cooling applications. *Passive cooling of buildings*. Santamouris, M. and Asimakopoulos, D. (Ed.) London, United Kingdom, James & James: 455-465.

Schild, P. (2003). *COMISEXCEL: a spreadsheet user interface for COMIS*, Norwegian Building Research Institute, Oslo, Norway, http://www.byggforsk.no/prosjekter/hybvent/COMISexcel.htm

Seem, J.E. (1987). Modelling of Heat in Buildings. Madison, USA, University of Wisconsin. PhD.

Shaviv, E., Yezioro, A., Capeluto, I.G. (2001). Thermal mass and night ventilation as passive cooling design strategy. *Renewable Energy* **24**(3-4): 445-452.

Sherman, M.H., Chan, R. (2004). *Building airtightness: research and practice*. Lawrence Berkeley National Laboratory report no. LBNL-53356, Berkeley, CA, USA.

Sobol', I.M. (1993). Sensitivity analysis for non linear mathematical models. *Math. Model. Comput. Exp.* **1**: 407-414.

Solarbau (2005). www.solarbau.de

Swami, M.V., Chandra, P.E. (1988). Correlations for pressure distributions on buildings and calculations on the wind induced ventilation on a cubic structure. *ASHRAE Transactions* **94**(1): 243-266.

Tamura, G.T., Chia, Y.S. (1976). Studies on exterior wall air tightness and air infiltration of tall buildings. *ASHRAE Transactions* **82**(1): 122-134.

Thevenard, D.J., Brunger, A.P. (2002). The development of typical weather years for international locations: part I, algorithms and part II, production. *ASHRAE Transactions* **108**(1):376-383, 480-486

Thomas, R., Ed. (1996). Environmental design: an introduction for architects and engineers. London, UK, E&FN Spon.

Trnsys 13.1 (1990). *A transient system simulation program*, Solar Energy Laboratory, University of Wisconsin, Madison, USA.

Trocine, L., Malone, L. (2000). *Finding important independent variables through screening designs: a comparison of methods.* 2000 Winter Simulation Conference IEEE, Orlando, USA, 749-754.

van der Aa, A. (2002). Pilot study report: School building Waterland, The Hague, The Netherlands. *In: Principles of Hybrid Ventilation*. Heiselberg, P. (Ed.) Aalborg, Denmark, Hybrid Ventilation Centre, Aalborg University.

van der Linden, A.C., Kerssemakers, M., Boerstra, A.C., Raue, A.K. (2000). Thermisch binnenklimaat als gebouwprestatie. *Bouwfysica* **11**(4): 13-18.

van der Linden, K., Boerstra, A.C., Raue, A.K., Kurvers, S.R. (2002). Thermal indoor climate building performance characterized by human comfort response. *Energy And Buildings* **34**(7): 737-744.

van der Linden, A.C., Boerstra, A.C., Raue, A.K., Kurvers, S.R., de Dear, R. (2006). Adaptive temperature limits: a new guideline in The Netherlands A new approach for the assesment of building performance with respect to thermal indoor climate. *Energy And Buildings* **38**(1): 8-17.

van Paassen, A.H.C., Liem, S.H., Gröninger, B.P. (1998a). *Control of night cooling with natural ventilation: sensitivity analysis of control strategies and vent openings*. 19th AIVC Conference, Oslo, Norway, AIVC, 438-447.

van Paassen, A.H.C., Broekhuizen, H.F., Verwaal, M. (1998b). *Prototype of night ventilator for cooling*. Delft University of Technology, http://projects.bre.co.uk/natvent/index.html.

VDI (1996). VDI 2078: cooling load calculation of air-conditioned buildings (VDI cooling load regulations).

VITO (2002). Energy indicators in the tertiary sector in Flanders. VITO, Mol, Belgium.

Warren, P.R., Parkins, L.M. (1984). Window opening behaviour in office buildings. *Building. Serv. Eng. Res. Technol.* **5**(3): 89-101.

Weber, A., Koschenz, M., Dorer, V., Hiller, M., Holst, S. (2003). *TRNFLOW, a new tool for the modelling of heat, air and pollutant transport in buildings within TRNSYS*. Eighth International IBPSA Conference, Eindhoven, Netherlands, 1363-1367.

White, M., Kolokotroni, M., Webb, B.C., Shaw, R., Mdaes, P. (1998). *Detailed Monitoring Report: Portland Street Low Energy Building, University of Portsmouth*. Building Research Establishment, http://projects.bre.co.uk/natvent/index.html

Wieringa, J. (1992). Updating The Davenport Roughness Classification. *Journal Of Wind Engineering And Industrial Aerodynamics* **41**(1-3): 357-368.

Wilkins, C.K., McGaffin, N. (1994). Measuring computer equipment loads in office buildings. *Ashrae Journal* **39**(12): 41-44.

Wilkins, P.E., Hosni, M.H. (2000). Heat gain from office equipment. *Ashrae Journal* **42**(6): 33-44.

Wouters, P. (2000). Quality in relation to indoor climate and energy efficiency: An analysis of trends, achievements and remaining challenges. Louvain-la-Neuve, Belgium, Université Catholique de Louvain. **PhD**.

Wouters, P., Heijmans, N., Loncour, X. (2004). *Outline for a general framework for the assessment of innovative ventilation systems*. Reshyvent WP 4: Standards and Regulations,

Zaccheddu, E. (1998). *Detailed monitoring report: The Velux building*. Sulzer Infra Lab Ltd, http://projects.bre.co.uk/natvent/index.html

Publications

International journals

Breesch, H., Bossaer, A., Janssens, A. (2005). Passive cooling in a low-energy building, *Solar Energy* **79** (6): 682-696

Breesch, H., Janssens, A. (2006). Building simulation to predict the performances of natural night ventilation: uncertainty and sensitivity analysis, *submitted to Building and Environment*

International conferences proceedings

Breesch, H., Janssens, A. (2005). *Uncertainty and sensitivity analysis to evaluate natural night ventilation design in an office building*, 26th AIVC Conference "Ventilation in relation to the energy performance of buildings", Brussel, België, 21-23 september 2005, ISBN 2-9600355-8-5, p. 3-8

Breesch, H., Janssens, A. (2005). *Building simulation to predict the performances of natural night ventilation: uncertainty and sensitivity analysis*, Building Simulation 2005, 9th IBPSA Conference, Montréal, Canada, 15-18 augustus 2005, ISBN 2-553-01152-0, p. 115-122

Breesch, H., Descheemaeker, K., Janssens, A., Willems, L. (2004). *Evaluation of natural ventilation systems in a landscaped office*, 21st International Conference Passive and low energy architecture (PLEA) 'Built environments and environmental buildings', Eindhoven, The Netherlands, 19-22 September 2004, ISBN 90-386-1636-8, p. 157-162

Breesch, H., Janssens, A. (2004). *Uncertainty and sensitivity analysis of the performances of natural night ventilation*, Roomvent 2004 Conference, Coimbra, Portugal, 5-8 September 2004, ISBN 972-97973-2-3

Breesch, H., Bossaer, A., Janssens, A. (2003). *Passive cooling in a low-energy building*, AIVC 2003 BETEC Conference 'Ventilation, Humidity Control and Energy', Washington DC, USA, 12-14 October 2003, ISBN 2-9600355-4-2, p. 145-150

Breesch, H., Janssens, A. (2002). *Simulating natural ventilation: coupling thermal and ventilation model*, EPIC 2002 AIVC Conference 'Energy efficient & Healthy building in Sustainable cities', Lyon, France, 23-26 October 2002, ISBN 2-86834-118-7, p. 741-746

National conferences proceedings

Breesch, H., Janssens, A. (2003). Building simulation to predict the performances of natural night ventilation: sensitivity analysis, 4[de] doctoraatssymposium FTW, Gent, 3 december 2003, paper 117

Breesch, H., Janssens, A. (2001). *Natural ventilation: theory and simulation*, 2de doctoraatssymposium FTW, Gent, 12 december 2001, paper 8

Breesch, H., Janssens, A. (2000). *How to Apply Building Simulation Tools in the Design of Natural and Hybrid Ventilation?*, 1ste Doctoraatssymposium FTW, Gent, 5 december 2000, paper 37